

## **A PDK1-dependent regulation of PLC1 activation is essential for cancer cell migration and invasion**

Raimondi, Claudio

For additional information about this publication click this link.

<http://qmro.qmul.ac.uk/jspui/handle/123456789/2346>

Information about this research object was correct at the time of download; we occasionally make corrections to records, please therefore check the published record when citing. For more information contact [scholarlycommunications@qmul.ac.uk](mailto:scholarlycommunications@qmul.ac.uk)

# **A PDK1-dependent regulation of PLC $\gamma$ 1 activation is essential for cancer cell migration and invasion**

**Claudio Raimondi**

**Supervisor: Marco Falasca**

**Co-supervisor: Tania Maffucci**

**Thesis submitted for the degree of PhD**

*Centre for Diabetes, Blizard Institute of Cell and Molecular Science, Barts and  
the London School of Medicine and Dentistry, Queen Mary, University of  
London*

*May 2011*

*I, Claudio Raimondi, declare that the work presented in this thesis is my own, unless stated otherwise, and is in accordance with the University of London's regulation for the degree of PhD.*

Claudio Raimondi

# Abstract

Phospholipase C $\gamma$ 1 (PLC $\gamma$ 1) is highly expressed in several tumours such as breast carcinomas and has been found overexpressed in metastases compared to primary tumour in breast cancer patients, indicating that PLC $\gamma$ 1 may be important in tumorigenesis and metastasis dissemination. PLC $\gamma$ 1 involvement in cancer cell motility and in cancer cell Matrigel invasion was investigated. Downregulation of PLC $\gamma$ 1 protein expression by siRNA or shRNA inhibited Matrigel cell invasion of highly invasive breast and melanoma cancer cell lines. Furthermore PLC $\gamma$ 1 protein downregulation inhibits intracellular calcium mobilisation upon EGF stimulation demonstrating the essential role of PLC $\gamma$ 1 in EGF-induced calcium release. In the effort to identify specific PLC $\gamma$ 1 inhibitors, Inositol (1,3,4,5,6) pentakisphosphate (InsP<sub>5</sub>) and 2-*O*-Bn-InsP<sub>5</sub>, a synthetic compound based on InsP<sub>5</sub> structure, were tested on Matrigel cell invasion and PLC $\gamma$ 1 activity. I found that InsP<sub>5</sub> and 2-*O*-Bn-InsP<sub>5</sub> reduce cell migration and Matrigel invasion in breast and melanoma cancer cell lines, with a complete inhibition displayed by 2-*O*-Bn-InsP<sub>5</sub> treated cells. Furthermore InsP<sub>5</sub> and 2-*O*-Bn-InsP<sub>5</sub> treatment reduces calcium release upon EGF stimulation, with a complete inhibition showed by 2-*O*-Bn-InsP<sub>5</sub> treated cells, suggesting a potential inhibition on PLC $\gamma$ 1 activity. Analysis of PLC $\gamma$ 1 phosphorylation in tyrosine 783 residue revealed that 2-*O*-Bn-InsP<sub>5</sub> inhibits EGF-induced PLC $\gamma$ 1 tyrosine phosphorylation. Kinase profile assay, performed *in vitro* to test the inhibitory effect of InsP<sub>5</sub> and 2-*O*-Bn-InsP<sub>5</sub> on different kinases, showed a specific inhibition by 2-*O*-Bn-InsP<sub>5</sub> of the 3-phosphoinositide-dependent-protein kinase 1 (PDK1) with an IC<sub>50</sub> of 26 nM. Knock down of PDK1 using siRNA and shRNA in MDA-MB-231 showed impairment in cell migration and Matrigel invasion and inhibition of EGF-induced calcium mobilisation. Co-immunoprecipitation and FRET analyses showed that PLC $\gamma$ 1 and PDK1 associate in a protein complex. My finding identified a novel pathway which involves PDK1 in PLC $\gamma$ 1 activation. Furthermore this work highlights PLC $\gamma$ 1 as a potential therapeutic target to prevent metastases spreading and identified 2-*O*-Bn-InsP<sub>5</sub> as a leading compound for development of anti-metastatic drugs.

# Tables of contents

<b>Abstract</b> .....	3
<b>Acknowledgements</b> .....	11
<b>List of Figures and Tables</b> .....	12
<b>Abbreviations</b> .....	18
<b>CHAPTER 1: INTRODUCTION</b> .....	19
<b>1.1 Phosphoinositides</b> .....	20
<b>1.1.1 Phosphatidylinositol-4,5-bisphosphate, PtdIns(4,5P)<sub>2</sub></b> .....	21
<b>1.1.1.1 PtdIns(4,5)P<sub>2</sub> and cytoskeleton remodelling</b> .....	22
<b>1.1.1.2 PtdIns(4,5)P<sub>2</sub> and membrane trafficking</b> .....	23
<b>1.1.2 Phosphatidylinositol-3,4,5-trisphosphate, PtdIns(3,4,5)P<sub>3</sub></b> ....	24
<b>1.1.2.1 PtdIns(3,4,5)P<sub>3</sub>-dependent AKT and PLC<math>\gamma</math>1</b> <b>activation</b> .....	24
<b>1.2 Phospholipase C (PLC)</b> .....	26
<b>1.2.1 Catalytic domain</b> .....	26
<b>1.2.2 EF Motifs</b> .....	28
<b>1.2.3 C2 domain</b> .....	28
<b>1.2.4 PH domain</b> .....	30
<b>1.2.5 PLC Isoenzymes</b> .....	32
<b>1.3 PLC<math>\gamma</math></b> .....	38
<b>1.3.1 Growth factors induced stimulation of PLC<math>\gamma</math>1</b> .....	39
<b>1.3.2 PI3K and PLC<math>\gamma</math>1 activation</b> .....	41
<b>1.3.3 PLC<math>\gamma</math>1 activation and integrins</b> .....	43
<b>1.3.4 Biological functions of PLC<math>\gamma</math>1</b> .....	46
<b>1.3.5 Overview of the cell migration process</b> .....	49
<b>1.3.6 PLC<math>\gamma</math>1 and Rac1</b> .....	51
<b>1.4 Role of PLC<math>\gamma</math>1 in cancer</b> .....	52
<b>1.5 The metastatic process</b> .....	56
<b>1.6 Breast cancer</b> .....	59
<b>1.7 3-Phosphoinositide-Dependent-Protein-Kinase-1 (PDK1) in cancer as</b> <b>potential therapeutic target</b> .....	61
<b>1.7.1 Biological functions of PDK1</b> .....	61

1.7.2	PDK1 in cancer .....	62
1.7.3	PDK1-dependent pathways .....	64
1.7.4	PDK1 as therapeutic target .....	68
1.8	Inositol phosphates: promising lead compound for anticancer molecule development .....	69
<b>CHAPTER 2: Materials and Methods.....</b>		<b>75</b>
2.1	Cell culture .....	76
2.1.1	Cell lines.....	76
2.1.2	Cell culture and propagation .....	77
2.1.3	Cell amplification and passage .....	77
2.1.4	Cryo-conservation and recovery of cell lines.....	78
2.2	Molecular Biology.....	78
2.2.1	Proteins.....	78
2.2.1.1	Western blotting analysis.....	78
2.2.1.1.1	Protein sample preparation from cell lysates.....	78
2.2.1.1.2	Bradford protein assay .....	79
2.2.1.1.3	Polyacrylamide Gel Electrophoresis (PAGE) and Western blot .....	80
2.2.1.1.4	Immunoblotting and analysis.....	81
2.2.1.2	Co-immunoprecipitation analysis .....	82
2.2.1.2.1	Co-immunoprecipitation analysis by Millipore Catch and release KIT.....	82
2.2.1.2.2	Endogenous co-immunoprecipitation analysis.....	83
2.2.1.3	GST-Pull down assay .....	83
2.2.2	RNA-interference .....	84
2.2.2.1	siRNA using Oligofectamine transfecting agent.....	84
2.2.2.2	siRNA using Hiperfect reagent .....	85
2.2.2.3	stable knock down using short hairpin RNA.....	85
2.2.2.3.1	Stable knock down of PLCg1 using pSUPER™.retro vector-based shRNA .....	85

	2.2.2.3.2	Inducible knock-down of PLC $\gamma$ 1 using pSUPERIOR <sup>TM</sup> vector-based shRNA	86
	2.2.2.3.3	Stable downregulation of PDK1 using pSUPER vector-based shRNA	86
2.2.3		DNA	88
	2.2.3.1	Ligation and transformation	88
	2.2.3.2	DNA digestion	88
	2.2.3.3	Plasmid preparation	89
	2.2.3.4	Miniprep	89
	2.2.3.5	Maxiprep	89
	2.2.3.6	Agarose gel	89
	2.2.3.7	Plasmid transfection	90
	2.2.3.8	PCR	91
2.2.4		RNA	92
	2.2.4.1	RNA extraction	92
	2.2.4.2	RNA Reverse transcription	92
	2.2.4.3	Real Time quantitative Polymerase Chain Reaction (RT-qPCR)	93
2.3		Imaging methods	94
	2.3.1	Ruffling Assay	94
	2.3.2	Calcium measurement Assay	94
	2.3.3	Incorporation of Fluorescein-conjugated InsP <sub>5</sub> (2-FAM-InsP <sub>5</sub> )	95
	2.3.4	Forster Resonance Energy Transfer by acceptor photo-bleaching	96
	2.3.5	Forster Resonance Energy Transfer by FACS	98
2.4		Cell Biology	100
	2.4.1	Cell counting	100
	2.4.2	Migration and invasion assay	100
	2.4.2.1	Cell migration assay	100
	2.4.2.2	Matrigel cell invasion assay	101
	2.4.3	Inositol phosphate assay	102
	2.4.4	[ <sup>3</sup> H]InsP <sub>5</sub> incorporation assay	103
2.5		Statistical analysis	103

<b>CHAPTER 3: PLC<math>\gamma</math>1 is essential for cancer cell migration and invasion .....</b>	<b>104</b>
<b>3.1 Introduction .....</b>	<b>105</b>
<b>3.2 Results.....</b>	<b>106</b>
<b>3.2.1 PLC activity is essential for MDA-MB-231 fibronectin-induced migration.....</b>	<b>107</b>
<b>3.2.2 Effect of a PLC<math>\gamma</math>1 mutant form constitutively recruited to the plasma membrane on fibronectin-induced cell migration.....</b>	<b>109</b>
<b>3.2.3 Downregulation of PLC<math>\gamma</math>1 expression using a pSUPERIOR construct containing specific shRNA targeting PLC<math>\gamma</math>1.....</b>	<b>111</b>
<b>3.2.4 Inducible downregulation of PLC<math>\gamma</math>1 expression using a pSUPERIOR construct .....</b>	<b>112</b>
<b>3.2.5 Cell invasion assay in breast cancer cells stably downregulated for PLC<math>\gamma</math>1 expression .....</b>	<b>114</b>
<b>3.2.6 Cell invasion assay in melanoma cells transiently downregulated for PLC<math>\gamma</math>1 expression.....</b>	<b>116</b>
<b>3.2.7 Analysis of cytoskeleton remodelling in MDA-MB-435.....</b>	<b>117</b>
<b>3.2.8 Analysis of cytoskeleton remodelling in TSA murine breast cancer cell line .....</b>	<b>119</b>
<b>3.3 Discussion .....</b>	<b>121</b>
<b>CHAPTER 4:PLC<math>\gamma</math>1 is the main PLC isoform involved in EGF- and FGF- induced calcium release and InsP<math>_3</math> production in breast cancer and endothelial cells.....</b>	<b>124</b>
<b>4.1 Introduction .....</b>	<b>125</b>
<b>4.2 Results.....</b>	<b>126</b>
<b>4.2.1 Effect of PLC<math>\gamma</math>1 downregulation on EGF-induced calcium release in MDA-MB-231 .....</b>	<b>126</b>
<b>4.2.2 Effect of PCL<math>\gamma</math>1 downregulation on EGF-dependent Inositol Phosphates accumulation.....</b>	<b>128</b>
<b>4.3 Discussion .....</b>	<b>129</b>
<b>4.4 PLC<math>\gamma</math>1 siRNA interference inhibits FGF-2 induced calcium release in</b>	

HUVEC cells .....	131
4.4.1 Calcium release assay upon FGF-2 addition.....	131
4.4.2 PI3K is required for FGF-2-induced calcium release .....	132
4.4.3 Effect of PLC $\gamma$ 1 and PLC $\gamma$ 2 downregulation on endothelial cell proliferation .....	133
4.5 Discussion .....	134

**CHAPTER 5: Effect of Ins(1,3,4,5,6)P<sub>5</sub> and 2-*O*-Bn-InsP<sub>5</sub> on cell migration, cell invasion and on PLC $\gamma$ 1 activity .....**136

5.1 Introduction .....	137
5.2 Results.....	138
5.2.1 InsP <sub>5</sub> inhibits fibronectin-induced migration in MDA-MB-231. 138	
5.2.2 InsP <sub>5</sub> inhibits cell invasion on Matrigel of MDA-MB-231 .....	139
5.2.3 Effect of InsP <sub>5</sub> on cell survival and proliferation in MDA-MB-231 Breast cancer cells .....	140
5.2.4 InsP <sub>5</sub> inhibits Matrigel cell invasion in human and murine breast cancer cell lines.....	141
5.2.5 InsP <sub>5</sub> does not affect cell proliferation and cell survival of MDA-MB-435, 4T1 and TSA.....	142
5.2.6 InsP <sub>5</sub> inhibits internal calcium release In MDA-MB-231 and MDA-MB-435 cell lines .....	144
5.3 Discussion .....	147
5.4 2- <i>O</i> -Bn-InsP <sub>5</sub> – a new synthetic compound based on InsP <sub>5</sub> structure.....	147
5.4.1 2- <i>O</i> -Bn-InsP <sub>5</sub> inhibits fibronectin-induced cell migration in MDA-MB-231.....	148
5.4.2 2- <i>O</i> -Bn-InsP <sub>5</sub> inhibits cell migration in a dose-dependent manner .....	149
5.4.3 2- <i>O</i> -Bn-InsP <sub>5</sub> inhibits cell invasion on Matrigel in different human and murine breast cancer cell lines.....	150
5.4.4 2- <i>O</i> -Bn-InsP <sub>5</sub> does not affect cell proliferation and cell survival in MDA-MB-435, 4T1 and TSA cell lines.....	152
5.4.5 2- <i>O</i> -Bn-InsP <sub>5</sub> inhibits calcium release response in MDA-MB-	

	231 and MDA-MB-435 upon EGF stimulation.....	154
5.4.6	2- <i>O</i> -Bn-InsP <sub>5</sub> inhibits PLC $\gamma$ 1 tyrosine phosphorylation upon EGF stimulation.....	156
5.5	Discussion .....	157
<b>Chapter 6: Potential involvement of ABC transporters on inositol polyphosphates transmembrane transport.....</b>		
<b>161</b>		
6.1	InsP <sub>5</sub> internalisation .....	162
6.1.1	Time-course of InsP <sub>5</sub> uptake.....	162
6.1.2	Probenecid and Glibenclamide inhibit 2-FAM-InsP <sub>5</sub> uptake...164	
6.1.3	ABCC1 transporter is involved in 2-FAM-InsP <sub>5</sub> uptake.....	166
6.1.4	ABCC1 is potentially involved in <sup>3</sup> H-InsP <sub>5</sub> uptake.....	168
6.1.5	Downregulation of ABCC1, but not ABCC5, inhibits InsP <sub>5</sub> uptake in MDA-MB-231 .....	170
6.1.6	Downregulation of ABCC1 expression inhibits <sup>3</sup> H-InsP <sub>5</sub> uptake .....	173
6.1.7	Downregulation of ABCC1 and ABCC5 protein levels in	
	MDA-MB-231.....	174
6.2	Discussion .....	175
<b>Chapter 7: PDK1-dependent PLC<math>\gamma</math>1 activation .....</b>		
<b>177</b>		
7.1	Transient downregulation of PDK1 in MDA-MB-231, MDA-MB-435 and A375M.....	178
7.1.1	PDK1 protein downregulation in MDA-MB-231, MDA-MB-435 and A375M.....	178
7.1.2	Transient downregulation of PDK1 protein expression inhibits calcium release upon EGF stimulation .....	180
7.1.3	Matrigel cell invasion is inhibited in breast cancer and Melanoma cell lines upon PDK1 downregulation. ....	182
7.2	Generation of MDA-MB-231 stably downregulated for PDK1 expression .....	183

7.2.1	Design of 22-nucleotide targeting sequence cloned in pSUPERIOR.retro.puro vector .....	184
7.2.2	Colony-PCR screening.....	187
7.2.3	Clones selection.....	188
7.3	Effect of PDK1 protein downregulation on Inositol phosphates production .....	190
7.4	The PDK1-dependent PLC $\gamma$ 1 regulation .....	192
7.4.1	Analysis of PLC $\gamma$ 1 protein level in MDA-MB-231 downregulated for PDK1 .....	192
7.4.2	Effect of downregulation of PDK1 on tyrosine phosphorylation of PLC $\gamma$ 1 in MDA-MB-231.....	193
7.5	Investigation of the mechanism of PDK1-mediated PLC $\gamma$ 1 activation..	196
7.5.1	Overexpression of PLC $\gamma$ 1 and PDK1 in HEK293 cells .....	196
7.5.2	Investigation of potential PLC $\gamma$ 1-PDK1 through co-immunoprecipitation analysis .....	198
7.5.3	GST pull-down experiments .....	200
7.5.4	GST pull down analysis of PDK1-PLC $\gamma$ 1 interaction .....	201
7.5.5	Co-immunoprecipitation analysis of endogenous PLC $\gamma$ 1 and PDK1 in MDA-MB-231.....	205
7.5.6	FRET analysis of PLC $\gamma$ 1/PDK1 protein interaction by confocal imaging .....	207
7.5.7	FRET analysis of PLC $\gamma$ 1/PDK1 protein interaction by FACS analysis .....	214
7.6	Discussion .....	216
<b>Chapter 8: Concluding discussion and future studies .....</b>		<b>219</b>
8.1	Discussion .....	220
8.2	Future works .....	224
<b>Bibliography .....</b>		<b>225</b>
<b>Appendices .....</b>		<b>239</b>

# *Acknowledgement*

I am grateful to my supervisor, Professor Marco Falasca and to my co-supervisor Dr. Tania Maffucci for the opportunity to work in their lab, and for their endless support, guidance and enthusiasm and scientific support. It is difficult to express in word my gratitude to these two great scientists that has always been there for me throughout these last 3 years, showing me how to better achieve my goal and how to improve my skills in all the aspects that this job requires.

I want to thank my group, present and prior members, for their guidance in the lab and for the friendly environment; all the collaborators that provided me with reagents, cell lines and advices and the all the people in Centre for Diabetes. A very special thank to my fiancé Anissa, with whom I shared my happiest but also most difficult times, for her support and for the endless scientific discussions that contributed to increase my knowledge and my critical skill. A special thank to Dr. Gianluca Baldanzi for sharing with me some original ideas about the difficult scientific world during my first year of PhD. At that time I did not understand, today I believe he was quite right. Finally I would like to thank my family, my parents my brother and my grandparents who have always believed in me and supported me in all the ways.

# *List of Figures and Tables*

*Figures:*

<b>Figure 1.1</b>	Structure of Phosphatidylinositol .....	20
<b>Figure 1.2</b>	Schematic representation of phosphoinositides kinases and phosphates enzymes involved in their synthesis .....	21
<b>Figure 1.3</b>	A)Enzymatic reaction catalyzed by PLCs B) Crystal structure of PLC $\delta$ 1 .....	27
<b>Figure 1.4</b>	Structure of EF motif of PLC $\delta$ 1 isoform .....	28
<b>Figure 1.5</b>	Structure of the C2 domain of PLC $\delta$ 1 .....	29
<b>Figure 1.6</b>	PLC $\delta$ 1 PH domain structures .....	31
<b>Figure 1.7</b>	Schematic representation of PLC isoenzymes structures .....	34
<b>Figure 1.8</b>	Regulation of PLC $\beta$ by GPCR .....	35
<b>Figure 1.9</b>	Schematic mechanism of activation of PLC $\epsilon$ .....	37
<b>Figure 1.10</b>	Representation of PLC $\gamma$ isoenzymes.....	38
<b>Figure 1.11</b>	Relief of the auto-inhibitory interaction .....	41
<b>Figure 1.12</b>	Crosstalk PI3K/PLC $\gamma$ 1 .....	43
<b>Figure 1.13</b>	Representation of integrins heterodimer .....	44
<b>Figure 1.14</b>	Model of ECM-integrin-induced PLC $\gamma$ 1 activation .....	46
<b>Figure 1.15</b>	Model of cofilin activation .....	48
<b>Figure 1.16</b>	Model of cell migration .....	50
<b>Figure 1.17</b>	Model of EGF-induced Rac1 activation downstream of PLC $\gamma$ 1.....	52
<b>Figure 1.18</b>	PLC $\gamma$ 1 is important in metastasis development and progression .....	55
<b>Figure 1.19</b>	Model of metastasis dissemination and initiation of a novel distant tumour .....	58

<b>Figure 1.20</b>	Molecular mechanism of AKT activation by PDK1 .....	66
<b>Figure 1.21</b>	Mechanism of activation of S6K and SGK kinases by PDK1 .....	68
<b>Figure 1.22</b>	Representation of the mechanism through which Ins(1,3,4,5,6)P <sub>5</sub> may inhibits AKT .....	70
<b>Figure 2.1</b>	Thermal-Cycler protocol for RT-qPCR .....	93
<b>Figure 2.2</b>	Donor and acceptor spectra generated with Fluorescence spectra viewer tool.....	97
<b>Figure 3.1</b>	(A) Pictures of transwell inserts (B) Quantification of migrating cells by cell counting .....	106- 107
<b>Figure 3.2</b>	Effect of PLC inhibition on fibronectin-induced cell migration .....	108
<b>Figure 3.3</b>	Cell migration in MDA-MB-231 expressing PALM-PLC $\gamma$ 1 .....	110
<b>Figure 3.4</b>	WB analysis of stable protein downregulation of PLC $\gamma$ 1 .....	111
<b>Figure 3.5</b>	Model of inducible protein downregulation using pSUPERIOR inducible system.....	112
<b>Figure 3.6</b>	Inducible downregulation of PLC $\gamma$ 1 .....	113
<b>Figure 3.7</b>	Analysis of Matrigel invasion in breast cancer cell lines.....	115
<b>Figure 3.8</b>	(A) PLC $\gamma$ 1 transient downregulation in A375M (B) Matrigel cell invasion assay .....	116- 117
<b>Figure 3.9</b>	(A) PLC $\gamma$ 1 is important for cytoskeleton remodelling in MDA-MB-435 (B) Quantification of membrane ruffles in MDA-MB-435.....	118- 119
<b>Figure 3.10</b>	(A) Phalloidin staining of actin cytoskeleton in unstimulated and EGF- or Serum-stimulated TSA (B) Quantification of membrane ruffling in TSA .....	120
<b>Figure 4.1</b>	PLC $\gamma$ 1 is essential for EGF-induced calcium mobilisation (A) Calcium increase in EGF-stimulated-MDA-MB-231 when PLC $\gamma$ 1 is expressed (B) Calcium increase in EGF-stimulated-MDA-MB-231 when PLC $\gamma$ 1 expression is downregulated.....	127
<b>Figure 4.2</b>	Inositol phosphate assay .....	129

<b>Figure 4.3</b>	Intracellular calcium increase in serum starved HUVEC.....	132
<b>Figure 4.4</b>	PI3K is required for FGF-2-induced calcium release.....	133
<b>Figure 4.5</b>	PLC $\gamma$ 2 but not PLC $\gamma$ 1 affects cell proliferation in HUVEC cells.....	134
<b>Figure 5.1</b>	InsP <sub>5</sub> inhibits fibronectin-induced migration .....	138
<b>Figure 5.2</b>	InsP <sub>5</sub> inhibits Matrigel invasion .....	139
<b>Figure 5.3</b>	Cell counting of MDA-MB-231 after 72 hours of treatment with InsP <sub>5</sub> .....	141
<b>Figure 5.4</b>	InsP <sub>5</sub> inhibits cell invasion on Matrigel of MDA-MB-435, 4T1 and TSA .....	142
<b>Figure 5.5</b>	Effect of InsP <sub>5</sub> on cell proliferation/survival .....	143
<b>Figure 5.6</b>	Effect of InsP <sub>5</sub> on EGF-induced intracellular calcium mobilisation in MDA-MB-231 .....	145
<b>Figure 5.7</b>	Effect of InsP <sub>5</sub> on EGF-induced intracellular calcium mobilisation in MDA-MB-435 .....	146
<b>Figure 5.8</b>	2- <i>O</i> -Bn-InsP <sub>5</sub> blocks fibronectin-induced migration.....	148
<b>Figure 5.9</b>	2- <i>O</i> -Bn-InsP <sub>5</sub> inhibits cell migration in a dose-dependent manner.....	149
<b>Figure 5.10</b>	2- <i>O</i> -Bn-InsP <sub>5</sub> inhibits cell invasion on Matrigel ...	151
<b>Figure 5.11</b>	Cell proliferation and cell survival upon 2- <i>O</i> -Bn-InsP <sub>5</sub> treatment .....	153
<b>Figure 5.12</b>	Effect of 2- <i>O</i> -Bn-InsP <sub>5</sub> on intracellular calcium mobilisation .....	154-155
<b>Figure 5.13</b>	PLC $\gamma$ 1 phosphorylation is inhibited by 2- <i>O</i> -Bn-InsP <sub>5</sub> treatment .....	157
<b>Figure 6.1</b>	Incorporation of 2-FAM-InsP <sub>5</sub> .....	163
<b>Figure 6.2</b>	Time course of 2-FAM-InsP <sub>5</sub> uptake in untreated cells and in MDA-MB-231 treated with probenecid and glibenclamide .....	165
<b>Figure 6.3</b>	2-FAM-InsP <sub>5</sub> is inhibited by MK-571 .....	167-168
<b>Figure 6.4</b>	<sup>3</sup> H-InsP <sub>5</sub> incorporation is inhibited by MK-571 .....	169
<b>Figure 6.5</b>	Effect of siRNAs targeting ABCC1 or ABCC5 on 2-FAM-InsP <sub>5</sub> uptake .....	171-172
<b>Figure 6.6</b>	Figure 6.6: Effect of siRNAs targeting ABCC1 or ABCC5 on <sup>3</sup> H-InsP <sub>5</sub> uptake .....	173

<b>Figure 6.7</b>	Quantification of ABCC1 and ABCC5 expression .....	174
<b>Figure 7.1</b>	Transient downregulation of PDK1 .....	179
<b>Figure 7.2</b>	PDK1 downregulation inhibits EGF-induced calcium release.....	181
<b>Figure 7.3</b>	Cell invasion on Matrigel of MDA-MB-231, MDA-MB-435 and A375M downregulated for PDK1 expression.....	183
<b>Figure 7.4</b>	Short hairpin constructs .....	185
<b>Figure 7.5</b>	pSUPERIOR.retro.puro digested with HindIII .....	186
<b>Figure 7.6</b>	Second digestion of pSUPERIOR.retro.puro with BglII.....	186
<b>Figure 7.7</b>	Colony PCR screening Colony PCR screening .....	187
<b>Figure 7.8</b>	Western blot analysis for PDK1 .....	189
<b>Figure 7.9</b>	Inositol phosphates levels in MDA-MB-231 stably downregulated for PDK1 .....	191
<b>Figure 7.10</b>	PLC $\gamma$ 1 expression in cells downregulated for PDK1 .....	193
<b>Figure 7.11</b>	Western blot analysis of MDA-MB-231 downregulated for PDK1 (siPDK1 or shPDK1) .....	195
<b>Figure 7.12</b>	Overexpression of PLC $\gamma$ 1 and HA-Flag-PDK1 in HEK293 cells .....	197
<b>Figure 7.13</b>	Co-IP analysis of PDK1/ PLC $\gamma$ 1 upon overexpression .....	199
<b>Figure 7.14</b>	Overexpression of PLC $\gamma$ 1 and GST-PDK1 .....	201
<b>Figure 7.15</b>	GST pull-down.....	202
<b>Figure 7.16</b>	GST Pull-down optimisation protocol .....	204
<b>Figure 7.17</b>	Co-immunoprecipitation of endogenous PDK1 and PLC $\gamma$ 1.....	205
<b>Figure 7.18</b>	Co-immunoprecipitation of PDK1 and PLC $\gamma$ 1 in MDA-MB-435.....	207
<b>Figure 7.19</b>	FRET images of MDA-MB-231 expressing exogenous PLC $\gamma$ 1 and PDK1 .....	209-211
<b>Figure 7.20</b>	Graphs representing donor and acceptor fluorescence .....	212
<b>Figure 7.21</b>	Quantification of FRET in MDA-MB-231.....	213
<b>Figure 7.22</b>	Quantification of FRET by FACS analysis .....	215

**Tables:**

<b>Table 1.1</b>	PLC family members and respective tissue expression .....	33
<b>Table 2.1</b>	Cell lines .....	76
<b>Table 2.2</b>	BSA Standard curve protein concentration .....	80
<b>Table 2.3</b>	List of Antibodies used for WB .....	81
<b>Table 2.4</b>	PLC $\gamma$ 1 targeting sequence cloned in pSUPER.retro vector .....	86
<b>Table 2.5</b>	PDK1 targeting sequence .....	87
<b>Table 2.6</b>	Transfection protocol .....	90
<b>Table 2.7</b>	Typical PCR master mix .....	91
<b>Table 2.8</b>	Typical thermal-cycler program for PCR .....	91
<b>Table 2.9</b>	RNA retrotranscription program .....	92
<b>Table 2.10</b>	Plasmids, primary and secondary antibodies used for FRET experiments by FACS .....	99
<b>Table 5.1</b>	Table 5.1: Percentage of MDA-MB-231, MDA-MB-435, 4T1, TSA treated with InsP <sub>5</sub> 50 $\mu$ M or 2- <i>O</i> -Bn-InsP <sub>5</sub> 50 $\mu$ M .....	150
<b>Table 6.1</b>	ABC inhibitors (concentration used) .....	165
<b>Table 7.1</b>	List of colonies chosen for plasmid purification .....	188
<b>Table 7.2</b>	IP buffers	202

## Abbreviations

ABP	actin binding proteins	MMp	matrix metalloproteinase
ATP	Adenosine triphosphates	mTOR	mammalian target of rapamycin
Bp	Bais pair	n	Number of value
BSA	Bovine Serum Albumin	NaCl	Sodium chloride
CaCl <sub>2</sub>	Calcium Chloride	NP40	Tergitol-type NP-40
CAPS	Ca <sup>2+</sup> -dependent activator protein for secretion	nt	Nucleotide
cDNA	Complementary DNA	Oligo(dt)	Oligodeoxythymidylic acid
DAG	Diacylglycerol	PAGE	Polyacrylamide gel electrophoresis
DAPI	4',6-diamidino-2-phenylindole	PBS	Phosphate buffer solution
ddH <sub>2</sub> O	Double-distilled water	PCR	Polymerase chain reaction
DMEM	Dulbecco's modified Eagle's medium	PDGF	platelet-derived growth factor
DMSO	Dimethyl sulfoxide (DMSO)	PDK1	3-Phosphoinositide-Dependent-Protein-Kinase-1
DNA	Deoxyribonucleic Acid	PH	Pleckstrin homology
dNTP	Deoxynucleotide triphosphate	PI3K	phosphoinositide 3-kinase
ECM	Extracellular Matrix Components	PIP <sub>3</sub>	Phosphatidylinositol-3,4,5-trisphosphate
EDTA	Ethylenediaminetetraacetic acid	PIP5K	PtdIns4P 5-kinases
EGF	Epidermal growth factor	PKA	cAMP-dependent protein kinase 1
EGFR	Epidermal growth factor receptor	PKC	protein kinase C
EHS	Engelbreth-Holm-Swarm	PKG	cGMP-dependent protein kinase
ER	oestrogen receptor	PLC	Phospholipase C
ERK	Extracellular-signal-related-kinase	PtdIns(4,5)P <sub>2</sub>	Phosphatidylinositol-4,5-bisphosphate
ErbB(s)	Epidermal growth factor family	PTEN	phosphatase tensin homology protein
FAK	focal adhesion kinase	PTHRP	parathyroid hormone related protein
FBS	Foetal Bovine Serum	RNA	Ribonucleic acid
FGF-2	Basic fibroblast growth factor	RPM	Revolutions per minutes
FRET	Forster Resonance Energy Transfer	RT	Room temperature
g	Relative centrifuge force	SDS	Sodium-dodecyl-sulphate
GAPDH	Glyceraldehyde-3-phosphates dehydrogenase	SEM	Standard error of the mean
GEF	guanine nucleotide exchange	SH	Src homology domain
GFP	Green fluorescent protein	shRNA	Short hairpin RNA
GPCR	G-protein-coupled-receptor	siRNA	Small interfering RNA
GPI	glycosylphosphatidylinositol	TEA	Tris-acetic acid-EDTA
GTP	Guanosine-5'-triphosphate	Thr	Threonine
Guanosine diphosphate	<b>Guanosine diphosphate</b>	TIM	triose-phosphate-isomerase
HUVEC	humbilical vein endothelial cells	TKR	tyrosine kinase receptor
IgG	Immunoglobulin G	TRPC3	transient Receptor Potential C3
InsP <sub>3</sub>	Inositol-(1,4,5)	Tyr	Tyrosine
InsP <sub>5</sub>	Inositol-(1,3,4,5,6)-pentakisphosphates	WB	Western blot
IP <sub>3</sub>	Inositol-(1,4,5)-trisphosphates		

# Publications, presentations and awards arising from this thesis

## Publications

**A PDK1-dependent regulation of PLC $\gamma$ 1 activation is essential for cancer cell migration and invasion.**

Raimondi C, Maffucci T, Falasca M. (Submitted)

**Class II phosphoinositide 3-kinase regulates exocytosis of insulin granules in pancreatic beta cells.**

Dominguez V, Raimondi C, Somanath S, Bugliani M, Loder MK, Edling CE, Divecha N, da Silva-Xavier G, Marselli L, Persaud SJ, Turner MD, Rutter GA, Marchetti P, Falasca M, Maffucci T.

*J Biol Chem.* 2011 Feb 11;286(6):4216-25. Epub 2010 Dec 2.

**A phosphoinositide 3-kinase/phospholipase  $\gamma$ 1 pathway regulates fibroblast growth factor-induced capillary tube formation.**

Maffucci T, Raimondi C, Abu-Hayyeh S, Dominguez V, Sala G, Zachary I, Falasca M. *PLoS One.* 2009 Dec 14;4(12):e8285

**Phospholipase  $\gamma$ 1 is required for metastasis development and progression.**

Sala G, Dituri F, Raimondi C, Previdi S, Maffucci T, Mazzeo M, Rossi C, Iezzi M, Lattanzio R, Piantelli M, Iacobelli S, Brogginini M, Falasca M. *Cancer Res.* 2008 Dec 15;68(24):10187-96.

### Boyden Chamber (Book chapter)

Falasca M, Raimondi C, Maffucci T.

Developmental Methods and Protocols Series: **Methods in Molecular Biology**, Vol. 769 Wells, Claire M.; Parsons, Maddy (Eds.) 2nd ed., 2011. A Humana Press product Hardcover, ISBN 978-1-61779-206-9

Due: July 29, 2011

### Targeting PDK1 in cancer (Review)

Claudio Raimondi and Marco Falasca

Current Medicinal Chemistry (in press)

## Awards

**2010 – Wellcome Trust Value in People Award 2010/11** supporting the project “Targeting PDK1 in breast cancer metastases” for 6 months.

**2010 – Best emerging investigator poster presenter award** – Breast Cancer Campaign Scientific Conference 2010 at the *Royal Society* (London)

**2009 – Best poster award** – Away-day-meeting for Diabetes and Metabolic Department, Queen Mary’s University

**2008 – Best poster award** – William Harvey Day, Queen Mary’s University

# **Chapter 1**

## **Introduction**

## Chapter 1:

### Introduction

#### 1.1 Phosphoinositides

Phosphoinositides are phospholipids within cell membranes. The general structure of the phosphoinositides comprises two fatty acid chains linked a glycerol moiety and to a water soluble inositol head-group, which can undergo differential phosphorylation (Figure 1.1).

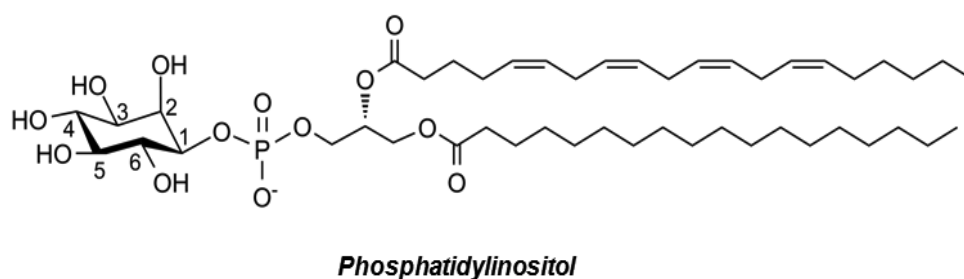


**Figure 1.1:** Structure of phosphatidylinositol, the compound for the synthesis of the whole family of phosphoinositides

The inositol group may be phosphorylated in different positions generating all the different components of the phosphoinositide family (Figure 1.2). Some phosphoinositides, such as the PtdIns(3,4,5)P<sub>3</sub>, play a role as second messenger. Several protein domains are able to bind the different phosphoinositides such as PH, FYVE, PX, PHD, FERM, GRAM, ENTH and ANTH domains. Nowadays it is well understood the role of phosphoinositides as second messengers and their role in cell signalling in healthy and pathological conditions.

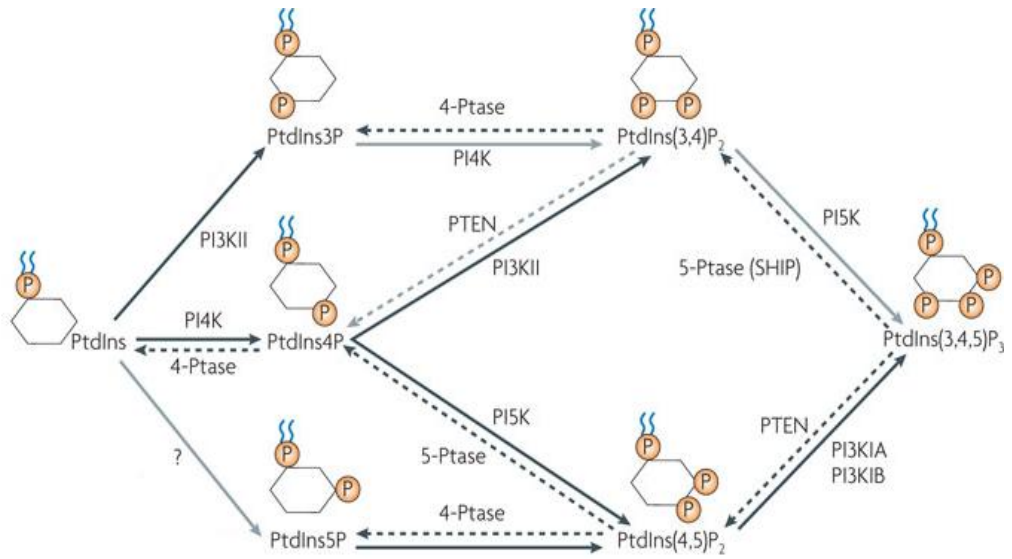


**Figure 1.2:** Schematic representation of phosphoinositides, kinases and phosphatases enzymes involved in their synthesis (adapted from Bunney and Katan, 2010).

Phosphoinositides metabolism is strictly controlled in cells since activation of signalling molecules has to be well defined both temporally and spatially. Some phosphoinositides, such as PtdIns(3,4)P<sub>2</sub> and PtdIns(3,4,5)P<sub>3</sub> are absent in resting cells and are synthesised only upon cellular stimulation. This process involves protein kinases and protein phosphatases, the last in general involved in switching off the signalling. Phosphoinositides are involved in many cellular processes, and dysfunction of their metabolism is observed in several diseases such as cancer and diabetes (Wymann and Schneiter, 2008).

### 1.1.1 Phosphatidylinositol-4,5-bisphosphate, PtdIns(4,5)P<sub>2</sub>

Phosphatidylinositol-4,5-bisphosphate [PtdIns(4,5)P<sub>2</sub>] represents 0.5% of total membrane lipids (Stephens et al., 2000). The major synthetic route of PtdIns(4,5)P<sub>2</sub> is the phosphorylation of PtdIns4P at the 5-position by PtdIns4P 5-kinases (PIP5K) (van den Bout and Divecha, 2009). Three different classes of PIP5K have been identified: PIP5K $\alpha$ , PIP5K $\beta$  and

PIP5K $\gamma$ . A minor synthetic route is represented by the synthesis through the action of PtdIns5P 4-kinases that phosphorylate PtdIns5P in position 4 (Rameh et al., 1997; Clarke et al., 2010). PtdIns(4,5)P<sub>2</sub> has been extensively studied since different second messengers are generated from this phosphoinositide. Indeed PtdIns(4,5)P<sub>2</sub> is the main substrate of the PI3K family which produces the second messenger PtdIns(3,4,5)P<sub>3</sub>. PtdIns(4,5)P<sub>2</sub> is also the substrate of Phospholipase C family members (PLCs). PLCs cleave the polar head group of PtdIns(4,5)P<sub>2</sub> generating diacylglycerol (DAG) and Inositol-(1,4,5)-trisphosphate (InsP<sub>3</sub>), which are second messengers that activate PKC and stimulate calcium release from internal stores (Irvine et al., 1984; Berridge and Irvine, 1989). PtdIns(4,5)P<sub>2</sub> has many functions within cell signalling. Some of its functions, closely related to this thesis, are described in the following chapter.

#### **1.1.1.1 PtdIns(4,5)P<sub>2</sub> and cytoskeleton remodelling**

PtdIns(4,5)P<sub>2</sub> plays an essential role in the regulation of cytoskeleton remodelling by binding to proteins such as cofilin, profilin, gelsolin. This interaction binds these proteins to the plasma membrane in a mechanism that prevents their activation. Hydrolysis of PtdIns(4,5)P<sub>2</sub> by phospholipase C (PLC) enzymes (Van Rheenen et al., 2007) releases these proteins from the plasma membrane in a well-defined spatial and temporal manner, stimulating actin polymerization. The actin binding proteins (ABP) cofilin interacts with monomeric and filamentous actin promoting actin filament disassembly and severing actin filaments. The actin filament severing activity contributes to create new barbed ends promoting new polymerization-competent filaments (Adrianantoandro and Pollard, 2006; Pavlov et al., 2007). Similarly, PtdIns(4,5)P<sub>2</sub> is involved in regulation of profilin and gelsolin, which play a central role in cytoskeleton remodelling and actin dynamics. The interaction between PtdIns(4,5)P<sub>2</sub> and profilin inhibits the activity of profilin as actin-monomer sequestering, stimulating actin polymerisation and cytoskeleton remodelling (Saarikangas et al., 2010). In particular profilin stimulates the incorporation of globular actin

in the actin filaments promoting their elongation. In parallel the ARP2/3 complex (Actin Related Proteins) associates to the side of a “Mother” filament creating a new nucleation site which initiates a branching filament (Nurnberg and Grosse, 2011). Equally, PtdIns(4,5)P<sub>2</sub> inhibits gelsolin actin filament severing activity by recruiting this protein to the plasma membrane (Saarikangas et al., 2010).

#### **1.1.1.2 PtdIns(4,5)P<sub>2</sub> and membrane trafficking**

PtdIns(4,5)P<sub>2</sub> is also directly involved in exocytosis (Martin et al., 1998), acting on plasma membrane proteins such as Ca<sup>2+</sup>-dependent activator protein for secretion (CAPS) and on vesicle proteins such as synaptotagmin (Di Paolo and De Camilli, 2006). Furthermore, PtdIns(4,5)P<sub>2</sub> appears to be required in the ATP-dependent priming process of neurosecretory vesicles. During the exocytosis PtdIns(4,5)P<sub>2</sub> is locally and transiently depleted by a PLC-dependent hydrolysis and is not detected on the membrane of the fusing granules (Hammond et al., 2006; Hammond and Schiavo, 2006).

Exocytosis is often coupled to compensatory endocytosis, which is dependent on PtdIns(4,5)P<sub>2</sub>. Compensatory endocytosis can occur through a clathrin-mediated mechanism or through alternative mechanisms which do not involve complete vesicle fusion or clathrin-mediated vesicle recycling (Gundelfinger et al, 2003). PtdIns(4,5)P<sub>2</sub> interacts with some endocytic clathrin adaptors such as AP-2, P180/CALM and epsin and binds to many other endocytic factors such as dynamin, which controls the fission reactions. Other actions of PtdIns(4,5)P<sub>2</sub> in endocytosis reflect its effects on the actin cytoskeleton, which is implicated in all internalization pathways (Di Paolo and De Camilli, 2006).

### **1.1.2 Phosphatidylinositol-3,4,5-trisphosphate, PtdIns(3,4,5)P<sub>3</sub>**

Phosphatidylinositol-3,4,5-trisphosphate, PtdIns(3,4,5)P<sub>3</sub>, is a well characterised second messenger. Indeed PtdIns(3,4,5)P<sub>3</sub> is barely detectable in resting normal cells but its amount increases transiently in stimulated cells. PtdIns(3,4,5)P<sub>3</sub> levels increase upon activation of some members of the family of enzymes phosphoinositide 3-kinase (PI3K), which phosphorylates PtdIns(4,5)P<sub>2</sub> on position 3. PI3K is a family of enzymes, comprising eight mammalian isoforms grouped into three classes and PtdIns(3,4,5)P<sub>3</sub> is the main *in vivo* product of class I isoforms. Class I A consists of a catalytic subunit and a regulatory subunit. The catalytic subunits consist of p110 $\alpha$ , p110 $\beta$ , or p110 $\delta$ , and are the product of three genes *PIK3CA*, *PIK3CB* and *PIK3CD*. The regulatory subunits consist of p85 $\alpha$ , p85 $\beta$  or p55 $\gamma$ . Class I B consists of only one catalytic subunit, p110 $\gamma$ , and two regulatory units, p84 and p101. *PIK3CA* is frequently mutated in cancers, and around eighty percent of these mutations occur in the helical or kinase domain of the enzyme leading to gain of function p110 $\alpha$  activity (Courtney et al., 2010; Wong et al., 2010). The levels of PtdIns(3,4,5)P<sub>3</sub> are negatively regulated by the phosphatase tensin homology protein (PTEN), which dephosphorylates PtdIns(3,4,5)P<sub>3</sub> in position 3 and therefore switches off the PI3K-activated pathway. PTEN is the second most frequently mutated gene in human cancer following *TP53* (Yuan and Cantley, 2008; Kok et al., 2009; Carracedo and Pandolfi, 2008). The lipid phosphatase activity is critical for PTEN tumour suppressor function. Therefore loss of PTEN activity leads to uncontrolled activation of the PI3K pathway, and the subsequent accumulation of PtdIns(3,4,5)P<sub>3</sub> leads to cell transformation.

#### **1.1.2.1 PtdIns(3,4,5)P<sub>3</sub>-dependent AKT and PLC $\gamma$ 1 activation**

Accumulation of PtdIns(3,4,5)P<sub>3</sub> has been observed in many cancers. For this reason the PtdIns(3,4,5)P<sub>3</sub>-dependent pathway has been intensively studied. The main effector activated downstream of PtdIns(3,4,5)P<sub>3</sub> is the protein kinase PKB/AKT, which controls different cellular functions.

AKT possesses a pleckstrin homology (PH) domain which specifically binds PtdIns(3,4,5)P<sub>3</sub> and PtdIns(3,4)P<sub>2</sub>, both produced by PI3K. The PH domain- PtdIns(3,4,5)P<sub>3</sub> interaction recruits AKT to the plasma membrane and this interaction causes a conformational change leading to its activation (Alessi et al., 1997; Sarbassov et al., 2005; Bellacosa et al., 2005; Calleja et al., 2007). At the plasma membrane, 3-phosphoinositide-dependent-protein-kinase-1 (PDK1) and mammalian target of rapamycin (mTOR), in particular the mTOR complex 2 (mTORC2), phosphorylates AKT at its residues in Thr308 and Ser473 respectively. The phosphorylation of AKT by PDK1 is PtdIns(3,4,5)P<sub>3</sub>-dependent (Alessi et al., 1997). In particular PDK1 possesses a PH domain which binds PtdIns(3,4,5)P<sub>3</sub>. This interaction allows AKT and PDK1 to co-localise at the plasma membrane and it is required for optimal phosphorylation of AKT (Waugh et al., 2009). Mice expressing a PDK1 mutated form unable to bind phosphoinositides present a strongly reduced AKT activation, insulin resistance and hyperinsulinaemia (Bayascas et al., 2008). Once phosphorylated, AKT activates different downstream effectors. AKT is involved directly and indirectly in many cellular processes, such as cell proliferation, growth and cell motility. For example the AKT-induced FOXO phosphorylation leads to the inhibition of the transcription of p21KIP and retinoblastoma-like-2, both inhibitors of cell cycle progression, and therefore it promotes progression through the cell cycle (Manning et al., 2007; Zhang et al., 2011). Furthermore activated AKT phosphorylates the pro-apoptotic Bcl-2 family member BAD, which is inactive in the phosphorylated form, and MDM2 that induces p53 degradation (Wymann 2008; Duronio 2008). PtdIns(3,4,5)P<sub>3</sub>-mediated AKT activation leads to stimulation of cell growth through mTOR activation, which is one of the major effectors in tumourigenesis. Also PtdIns(3,4,5)P<sub>3</sub> contributes to cell migration and cytokinesis. Indeed, another downstream effector of PtdIns(3,4,5)P<sub>3</sub> is Phospholipase C gamma 1 (PLC $\gamma$ 1) that translocates to the plasma membrane after cellular stimulation with growth factors such as EGF or PDGF in a PtdIns(3,4,5)P<sub>3</sub> dependent manner (Falasca et al., 1998). PLC $\gamma$ 1 plasma membrane

translocation is triggered by the PH domain which specifically binds the PtdIns(3,4,5)P<sub>3</sub> and is essential for its activation.

## **1.2 Phospholipase C (PLC)**

Historically, phospholipase C (PLC) was identified as an important enzyme involved in phosphoinositide metabolism (Hokins 1953, Michell 1975). It was only in the 80's that the link between the water soluble PLC product Ins(1,4,5)P<sub>3</sub> and the release of calcium from intracellular stores was identified (Streb et al., 1983; Irvine et al., 1986). Several different PLC isoforms are currently known (see chapter 1.2.5), sharing common regions/domains, called X and Y flanked by EF motifs, which form the conserved catalytic domain. However different protein modules, such as PH domains or other protein binding modules are specific to each distinct isoform and are responsible for the different mechanisms of enzymatic activation and regulation. The following chapters will focus on the functions of domains common to all PLC isoenzymes.

### **1.2.1 Catalytic domain**

The PLC isoenzymes catalyze the hydrolysis of the phosphodiesteric bond between the phosphoinositol headgroup and diacylglycerol (Figure 3A) (Bunney and Katan, 2010). The catalytic domain possesses alternating  $\alpha$ -helixes and  $\beta$ -sheets and resembles an incomplete triose-phosphate-isomerase (TIM)  $\alpha/\beta$  barrel (Figure 1.3B). The enzymatic reaction is catalysed by specific aminoacids in the catalytic domain which are conserved among the different family members (Hondal et al., 1998). In particular, production of a cyclic-1,2-inositol,4,5-bisphosphate intermediate is catalysed by histidine 392, which binds to the proton of the 2-Hydroxyl of the inositol headgroup residues that acts as general base creating a cyclic intermediate (Essen et al., 1997). This intermediate is quickly hydrolysed in Ins(1,4,5)P<sub>3</sub>, while His-311 protonates the DAG leaving group (Figure 1.3A). The catalytic domain has been shown to be

able to bind calcium ions. Calcium binding has been reported to be essential for catalytic activity since single mutation of the calcium binding Glu-341 within the TIM barrel inhibits calcium binding to the catalytic domain impairing enzymatic activity (Cheng et al.1995).

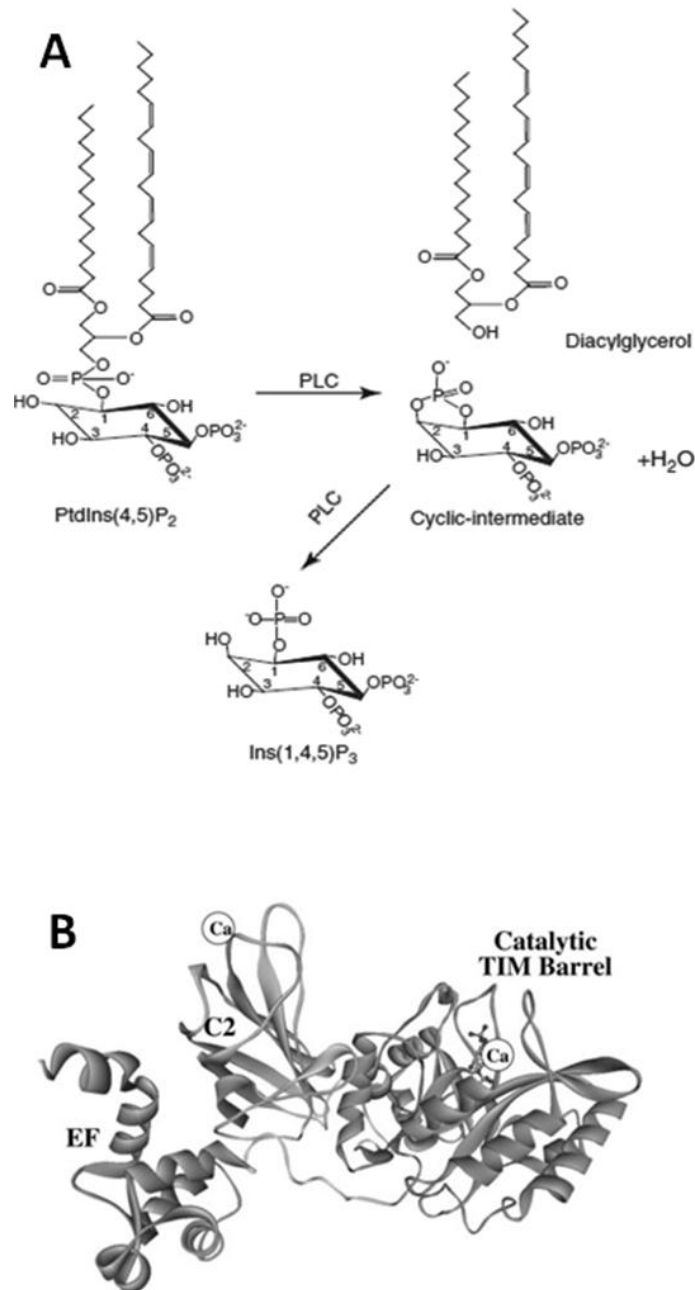


**Figure 1.3:** **A)** Enzymatic reaction catalysed by PLC isoenzymes (adapted from Bunney and Katan, 2010); **B)** Crystal structure of PLCδ1 (PH domain excluded) (Rebecchi et al, 2000)

### 1.2.2 EF Motifs

The N-terminal domain consists of an EF motif, a Helix loop Helix domain found in all the PLCs and common to calcium binding proteins. PLC isoforms can have up to four EF domains organised in paired units ( $N_{\text{term}}\text{-EF}_1\text{-EF}_2\text{-EF}_3\text{-EF}_4\text{-C}_{\text{term}}$ ) (Figure 1.4). The role of PLC EF domains in calcium binding is controversial. Indeed the EF<sub>3</sub> and EF<sub>4</sub> motifs do not show metal binding during structural analysis. EF<sub>1</sub> and EF<sub>2</sub> contain calcium ligands (Essen et al.,1996). However there is no evidence showing that EF motifs in PLC isoforms bind to calcium ions. Deletion of EF<sub>3</sub> and EF<sub>4</sub> in PLC $\delta$ 1 completely blocks PLC enzymatic activity, indicating that this protein domain is essential for the correct function of the catalytic activity together with the TIM barrel domain (Nakashima et al., 1995).

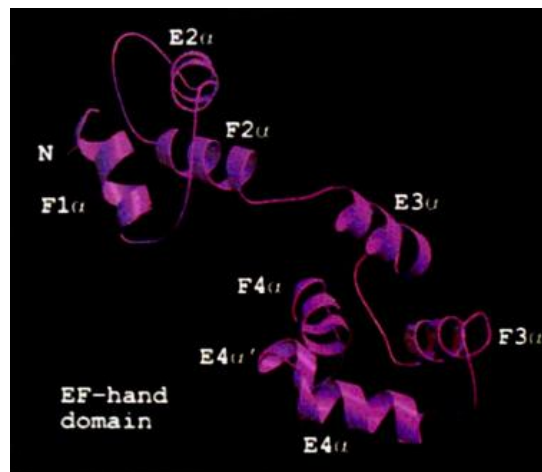


**Figure 1.4:** Structure of EF motifs of PLC $\delta$ 1 isoform (Essen et al., 1996)

### 1.2.3 C2 domain

The C2 domain is a protein module of ~120 aminoacids present in different enzymes such as PKCs cPLA<sub>2</sub> and PLCs. C2 domains possess 8 antiparallel  $\beta$ -sheets, which define three loops essential for calcium

binding (Figure 1.5). It has been proposed that C2 domain of PLCs can interact with phospholipids facilitating the tethering to the plasma membrane of the enzymes. Two possible mechanisms have been proposed: the bridging mechanism that involves calcium ions being sandwiched between the C2 domain and the phospholipid (Swairjo et al 1995). Alternatively, it has been proposed that calcium binding does not cause conformational changes but it is essential for electrostatic potential change essential for a calcium-mediated binding of the target molecule (Newton et al.,1995). Therefore the C2 domain, together with the PH domain when present, could represent a second site for the binding of phosphoinositides important for the correct orientation of the catalytic domain (Bunney and Katan, 2010).

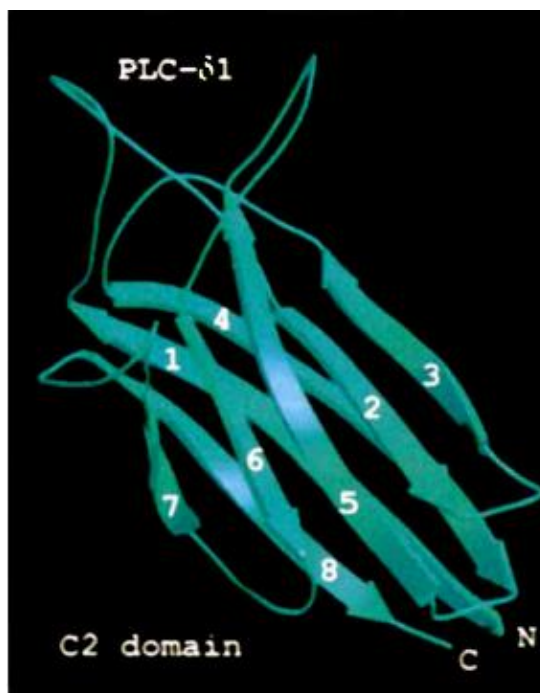


**Figure 1.5:** Structure of the C2 domain of PLC $\delta$ 1 (Essen et al., 1996)

#### 1.2.4 PH domains

The PH domain was first identified in the protein pleckstrin, the main substrate of PKC. Currently several proteins have been discovered containing the PH domain (Musacchio et al., 1993; Lemmon et al., 1996); among them PLC $\delta$ 1, PLC $\gamma$ 1, PDK1 and AKT. The PH domain is a protein module consisting of ~120 amino acids with no catalytic activity. The sequence identities among the different PH domains are not sufficient to support structural homology. However it has been found that the secondary and tertiary structures are conserved among the different PH domains (Lemmon et al., 1995). Each domain consists of two nearly orthogonal antiparallel  $\beta$ -sheets of four and three strands and an amphipathic  $\alpha$ -helix localised at the C-terminal portion of the domain (Figure 1.6). Each PH domain presents a well-defined charge polarisation. In particular the  $\beta$ 1/  $\beta$ 2,  $\beta$ 3/ $\beta$ 4 and  $\beta$ 6/ $\beta$ 7 loops represent the most variable region in length and sequence. These regions define the positively charged portion needed for ligand interaction and recognition and define the binding pocket which presents the sequence motif  $KX_n(K/R)XR$  (Ferguson et al.,1995) . The lysine (K) and arginine (R) represent the positive charged core responsible for the interaction with the phosphate groups. The side chains are responsible for further interactions which defines the identity of the ligand and the binding affinity (Lemmon and Ferguson, 2000).

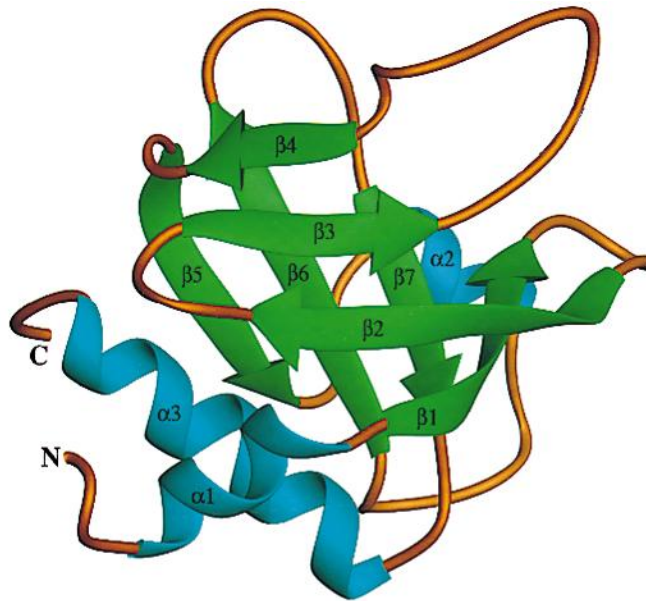


**Figure 1.6:** PLC $\delta$ 1 PH domain structures (adapted from Lemmon et al., 1996)

It has been noted that the majority of proteins hosting PH domains require membrane association to carry out their functions. The original idea was that PH domains were involved in protein-protein interactions, in similar manner to SH2 and SH3 domains (Gibson et al., 1994). Initial evidence suggested the  $\beta\gamma$  subunits of the heterotrimeric G protein as a potential PH domains target (Touhara et al., 1994; Tsukada et al., 1994). However *in vitro* experiments using lipid vesicles identified the phosphoinositides as the main target of PH domain (Harlan et al.1994). Since the original identification, other PH domains were shown to bind with high affinity and stereospecificity for specific phosphoinositides headgroups (Kavran et al., 1998). The PLC $\delta$  PH domain was identified to specifically interact with PtdIns(4,5)P<sub>2</sub>, leading to a plasma membrane recruitment of the enzyme and increasing its processivity (Garcia et al., 1995; Lemmon et al., 1995). However few PH domains, such us PLC $\delta$ 1 PH domain, bind to phosphoinositides with high specificity. Most PH domains, such as PLC $\gamma$ 1 PH domain can bind several phosphoinositides with different affinity and low specificity. The phosphoinositides/PH domain interaction has been demonstrated to be required for protein translocation to the plasma

membrane. A 'tandem model' has been proposed as potential mechanism that stabilises a weak interaction of PH domain through a co-operation with other domains of the host protein (Maffucci and Falasca, 2001). The PLC $\gamma$ 1 PH domain was demonstrated to be essential for PLC $\gamma$ 1 plasma membrane recruitment and subsequent enzyme activation (Falasca et al., 1998), together with PLC $\gamma$ 1 interaction with the phosphorylated EGF receptor.

The PH domains bind to the phosphoinositide head groups but also to the soluble isolated head groups of phosphoinositides. The PH domain of PLC $\delta$ 1, for example, binds to the soluble head group of PtdIns(4,5)P<sub>2</sub>, D-*myo*-Ins(1,4,5)P<sub>3</sub>. Similarly Grp-1 PH domain binds with high affinity to D-*myo*-Ins(1,3,4,5)P<sub>4</sub>, the soluble PtdIns(3,4,5)P<sub>3</sub> head group. Interestingly, the isolated head group may show a higher affinity for the PH domain binding compared to the head group membrane-embedded. This is the case of Ins(1,4,5)P<sub>3</sub>, which is able to bind to PLC $\delta$ 1 PH domain with an higher affinity ( $K_D=0.21 \mu\text{M}$ ) compared to PtdIns(4,5)P<sub>3</sub> ( $K_D=1.66 \mu\text{M}$ ), leading to the displacement of PLC $\delta$ 1 when Ins(1,4,5)P<sub>3</sub> is generated, in an auto-inhibitory mechanism (Lemmon et al., 1995; Kavran et al., 1998, Lemmon, 2008). The properties of PH domains to bind to the soluble phosphoinositide head groups opened the field for a novel strategy, aiming to antagonise the activation of PH domain containing proteins by inhibiting their translocation to the plasma membrane. Indeed since different PH domains present different affinities for different inositol phosphates, it may be possible to specifically block a particular membrane-targeted protein using inositol phosphate derivative compounds.

### **1.2.5 PLC Isoenzymes**

Several PLCs are known, diverging for aminoacid sequence, structure, regulation and tissue localisation. In particular the PLC isoenzyme family

is composed of the following members, which are present in the tissues listed in Table 1.1.

Member	Isoforms	Tissue expression (Suh et al., 2008)
PLC $\beta$	PLC $\beta$ 1, PLC $\beta$ 2, PLC $\beta$ 3, PLC $\beta$ 4	PLC $\beta$ 1: Brain, intestine, prostate, ovary PLC $\beta$ 2: Mainly hematopoietic tissue; present in ovary and brain PLC $\beta$ 3: Brain, liver, parotid gland, skin, ovary PLC $\beta$ 4: Mainly brain
PLC $\gamma$	PLC $\gamma$ 1, PLC $\gamma$ 2	PLC $\gamma$ 1: ubiquitous PLC $\gamma$ 2: Hematopoietic tissue
PLC $\delta$	PLC $\delta$ 1 PLC $\delta$ 3 PLC $\delta$ 4	PLC $\delta$ 1: Brain, lungs, muscles, testis PLC $\delta$ 3: Brain, heart, muscles, testis, kidney PLC $\delta$ 4: Ubiquitous with high levels of expression in brain, muscles and kidney
PLC $\epsilon$	PLC $\epsilon$ 1a, PLC $\epsilon$ 1b	High expression in heart; present in brain, lungs, colon
PLC $\zeta$	PLC $\zeta$	Sperm-specific
PLC $\eta$	PLC $\eta$ 1, PLC $\eta$ 2	High level in brain and kidney; low level in lungs, intestine and pancreas

**Table 1.1:** PLC family members and respective tissue expression

Beside the tissue localisation, the most important difference among the PLC isoenzymes is the modality of their activation and their structure.

Schematic structures of the different PLC isoenzymes are illustrated in Figure 1.7.

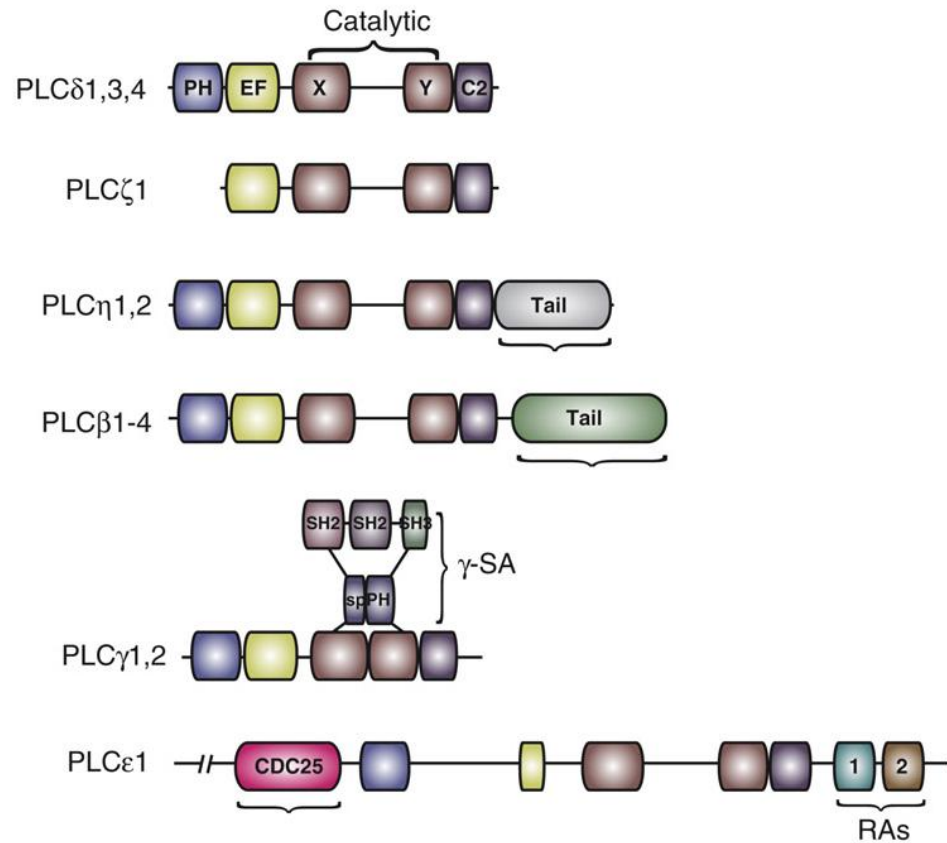


**Figure 1.7:** Schematic representation of PLC isoenzymes structures showing the differences in protein domains present in the family members (adapted from Bunney and Katan., 2010)

Different extracellular stimuli activate distinct PLC isoenzymes through different molecular mechanisms. However some stimuli can activate different PLC isoenzymes simultaneously, which complicate the understanding of the role of each single isoform. In this chapter the main mechanism of activation of all PLCs, except PLC $\gamma$ , are described. PLC $\gamma$  will be discussed in the following chapter 1.3.

## PLC $\beta$

The PLC $\beta$ s are activated by the rhodopsin superfamily membrane receptors which respond to a plethora of stimuli. These receptors belong to the class of G-protein-coupled-receptor (GPCR) and activate G-proteins to activate signal transduction. Among the different PLCs, PLC $\beta$ , but not PLC $\delta$  or PLC $\gamma$ , are activated by G-proteins (Rebecchi and Pentylala, 2000). The G-proteins form a heterotrimeric complex in the inactive GDP-binding state formed by G $_{\alpha}$ , G $_{\beta}$  and G $_{\gamma}$  subunits. Upon stimulation of the receptor, the G $_{\alpha}$  subunit is activated through exchanging GDP with GTP. This event causes the dissociation of G $_{\alpha}$  from G $_{\beta\gamma}$ . The GTP-bound G $_{\alpha}$  subunit, together with the G $_{\beta\gamma}$  heterodimer, activate PLC $\beta$  isoenzymes. It has to be pointed out that within the PLC $\beta$  isoenzymes, each enzyme shows different responsiveness to the different subunits, indicating a subtle regulation of their differential activation (Rebecchi et al., 2000). PLC $\beta$ 1 is the least sensitive to G $_{\beta\gamma}$  activation and PLC $\beta$ 4 is completely insensitive to G $_{\beta\gamma}$  (Figure 1.8). Recent works demonstrate that PLC $\beta$  can also be activated by the Rho-GTPase family member Rac, which is able to interact with the PH domain (Snyder et al., 2003).

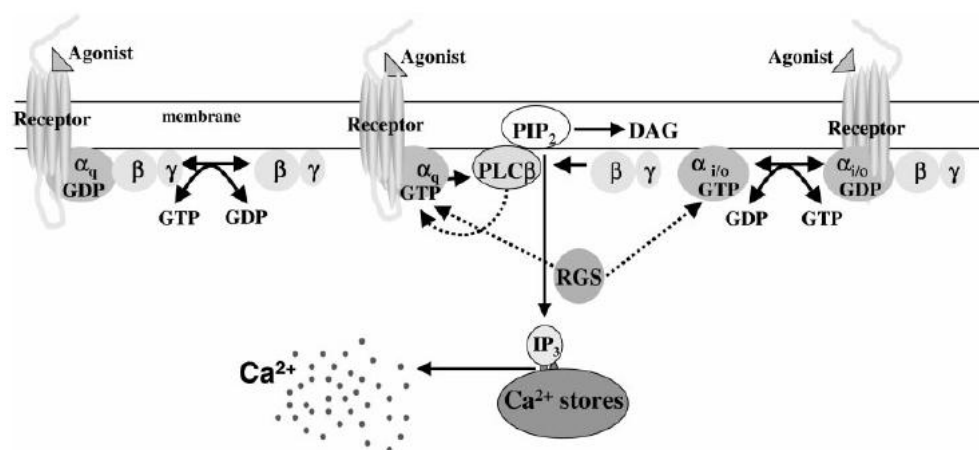


**Figure 1.8:** Regulation of PLC $\beta$  by GPCR (Rebecchi et al., 2000)

### *PLC $\delta$*

A different mechanism controls the activation of PLC $\delta$  isoenzymes. PLC $\delta$ s are the most sensitive to intracellular calcium variation compared to other PLC isoenzymes. PLC $\delta$ 1, the most studied of its family, can be activated by calcium and in turn it can amplify the calcium signal. PLC $\delta$ 1 can also be activated by  $\alpha_1$ -adrenergic receptors through atypical G-protein (G<sub>h</sub>) and by G<sub>i</sub> coupled receptor agonists (Murthy et al., 2004) and RhoGAP which stimulates PLC $\delta$ 1 activity up to 10-fold (Rebecchi et al., 2000).

### *PLC $\epsilon$*

In 2001 a novel group of PLC was identified. PLC $\epsilon$  isoenzymes are the newest and most complex PLC isoenzymes since they present the highest number of different protein domains, which regulate their activation (Kelley, et al 2001). PLC $\epsilon$  is activated by Ras family members. In particular PLC $\epsilon$  possesses two RA domains that associate with Ras and Rap1 and are essential for PLC $\epsilon$  activation (Figure 1.9) (Song et al., 2002). Notably, Ras-mediated PLC $\epsilon$  activation induces translocation of the enzyme to the plasma membrane, while Rap1-induced activation recruits the enzyme to the perinuclear region (Song et al., 2002). Furthermore the PLC $\epsilon$  family presents a CDC25 homology domain. The CDC25 homology domain was first identified in the CDC25 protein isolated from *S. cerevisiae*, and possesses guanine nucleotide exchange (GEF) factor properties for RAS proteins. The CDC25 domain of PLC $\epsilon$  has GEF activity towards RAP1, but not towards any other Ras members, therefore it is able to stimulate Rap1 GTP binding and activation which in turn activates PLC $\epsilon$  activity and perinuclear translocation of the enzyme (Jin et al., 2001). In addition to Ras family members, PLC $\epsilon$  are activated by a plethora of stimuli. Ligands able to bind GPCRs, such as lysophosphatidic acid or sphingosine-1-phosphate, can activate

PLC $\epsilon$  isoenzymes together with PLC $\beta$  isoenzymes. Growth factors such as EGF, activate PLC $\epsilon$  as well as the PLC $\gamma$  isoforms (Citro et al., 2007).

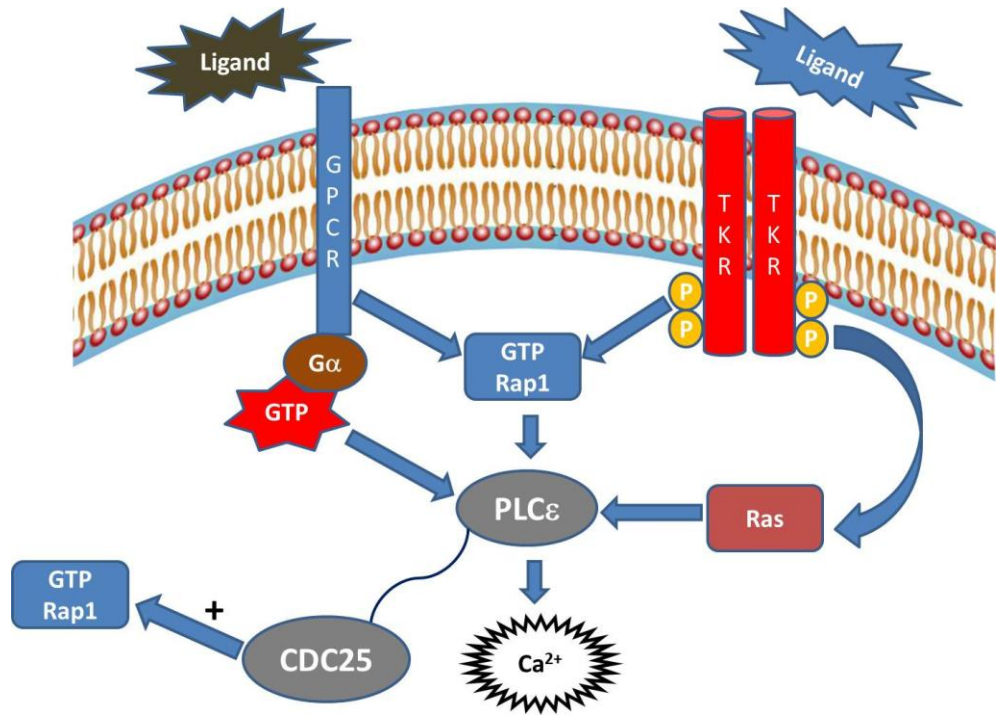


**Figure 1.9:** Schematic mechanism of activation of PLC $\epsilon$  showing the activation of the enzyme by GPCR through G $\alpha$  subunit and RAP1 and by RTKs which are able to activate PLC $\epsilon$  through activation of RAS and RAP1. The CDC25 homology domain of PLC $\epsilon$ , illustrated in the figure, acts as a GEF for RAP1, increasing its activation, which in turn contributes to a sustained activation of PLC $\epsilon$ .

### PLC $\zeta$

PLC $\zeta$  is a sperm-specific PLC isoform. Recombinant protein injected in egg cells causes calcium oscillation. PLC $\zeta$  isoenzyme is the shortest of the family and lacks the PH domain. The lack of PH domain, important for phosphoinositide binding, raised the question of how the enzyme is able to maintain processive substrate hydrolysis. It has been shown that the C2 domain is sufficient for membrane tethering of the enzyme and its deletion inhibits calcium oscillations upon PLC $\zeta$  activation (Suh et al., 2008).

## *PLC $\eta$*

PLC $\eta$  activation is still not completely understood. The plasma membrane localisation of the enzyme is independent from extracellular stimuli and is dependent on the PH domain. Indeed deletion of PH domain induces cytosolic localisation of the enzyme. Recent data showed that PLC $\eta$ 1 is involved in the signal amplification downstream of GPCR and is activated by intracellular calcium. Indeed LPA-induced calcium release was inhibited in PLC $\eta$ 1 knockdown cell lines (Kim et al., 2011).

### 1.3 PLC $\gamma$

The PLC $\gamma$  subgroup includes two members: PLC $\gamma$ 1 and PLC $\gamma$ 2. PLC $\gamma$ 1 is ubiquitous, while PLC $\gamma$ 2 is mainly expressed in the hematopoietic system although it was originally identified in brain tissues (Rebecchi et al., 2000; Suh et al, 2008). The detailed structure of PLC $\gamma$  is illustrated in Figure 1.10.

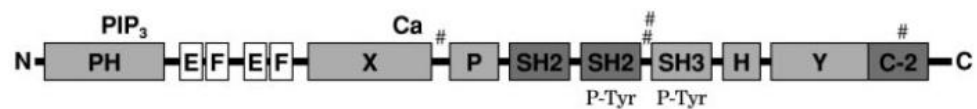


**Figure 1.10:** Representation of PLC $\gamma$  isoenzymes with their different protein domains and the position of known phosphorylation sites (Rebecchi et al., 2000).

PLC $\gamma$  isoenzymes possess some unique protein modules that are essential for enzyme regulation. The X and Y domains, together with the EF domain are common to the other PLC isoforms. As indicated in Figure 1.10 PLC $\gamma$  members also present two SH2 domains, one SH3 domain, a split PH domain and the N-terminal PH domain (Rebecchi et al., 2000). This long region is inserted between the X and Y domains which form the catalytic domain and it has an important role in regulating PLC $\gamma$  catalytic activity (Katan and Williams, 1998). The SH2 domain (Src homology

domain 2) is responsible for protein-protein interaction, recognising specific phosphorylated on tyrosine. Indeed the SH2 domains are essential for interaction with phosphorylated tyrosine residues in activated tyrosine kinase receptors, which dimerise upon ligand engagement and get auto-phosphorylated in tyrosine residues. The SH3 domain recognizes and interacts with proteins expressing polyproline sequences. PLC $\gamma$  family members possess an N-terminal PH domain (see chapter 1.2.4) and a split PH domain. The N-terminal PH domain is essential for PLC $\gamma$ 1 activation and binds PtdIns(3,4,5)P<sub>3</sub> (with a K<sub>D</sub>=1 $\mu$ M) (Falasca et al.,1998). The synthesis of PtdIns(3,4,5)P<sub>3</sub> increases the Ins(1,4,5)P<sub>3</sub> production and the following intracellular calcium release, potentially via enhanced PtdIns(4,5)P<sub>2</sub> substrate availability due to PtdIns(3,4,5)P<sub>3</sub>-mediated recruitment of PLC $\gamma$ 1 to the plasma membrane through the PH domain (Bae et al., 1998; Rameh et al., 1998). The split PH possesses its two halves flanking the SH2-SH2-SH3 domains and its function is still not completely understood. Recent data showed that the split PH domain is required for the direct interaction of PLC $\gamma$ 1 with the transient Receptor Potential C3 (TRPC3) channel and is not involved in phosphoinositides binding (van Rossum et al, 2005) (Wen et al., 2006). However another report showed that the split PH domain of PLC $\gamma$ 1 is involved in phosphoinositides binding, in particular in PtdIns(4)P and PtdIns(4,5)P<sub>2</sub> binding (Kim et al., 2004).

### **1.3.1. Growth factor-induced stimulation of PLC $\gamma$ 1**

PLC $\gamma$  family is composed of two members: PLC $\gamma$ 1 and PLC $\gamma$ 2. Although PLC $\gamma$ 1 is ubiquitarily expressed, PLC $\gamma$ 2 is expressed mainly in the hematopoietic tissue. This introductory chapter will focus on PLC $\gamma$ 1 isoenzyme, which was the focus of my PhD project.

PLC $\gamma$ 1 is activated by different growth factors such as EGF, PDGF and FGF, which activate their respective tyrosine kinase receptors (TKR)

(Nishibe et al., 1990; Mohammadi et al., 1992; Rhee, 2001). Engagement of the ligand to the TKR induces the dimerisation of the receptor and its auto-phosphorylation in tyrosine residues. The phosphorylated receptors recruit PLC $\gamma$ 1 and this allows TKRs to phosphorylate PLC $\gamma$ 1 in specific tyrosine residues. The protein-protein interaction between PLC $\gamma$ 1 and TKRs is promoted by the SH2 domain present in the PLC $\gamma$  family, which recognizes the phosphotyrosine residues on the activated TKRs. Both SH2 domains are involved in the interaction, with a more specific role for the N-terminal SH2 compared to the C-terminal SH2 domain (Chattopadhyay et al., 1999; Poulin et al., 2000). Indeed mutation of the C-terminal SH2 domain, which inhibits the SH2 binding to its target, causes a slight reduction of PLC $\gamma$ 1 phosphorylation and activation. On the contrary, mutation targeting the N-terminal SH2 completely inhibited PLC $\gamma$ 1 phosphorylation and activation. Therefore, the N-terminal-SH2 and the C-terminal-SH2 domains of PLC $\gamma$ 1 play different roles in PLC $\gamma$ 1 regulation (Stoica et al., 1998).

Growth factor stimulation induces PLC $\gamma$ 1 recruitment to the membrane and interaction with TKRs, which in turn phosphorylate PLC $\gamma$ 1 at specific tyrosine residues: Tyr 771, Tyr 783 and Tyr 1253. The phosphorylation is essential for PLC $\gamma$ 1 activation (Kim et al., 1990; Kim et al. 1991; Bunney and Katan, 2010) although plasma membrane recruitment through the PH domain is essential (Falasca et al., 1998). Mutation of Tyr 783 to phenylalanine (Phe) completely inhibits PLC activity upon EGF or PDGF stimulation. On the contrary substitution of Tyr 1253 or Tyr 771 causes limited or no inhibition. These data indicate that phosphorylation at Tyr 771 and Tyr 1253 is dispensable, whereas phosphorylation at Tyr 783 is essential for PLC $\gamma$ 1 activation (Kim et al., 1991; Sekiya et al., 2004). Evidence showed that PLC $\gamma$ 1 is maintained in an auto-inhibitory conformation that keeps the enzyme in an inactive form in the absence of extracellular stimulation. The inhibition is promoted by the X-Y linker, constituted by SH2-SH2-SH3 domain that occludes the access of the substrate to the catalytic domain. In particular it has been demonstrated

that a minimal inhibitory protein module consists of the C-terminal-SH2 and that phosphorylation of Tyr 783 is essential for relieving of the auto-inhibitory interaction (Gresset et al., 2010) (Figure 1.11). A relative stabilising contribution to the auto-inhibitory interaction has been attributed to the split PH domain. Indeed mutation of this domain slight increases the activity of the purified PLC $\gamma$ 1 enzyme *in vitro* (Gresset et al., 2010).

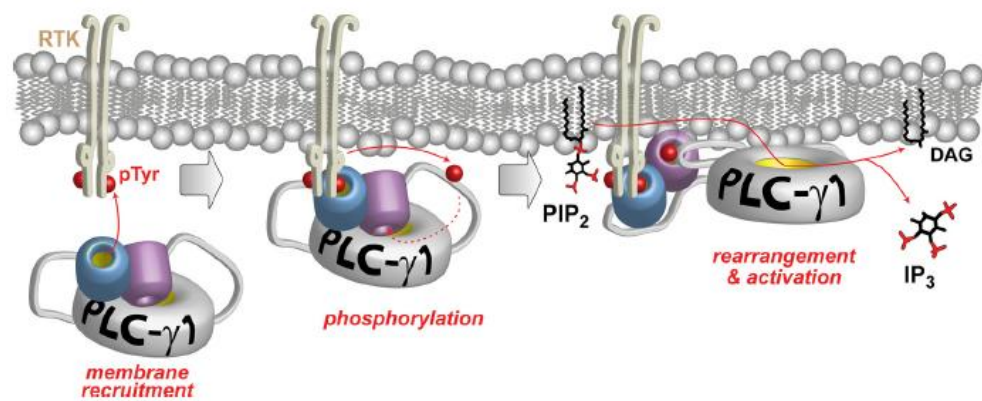


**Figure 1.11:** Relief of the auto-inhibitory interaction. The catalytic domain (represented in grey) is inhibited by the interaction with the C-SH2 (purple cylinder). Phosphorylation of the TRK provides the docking site for the N-SH2 (blue cylinder). The following phosphorylation (red sphere) induces a conformational change that releases the catalytic domain from the auto-inhibitory interaction (Gresset et al., 2010).

### 1.3.2 PI3K and PLC $\gamma$ 1 activation

The mechanism described in the previous chapter explained the mechanism of PLC $\gamma$ 1 activation by TKRs. However it has to be noted that the recruitment to the membrane is not only due to the interaction of N-

terminal-SH2 with the receptor. The PLC $\gamma$ 1 PH domain is essential for the growth factor-induced membrane translocation of PLC $\gamma$ 1. As described in chapter 1.2.4, it has been shown that PLC $\gamma$ 1 PH domain specifically binds to the PI3K product PtdIns(3,4,5)P<sub>3</sub> (Falasca et al., 1998). Specifically, mutation of the  $\beta$ 3/ $\beta$ 4 loop of the PH-PLC $\gamma$ 1 completely abolishes the membrane translocation of PH-PLC $\gamma$ 1 upon PDGF stimulation. Therefore the PH domain is essential for PLC $\gamma$ 1 plasma membrane recruitment (Falasca et al., 1998).

By expressing the GFP-tagged PLC $\gamma$ 1 PH domain in live cells, it is possible to follow the growth factor-induced translocation of the PH domain in living cells. The GFP-PH translocation to the plasma membrane starts within 3-5 minutes from stimulation with PDGF and becomes more evident within 15 minutes. It localizes with ruffles-like structures and gradually disappears from the plasma membrane after 30 minutes from stimulation (Falasca et al., 1998). Inhibition of PI3K using the irreversible PI3K inhibitor wortmannin blocks the PDGF-induced translocation of overexpressed recombinant GFP-PH-PLC $\gamma$ 1. This study demonstrated that there is a crosstalk between PLC $\gamma$ 1 and PI3K pathway and added important information to understand the mechanism of PLC $\gamma$ 1 activation (Figure 1.12). Furthermore the observation that PH/PtdIns(3,4,5)P<sub>3</sub> interaction is essential for PLC $\gamma$ 1 activation suggested the possibility of inhibiting PLC $\gamma$ 1 activation using molecules that block PLC $\gamma$ 1 translocation by competing with this interaction.

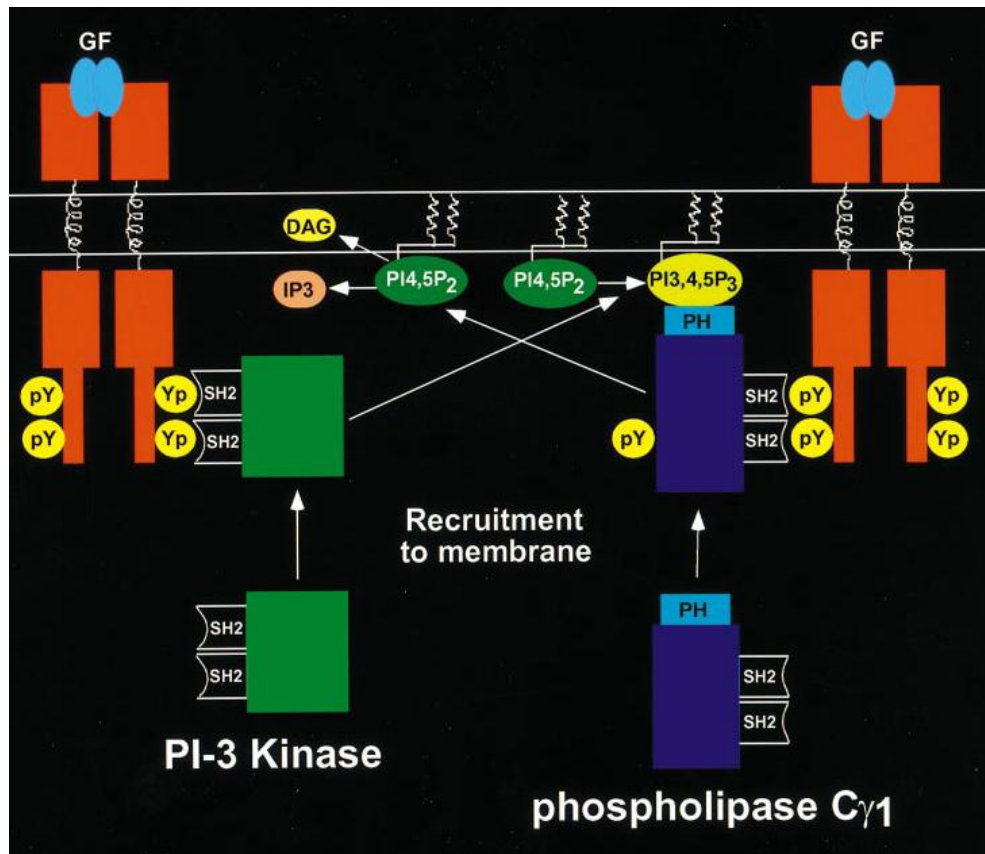


**Figure 1.12:** Crosstalk of PI3K/PLC $\gamma$ 1: PLC $\gamma$ 1 and PI3K are activated by growth factors. Binding of PtdIns(3,4,5)P<sub>3</sub> to PLC $\gamma$ 1 the PH domain and the interaction of SH2 domains of PLC $\gamma$ 1 with phosphotyrosine of TKRs lead to translocation of PLC $\gamma$ 1 to the plasma membrane and its activation (Falasca et al., 1998).

### 1.3.3 PLC $\gamma$ 1 activation and integrins

Extracellular Matrix Components (ECM) represent the main tissue's mechanical support and a barrier for cell migration. ECM components provide the substrates for cellular migration triggering outside-in signalling promoting cell migration. Integrins are a family of glycoproteins, composed of  $\alpha$ -subunits and  $\beta$ -subunits, which are responsible for cellular interaction with ECM components. Integrins form specific heterodimers with different binding specificity to ECM components. Each heterodimer presents an extracellular domain required for ECM component engagement and an intracellular domain responsible

for the propagation of the outside-in signal (Figure 1.13) (Friedl and Wolf, 2003).

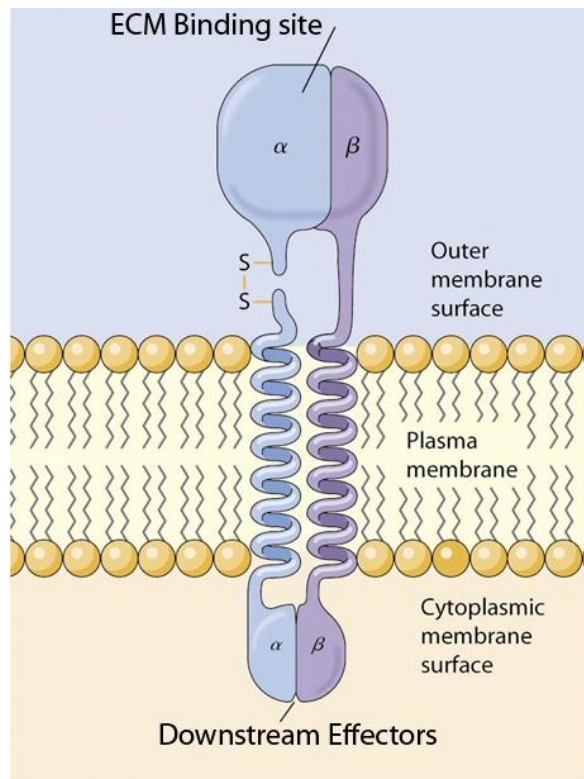


**Figure 1.13:** Representation of integrins heterodimer (adapted from Cooper, 2000).

The outside-in signal activated by engaged integrins leads to activation of downstream pathways that control survival and migration. The focal adhesion kinase (FAK) is phosphorylated after integrin engagement with ECM components. FAK presents a FERM domain able to interact with growth factor receptors and the  $\beta$ -integrin subunit. Following integrin engagement FAK gets autophosphorylated at Tyr 397, the main phosphorylation site of the protein (Sieg et al., 2000). This activated conformation promotes the interaction with the kinase Src which is mediated by the Src SH2 and SH3 domains that recognise FAK phosphotyrosine and FAK proline-rich sequence respectively (Thomas et al., 1998; Frame et al., 2010). Therefore ECM-integrin engagement activates FAK and Src together with other effectors such as PI3K and ERK, promoting cell survival and cellular migration. PLC $\gamma$ 1 is also able to

interact with the phosphorylated form of FAK through its C-terminal SH2 domain. This interaction stimulates the tyrosine phosphorylation of PLC $\gamma$ 1 and its enzymatic activity, although FAK is not directly involved in PLC $\gamma$ 1 phosphorylation (Zhang et al., 1999). ECM-integrins engagement activates PLC $\gamma$ 1, as indicated by PLC $\gamma$ 1 tyrosine phosphorylation in cells seeded on Matrigel or fibronectin (Langholz et al., 1997; Tvorogov et al., 2004) and it is important for cell migration and changes in morphology upon integrin engagement (Kassis et al 1999; Jones et al., 2005). Indeed, an integrin-blocking antibody inhibits PLC $\gamma$ 1 phosphorylation. Similarly, PLC $\gamma$ 1 inhibition through specific siRNAs or using the pan-PLC chemical inhibitor U73312 blocks the integrin induced cellular morphology change and cell migration. It has been demonstrated that the ECM-integrin induced PLC $\gamma$ 1 activation occurs downstream of Src kinase, which phosphorylates PLC $\gamma$ 1 in Tyr 783. Indeed inhibition of Src with the specific Src-inhibitor PP2, blocks Ins(1,4,5)P<sub>3</sub> production and calcium release (Jones et al., 2005) (Figure 1.14). Furthermore PLC $\gamma$ 1 and Src co-immunoprecipitate in a complex together with GIT1, that acts as a molecular adapter between PLC $\gamma$ 1 and Src (Haendler et al., 2003).

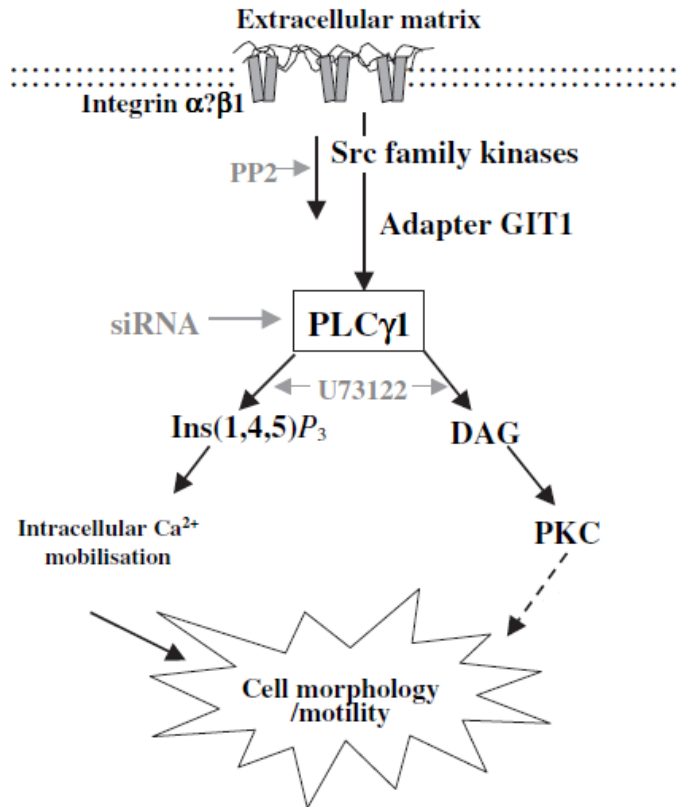


**Figure 1.14:** Model of ECM-integrin-induced PLC $\gamma$ 1 activation (adapted from Jones et al., 2005)

### 1.3.4 Biological functions of PLC $\gamma$ 1

In the previous chapter the different modalities of PLC $\gamma$ 1 activation were described. This chapter will focus on the role of PLC $\gamma$ 1. Mice PLC $\gamma$ 1 $^{-/-}$  are not viable and die after the first week of gestation. In particular mice PLC $\gamma$ 1 $^{-/-}$  develop normally at E8.5, but at E9.5 are markedly reduced in size and die in the following stages. These data indicate that PLC $\gamma$ 1 plays an essential role in development (Ji et al., 1997). Fibroblasts isolated from these embryos proliferate normally upon addition of different mitogenic factors but fail to mobilize calcium upon EGF stimulation (Ji et al., 1998). However other reports showed that PLC $\gamma$ 1 promotes cell growth in fibroblasts in a catalytic-independent mechanism (Huang et al., 1995). In particular the SH3 domain of PLC $\gamma$ 1 has been reported to interact with the Ras exchange factor SOS1, promoting Ras activation (Kim et al., 2000).

Similarly the SH3 domain of PLC $\gamma$ 1 interacts with the protein kinase Jak2 in a process implicated in the modulation of growth hormone signalling (Choi et al., 2006). Several lines of evidence suggest a catalytic-independent role of PLC $\gamma$ 1 as guanine nucleotide exchange factor (Ye et al., 2002; Choi et al., 2004) and also as a key regulator of agonist-induced Ca<sup>2+</sup> entry (Patterson et al., 2002). Analysis of mouse embryos revealed that PLC $\gamma$ 1 is essential in angiogenesis. Embryos PLC $\gamma$ 1<sup>-/-</sup> showed no erythropoiesis, reduced vasculogenesis and reduced levels of vascular endothelial growth factor (VEGF) receptor expression (Liao et al., 2002). Similarly, mutation of the PLC $\gamma$ 1 orthologue causes defects in arteries formation (Lawson et al., 2003) in zebra fish. In umbilical vein endothelial cells (HUVEC), FGF-2 activates PLC $\gamma$ 1 in a PI3K-dependent manner. In these cells pharmacological inhibition or downregulation of PLC $\gamma$ 1 inhibits the FGF-2 induced cell migration and the tubulogenesis *in vitro* (Maffucci et al., 2009). Altogether these data indicate that, although PLC $\gamma$ 2 is the PLC isoform specifically expressed in the hematopoietic tissue, PLC $\gamma$ 1 is essential in early stage of development and the two isoforms have not overlapping roles.

It has been reported that PLC $\gamma$ 1<sup>-/-</sup> fibroblasts show a significant decrease in fibronectin-induced adhesion compared to normal fibroblasts (Tvorogov et al., 2005). Furthermore inhibition of PLC $\gamma$ 1 by siRNA or pharmacological inhibition affects cell morphology of cells seeded on ECM components such as Matrigel. In particular both HUVEC endothelial cells and cancer cells such as BE (colon carcinoma) and DU145 (prostate cancer) showed a rounded morphology when plated on Matrigel upon PLC $\gamma$ 1 knockdown or after treatment with U73122 (Jones et al., 2005). PLC $\gamma$ 1 plays an important role in cell movement regulation and cytoskeleton remodelling upon integrin engagement or growth factor stimulation. Inhibition of PLC $\gamma$ 1 reduces growth factor-induced cell motility in cancer cell lines and endothelial cells (Kassis et al., 1999; Maffucci et al., 2009). EGF-induced motility has been extensively investigated in cancer cell lines. EGF stimulation induces cytoskeleton

rearrangement, stimulating actin filament polymerisation (Chan et al., 1998). As described in chapter 1.1.1.1 PLC $\gamma$ 1 is involved in the regulation of actin polymerisation activating actin binding proteins (ABPs) such as cofilin, profilin and gelsolin through hydrolysis of PtdIns(4,5)P<sub>2</sub> (Wang et al., 2007). PLC $\gamma$ 1 inhibition blocks the cofilin activity and inhibits the early actin polymerisation and the generation of new barbed ends (Figure 1.15) (Mouneimne et al., 2004). During chemotaxis, the asymmetric actin polymerization generates a cell polarity towards the stimulus, essential for chemotaxis and for cell directionality. Chemotaxis assays showed that the normal EGF-induced polymerisation of actin filaments at the leading edge of the cells, which induces a well-defined cell polarity, is completely blocked following inhibition of PLC $\gamma$ 1. Indeed cells treated with U73122 failed to develop a well-defined cell polarity indicating that PLC $\gamma$ 1 is essential for protrusion formation upon EGF stimulation (Jones et al., 2005). The activation of PLC $\gamma$ 1 at the leading edge is PI3K dependent. Indeed inhibition of PI3K pathway inhibits PLC $\gamma$ 1 translocation at the leading edge (Piccolo et al., 2002).

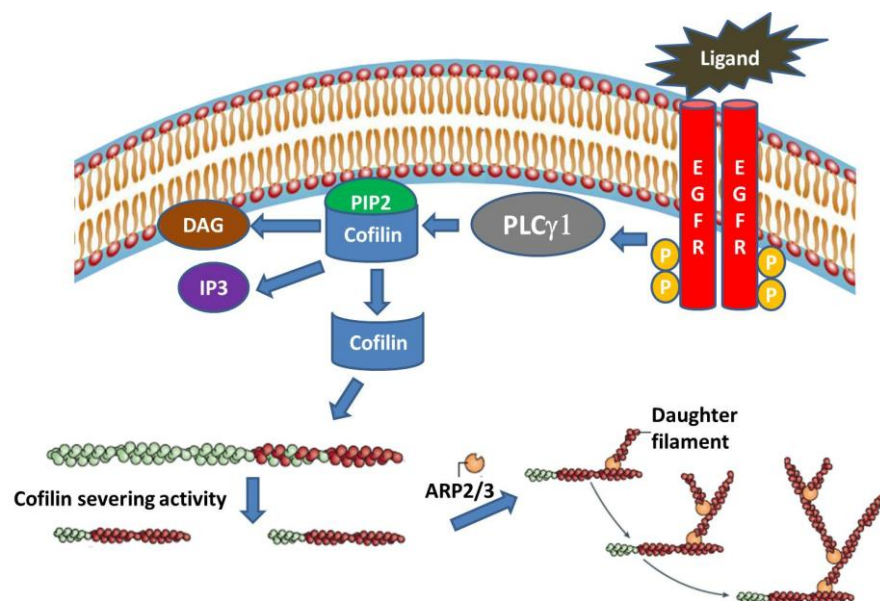


**Figure 1.15:** Model of cofilin activation (adapted by Wang et al., 2007)

### **1.3.5 Overview of the cell migration process.**

The ability of cells to migrate and to move towards a chemo-attractant is an important process occurring in many physiological conditions such as embryogenesis, wound healing and the immune system response. Cell migration and invasion play also a very important role in cancer, allowing tumour cells to invade the surrounding tissue and eventually leading to dissemination of cancer cells during the metastatic process. Extracellular Matrix Components (ECM) represent the main tissue's mechanical support and a barrier for cell migration. Integrins play an essential role in ECM-induced signalling (see chapter 1.3.3), and growth factors stimulate cell motility. During cell migration, integrins become locally enriched in regions of the plasma membrane defined as focal complexes which eventually evolve in focal contact regions (Burrige and Chrzanowska-Wodicka, 1992). The composition of focal complex depends on the relative abundance of the different ECM components and results in local enrichment of integrin heterodimers accordingly to the different ECM components available. Upon integrin engagement and growth factor stimulation, the cytoskeleton remodelling machinery becomes activated. In this process PI3K, PLC $\gamma$ 1 and the Rho family of small GTPase play an essential role stimulating cytoskeleton remodelling and the formation of cell protrusion at the leading edge of the cells (see chapter 1.1.1.1 and 1.3.4). The ECM-engaged integrins are able to associate with  $\alpha$ -actinin, tensin, vinculin that bind integrins directly to the cytoskeleton, creating a direct link between focal adhesions and cytoskeleton (Figure 1.16-1,2) (Zamir and Geiger, 2001). These complexes are essential to generate the forces necessary to extend cellular protrusion. During the initial steps, when little adhesion is present at the leading edge, actin filament elongation extends the leading edge pushing the membrane in an outward direction. Movements within the ECM often require proteolysis of the ECM itself allowing the cells to create a path of migration. For this reason membrane-type matrix metalloproteinase enzymes are required for ECM digestion in order to create the space for cellular migration (Figure 1.16-3)

(Friedl and Wolf, 2003). Late the contraction driven by myosin II along the stress fibres leads to the contraction of the cell body towards the leading edge, pushing the cells forward (Figure 1.16-4). The coordinated sequence of these steps leads to the movement of the cell on the ECM or toward a chemo-attractant. Inhibition of one of these phases results in inhibition of cell migration and motility. As described in chapter 1.3.4, PLC $\gamma$ 1 is an important hub in cell motility regulation. Indeed its inhibition reduced cell motility upon growth factor and integrin-engagement stimulation, due to its important role in regulating the cytoskeleton remodelling through the activation of effectors such as Rac1 and cofilin (Li et al., 2009; Mouneimne et al., 2004; van Rheenen et al., 2007).

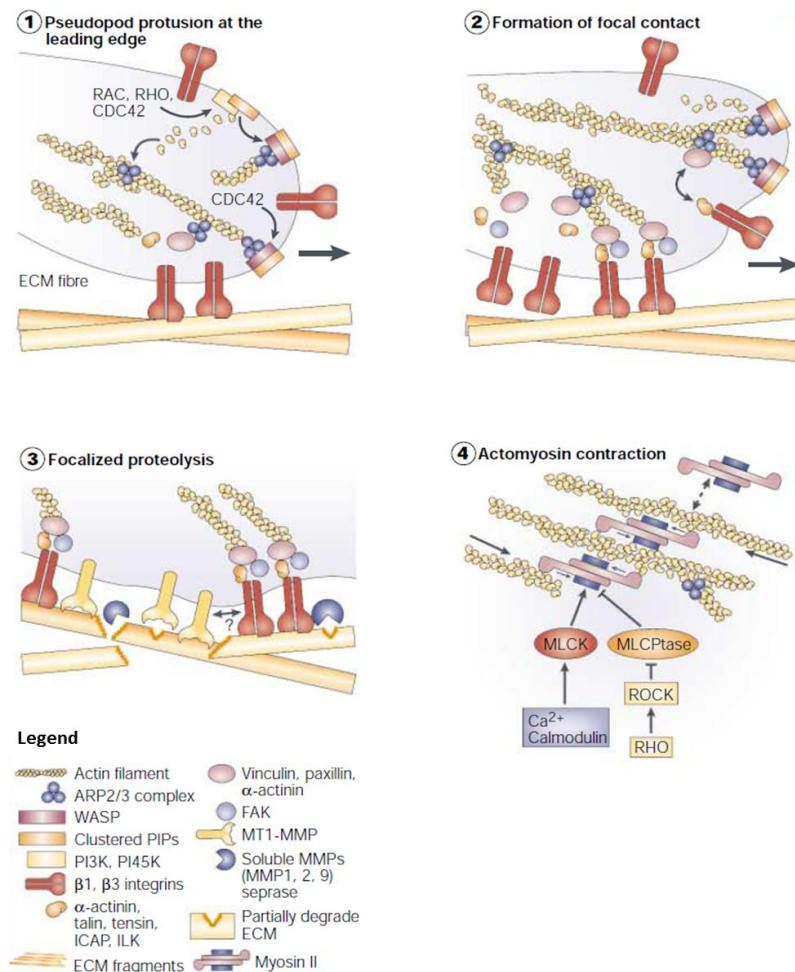


**Figure 1.16:** Model of cell migration summarising the process in 4 steps: 1-pseudopod protrusion at the leading edge, 2-formation of focal contact,

3- focalized proteolysis, 4-actomyosin contraction (Friedl and Wolf, 2003).

### **1.3.6 PLC $\gamma$ 1 and Rac1**

The Rho GTPase family belongs to the Ras superfamily and has an important role in cytoskeleton rearrangement and actin polymerisation. The small GTPases are guanine-nucleotide-binding proteins which are in an “OFF” conformation when bound to GDP but switch to an “ON” conformation when bound to GTP. The cycling between the two forms is controlled by the activity of GEFs proteins (Guanine Exchange Factor), which induces the release of GDP from the small GTPase proteins and its replacement with GTP and GAPs (GTPase activating protein) which activate the GTPase activity and induce the hydrolysis of GTP to GDP. The Rho family presents, among other members, three subfamilies that control different processes within the cytoskeleton remodelling: Cdc42, Rac and Rho subclasses. In particular, Rho members are involved in formation of stress fiber and focal adhesion, Cdc42 in filopodia organisation and Rac in lamellipodia and membrane ruffles formation. Rac in particular activates the WASP and WAVE proteins that in turn activate the ARP2/3 complex and therefore induce actin nucleation (Haesman and Ridley, 2008). These structures are essential for cellular migration and motility. Both PLC $\gamma$ 1 and Rac1 have been shown to regulate cytoskeleton remodelling upon EGF stimulation (Wells et al., 2002; Ridley et al, 1992). A direct link exists between PLC $\gamma$  isoforms and Rac1. While binding of Rac1 to the split PH domain of PLC $\gamma$ 2 is important for the Rac1-dependent activation of PLC $\gamma$ 2 (Walliser et al., 2008), the direct interaction of Rac1 with PLC $\gamma$ 1 promotes Rac1 activation (Jones and Katan, 2007). Indeed PLC $\gamma$ 1 associates with Rac1 upon EGF stimulation and promotes its activation. The SH3 domain of PLC $\gamma$ 1 is essential for this interaction and mutation of this domain abrogates Rac1 binding and its activation (Figure 1.17) (Li et al., 2009). Similarly, downregulation of PLC $\gamma$ 1 inhibits EGF- and serum-induced

activation of Rac1. It has been shown that PLC $\gamma$ 1 is a GEF specific for Rac1, which is consistent with the ability of PLC $\gamma$ 1 to activate Rac1. In particular the SH3 domain of PLC $\gamma$ 1 is responsible for the GEF activity. Indeed *in vitro* assay showed that PLC $\gamma$ 1 SH3 domain alone induces Rac1-GTP binding. (Li et al., 2009).

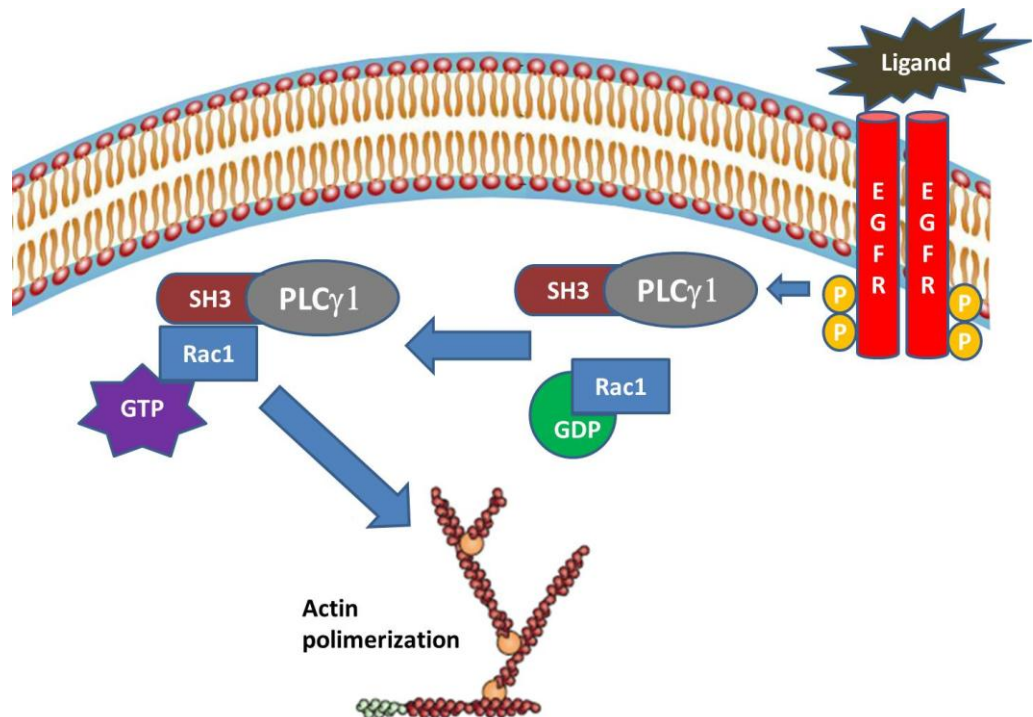


**Figure 1.17:** Model of EGF-induced Rac1 activation downstream of PLC $\gamma$ 1

#### 1.4 Role of PLC $\gamma$ 1 in cancer

As a key downstream effector of EGF receptor (EGFR), PLC $\gamma$ 1 is likely to be involved in tumour progression. EGFR family members are often overexpressed in many cancers such as prostate, breast, head and neck cancers and many others (Agus et al., 2002; Scagliotti et al., 2004). Increased PLC $\gamma$ 1 expression was reported in breast carcinoma samples compared to healthy tissue, although this study did not connect the overexpression pattern to any particular stage of the disease (Arteaga et

al., 1991). In parallel other studies demonstrated the activation of PLC $\gamma$ 1 downstream of EGF. In particular, EGFR overexpression in fibroblasts induced PLC $\gamma$ 1 phosphorylation and increased motility upon EGF stimulation. Pharmacological inhibition of PLC $\gamma$ 1 or expression of a PLC $\gamma$ 1 dominant negative inhibited cell migration but it had no effect on EGF-induced mitogenesis, demonstrating the specific role of PLC $\gamma$ 1 in cell motility (Chen et al., 1994).

Increased cell motility plays an essential role in invasive cancers and metastasis. The role of PLC $\gamma$ 1 in cell invasion was assessed *in vivo* by injecting mice with DU145 prostate cancer cells expressing a PLC $\gamma$ 1 dominant negative mutant (PLCz). This dominant negative mutant of PLC $\gamma$ 1 inhibited primary tumour spreading and local invasion. Notably PLC $\gamma$ 1 inhibition had no effect on cell growth confirming the main role of PLC $\gamma$ 1 in cell invasion downstream of EGFR (Turner et al., 1997). Further *in vitro* invasion experiments using different breast and prostate cancer cell lines showed the broad role of PLC $\gamma$ 1 in cell invasion. Indeed pharmacological inhibition of PLC $\gamma$ 1 was able to inhibit *in vitro* Matrigel invasion in all the cell lines tested (Kassis et al., 1999), demonstrating the role of PLC $\gamma$ 1 in cell invasion. These results highlighted PLC $\gamma$ 1 as a potential target to inhibit carcinoma.

Although these reports provided a “proof of concept” that PLC $\gamma$ 1 can be targeted to inhibit tumour invasion, there was no clear *in vivo* proof of its importance in the metastatic process. The MMTV-PyVmT and TRAMP mice models, which respectively express the oncogenic Mice Mammary Tumour virus and the Polyoma middle T antigen, develop respectively breast cancer and prostate cancer and therefore represent a good model to study metastasis arisen from oncogene-induced primary tumour. The expression of breast- and prostate-localised PLCz dominant negative peptide had no effect on the primary tumour size but decreased the invasiveness of primary tumours and, most importantly, reduced formation of distant lung metastasis, showing the importance of PLC $\gamma$ 1 in

metastasis development (Shepard et al., 2007). A recent work published by our laboratory, in which I contributed as co-author, showed that downregulation of PLC $\gamma$ 1 had no effect on primary xenografted tumour whereas it inhibited the development of lung metastases derived from human breast cancer cell line MDA-MB-231 injected in the tail vein (Figure 1.18A) (Sala et al., 2008). In particular the downregulation of PLC $\gamma$ 1 in the injected MDA-MB-231 was achieved using specific shRNAs which were expressed in a stable or tetracycline inducible system. The shRNA represents a more specific system compared to the dominant negative system used in previous works. Furthermore the inducible downregulating system allowed us to downregulate PLC $\gamma$ 1 after the injection. Mice injected with breast cancer cells MDA-MB-231 stably downregulated for PLC $\gamma$ 1 showed inhibition of lung metastases development compared to mice injected with cell expressing PLC $\gamma$ 1 (Sala et al., 2008). To further understand the role of PLC $\gamma$ 1 in metastasis, mice were injected with MDA-MB-231 expressing the tetracycline inducible downregulating system targeting PLC $\gamma$ 1. Mice were not treated with tetracycline after the injection in order to maintain the expression of PLC $\gamma$ 1 in the cancer cells. Micro-metastases were detectable after 15 days from the injection. Therefore after 15 days from the injection, mice where treated with tetracycline, in order to activate the tetracycline-induced downregulation of PLC $\gamma$ 1 in the cancer cells. PLC $\gamma$ 1 downregulation induced regression of lungs metastases (Figure 1.18B). In fact, four of five lung tissues in both stable and inducible PLC $\gamma$ 1 knockdown were completely metastasis-free and only one mouse showed few metastases (Sala et al., 2008). These data showed that PLC $\gamma$ 1 is important in the early steps of metastases development and, more important, that it is required for metastatic development since its downregulation induces metastases regression. These data enhanced the importance of PLC $\gamma$ 1 in cancer cell invasion highlighted by previous work and suggested that PLC $\gamma$ 1 may represent a novel anti-metastatic strategy.

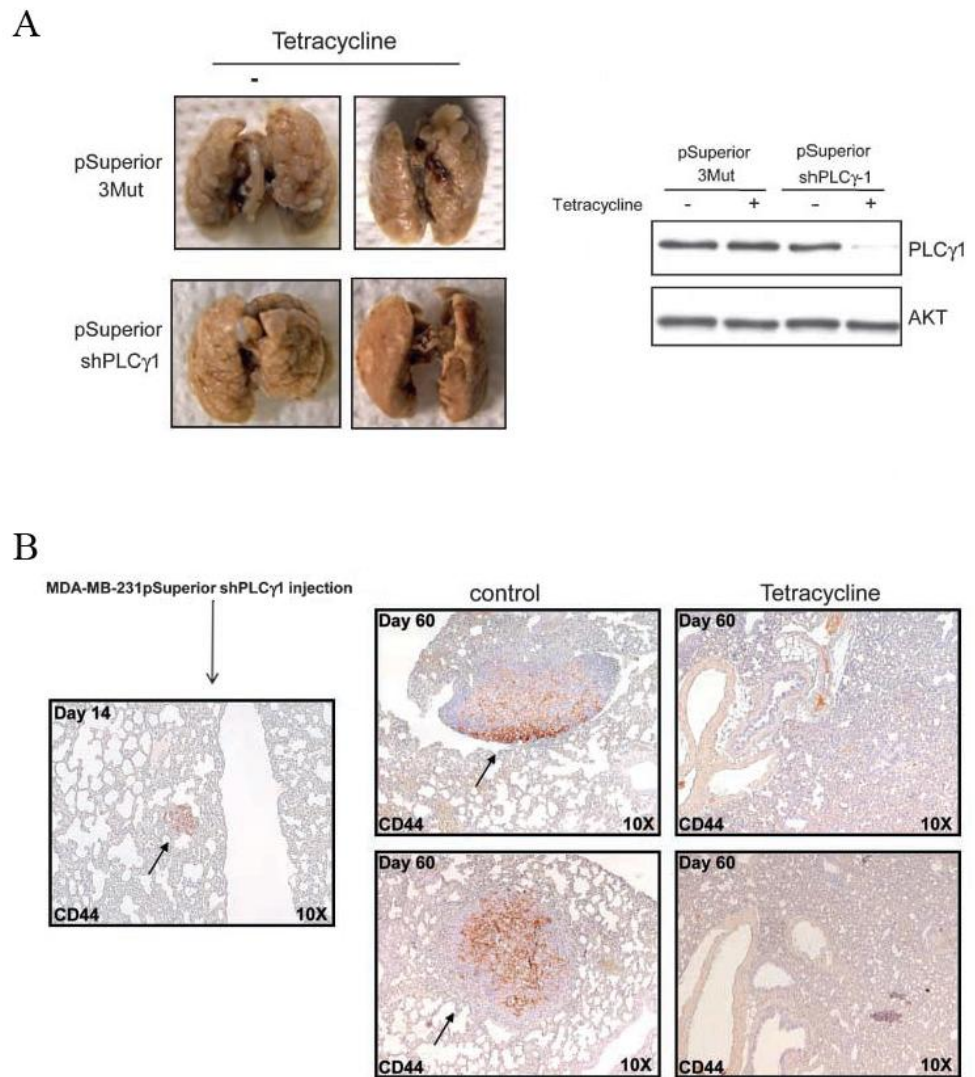


**Figure 1.18:** PLC $\gamma$ 1 is important for metastasis development and progression. **A)** Control MDA-MB-231 expressing a tetracycline inducible non-targeting sequence (3MUT) and MDA-MB-231 expressing a tetracycline inducible targeting shRNA for PLC $\gamma$ 1 (shPLC $\gamma$ 1), were injected in mice and lung metastases were assessed after 60 days from the injection. Downregulation of PLC $\gamma$ 1 protein level upon induction by tetracycline was assessed by western blot. **B)** Representative lung sections from untreated mice or mice treated with tetracycline after 14 days from injection are shown. Arrows indicate micrometastases (Sala et al., 2008).

## 1.5 The metastatic process

The initiating events in the arising of cancer are mutating oncogenic events, defined tumour initiating mutations that provide cells with enhanced proliferation rate, resistance to cell death and chromosomal and genetic instability (Figure 1.19-a,b) (Fidler, 2002). Mutation of EGFR and altered PI3K pathway, due to PI3K overexpression or inactive mutations of PTEN or its deletion are a well-established example of oncogenic events (Kok et al., 2009; Gonzalez-Angulo et al., 2011). In some cases tumour cells migrate from the primary tumour to distant healthy tissues initiating a second cancerous lesion called metastasis. Often metastasis remains dependent on such alterations, and inhibition of those pathways leads to tumour and metastatic regression. However, very often, metastases develop new mutations and become resistant to treatment, resulting in poor prognosis. Cells crossing the tissue boundaries find themselves in a different environment and altered pathways help these cells to survive and proliferate (Nguyen et al., 2009). The initiation of a novel tumour occurs in specific host organs whose microenvironment stimulates metastasis development. In particular physical characteristics of the organ structure and specific cytokines, determine the homing of metastatic cancer cells. For example expression of epiregulin, prostaglandin G/H, matrix metalloproteinase 1 (MMP1) and MMP2 in breast cancer cell lines has been implicated in breast cancer lung metastasis (Minn et al., 2007). The mutual relationship between the origin of cancer cells and the site for metastasis development was observed by Paget more than 100 years ago when he compared cancer cells to the “seed” and the specific host organ as the “soil” and highlighted the “*conditio sine qua non*” seed and soil has to be compatible (Fidler, 2002). The metastatic process can be subdivided into intravasation, survival in the circulation, extravasation and colonisation at distant site (Fidler, 2003; Nguyen et al., 2009). During this process, usually characterised by tumour-driven-angiogenesis, the tumour reaches the tissue boundaries allowing some cancer cells to enter the circulatory system (Figure 1.19-

c,d), during the intravasation phase. Cells entering the circulatory system undergo mechanical stress and they are targeted by the immune system. Therefore only few cells survive during this phase, which eventually is followed by extravasation. In this phase cells expressing extravasation genes such as metalloproteinases genes (MMPs) and CCL5 are characterised by enhanced ability to adhere to the blood vessel wall, to invade distant tissues and to initiate novel distant tumours (Figure 1.19-e) (Nguyen et al., 2009). It is well established that different steps are necessary for development of metastatic tumours and each step requires a highly selective process which selects cancer cells with metastatic characteristics. This is due to the fact that metastases are the results of a high selective process that selects populations of cancer cells presenting enhanced expression of metastasis initiating genes and metastasis progression-related genes which allows them to resist the environment of the newly colonised organ and often confers resistance to anti-cancer treatments. For example parathyroid hormone related protein (PTHrP) and interleukin 11 (IL-11) expression enable breast cancer cells to generate osteolytic metastases but they have no effect on primary tumour growth (Yin et al., 1999; Kang et al., 2003). The increased invasiveness and the ability of cancer cells to reach and colonise distant tissues are the main characteristics of metastasis. The tumour cell invasion role is a complex process whereby a group of epithelial-derived cells invade adjacent tissue in a coordinated fashion. The invasion is accompanied by cell proliferation and morphogenic differentiation. In this context the fact that PLC $\gamma$ 1 has been demonstrated to be essential for metastasis development and progression (chapter 1.4), but not for primary tumour growth, highlights PLC $\gamma$ 1 as an important determinant protein for metastasis development and a potential antimetastatic target.

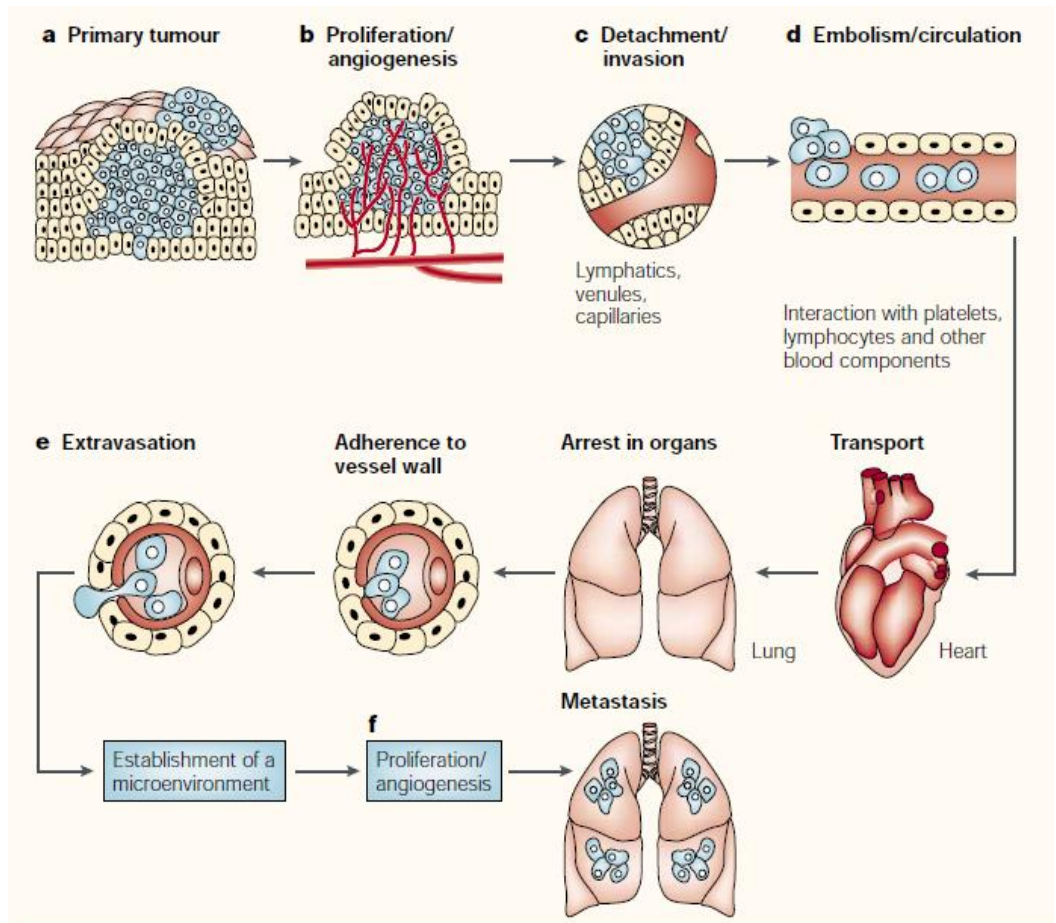


**Figure 1.19:** Model of metastasis dissemination and initiation of a novel distant tumour (Fidler, 2002).

## 1.6 Breast cancer

In 2008 47,700 woman were diagnosed with breast cancer in UK (Official Cancer Research UK cancer statistical analysis). Breast cancer is a heterogeneous disease and therefore treatments have different outcomes according to the origin of the carcinoma and the tumour stage. The breast gland consists of lobules and ducts. In particular lobules present a luminal compartment surrounded by luminal cells. Ducts consist of ductal cells which define a tubular structure necessary for carrying the milk secreted in the lobules. Cancer cells can originate from both ducts (ductal carcinoma) and lobules (lobular carcinoma). Histopathological classification defines breast cancer as carcinoma *in situ*, when it is still limited by the basal membrane of the ducts and therefore it is not spread. The invasive carcinoma presents local infiltration of cancer cells and fixation of the tumour to skin and the underlying pectoralis fascia. Breast cancer-derived metastases may be found in lymph node, lungs, brain and bones. In general breast cancers are classified according to the tumour size (T), presence of nodule (N) and distant metastases occurrence (M). However molecular biology approaches, such as microarray analysis of breast cancer patient tissues, classify breast cancer on the basis of gene expression signature as: normal breast-like, ERBB2, basal-like and luminal-like breast cancer. In particular luminal breast cancer-like is associated with high levels of oestrogen receptor (ER), while normal breast-like, ERBB2, and basal-like breast cancers are associated with low level of ER (Perou et al., 2000; Sorlie et al., 2001). Tumours overexpressing ER depend on oestrogen for proliferation, therefore these tumours are responsive to hormone therapy. However selective pressure contributes to select ER<sup>-</sup> cell populations, which are not dependent on oestrogen to proliferate and therefore are resistant to hormone therapy context. Generally in breast cancer, selective pressure contributes to the generation of ERBB2 and EGFR gene amplification. The overexpression of these receptors provides the tumour cells with enhanced growth and motility. EGFR and ERBB2 belong to the family of epidermal growth

factor receptors composed by EGFR/ERBB1, ERBB2, ERBB3 and ERBB4. Ligand binds to the extracellular domain, induces heterodimerisation and activates receptor autophosphorylation activating the downstream pathways. The ERBBs receptors present heterogeneous characteristics. ERBB2 for example possesses an extracellular domain but no ERBB2 ligand is known, while ERBB3 possesses a non-functional kinase domain. However ERBB3 seems to be essential for the tumorigenesis induced by ERBB2. Increased expression of ERBB3 potentiates the ERBB2 induced transformation, while ERBB3 loss inhibits ERBB2-induced transformation. Since the epidermal growth factor has a crucial role in breast cancer, specific drugs targeting the HERBB receptors were developed. For example, Trastuzumab is a monoclonal antibody that recognizes the extracellular domain of ERBB2 receptor, inhibiting the activation of the receptor (Molina et al., 2001). In the case of ERBB2 overexpressing metastatic breast cancers, Trastuzumab extended the progression-free and recurrence-free survival when combined with cytotoxic drugs like taxanes or cisplatin (Burstein et al., 2007). Trastuzumab and hormone therapy are a valid therapy in case of ER<sup>+</sup> and ERBB2-overexpressing breast cancers. However about 15% of breast cancer tumours belong to the basal-like breast cancer subtype, which are also ER<sup>-</sup>. The almost totality of this subtype do not present expression of oestrogen, progesterone and ERBB2 receptors and therefore are called triple negative (Bauer et al., 2007). Triple negative cancer patients have poor prognosis and do not respond to endocrine therapies or ERBB2 targeting therapies. It has been demonstrated that triple negative phenotype correlates with mutation of the tumour suppressor BRCA1 and EGFR is often overexpressed in this tumour type. Clinical trials, which employ an EGFR targeting approach such as the tyrosine kinase inhibitor lapatinib and the EGFR-targeting antibody Cetuximab, showed a positive response when combined with genotoxic treatments such as carboplatin and DNA-damaging treatment (Cleator et al., 2007). The overall progress in breast cancer treatment and molecular mechanisms involved in breast cancer, early diagnosis and screening programs contributed to decrease

mortality rate of 37% compared to 1989 (Breast cancer UK, 2009). However, very little progress has been done in curing metastatic breast cancer. Despite the therapeutic improvements about 30% of patients with breast cancer develop recurrent advanced metastases, indicating no significant advances in anti-metastatic treatment for metastatic breast cancer, and for metastasis spreading in general. Currently no effective anti-metastatic drugs are available and metastasis remains the main cause of cancer-related death.

### **1.7 3-Phosphoinositide-Dependent-Protein-Kinase-1 (PDK1) in cancer as potential therapeutic target**

Cancer cell proliferation and survival is tightly regulated by hormones and growth factors that activate specific intracellular pathways inside the cell. Understanding the signalling pathways involved in these processes may help us to find predictive factors for tumour aggressiveness and develop new anticancer drugs. Among the different pathways, signals transmitted by the PI3K/AKT pathway have proven to be important for cell survival in many cell types (Chapter 1.1.2). Although Akt is considered to be one of the key enzymes regulating growth and proliferation of cancer cells, there is increasing evidence that Akt-independent pathways, downstream of PI3K activation, may also play a crucial role in driving tumour progression. In this respect, the existence of PDK1-mediated/Akt-independent pathways has been recently identified (Vasudevan et al., 2009). Despite the importance of PDK1 in cell signalling, less attention has been paid to this kinase for its role in cancer and as a therapeutic target.

#### **1.7.1 Biological functions of PDK1**

The role of PDK1 has been investigated *in vivo* in yeast, *Drosophila* (Casamayor et al., 1999; Cho et al., 2001; Lawlor et al., 2002) and mice.

In the examined organism the absence of PDK1 is lethal. Mice PDK1<sup>-/-</sup> lack branchial arches and exhibit problems in neural crest specification and forebrain development, and several disruptions in the development of a functional circulatory system, which eventually causes death at E9.5 (Lawlor et al., 2002). In order to study the role of PDK1 in development, hypomorphic mice for PDK1 were generated showing a reduced expression of PDK1 in all tissues. These mice showed a decreased body size of 40-50% compared to the wild type littermates, but showed no significant differences in the activation of AKT induced by insulin compared to their littermates. Analysis of organs revealed that the difference in size is due to a decreased cell size rather than reduction in cell number. Furthermore mice expressing a PDK1 mutated form unable to bind phosphoinositides present a strongly reduced AKT activation, insulin resistance and hyperinsulinaemia (Bayascas et al., 2008).

### **1.7.2 PDK1 in cancer**

Hyperactivation of the PI3K/PDK1/AKT pathway is found in many human cancers. As described in chapter 1.1.2, PTEN is often mutated in human cancer and its absence causes a hyperactivation of the mitogenic signal promoted by PI3K, promoting tumorigenesis. The hypomorphic PDK1 mice model was a useful tool to investigate the role of PDK1 under increased PI3K signalling pathway. Hypomorphic PDK1 mutations in mice showed increased resistance to develop tumours when crossed with mice PTEN<sup>+/-</sup> indicating that PDK1 can be an important therapeutic target in cancers that present hyperactivation of the PTEN/PI3K/AKT pathway (Bayascas et al., 2005). PDK1 plays a pivotal role in breast cancer development. Increased copy number of PDK1 is often present in human breast cancer compared to normal breast epithelia and correlates with upstream PI3K pathway activation. In particular, increased copy number of PDK1 correlates with the presence of activating mutation of PI3K class 1 p110 $\alpha$  or with ERBB2 overexpression (Maurer et al., 2009). Furthermore, using an RNA interference library targeting 779 kinases and related proteins, the PDK1 signalling pathway has been identified as a strong

determinant of sensitivity to multiple ER $\alpha$  antagonists, including tamoxifen the most commonly used drug to treat breast cancer whose usefulness is limited by the development of resistance (Iorns et al., 2009; Peifer and Alessi, 2009). Whether PDK1 is essential for tumourigenesis initiation or it is required in later stages is still unclear. Overexpression of PDK1 in non tumourigenic breast epithelial cell line MCF10A does not alter cell growth and the normal multiacinar morphology in three-dimensional culture conditions. Strikingly, co-overexpression of PDK1 and of the active mutant rat homolog of ERBB2 in MCF10A causes a profoundly distorted three-dimensional multiacinar organization and confers increased cell motility regardless of the presence of chemo-attractant (Maurer et al., 2009). Indeed, PDK1 positively regulates ROCK1 in a kinase-independent manner. ROCK1 is a protein kinase involved in the phosphorylation of the myosin light chain and it is therefore involved in acto-myosin contractility. In particular promoting ROCK1 is essential for cell motility in three-dimensional conditions and *in vivo*. Several studies have shown that upregulation of Rho-ROCK signalling in tumours is linked to increased invasion and metastatic potential (Pinner and Sahai, 2008). Noteworthy, the PDK1-dependent regulation of ROCK1 seems particularly important in three-dimensional environments. Interestingly, knock down of PDK1 has no effect on cell growth under standard tissue culture conditions in a panel of breast, colon, lungs and prostate cancer cell lines. However pharmacological inhibition of PDK1 or PDK1 knockdown inhibits cell growth in three-dimensional culture conditions on Matrigel or the anchorage-independent growth. Furthermore PDK1 inhibition inhibits Matrigel cell invasion in breast cancer cell lines, prostate cancer and melanoma (Pinner and Sahai, 2008; Nogashima et al., 2010), in line with data showed in this thesis.

### 1.7.3 PDK1-dependent pathways

3-phosphoinositide-dependent-protein kinase 1 (PDK1) is a kinase belonging to family of the AGC kinases. The AGC kinase family includes serine and threonine kinases with high identity of their catalytic domain to cAMP-dependent protein kinase 1 (PKA), cGMP-dependent protein kinase (PKG) and protein kinase C (PKC). The AGC kinases possess a conserved bi-lobed structure which defined the catalytic domain. The amino-terminal small lobe and the carboxy-terminal large lobe sandwich one ATP molecule essential for the subsequent substrate phosphorylation. Many AGC kinases possess two phosphorylation sites that regulate their activation: the activation loop, which is located within the kinase domain, and the hydrophobic motif which is located in a region adjacent to the catalytic domain. Phosphorylation of these sites increases the kinase activity and leads to enzymatic full activation. PDK1 was originally discovered in 1997 as the kinase responsible for the phosphorylation of AKT activation loop at the residue threonine 308, essential for enzyme activation (Alessi et al., 1997). Furthermore AKT phosphorylation at Thr308 was dependent *in vitro* on PtdIns(3,4,5)P<sub>3</sub> concentration, linking PDK1 to the upstream activation of PI3K. PDK1 is a protein of 556 amino acids that possesses a catalytic domain and a PH domain. As a member of the AGC kinase, PDK1 shows a phosphorylation site in S241 which is located in the activation loop. The PDK1 activation loop is phosphorylated in resting cells and this event is not affected by growth factor stimulation. Phosphorylation of PDK1 at S241 is catalysed by an autophosphorylation reaction *in trans*, meaning that PDK1 is autophosphorylated by another PDK1 molecule (Wick et al., 2003). Therefore PDK1 kinase activity is constitutively active and regulation of PDK1-activated signalling involves other mechanisms. The first mechanism was discovered investigating the steps involved in AKT-T-loop phosphorylation in living cells. PDK1 is localised at the plasma membrane because of the interaction of its PH domain with the phosphoinositides PtdIns(3,4,5)P<sub>3</sub>, PtdIns(3,4)P<sub>2</sub> and PtdIns(4,5)P<sub>2</sub>, with

the highest affinity towards the PI3K lipid products (Currie et al., 1999). The affinity of PDK1-PH domain for the PI3K products suggested a potential PI3K-dependent PDK1 membrane translocation. Although PDK1 membrane localisation has been largely investigated and supported, the dynamic of this localisation is controversial. Whether PDK1 translocates to the plasma membrane following growth factor stimulation, or it is constitutively localised to the plasma membrane is still debated. Growth factor-induced PDK1 membrane translocation was observed by confocal analysis (Anderson et al., 1998; Filippa et al., 2000). However another study employing high resolution electron microscopy analysis revealed a constitutive PDK1 membrane localisation without further translocation following growth factor stimulation (Currie et al., 1999). PDK1 membrane localisation is essential for AKT phosphorylation at Thr308. Growth factor-induced AKT membrane translocation leads to PDK1 and AKT co-localisation at the plasma membrane following PI3K activation, since both proteins bind PtdIns(3,4,5)P<sub>3</sub>. AKT membrane recruitment causes conformational changes in AKT which allow the phosphorylation of AKT by PDK1 (Calleja et al., 2007) (Figure 1.20). Expression of a mutant AKT constitutively associated to the membrane resulted in full AKT phosphorylation at Thr308 in unstimulated cells (Andjelkovic et al., 1997), which may occur only in the presence of a membrane located PDK1 pool. On the contrary, mutation of the AKT-PH domain that abolishes AKT membrane recruitment strongly decreases AKT phosphorylation. Similarly, mutation or deletion of PDK1-PH domain strongly reduces AKT phosphorylation (Currie et al., 1999). PDK1-dependent AKT phosphorylation is therefore promoted by the co-localisation of both proteins to the plasma membrane, mediated by the interaction of the respective PH-domains with the PtdIns(3,4,5)P<sub>3</sub>.

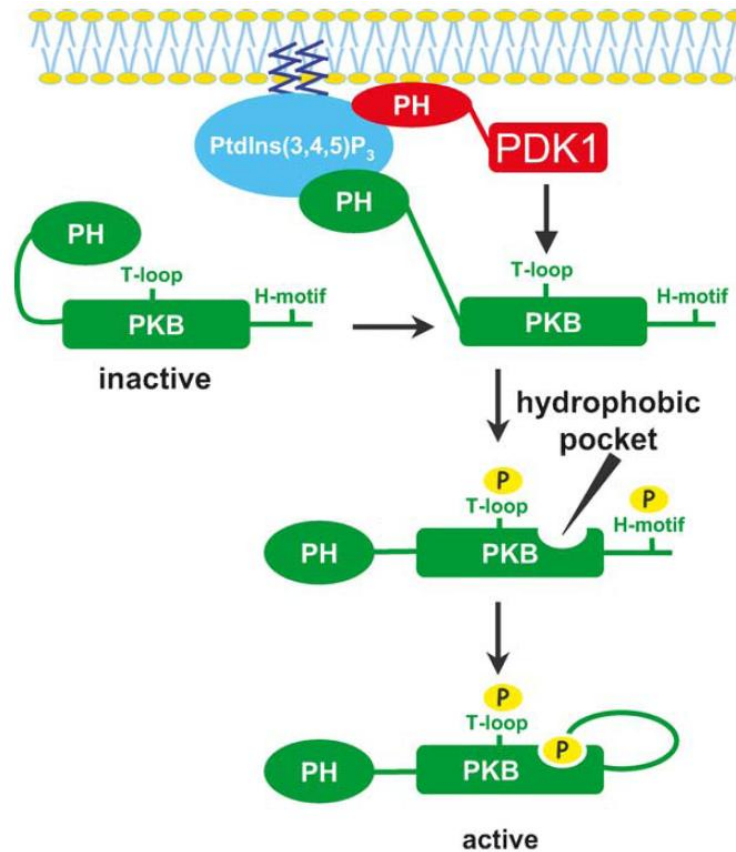


**Figure 1.20:** Molecular mechanism of AKT activation by PDK1 (adapted from Mora et al., 2004)

A recent study reported that PDK1 exists as a homodimeric complex through PH domain interaction of two PDK1 monomers, and that this interaction is important in the regulation of AKT phosphorylation. Extracellular stimulation increases the basal homodimerisation in live cells in the cytosol and at the plasma membrane in a PI3K-dependent manner. Deletion of the entire PH domain or mutation of the threonine 513 within the PH domain, which is phosphorylated by PDK1 itself, inhibits the homodimer formation, favouring the monomeric PDK1 fraction and increases AKT Thr308 phosphorylation (Masters et al., 2010). This report identified the monomeric PDK1 form as a more active form in activating AKT compared to the homodimeric PDK1 form which resulted in an inhibited conformation. Therefore different mechanisms are

involved in AKT activation and the different steps showed above demonstrate a fine regulation of PDK1 pathway (Figure 1.20).

Although PDK1 was discovered for its ability to phosphorylate AKT, many other kinases are now known to act downstream of PDK1. For example the AGC kinases members serum glucocorticoid kinase (SGK), p70 ribosomal protein S6 kinases (S6K), p90 ribosomal protein S6 kinase (RSK), P21-activated kinases 1 (PAK1) and atypical protein kinase C (PKC) isoforms are known to be direct targets of PDK1, which phosphorylates specific serine/threonine residues of their activation loops (Mora et al., 2004). For this reason PDK1 has a main role in controlling cell proliferation, survival and cell motility and it has been termed “master AGC kinase”. The mechanism of activation of the PDK1-dependent kinases differs from the AKT activation mechanism. These protein kinases lack the PH domain but possess a hydrophobic motif that interacts with PDK1. The hydrophobic motif, also called PDK1 interacting fragment (PIF), lies in a conserved Phe-Xaa-Xaa-Phe/Tyr-Ser/Thr-Phe/Tyr sequence that undergoes phosphorylation in serine or threonine (Pearce et al., 2010). Phosphorylation of this site increases the binding of PDK1 to the hydrophobic motif, leading to the phosphorylation of the targeted kinases activation loop (Pullen et al., 1998; Alessi et al., 1998) (Figure 1.21). Mutagenesis of the hydrophobic motif decreases the PDK1-dependent phosphorylation of the activation loop. PDK1 is the only member of the AGC kinase family that lacks the hydrophobic motif, but structural analysis revealed that PDK1 presents a hydrophobic pocket, termed PDK1 interacting fragment pocket (PIF pocket), which is essential for PDK1 interaction with the hydrophobic motif of the targeted protein kinases (Biondi et al 2002). Mutations within the PDK1 PIF pocket abolish the binding of PDK1 to PKC, S6K and SGK1 and their subsequent phosphorylation and activation (Biondi et al., 2002). Therefore the PIF pocket represents a docking site that binds the PIF hydrophobic motif and promotes the phosphorylation of the activation loop of the targeted kinase.

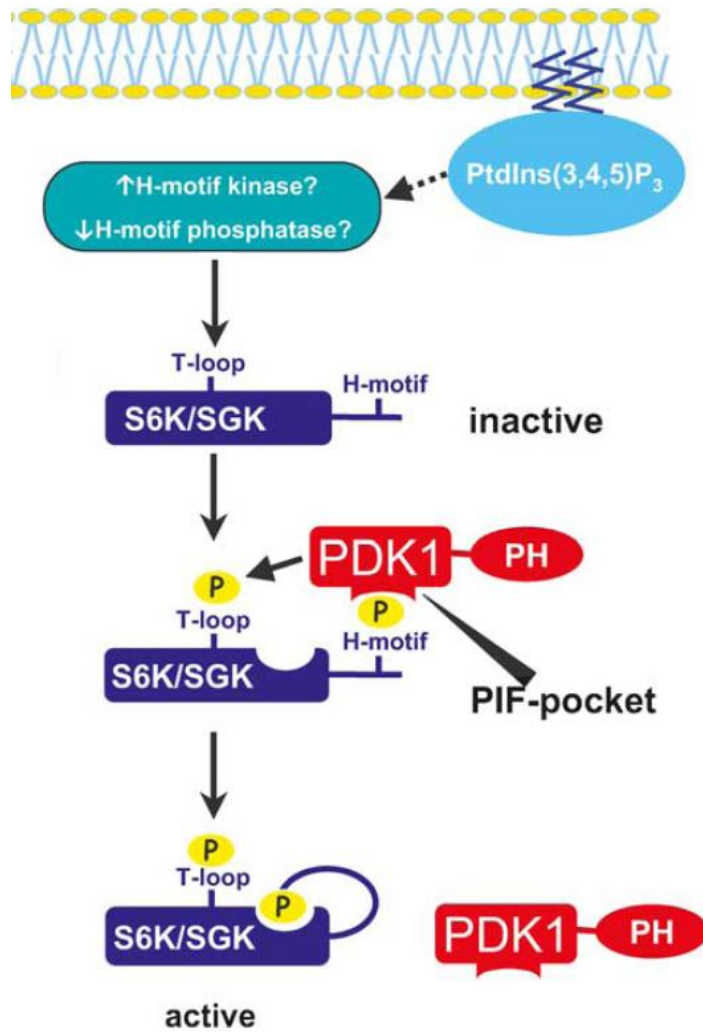


**Figure 1.21:** Mechanism of activation of S6K and SGK kinases by PDK1 (adapted from Mora et al., 2004)

#### 1.7.4 PDK1 as therapeutic target

Although several data showed that PDK1 plays an important role in cancer, no inhibitors were found to specifically inhibit PDK1. Many compounds able to inhibit PDK1 are small molecule inhibitors belonging to the class of ATP-competitive protein kinases inhibitors. These inhibitors compete for the ATP-binding to the kinase domain but often present off-target effects, being able to compete with the ATP binding of other protein kinases (Peifer and Alessi, 2008). Biochemical and structural data on the mechanism of action of PDK1 indicate that two additional

classes of PDK1 inhibitors could be exploited as druggable targets: the PIF pocket binding allosteric ligands and the PH domain competitors. A compound has been recently discovered in recent work performed by my group. The 2-O-*Bn*-InsP<sub>5</sub> is an inositol derivative compound with specific PDK1 inhibitor activity presenting anticancer and pro-apoptotic properties *in vivo*, able to block AKT Thr308 phosphorylation in cell lines and in excised tumours (Falasca et al., 2010). It has been proposed that inositol phosphates can bind PDK1 PH domain and retain this kinase in the cytosol, preventing Akt phosphorylation at Thr308 (Komander et al., 2004). New specific and potent inhibitors such as GSK2334470 (Najafov et al., 2010) and a pyridinonyl-based compound (Nagashima et al., 2010) were recently characterised and showed high selectivity and high potency in inhibiting PDK1. Therefore an increasing number of reports discovered the importance of PDK1 as a central hub in cancer development. However in the future it will be important to investigate *in vivo* the pharmacological inhibition of PDK1 on tumour models, and eventually determine the pharmacokinetic and metabolic properties of specific PDK1 inhibitors identified for pre-clinical trials.

### **1.8 Inositol phosphates: promising lead compound for anticancer molecule development**

Key enzymes such as AKT, PDK1 and PLC $\gamma$ 1 which are involved in cell proliferation, resistance to apoptosis and increased cell motility possess a PH domain that interacts with phosphoinositides and in particular with the 3-phosphorylated- phosphoinositides, in a mechanism that is essential for the enzyme activation. As described in chapter 1.2.4 it has been reported that PH domains can also bind to inositol polyphosphates, the soluble head-group of phosphoinositides. For instance Grp1-PH domain binds with high affinity the Ins(1,3,4,5)P<sub>4</sub> with a K<sub>D</sub> of 27.3 nM and with lower affinity to other inositol polyphosphates (Lemmon et al., 1998). Similarly, structural studies showed that BTK-PH domain and AKT-PH domain

binds to Ins(1,3,4,5)P<sub>4</sub>. BTK-PH domain interacts with 3-, 4- and 5-phosphates with the side chains of two acidic residues and with the backbone of the L1/L2 loop. This high number of contacts is sufficient to guarantee a stable interaction and accounts for the high affinity and specificity of the Btk PH domain for Ins(1,3,4,5)P<sub>4</sub> over Ins(1,4,5)P<sub>3</sub> (Maffucci and Falasca 2001). In the case of AKT PH domain, the interaction with Ins(1,3,4,5)P<sub>4</sub> leaves the 6-OH group exposed to the solvent, suggesting that the binding site could accommodate the phosphate group presented in the Ins(1,3,4,5,6)P<sub>5</sub> (Thomas et al 2003). These data suggested that inositol polyphosphates may be used as phosphoinositides antagonist, competing for binding the PH domain (Figure 1.22).

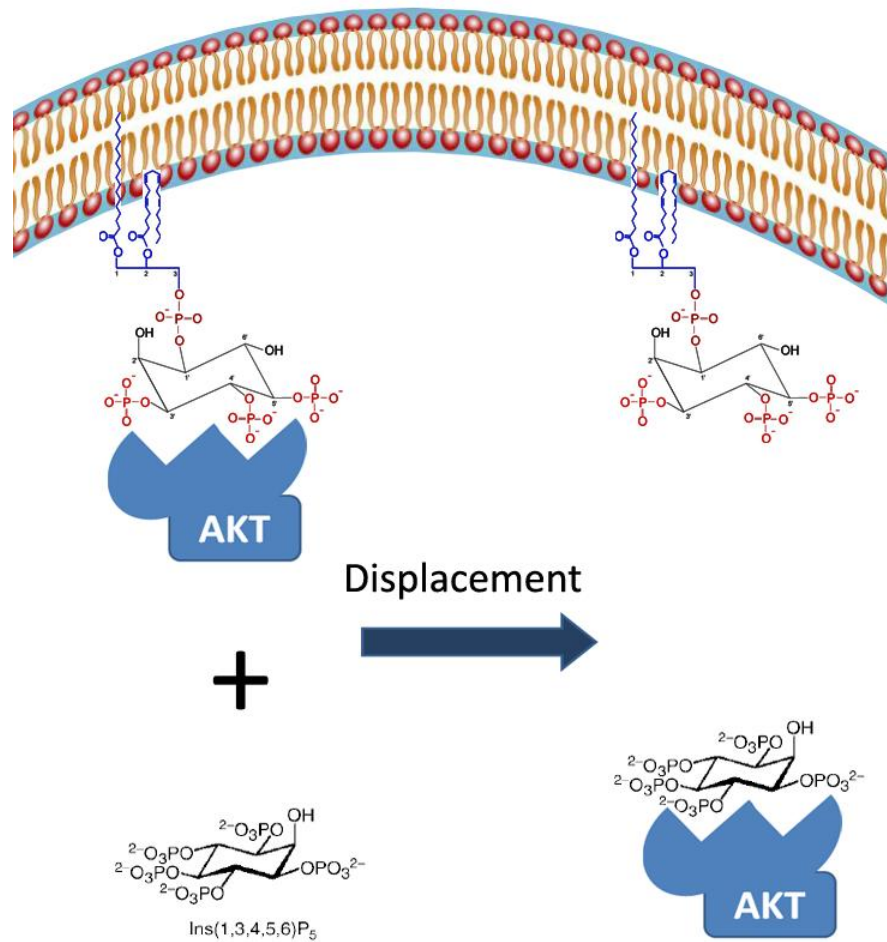


**Figure 1.22:** Representation of the mechanism through which Ins(1,3,4,5,6)P<sub>5</sub> may inhibit AKT by competing with PtdIns(3,4,5)P<sub>3</sub> for binding AKT-PH domain.

It has been proposed that just as specific phosphoinositides activate different pathways in cells, specific inositol phosphates may block those pathways acting as specific antagonists (Berrie and Falasca, 2000). About 20 years ago it was discovered that a diet rich in inositol hexakisphosphate (InsP<sub>6</sub>), named also phytic acid, correlates negatively with colon cancer (Vucenik et al., 2003). It was demonstrated that InsP<sub>6</sub> is internalized by cancer cells (Vucenik et al., 1994). Analysis of <sup>3</sup>H labelled InsP<sub>6</sub> uptake and metabolism showed that InsP<sub>6</sub> is quickly uptaken in colon cancer cell lines and after 1 hour 56% of radioactivity is in InsP<sub>6</sub> form while the rest is in form of dephosphorylated inositol phosphates metabolic products (Sakamoto et al., 1993).

InsP<sub>6</sub> is a dietary supplement with antioxidant properties and it is also found in mammalian cells (Szwergold et al., 1987). InsP<sub>6</sub> has been found to be active in inhibiting tumour growth of leukemic hematopoietic cell line, breast, hepatoma, colon cell lines *in vitro* with different degrees of sensitivity accordingly to the cell lines (Shamsuddin et al., 1999; Singh et al., 2003). Furthermore InsP<sub>6</sub> showed protective effect for colon and breast cancer induced by different carcinogens and metastases formation in mice models injected with fibrosarcoma cells (Vucenik et al., 2003) and presents antiangiogenic properties *in vitro* and *in vivo* being able to inhibit tubulogenesis *in vitro* and blood vessel neogenesis induced by b-FGF *in vivo* (Vucenik et al., 2004). Treatment of Transgenic Adenocarcinoma of Mouse Prostate (TRAMP) mice with InsP<sub>6</sub> in drinking water reduced the progression of prostate cancer lesions without any toxicity (Raina et al., 2008). All these evidences together points out that InsP<sub>6</sub> is able to prevent tumour growth and correlates with etiological evidences that diet rich in InsP<sub>6</sub>-containing foods associates with protection against colon and prostate cancer (Vucenik et al., 2003). InsP<sub>6</sub> was shown to enhance the effect of Tamoxifen and Doxorubicin in breast cancer cell lines MDA-MB-231 and MCF7 and in breast cancer cells derived from primary tumour, in a synergistic manner *in vitro*, suggesting the potential usage of this compound as adjuvant therapy (Tantivejkul et

al., 2003). However the  $IC_{50}$  of  $InsP_6$  in inhibiting tumour cell growth *in vitro* is between 1.26mM and 4.18mM according to the sensitivity of cancer cells. Although  $InsP_6$  treatment does not result in toxic effect in mice even at elevated concentrations (Ullah et al., 1990, Vucenik et al., 1995; Raina et al., 2008), it has to be noted that concentration of  $InsP_6$  (up to millimolar range) may result in reduced levels of multivalent cations and subsequent cell death due to its polyvalent cation-binding-properties (Torres et al., 2005). Moreover the high dose required to inhibit cell growth underlines a lack of molecular selectivity and specificity. One or more catabolic products of the  $InsP_6$  metabolism within the cells may be the  $InsP_6$ -derivated active compounds responsible for the biological effects of  $InsP_6$ . This could also explain the high doses needed to inhibit tumour growth. It was recently demonstrated that *in vivo* exogenous  $IP_6$  is rapidly dephosphorylated in plasma to inositol and to lower IPs (Eiseman et al., 2011). Moreover several lines of evidence suggest that the gut flora plays an essential role in  $InsP_6$  dephosphorylation and absorption. Indeed animals lacking the gut flora fail to incorporate detectable  $InsP_6$  (Wise and Gilbert, 1982; Sakamoto et al., 1993). These data suggest that although inositol phosphates present anti-tumour effects their effectiveness could be limited on tumour distant from the gastro-intestinal tract (Eiseman et al., 2011).

The effect of inositol phosphates has been tested *in vitro* and *in vivo* on tumour growth in the last 10 years. In particular among all the inositol polyphosphates, the inositol tetrakisphosphates  $Ins(1,4,5,6)P_4$  and pentakisphosphates  $Ins(1,3,4,5,6)P_5$  were found to inhibit cell growth and the anchorage-independent growth in breast cancer, ovarian and small cell lung cancer (SCLC) cell lines. Furthermore pre-treatment of cells with 50 $\mu$ M  $Ins(1,4,5,6)P_4$  blocked the growth factor-induced membrane translocation of overexpressed GFP-PH-AKT, indicating that this compound might be a selective inhibitor of PI3K/AKT pathway. Indeed, cell lines whose cell growth is PI3K independent and insensitive to the PI3K inhibitors LY294002 and Wortmannin, are also insensitive to

Ins(1,4,5,6)P<sub>4</sub> treatment (Razzini et al., 2000). Further work demonstrated that Ins(1,3,4,5,6)P<sub>5</sub> is the most potent inhibitor of PI3K/AKT pathway among the totality of inositol phosphates. Indeed Ins(1,3,4,5,6)P<sub>5</sub> induced apoptosis in ovarian cancer similarly to cisplatin and etoposide treatment and inhibited AKT S473 phosphorylation in ovarian and breast cancer cell lines that present increased activation of PI3K pathway. On the contrary proliferation of MDA-MB-231 and MCF7, which do not possess a constitutively activated PI3K/AKT pathway, were insensitive to Ins(1,3,4,5,6)P<sub>5</sub> treatment (Piccolo et al., 2004). *In vivo* experiments showed that Ins(1,3,4,5,6)P<sub>5</sub> blocks tumour growth in ovarian cancer cell line SKOV3 xenografted in mice and inhibits AKT S473 and T308 phosphorylation and also inhibits FGF-2-induced angiogenesis. Indeed Ins(1,3,4,5,6)P<sub>5</sub> prevents cell migration and tubulogenesis induced by FGF-2 in human umbilical vein endothelial cells (HUVEC) both *in vitro* and *in vivo* through the inhibition of PI3K/AKT pathway which is also involved in the angiogenesis process (Maffucci et al., 2005). Therefore targeting PI3K/AKT pathway is an attractive therapeutic target as much as the possibility to use natural compounds such as Ins(1,3,4,5,6)P<sub>5</sub> or synthetic derivative compound in order to inhibiting this pathway.

Since mono therapy in cancer treatment showed limited effects, adjuvant therapies are often applied to cancer patient. In this prospective *in vitro* treatment of SKOV3 cells with Ins(1,3,4,5,6)P<sub>5</sub> and cisplatin, the main anticancer drug used for ovarian cancer treatment, showed a more than additive effects providing evidence that this compound is able to sensitise cancer cells to the cytotoxic anti-cancer drugs (Piccolo et al., 2004).

The constant research for novel PI3K/AKT pathway inhibitors, characterised by decreased toxic effects and improved potency and selectivity, induced my group in the last years to test inositol derivative compounds for their ability to inhibit the PI3K/AKT pathway. It was recently published that a benzene-tetrakisphosphate compound [Bz(1,2,3,4)P<sub>4</sub>], an inositol phosphate surrogate, binds to AKT PH domain

with similar affinity to Ins(1,3,4,5)P<sub>4</sub> (Mills et al., 2007). Modification of the Ins(1,3,4,5,6)P<sub>5</sub> and analysis of X-ray structure of AKT PH domain showed that a tyrosine residue near the 6-OH of bound Ins(1,3,4,5,6)P<sub>4</sub> might interact with an aromatic group. As reported in Falasca et al., 2010, among different inositol phosphates tested on AKT activation, 2-*O*-Bn-InsP<sub>5</sub> resulted in AKT inhibition. In particular, 2-*O*-Bn-InsP<sub>5</sub> was more effective than Ins(1,3,4,5,6)P<sub>5</sub> in inhibiting growth and inducing apoptosis in SKBR3 and SKOV3 cell lines, which are sensitive to Ins(1,3,4,5,6)P<sub>5</sub> treatment. Strikingly, 2-*O*-Bn-InsP<sub>5</sub> induced apoptosis in Ins(1,3,4,5,6)P<sub>5</sub>-resistant cell lines such as prostate cancer PC3, pancreatic cancer ASPC1 and breast cancer MDA-MB-468, inhibiting the phosphorylation of AKT in Ser473 and Thr308 *in vitro*. *In vivo* xenograft experiments using PC3 cells showed that 2-*O*-Bn-InsP<sub>5</sub> inhibited tumour growth and phosphorylation of AKT at Ser473 and Thr308, while Ins(1,3,4,5,6)P<sub>5</sub> had no effect on tumour growth and AKT phosphorylation. Kinase profiling showed that 2-*O*-Bn-InsP<sub>5</sub> is a very specific and potent inhibitor of PDK1 which is involved in AKT activation (Falasca et al., 2010).

# **Chapter 2**

## **Materials and Methods**

## 2.1 Cell culture

### 2.1.1 Cell lines

The cell lines used in the experiments performed in this thesis are listed in Table 2.1 Cells were available in the laboratory of Professor Marco Falasca unless otherwise stated.

<b>MDA-MB-231</b>	<p><b>Organ:</b> mammary gland; breast  <b>Disease:</b> adenocarcinoma  <b>Derived from metastatic site:</b> pleural effusion  <b>Cell Type:</b> epithelia</p> <p>The cell line originates from a pleural effusion of an earlier breast adenocarcinoma. MDA-MB-231 shows aneuploidy (modal number = 64, range = 52 to 68), with chromosome counts in the near-triploid range.</p>
<b>MDA-MB-435</b>	<p><b>Organ:</b> mammary gland; breast  <b>Disease:</b> adenocarcinoma  <b>Derived from metastatic site:</b> pleural effusion  <b>Cell Type:</b> epithelial</p> <p>A controversy originates about the true origins of these cells. MDA-MB-435 cell line was identified as breast cancer cells. Marker expression studies and genomic analysis questioned the breast origin and classified this cell line as melanoma cell line (Elison et al., 2002; Garraway LA). Recent update confirmed the MDA-MB-435 as a poorly differentiated breast tumour cell line with expression of both melanocytic and epithelial markers (Chambers 2009)</p>
<b>TSA</b>	<p><b>Organism:</b> <i>Mus Musculus</i>  <b>Organ:</b> mammary gland</p> <p>TSA is an aggressive and poorly immunogenic cell line established from a moderately differentiated mammary adenocarcinoma that arose spontaneously in a multiparous BALB/c mouse.</p>
<b>A375M</b>	<p><b>Organ:</b> Skin  <b>Disease:</b> Invasive melanoma</p>
<b>HEK293T</b>	<p><b>Organ:</b> embryonic kidney  <b>Cell type:</b> transformed with adenovirus 5 DNA</p>
<b>4T1</b>	<p><b>Organism:</b> <i>Mus musculus</i>  <b>Organ:</b> mammary gland  <b>Disease:</b> tumour</p> <p>4T1 cell line is a mouse syngenic model of breast cancer. 4T1 produces highly metastatic tumors in BALB/c mice that can metastasise to the lung, liver, lymph nodes and brain while the primary tumor is growing in situ.</p>

<b>HUVEC</b>	<b>Organ:</b> Human umbilical vein <b>Cell type:</b> Endothelial HUVEC are responsive to cytokine stimulation and are commonly used for physiological and pharmacological investigations.
--------------	---

### 2.1.2 Cell culture and propagation

MDA-MB-231 and Human embryonic kidney cells were cultured in DMEM growth media (Invitrogen) supplemented with 10% (v/v) Foetal Bovine Serum (FBS) (Invitrogen), Sodium Pyruvate 1% (v/v), 1X L-glutamine/penicillin/streptomycin (Invitrogen) and 0.1% gentamycin (v/v) (Invitrogen, UK). MDA-MB-435, 4T1, TSA and A375M were cultured in RPMI 1640 growth media (Invitrogen or PAA, UK) supplemented with 10% (v/v) Foetal Bovine Serum (FBS), Sodium Pyruvate 1% (v/v), 1X L-glutamine/penicillin/streptomycin and 0.1% gentamycin (v/v). Cells were seeded in tissue culture treated plastic 10 cm dishes or the appropriate 6 cm petri dishes, multi-well dishes (BD, UK) and grown in humidified incubator at 37°C in a 5% CO<sub>2</sub> atmosphere.

### 2.1.3 Cell amplification and passage

All cells lines were passaged when 80-85% confluent. Growth medium was aspirated and cells were washed twice in 5ml of sterile phosphate buffered saline solution (PBS) (PAA, Austria) for 20-30 seconds and then incubated with 3ml of trypsin (0.25%)/EDTA(0.2g/l) (PAA, Austria) solution to detach the cells. After 3-5 minutes, cells were harvested in 5ml of the appropriate complete growth media and gently pipetted up and down before being pelleted by centrifugation at 250g for 5 minutes at room temperature in 15ml or 50ml centrifuge tubes (Falcon-BD, UK). Cell pellets were resuspended in the appropriate growth media and re-plated as required in new tissue culture plates. Cells were passaged every 2-3 days. Growth media was changed every 48 hours when needed.

#### **2.1.4 Cryo-conservation and recovery of cell lines**

Cells in a 10 cm petri dishes were detached when 80-85% confluent. Cells were washed in 1X PBS and incubated with 3ml of trypsin (0.25%)/EDTA(0.2g/l) solution to detach the cells. After 3-5 minutes, cells were harvested in 5ml of the appropriate complete growth media and recovered by centrifugation at 250g for 5 minutes at room temperature. Cell pellets were resuspended in 1ml of 90% FBS:10% DMSO (Sigma Aldrich, UK) freezing solution and the total volume transferred in cryovials (VWR) for cell storage in aliquots of 1ml per cryovial. Cells were wrapped in tissue paper and stored at -80°C in a polystyrene box for a time minimum of 24 hours up to 1 month before being transferred into liquid nitrogen for long term storage.

## **2.2 Molecular Biology**

### **2.2.1 Proteins**

#### **2.2.1.1 Western blotting analysis**

##### **2.2.1.1.1 Protein sample preparation from cell lysates**

Cell were plated in tissue culture treated 6 well plates. Cells were detached from 10 cm petri dishes when 80-85% confluent as described in chapter 2.1.3. The pellet was resuspended in 10 ml of growing media and an aliquot of 2 ml of the resuspended pellet was diluted in 10 ml of growing media. Then 2 ml of the diluted resuspension were added in each well of a 6-well plate. Alternatively 1 ml of the diluted resuspension was added in each well of a 12-well plate. When necessary, the day after being plated, cells were cultured in serum free growth media for 24 hours before stimulation and then lysed. Cells were washed twice in 1X PBS and lysed in 200µl of cold NP-40 lysis buffer (50mM Tris-pH 8.0; 50mM KCl, 1% (v/v) NP-40) containing 1X protease inhibitor

cocktail (Sigma-Aldrich, UK) and 1X phosphatase inhibitor cocktail II (Sigma-Aldrich, UK). Scrapers were used to detach the cells from the plastic dish and destroy cellular integrity. Lysate was collected in 1,5 ml tubes (VWR, UK) and cleared from cell debris and cell membrane by centrifugation at 10,000g for 3 minutes. The supernatant was transferred to a new 1.5 ml tube used for protein quantification and subsequent western blot analysis. Cell lysates were stored at -20°C or -80°C for long conservation.

#### **2.2.1.1.2 Bradford protein assay**

Protein concentration was determined by Bradford protein assay. Bovine Serum Albumin (BSA) (Sigma-Aldrich, UK) was used to establish a standard calibration curve for protein quantification. Table 2.2 shows a typical standard curve preparation. 1µl of lysate was added to 199µl of 1X Bradford solution (Bio-Rad, UK). The absorbance of the standards and of the samples was measured at 595 nm using a plate reader. A linear calibration curve was set using Microsoft Excel® plotting BSA concentration (X axis) and absorbance value (Y axis). The linear equation for the standard curve was calculated by the software. Standard curve with a minimum  $r^2=0.97$  was used to determine sample protein concentration. The unknown protein concentration of the lysates was calculated using the following formula:

$$\text{Abs}=\text{mx}+\text{b}$$

Abs=Absorbance; m=slope of the line; x=protein concentration; b=Y intercept

Protein samples were diluted in 5X denaturing sample buffer (see Appendix 1.1) and heated at 95°C for 5 minutes. The denatured protein samples were used for Polyacrylamide Gel Electrophoresis (PAGE) and Western blot analysis. The denatured sample buffers were stored at 4°C or at -20 for short and long period storage respectively.

Table 2.2: BSA Standard curve protein concentration

Biorad protein assay	1X Bradford reactive	BSA 200 µg/ml (µl)	BSA (µg/ml)
<b>Standard curve</b>	200	0	0 µg/ml
	198	2	0.4 µg/ml
	196	4	0.8 µg/ml
	194	6	1.2 µg/ml
	192	8	1.6 µg/ml

1X Bradford solution was prepared diluting 5X Bradford Bio-Rad protein assay solution (Bio-Rad Laboratories, UK) in ddH<sub>2</sub>O.

### 2.2.1.1.3 Polyacrylamide Gel Electrophoresis (PAGE) and Western blot

Two dedicated glass plates were assembled in a gel electrophoresis apparatus (Bio-Rad Laboratories, UK). A 10% resolving polyacrylamide gel solution was prepared and poured between the two glass plates, overlaid with 1.5ml of water and left at RT for 20-25 minutes to polymerize. Then, the water was removed and a 5% stacking solution was added on top of the previously set resolving gel and cast with 10 or 15 sample combs on top. Polymerization was allowed at RT for about 30 minutes (see appendix 1.2 and 1.3).

After removing the comb, each well of the gel was washed with ddH<sub>2</sub>O. Previously denatured protein samples were loaded on the gel and gel electrophoresis performed in 1X running buffer (Appendix 1.4). A constant

voltage of 120V was used for gel-electrophoresis. Electro-blotting from the gel onto a Protran® nitrocellulose membrane filter (Whatman, UK) was performed in 1X transfer buffer (see appendix 1.5) using a dedicated apparatus (Bio-Rad Laboratories). Transfer was performed at constant current of 400mA for 1 hour and 30 minutes at RT in presence of a dedicated icepack within the tank. The correct protein transfer was assessed by staining with Ponceau solution (Applichem GmbH, UK). The solution was incubated for 2 minutes at RT. Membrane were washed in ddH<sub>2</sub>O in order to remove the excess of Ponceau solution and visualize protein staining.

#### 2.2.1.1.4 Immunoblotting and analysis

Nitrocellulose membrane was incubated with a solution of 5% milk (w/v) (Invitrogen) in PBS-0.05%Tween-20 (v/v) for 30 minutes before being transferred in PBS-0.05%Tween-20 (v/v) solution containing the diluted primary antibody (table 2.3) and incubated at 4°C overnight in agitation. The following day the membrane were washed 3X for 10 minutes in PBS-0.05%Tween-20 (v/v) and incubated with agitation at RT for 1 hour with the appropriate peroxidase-conjugated secondary antibodies anti-mouse (GE Healthcare, UK) (1:8,000), anti-rabbit (Sigma-Aldrich, UK) (1:8,000) or anti-goat (GE Healthcare, UK) (1:20,000) diluted in PBS-0.05%Tween-20 (v/v). Membranes were then washed 3X 5 minutes in PBS-0.05%Tween-20 (v/v) and 1X 5 minutes in PBS before being incubated with ECL Plus Mix solution (Amersham Bioscience, UK) for 1 minute, sealed in a plastic sheet and exposed to chemiluminescence sensitive film (Kodak) in a dedicated cassette, usually from 15 seconds to 10 minutes.

Table 2.3: List of Antibodies used for WB

Antibody	Company	Catalog #	Host	Dilution
PLC $\gamma$ 1	Santa Cruz	SC-7290	Mouse	1:1000
pPLC $\gamma$ 1	Cell signalling	2821	Rabbit	1:500

<b>PDK1</b>	Cell signalling	3062	Rabbit	1:500
<b>PLC<math>\gamma</math>2</b>	Santa Cruz	SC-5283	Mouse	1:500
<b>AKT 1/2/3</b>	Santa Cruz	Sc-8312	Rabbit	1:1000
<b>pAKT Ser473</b>	Santa Cruz	Sc-7985	Rabbit	1:500
<b>pAKT Thr308</b>	Cell signalling	2965	Rabbit	1:500
<b>ERK1/2</b>	Santa Cruz	sc- 135900	Goat	1:1000
<b>Anti-HA</b>	Sigma-Aldrich	H3663	Mouse	1:500
<b>GAPDH</b>	Sigma-Aldrich	G9545	Rabbit	1:2500

### 2.2.1.2 Co-immunoprecipitation analysis

#### 2.2.1.2.1 Co-immunoprecipitation analysis by Millipore Catch and release KIT 2.0 (Millipore, US)

Co-immunoprecipitation in overexpressing conditions was performed using HEK293 cells transfected with pOZ-PDK1 and PRK5-PLC $\gamma$ 1 constructs as indicated in “plasmid transfection” paragraph. Three six centimetre dishes were used for each co-immunoprecipitation. Cells were lysed using the NP-40 lysis buffer (50mM Tris-pH 8.0, 50mM KCl, 1% (v/v) NP-40) containing protease and phosphatase inhibitors. Protein lysates were cleared from cell debris by centrifugation step at 10,000 RPM for 3 minutes at 4°C. In parallel, spin columns from the kit were washed by adding 400 $\mu$ l of 1X catch and release wash buffer and centrifuged for 30 seconds at 2,000g. Then 500  $\mu$ g of protein were loaded onto the spin columns together with 3 $\mu$ g of primary antibody or 3 $\mu$ g of IgG as negative control, and with 10 $\mu$ l of antibody capture

affinity ligand. 1X wash buffer was added to provide a final volume of 500  $\mu$ l. Columns were incubated at 4°C overnight. The day after spin columns were centrifuged for 30 seconds at 2,000g and the flow-through collected. This fraction was used later to check the immunoprecipitation efficiency by western blot analysis. Spin columns were washed 3 times with 1X washing buffer and spinned at 2,000g for 30 second for each wash. The immunoprecipitated complex was eluted in 70  $\mu$ l of 1X denaturing sample buffer by centrifugation at 2,000g for 1 minute. The eluted fraction was heated at 95°C for 5 minutes before western blot analysis.

#### **2.2.1.2.2 Endogenous co-immunoprecipitation analysis**

Endogenous co-immunoprecipitation assay was performed using three confluent 10 cm petri dishes of MDA-MB-231, MDA-MB-435 and A375M. Cells were lysed using the NP-40 lysis buffer (50mM Tris-pH 8.0, 50mM KCl, 1% (v/v) NP-40) containing protease and phosphatase inhibitors. In both cases 1 mg of the whole protein lysed was mixed with 3  $\mu$ g of anti-PLC $\gamma$ 1 antibody (Santa Cruz Biotechnology Inc., US) and incubated on a rotating wheel overnight at 4°C to a final volume of 700  $\mu$ l in IP buffers. The following day the mix was centrifuged at 10,000g for 3 minutes and transferred to a new clean tube. The mixture was then incubated with 30  $\mu$ l of protein G Sepharose 4 fast flow (GE Healthcare, UK) and incubated on a rotating wheel at 4°C for 1 hour. Beads were centrifuged at 2,000g for 1 minute. Then, supernatant was removed and the beads were washed three times with IP buffer on a rotating wheel at 4°C for 5 minutes. Then beads were resuspended in 50  $\mu$ l of 2X sample buffer and heated at 95°C for five minutes. The supernatant was analysed by SDS-PAGE electrophoresis and western blot.

#### **2.2.1.3 GST-Pull down assay**

Three sets of three 6-cm petri dishes, previously seeded with HEK293, were transfected respectively with PRK5-PCL $\gamma$ 1, pEBG2T-GST-PDK1 and pEBG2T-GST empty vector. 24 hours from transfection cells were lysed in lysis buffer (50mM Tris-pH 8.0, 50mM KCl, 1% NP-40) containing protease

and phosphatases inhibitors. Lysates were cleared by centrifugation at 10,000g for 3 minutes at 4°C. 500 µg of HEK293 overexpressing GST-empty vector and 500 µg of HEK293 lysate overexpressing GST-PDK1 were incubated separately with 20 µl of G4510 glutathione-Sepharose-beads (Sigma-Aldrich) for 1 hour at 4°C. The beads were washed 3X in washing buffer for 5 minutes at 4°C. Beads were incubated with 500 µg of protein lysate of HEK293 overexpressing PLCγ1 overnight on a rotating wheel at 4°C in a total volume of 1 ml in IP buffer. The following day beads were harvested and washed 3X with IP washing buffer and the beads resuspended in 50 µl of denaturing sample buffer and heated at 95°C for 5 minute (see appendix 1.1). Supernatant was analysed by SDS-PAGE electrophoresis and western blot.

## **2.2.2 RNA-interference**

### **2.2.2.1 siRNA using Oligofectamine transfecting agent**

Transient knock down of target proteins was achieved using siRNA duplex technology. siRNAs were purchased from Dharmacon, USA (Appendix 2.2). Transfection of MDA-MB-231 and MDA-MB-435 was performed using Oligofectamine<sup>TM</sup> (Invitrogen, UK) following the manufacturer's instruction for transfection of adherent cells seeded in 6-well plates.  $2 \times 10^6$  cells/well were seeded the day before transfection in complete growth media and incubated at 37°C/5% CO<sub>2</sub>. A mix (A) of 5µl siRNA duplexes (stock solution of 20 µM) and 180 µl of serum-free, penicillin-streptomycin-free Optimem<sup>TM</sup> (Invitrogen, UK) was prepared. In parallel a mix (B) of 7.5µl of Oligofectamine<sup>TM</sup> and 7.5 µl of serum-free, penicillin-streptomycin-free Optimem<sup>TM</sup> (Invitrogen, UK) was prepared. The two mixes were incubated for 7 minutes at RT. Subsequently the content of the tubes was mixed and incubated 25 minutes RT resulting (total volume of 200 µl). Cells were washed in 1X PBS solution and 800 µl of Optimem<sup>TM</sup> plus the 200 µl of transfecting mix were added to each well and incubated for 4 hours at 37°C

/5% CO<sub>2</sub>. At the end of the incubation time, 500 µl of 30% FBS Optimem™ (v/v) were added to the 6 well and incubated overnight at 37°C/5%CO<sub>2</sub>. The following day cells were washed with 1X PBS solution and incubated with normal growth media for the indicated time before the experiment. Cells transfected with a pool of non-targeting siRNA (Applied Biosystem/Ambion Inc., USA) were used at the same final concentration as negative control in all the experiments.

#### **2.2.2.2 siRNA using Hiperfect reagent**

Transient knock-down of target proteins was achieved using siRNAs in A375M cell line. Cells were transfected using Hiperfect® transfecting agent (Qiagen Ltd, UK) following the protocol provided by the manufacturer, optimised for transfection of adherent cells in 6-well plate. 2X10<sup>6</sup> cells were seeded in 6 well plates and grown in complete RPMI growth media at 37°C/5%CO<sub>2</sub>. The day after, 100µl of Optimem™ were mixed with 7.5 µl of 20µM siRNA stock solution and 18µl of Hiperfect® in a tube and mixed by vortexing for 5 seconds. The mix was incubated for 10 minutes at RT and then added to the growth media in the 6-well plate. The cells were incubated with the transfection complex overnight at 37°C/5%CO<sub>2</sub> and media was replaced the following day. Cells transfected with a pool of non-targeting siRNA (Applied Biosystem/Ambion Inc., USA) were used at the same final concentration as negative controls in all the experiments.

#### **2.2.2.3 stable knock down using short hairpin RNA**

##### **2.2.2.3.1 Stable knock-down of PLCγ1 using pSUPER™.retro vector-based shRNA**

MDA-MB-231, MDA-MB-435 and TSA cell lines stable knock-down for PLCγ1 were previously generated in the lab using the pSUPER™.retro vector-based RNAi system (Oligoengine Inc. USA). A 19 nucleotide sequence derived from the mRNA PLCγ1 transcript were cloned in the vector

following the vector instruction. A 3 point-mutated non-targeting sequence was cloned in the vector and used as control for all the experiments (see table 2.4)

Table 2.4: The PLC $\gamma$ 1 targeting sequence cloned in pSUPER.retro vector together with the position in the cDNA is indicated. 3-point mutation of the control non-targeting sequence is indicated in **RED**.

PLC $\gamma$ 1 targeting sequence: GAACAACCGGCTCTTCGTC
Position in cDNA 2791nt of 5205
3MUT control non-targeting sequence: GAACAACCG <b>ACG</b> TTTCGTC

#### **2.2.2.3.2 Inducible knock-down of PLC $\gamma$ 1 using pSUPERIOR<sup>TM</sup> vector-based shRNA**

Inducible downregulation of PLC $\gamma$ 1 was achieved using the (Oligoengine Inc. USA) vector-based system. MDA-MB-231 cells expressing the inducible downregulating system was previously generated in the lab. These cells express the tetracycline repressor encoded by the vector pCDNA<sup>TM</sup>6/TR (Invitrogen) and the pSUPERIOR vector-based RNA. The targeting sequence and the control non-targeting illustrated in table 2.4, were cloned in the pSUPERIOR.retro.puro as indicated by the manufacturer.

#### **2.2.2.3.3 Stable downregulation of PDK1 using pSUPER vector-based shRNA.**

Stable downregulation of PDK1 was achieved using the pSUPERIOR<sup>TM</sup>.retro.puro. The PDK1 targeting sequence was designed based on PDK1 targeting sequence used by Sahai et al., 2008. A Pair of forward and reverse oligonucleotides, which comprise identical motifs in an inverted orientation separated by a 9 nt spacer, were generated. The extremities were

designed in order to present BglII and HindIII sticky ends. A control non-targeting sequence was designed by mutating 5 nucleotides in the sequence (see table 2.5). 5 µg of vector were digested overnight with BglII and HindIII restriction enzymes (Fermentas, UK) according to the manufacturer's instruction. The cut plasmid was run on 1% agarose gel and extracted from the gel using the Genejet™ gel extraction kit (Fermentas, UK) following the manufacturer's instruction.

Table 2.5 The 21 target sequence in PDK1 mRNA molecule is indicated together with the position in the mRNA transcript. The target sequence is indicated in bold while the BglII and HindIII sites together with the 5-pointed mutation are indicated in grey.

<p>PDK1 targeting sequence: <b>GACCAGAGGCCAAGAATTTTA</b></p> <p>Position in mRNA 1658 nucleotide</p>	
<p>Forward and reverse oligonucleotides designed to target PDK1 expression.</p> <div style="text-align: center;"> <p><b>Sense target sequence</b>                      <b>Anti-sense target sequence</b></p> <p><b>Bgl II</b>                      <b>Hind III</b></p> <p>5'- GATCCCC<b>GACCAGAGGCCAAGAATTTTA</b> TTCAAGAGAT <b>AAAATTC TTGGCCTCTGGTC</b> TTTTTA-3'</p> <p>3'-----GGG CTGGTCTCCGTT CTAAAT AAGTT CTCTA TTTTAAGAACCGGAGACCAG AAAAATTCGA-5'</p> <p style="text-align: center;">Loop</p> </div>	
<p>Forward and reverse oligonucleotides designed with 5-point-mutation in order to generate a control non-targeting sequence.</p> <div style="text-align: center;"> <p><b>Sense target sequence</b>                      <b>Anti-sense target sequence</b></p> <p><b>Bgl II</b>                      <b>Hind III</b></p> <p>5'- GATCCCC<b>GACAGGAGGTCAAGGATTTGA</b> TTCAAGAGAT TCAAATCCTTGACCTC CTGTC TTTTTA-3'</p> <p>3'-----GGGCTGTC CTCCAGTT CCTAAACT AAGTT CTCTA AGTTTAGGAACTGGAGGACAG AAAAATTCGA-5'</p> <p style="text-align: center;">Loop</p> </div>	

### **2.2.3 DNA**

#### **2.2.3.1 Ligation and transformation**

Inserts were ligated in a previously digested vector mixing insert and linearized vector at a 3:1 molar ratio. 1 unit of T4 ligase (Fermentas, UK) was mixed with 50 ng of vector and the insert together with 2 µl of 10X T4 ligase buffer and made up to a final volume of 20 µl. The ligation reaction was incubated at RT overnight. Control reactions were performed without the inserts.

The generated constructs were transformed in DH $\alpha$  strain bacterial cells. Bacteria were thawed on ice for 20 minutes. 5 µl of ligation mixture were added to the cells and incubated on ice for 20 minutes. Cells were heat-shocked at 42°C for 60 seconds and held directly on ice for 30 seconds. 500 µl of pre-warmed LB media was added to the bacteria and the mixture was incubated at 37°C for 1 hour in agitation at 200 rpm. Then cells were spun down at 500 g for 3 minutes and resuspended in 250 µl of LB before being plated on LB-agar plates (LB media with 1,5% (w/v) bacteriological agar) containing 100 mg/ml ampicillin or 100 mg/ml Kanamycin according to the resistance conferred by the vector. The inoculated plates were incubated overnight at 37°C.

#### **2.2.3.2 DNA digestion**

Fastdigest® enzymes (Fermentas, UK) were used for all the restriction reactions. 1 µg of vector was digested mixing 1 µl of enzyme together with 2 ml of 10X fastdigest® buffer in a final volume of 20 µl. The Digestion reaction was performed for 30 minutes at 37°C. DNA digestion was assessed by agarose gel electrophoresis.

### **2.2.3.3 Plasmid preparation**

Plasmids were extracted and purified from bacteria using the spin miniprep kit (Qiagen, UK) for small-scale plasmid preparation, or the QIA filter plasmid maxi kit (Qiagen, UK) for the large-scale plasmid preparation.

### **2.2.3.4 Miniprep**

For small-scale preparation, resistant colonies obtained from the inoculated plates were picked individually using sterile tips and grown overnight in 5 ml of LB media at 37°C with agitation (200 rpm) containing the appropriate antibiotic for selection. The DNA plasmid was then extracted following the manufacturer's instructions.

### **2.2.3.5 Maxiprep**

For large scale preparation 300 ml of LB media supplemented containing the appropriate antibiotic for selection were inoculated with 2 ml starter culture, prepared as indicated in "miniprep" section, and incubated with agitation (200 rpm) overnight at 37°C. Plasmids were extracted according to the manufacturer's instructions.

### **2.2.3.6 Agarose-gel electrophoresis**

A 1% agarose (Sigma, Aldrich, UK) (v/w) solution in 1X TAE buffer (see appendix 1.6) was prepared heating the solution until the total amount of agarose was dissolved. The solution was cooled down at RT for 10 minutes. Ethidium bromide was added to a final concentration of 0.5 µg/ml and the mixture was poured into a gel-casting tray, cast with sample combs and left to set at RT. The set gel was transferred on an electrophoresis apparatus filled with 1X TAE buffer. The samples were diluted in 5X loading buffer (New England Biolabs, UK) and loaded on the gel in parallel to 5 µl of 1-KB ladder (Fermentas, UK) for size comparison. The gel was run at 100 V for 30-60 minutes and DNA visualised under UV transillumination.

### 2.2.3.7 Plasmid transfection

Transfection of mammalian cells was performed using Lipofectamine™ (Invitrogen, UK) following the manufacturer's instructions. The amount of Lipofectamine™ and DNA was optimized according to the cell line used (Table 2.5). A "mix A" and a "mix B", containing respectively Lipofectamine™, Optimem™ and DNA/ Optimem™ were prepared as illustrated in Table 2.6. The two mixes were incubated separately at RT for 15 minutes before being mixed and left to incubate for further 15 minutes at RT. Cells were washed with 1X PBS and incubated with the mix plus serum free Optimem™ to the final volume indicated. After 4 hours, cells were washed in 1X PBS and incubated in complete growth media for 24 hours or 48 hours depending on the experiment.

Table 2.6: Transfection protocol optimized for HEK293 and MDA-MB-231 in different culture dishes/plate

Cell line	Plate	Lipofectamine/Optimem (Mix A)	DNA/Optimem (Mix B)	Total Volume
<b>HEK293</b>	6 cm dishes	10 µl/200 µl	5 µg/200 µl	2 ml
<b>MDA- MB-231</b>	12-well plate	2 µl/50 µl	1 µg/50 µl	500 µl
	6 cm dishes	12 µl/200 µl	5µg/200 µl	2 ml

### 2.2.3.8 Polymerase chain reaction (PCR)

25 ng of plasmid was used as template using the “Maxima® hot start PCR master mix 2X”. A typical PCR reaction is illustrated in table 2.7 and 2.8.

Table 2.7: Typical PCR master mix

	Sample	Control
<b>Maxima® hot start PCR master mix 2X</b>	25 µl	25 µl
<b>Forward primer (100 mM)</b>	0.5 µl	0.5 µl
<b>Reverse primer (100 mM)</b>	0.5 µl	0.5 µl
<b>Template DNA</b>	5 µl	-
<b>H<sub>2</sub>O</b>	19 µl	24 µl
<b>Total Volume</b>	50	50

Table 2.8: Typical thermal-cycler program for PCR

	Temperature (°C)	Time	Cycles
<b>Initial denaturation/enzyme activation</b>	95	4 min	1
<b>Denaturation</b>	95	30 sec	35
<b>Annealing</b>	57	30 sec	
<b>Extension</b>	72	40 sec	
<b>Final extension</b>	72	10 min	1
<b>Hold</b>	4	Indefinite	

## 2.2.4 RNA

### 2.2.4.1 RNA extraction

Total RNA was extracted from  $2 \times 10^5$  cells seeded on 6 wells multiplate using the RNeasy kit (Qiagen, UK) following the manufacturer's instructions.

### 2.2.4.2 RNA Reverse transcription

Total RNA was retro-transcribed using the SuperScript II reverse transcriptase kit (Invitrogen, UK). 1  $\mu$ g of RNA was diluted in a mix containing oligod(T) and random primers (25mg/ml), dNTP mix (0.5 mM) to a final volume of 12  $\mu$ l. The mix was heated to 65 degrees for 5 minutes in a PCR thermal-cycler block and quickly moved on ice. A mix of 1X first strand buffer, DTT (5mM) and RNase OUT (40 units) (Invitrogen, UK) was added and the mix was heated at 42°C for 2 minutes in a PCR thermal-cycler, where 200 units of SuperScript II reverse transcriptase were added to the reaction. The PCR thermal-cycler was programmed as follows:

Table 2.9 RNA retrotranscription program indicated in manufacturer's instruction

	Temperature (°C)	Time (min)
<b>SuperScript II thermal-cycler program</b>	25	10
	42	50
	70	15
	4	(until tube collection)

### 2.2.4.3 Real Time quantitative Polymerase Chain Reaction (RT-qPCR)

For quantitative PCR 100 ng of cDNA was mixed with 12.5  $\mu$ l of 2X Maxima® SYBR green/Fluorescein qPCR master mix (Fermentas), 2.5  $\mu$ l of 10  $\mu$ M stock solution of forward and reverse primers to a final volume of 25  $\mu$ l. The ABI 7500 Real-Time PCR system was programmed as indicated in Figure 2.1. For each qPCR reaction a fragment from GAPDH cDNA was amplified as internal control. Relative quantification of gene was calculated using the relative ddCT analysis mode of the ABI 7500 Real-Time PCR system software.

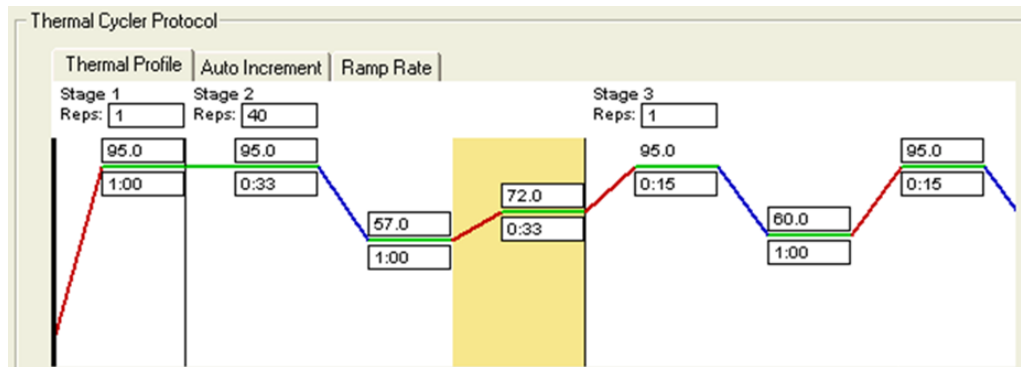


Figure 2.1: Thermal-Cycler protocol for RT-qPCR reaction using the 7500 ABI 7500 Real-Time PCR system software

## **2.3 Imaging methods**

Zeiss LSM Meta 510 or Zeiss LSM 510 inverted equipped with 405 nm, 488 nm, 543 nm , 594 nm lasers were used for all the fluorescence studies.

### **2.3.1 Ruffling Assay**

Cells were seeded on coverslips (VWR, UK) ( $1 \times 10^5$  per coverslip). Cells were starved overnight and then stimulated with 10% serum supplemented media or EGF (20ng/ml). After two washes in cold 1X PBS, cells were fixed in 4% paraformaldehyde for 30 minutes at room temperature. Cells were permeabilized in 1XPBS/0.25% Triton-X-100 for 2.5 minutes at RT. Unspecific staining was prevented blocking the coverslips with a solution 1X PBS/0.1% BSA for 30 minutes at RT. Alexa Fluor 594-Phalloidin (Invitrogen, UK) was added at 1:1000 dilution in PBS and incubated for 1 hour at 37°C. Hoechst 33342 5µg/ml (Sigma-Aldrich, UK) was added for nuclei staining. Coverslips were mounted on glass slides using the anti-fade Vektashield (Vector Laboratories, UK) and incubated for 1 hour at 4°C. Samples were analysed using Carl Zeiss™ confocal microscope LSM 510 Meta equipped with a 63X oil objective. DAPI was excited with laser 405nm wavelength while Alexa Fluor 594 dye was excited at 594nm and emission was measured at 620nm. All images were processed using LSM Image browser from Zeiss.

### **2.3.2 Calcium measurement Assay**

The fluorescent calcium indicator, Fluo-4 AM (Invitrogen, UK), was used to measure changes in intracellular calcium.  $4 \times 10^5$  cells were seeded on a bottom-glassed chamber for confocal live microscopy (Labtech Ltd, UK). The following day, cells were starved in serum free medium overnight. In case of siRNA transfection, cells were transfected in a 6 well-plate (chapter 2.2.2.1, 2.2.2.2) and 24 hours after transfection they were detached and seeded on the bottom-glassed chambers as described above. The following day each well

was incubated with 200  $\mu$ l of HBSS (Invitrogen, UK), containing 0.5% BSA (Sigma-Aldrich, UK), 2mM CaCl<sub>2</sub> (Sigma-Aldrich, UK), 4 $\mu$ M Fluo-4 for 45 minutes at 37°C/10%CO<sub>2</sub>. After loading, cells were washed twice in HBSS 0.5% BSA 2mM CaCl<sub>2</sub> and left in the same solution for 30 minutes for de-esterification of the Fluo-4-AM dye. Where indicated inhibitors were added during the de-esterification step for a total time of 30 minutes. The samples were protected from light during all the passages. The samples were moved in the confocal facilities and analysed using the LSM 510 inverted confocal microscope equipped with a chamber for live imaging at 37°C supplied with 5% CO<sub>2</sub> using a 20X objective. ZEN Carl Zeiss software was used for acquisition. The confocal was set in a time lapse acquisition mode acquiring a picture every 1.27 seconds, recording the fluorescence emitted by the Fluo-4 using a 505-545 nm pass-band filter. After recording basal fluorescent for 20 seconds cells were then stimulated with EGF (20ng/ml) and fluorescent was measured for 10 minutes. Analysis of fluorescence intensity was performed with ZEN™ Carl Zeiss software. Specifically, thirty cells were gated and variation of fluorescence intensity was measured for each sample. The average of intensity per time point was calculated and a chart of fluorescence on time was generated.

### **2.3.3 Incorporation of Fluorescein-conjugated InsP<sub>5</sub> (2-FAM-InsP<sub>5</sub>)**

MDA-MB-231 cells were seeded on coverslips in 12-well dishes at 60% of confluence and pre-treated with the indicated inhibitors for 2 hours. Cells were incubated with 2-FAM-InsP<sub>5</sub> (25  $\mu$ M) (provided by Professor Potter, Bath University, UK) or fluorescein (25  $\mu$ M) (Sigma-Aldrich) with or without the inhibitors for the indicated times. In the case of MDA-MB-231 transfected with siRNA targeting ABCC1 and ABCC5 and a scrambled non-targeting sequence, cells were seeded in a 12-well plate at a density of 50% of confluence, after 24 hours from transfection. Cells were then incubated with 2-FAM-InsP<sub>5</sub> or fluorescein for the indicated time points. In all cases cells were fixed in paraformaldehyde 4% (v/v) for 20 minutes and mounted on glass

slides. Fluorescence was measured by confocal analysis using an LSM 510 meta exciting the dye with the 488 laser with a 505-515 nm filter. Cell fluorescence was measured using the Carl Zeiss LSM software. Intracellular fluorescence was measured gating 40 cells for each time point of the experiments and mean fluorescence calculated.

#### **2.3.4 Forster Resonance Energy Transfer by acceptor photo-bleaching**

Direct protein–protein interactions were visualized using FRET whereby energy from an excited donor is transferred to an acceptor in very close proximity. The measurement of the energy transfer was monitored by following the fluorescence emission of the donor–acceptor couple and gave a reasonable approximation of the proximity and interaction between the two molecules, assuming that the emission spectrum of the donor overlapped with the excitation spectrum of the acceptor. The efficiency of this process was used to estimate the proximity and thus the interaction between PLC $\gamma$ 1 and PDK1 in MDA-MB-231 cells in overexpressing conditions.

Cells were seeded on coverslips in a 12-well plate at a density of 50% of confluence. Cells were co-transfected with PRK5-PLC $\gamma$ 1 and pOZ-PDK1 and after 24 hours from transfection cells were serum deprived overnight. The following day, cells were stimulated with a solution of DMEM + EGF (50 ng/ml) at the indicated time points before being fixed in paraformaldehyde 4% (v/v) for 30 minutes at RT. Cells were permeabilized in 1X PBS/0.25% Triton-X-100 for 2.5 minutes at RT. Unspecific staining was prevented by blocking the coverslips with a solution 1X PBS/0.1% of BSA for 30 minutes at RT. Primary antibodies anti-mouse-PLC $\gamma$ 1, (Santa Cruz Biotechnology, US) and anti-rabbit-PDK1 (Cell Signaling Technology Inc., USA) were diluted 1:50 in 50  $\mu$ l/coverslip of 1X PBS/0.1% BSA. The day after cells were washed 3X in 1X PBS/0.1% BSA and incubated with secondary antibodies anti-mouse-Alexa488 (Invitrogen, UK) and anti-rabbit Alexa555 (Invitrogen, UK) (The spectra of the two secondary antibodies are showed in Figure 2.2).

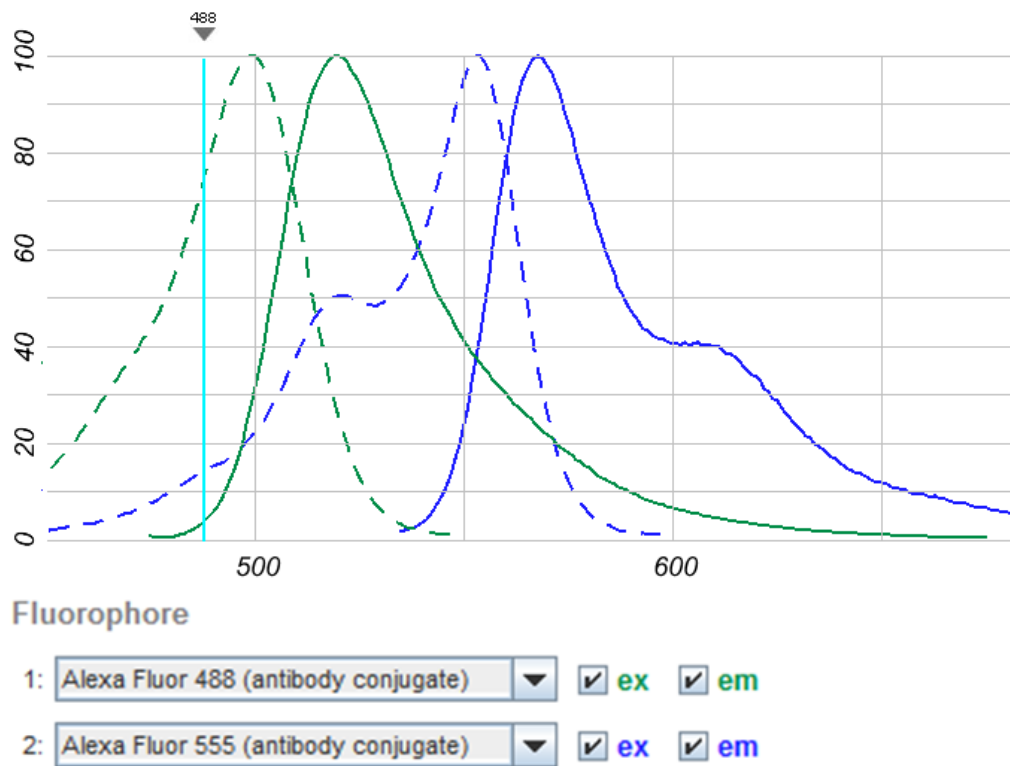


Figure 2.2: Donor and acceptor spectra generated with Fluorescence spectra viewer tool (<http://www.invitrogen.com/site/us/en/home/support/Research-Tools/Fluorescence-SpectraViewer.html>)

Cells were then washed 3X with 1X PBS and mounted on glass coverslips using Vectashield mounting media. Spectral imaging analysis was performed on Carl Zeiss LSM 510 meta. Cells were imaged with excitation  $\lambda=488$  nm and  $\lambda=543$  nm laser line and emission spectra were collected respectively in two different channels of the PMT detector. Reference spectra were generated from coverslips incubated separately with the two Alexa-conjugated secondary antibodies alone in order to generate single positive samples and all data were corrected for crosstalk and background fluorescence. The FRET efficiency was measured by acceptor photo-bleaching according to the method by Guillaud et al., 2008 where the de-quenching of the donor emission is a direct measure of the FRET efficiency. Cells were imaged with  $\lambda=543$  nm laser line to visualise PDK1 (acceptor) fluorescence and  $\lambda=488$  nm laser line to visualize PLC $\gamma$ 1 (donor) fluorescence. A selected area of the cell was repeatedly

photobleached with  $\lambda = 543$  nm laser line at full power for 1 minute and FRET efficiency was measured as the increase (or dequenching) of PLC $\gamma$ 1 fluorescence after photo-bleaching in the selected area. All fluorescence measurements were performed in MetaMorph software (Molecular Devices Inc., US).

Two independent areas in the bleached zone and one area in the non-bleached zone were analysed in parallel to ensure that the FRET efficiency values were not artefacts due to the photo-bleaching protocol. FRET efficiency was calculated using the following equation:

$$E = [1 - (\text{Donor.before} - \text{BCK.before}) / (\text{Donor.after} - \text{BCK.after})] \times 100$$

Donor.before = fluorescence intensity of PLC $\gamma$ 1 before photobleaching

BCK.before = background intensity before photobleaching

Donor.after = fluorescence intensity of PLC $\gamma$ 1 after photobleaching

BCK.after = background intensity after photobleaching. As a negative control, GFP was used as donor, was used to validate the system.

### **2.3.5 Forster Resonance Energy Transfer by FACS**

MDA-MB-231 were transfected with pOZ-PDK1 and PRK5-PLC $\gamma$ 1 either individually or in combination. 48 hour after transfection cells were detached by incubating with 1X PBS + 0.2% EGTA (w/v) solution for 20 minutes. Cells were spin at 1,200 RPM for 5 minutes and resuspended in 1 ml of media serum free supplemented with EGF (50 ng/ml) for 5 and 10 minutes. Cells were then fixed in 2% paraformaldehyde solution for 15 minutes. Cells were pelleted at 1,200 RPM for 5 minutes and permeabilized in 1XPBS/0.25% Triton-X-100 solution for 2.5 minutes at RT. Cells were centrifuged at 1,200 RPM for 5 minutes and resuspended in 1X PBS/0.1% BSA blocking solution for 30 minutes at RT. Cells were then pelleted at 1,200 RPM for 5 minutes and

resuspended in 400  $\mu$ l blocking solution containing anti-PLC $\gamma$ 1 or anti-PDK1 antibodies either individually or in combination (Table 2.10). Cells were incubated overnight at 4°C. The following day cells were centrifuged at 1,200 RPM for 5 minutes and washed three times for 5 minutes in blocking solution before being resuspended in 500  $\mu$ l of blocking solution and read with a Canto II FACS (Becton, Dickinson BD; UK)

Table 2.10: Plasmids, primary and secondary antibodies used for FRET experiments by FACS:

Constructs	Primary antibodies R=Rabbit; M=Mouse	Secondary antibodies (Alexa-555/Alexa-488 conjugated)
<b>pCDNA (Negative control)</b>	-	Alexa 488 (anti-mouse)
<b>pCDNA (Negative control)</b>	-	Alexa 555 (anti-mouse)
<b>pOZ-PDK1 (Single positive)</b>	anti-PDK1(R)	Alexa-488 (anti-rabbit)
<b>pOZ-PDK1 (single positive)</b>	anti-PDK1(R)	Alexa-555 (anti-rabbit)
<b>PRK5-PLC<math>\gamma</math>1 (single positive)</b>	anti-PLC $\gamma$ 1(M)	Alexa-488 (anti-mouse)
<b>PRK5-PLC<math>\gamma</math>1 (single positive)</b>	anti-PLC $\gamma$ 1(M)	Alexa-555 (anti-mouse)
<b>pEGFP/PRK5PLC<math>\gamma</math>1</b>	anti-PLC $\gamma$ 1(M)	Alexa-555 (anti-mouse)
<b>pEGFP/pOZ-PDK1</b>	anti-PDK1(R)	Alexa-555( Anti-rabbit)
<b>pOZ-PDK1/PRK5-PLC<math>\gamma</math>1</b>	anti-PLC $\gamma$ 1(M) anti-PDK1(R)	Alexa-488 (anti-rabbit) Alexa-555 (anti-mouse)
<b>pOZ-PDK1/PRK5-PLC<math>\gamma</math>1</b>	anti-PLC $\gamma$ 1(M) anti-PDK1(R)	Alexa-488 (anti-rabbit) Alexa-555 (anti-mouse)

Cells were gated according to forward and sideward scatter (FSC/SSC). All samples were excited with 488 nm laser and emission measured at 555 nm. The single positive samples stained with Alexa-555 conjugated secondary antibodies allowed to measure the background emission of the dye when excited with the 488 nm laser. The single positive samples stained with Alexa-488 conjugated secondary antibodies allowed removing of bleed-through fluorescence of the donor (Alexa-488) in the FRET channel by adjusting the photomultiplier tube (PMT) voltages and compensating for Alexa-488 and Alexa-555 dyes to specifically assess FRET in double positive cells. Cells co-transfected with pEGFP and PLC $\gamma$ 1 or PDK1 were used as negative controls of FRET. Data

were acquired using FACS Diva software (Becton, Dickinson BD; UK). Data were analysed with FlowJo Software (Treestar, US) with the help of Dr. Gary Warnes.

## 2.4 Cell Biology

### 2.4.1 Cell counting

Cells were seeded in 12-well plates at a density of  $1 \times 10^5$ . Cells were grown in 10% FBS supplemented growth media or in serum-free media. When indicated cells were treated with inhibitors. In all the experiments described cells were washed with 1X PBS and detached by incubating with trypsin (0.25%)/EDTA(0g/l) (PAA, Austria) solution. Trypsin was neutralized by adding 1 volume of growth media supplemented with 10% FBS (v/v) and the cell suspension was transferred in 1.5 ml Eppendorf tube (VWR, UK). Cells were centrifuged at 4,000g for 5 minutes. The supernatant was then removed and the pellet was resuspended in 150  $\mu$ l of growth media. Cells were manually counted using a Burker chamber. 10  $\mu$ l of cell suspension were added into the Burker chamber. All fields delimited by the grid of the chamber were counted and cell number calculated according to the formula:

$$\text{Cells number/ml} = \frac{1}{n} \sum_{i=1}^n x_i * 10,000$$

### 2.4.2 Migration and invasion assay

#### 2.4.2.1 Cell migration assay

MDA-MB-231, MDA-MB-435, TSA, 4T1 and A375M cell lines were cultured overnight in 6 wells multi-dishes and serum starved overnight before the experiment. Polycarbonate transwell insert 8.0  $\mu$ m diameter pores, 10mm diameter (Nunc, Thermo Scientific, UK) were coated overnight at 4°C with a solution of 10 $\mu$ g/ml of Fibronectin (Sigma-Aldrich, UK) in 1X PBS. The following day the inserts were washed in PBS 1X for few seconds and

transferred in a blocking solution of DMEM or RPMI containing 0.5% BSA for 1 hour at 37°C. When indicated cells were pre-treated with inhibitors for 1 hour before being trypsinized and pelleted. The pellet was resuspended in 2ml of RPMI or DMEM 0.5% BSA according to the cell type. Cells were counted and a suspension of 10,000 cells in 150µl was homogenously added in the upper chamber. The lower chamber was filled with 500µl of RPMI or DMEM 0.5% BSA according to the cell type. Cells were allowed to migrate for 4 hours at 37°C 5% CO<sub>2</sub>. Before fixing, non-migrated cells were removed from the upper surface of the porous membrane with a cotton bud. Cells underneath were then fixed in 4% paraformaldehyde solution for 20 minutes and washed in 3X in 1X PBS solution for 1 minute. Subsequently inserts were stained with 0.1% crystal violet solution (v/w) for 10 minutes, then washed 3X with 1X PBS and dried. Cells were counted using a Leica phase-light microscope using a 10X magnitude objective. A minimum of five fields per transwell were counted and an average of migrated cells/field was calculated.

#### **2.4.2.2 Matrigel cell invasion assay**

MDA-MB-231, MBA-MB-435, TSA, 4T1, A375M cell lines were cultured overnight in 6 well multi-dishes and serum-starved overnight before the experiment. The following day Matrigel pre-coated insert (8.0 µm diameter pores, 10mm diameter) were re-hydrated for 1 hour adding 500ul of RPMI or DMEM in the upper and lower compartment, according to the cell type to be seeded on the insert. When indicated, cells were pre-treated with inhibitors for the appropriated time before being detached from the 6-well dishes by trypsinisation. Cells were pelleted and resuspended in 2ml of 1%FBS DMEM or RPMI 1640 according to the cell type. Cells were counted and a suspension of 500µl of media containing 10,000 cells (60,000 in the case of MDA-MB-435) was seeded on the upper chamber of the insert. The lower chamber was filled with 500µl of 10% FBS RPMI or DMEM media according to the cell type used. Cell invasion was allowed for 36 hours. After 36 hours the upper face of the porous membrane was delicately cleaned with a cotton bud in order

to remove the non-invading cells. The cells that successfully invade the Matrigel were fixed in 4% paraformaldehyde solution (w/v) for 25 minutes. Inserts were washed 3X for 1 minute using 1X PBS solution. Cells were stained with 0.1% crystal violet solution (v/w) for 10 minutes, then washed 3X with 1X PBS and the dried. Cells were counted using a Leica phase-light microscope using a 10X magnitude objective. A minimum of five fields was counted per insert. Each invasion experiment was performed in duplicate and the average of invading cells/fields was calculated.

### **2.4.3 Inositol phosphate assay**

Cells were seeded on in 12-well plate at a density of  $8 \times 10^5$  cells per well. AG 1-X8 analytical grade anion exchange resin (formate form, 200–400 mesh, BioRad, UK) was re-hydrated overnight in H<sub>2</sub>O. The following day cells were labeled with 0.5  $\mu$ Ci/well [<sup>3</sup>H]myo inositol (PerkinElmer, US) in inositol free medium M199 (Sigma-Aldrich, UK). After 24 hours, cells were incubated in M199 containing 10 mM Hepes, pH 7.4 (Invitrogen, UK) and 20 mM LiCl (Sigma, UK) for 15 min before stimulation. A solution of M199 plus EGF (20 ng/ml) was prepared and used to stimulate the cells at the indicated time points. Cells were then lysed with 1 ml of ice cold 0.1 M HCOOH. In parallel, 3 ml of the re-hydrated resin were added to each column and left to set for 5 minutes. Columns were washed with 10 ml of H<sub>2</sub>O before loading the cell lysate. Free inositol was eluted and collected by elution with 10 ml of H<sub>2</sub>O and radioactivity counted by liquid radioactivity counting. Columns were washed with 5 ml of H<sub>2</sub>O. Glycophosphatidylinositols (GPI) were eluted using 5 ml of “solution A” containing (5 mM Na<sub>2</sub>B<sub>4</sub>O<sub>7</sub>, 160 mM NH<sub>4</sub>HCOO), collected and radioactivity counted by liquid radioactivity counting. After washing with 5 ml of solution A, inositol phosphates were eluted with 2 ml of NH<sub>4</sub>HCOO 1M and radioactivity counted by liquid scintillation. Radioactivity measured in the inositol fraction was used to normalise the radioactivity content of the samples.

Inositol phosphate production was expressed as percentage of inositol phosphate produced compared to the control unstimulated sample.

#### **2.4.4 [<sup>3</sup>H]InsP<sub>5</sub> incorporation assay**

MDA-MB-231 transfected with siRNA targeting ABCC1 and ABCC5 and a scrambled non-targeting sequence were seeded in a 12-well plate at a density of 50% of confluence 24 hours after transfection. In case of treatment with the ABCC1 inhibitor MK571 MDA-MB-231 were pre-treated with MK-571 (40µM) for 2 hours in 10% FBS growth media at 37°C/5% CO<sub>2</sub>. In the case of MDA-MB-231 transfected with siRNAs, cells were then incubated with 2 µl/well of [<sup>3</sup>H]InsP<sub>5</sub> for 1 hour minutes. In the case of MDA-MB-231 pre-treated with MK-571 cells were incubated with [<sup>3</sup>H]InsP<sub>5</sub> (2µl/well) for 2 second as basal incorporation and for 15 and 30 minutes. Cells were washed 3X with cold 1X PBS to remove the non-incorporated [<sup>3</sup>H]InsP<sub>5</sub>, then lysed on ice using 1 ml of HClO<sub>4</sub> 0.6M + 0.20 mg/ml Inositol Hexakisphosphate (IP<sub>6</sub>) solution and incubated on ice for 5 minutes. The whole lysate was diluted in 6 ml of scintillation liquid and radioactivity assessed by radioactivity counting. Radioactivity counts were normalized for the protein concentration of a duplicate 12 plate-dishes seeded and treated in parallel with “cold” InsP<sub>5</sub> as a duplicate. In the case of cells transfected with siRNAs incorporation was expressed as percentage of incorporation of scrambled after 1 hour of incorporation. In the case of cells treated with KM-571 incorporation was expressed as fold increase of basal incorporation.

#### **2.5 Statistical analysis**

Statistical analyses were carried out using the one-tailed, paired *t*-test using Microsoft Excel®.

**Chapter 3**  
**PLC $\gamma$ 1 is essential for cancer cell  
migration and invasion**

### 3.1 Introduction

PLC $\gamma$ 1 is activated by integrins engagement to the ECM and it also plays an important role in growth factor-induced cell motility, being activated by tyrosine kinase receptors for EGF, FGFs, NGF, VEGF, HGF and IGF-1 (Wells et al., 2002). Recent evidence produced by our group confirmed the pivotal role of PLC $\gamma$ 1 in malignant cell invasion and its role in metastasis development and progression (Sala et al., 2008).

During metastasis, malignant cells are able to “escape” from the primary tumour through the circulatory or lymphatic system, invading distant healthy tissues to initiate a new malignant lesion. Cell motility is critical for this process to occur and the mechanisms involved in regulation of cell motility are the results of an intricate network of signals activated by different growth factors, chemo-attractant and ECM components *in vivo*. The first *in vitro* tool to study cell motility was built by Boyden, therefore it was called Boyden chamber and was initially used to study leukocyte chemotaxis. It consists of two medium-filled chamber separated by a microporous membrane (Falasca et al., 2011). Cells are seeded in the top compartment and allowed to migrate for an appropriate incubation time toward chemotactic agents present in the bottom chamber media, such as growth factors or ECM components used to coat the porous membrane. Since the cells migrate from the upper compartment to the lower one through a porous membrane, the Boyden chambers are also called transwell chambers. Once the cells pass through the membrane they remain adherent to it. For this reason the cells need to be fixed on the membrane and stained to allow quantification based on manual counting using a phase contrast microscope.

In order to investigate the role of PLC $\gamma$ 1 in cell migration and 3D Matrigel invasion in cancer cell lines, I performed cell migration and cell invasion assays using different cancer cell lines (breast and melanoma cell lines) upon PLC $\gamma$ 1 inhibition by chemical and molecular biology approaches. Cytoskeleton remodelling was also analysed in those cell lines in order to investigate a potential role of PLC $\gamma$ 1 in this process.

### 3.2 Results

Migration of breast cancer cell line MDA-MB-231 was analysed *in vitro* using the transwell assay. The transwell inserts used in this assay consist of a porous polycarbonate membrane with an average porous size of 8  $\mu\text{m}$ . The inserts were coated with fibronectin, an ECM component, used as chemo-attractant. Cells were seeded in the upper chamber of the insert and allowed to migrate for 4 hours before being fixed in paraformaldehyde and stained with crystal violet. Cell migration was calculated by manual cell counting using a 10x magnification of a phase contrast microscope.

In order to determine the appropriate number of cells to be used in the assay, a preliminary experiment was performed using three different amounts of cells per transwell (5,000; 10,000; 20,000). Pictures in Figure 3.1A show representative fields of cell migrated on transwell insert. This experiment indicated that the optimal experimental condition to perform the assay was obtained when 10,000 cells were seeded on the inserts, which led to an average of 100 cells migrated through the porous membrane per fields, a reasonable number for the cell counting (Figure 3.1B).

**A**

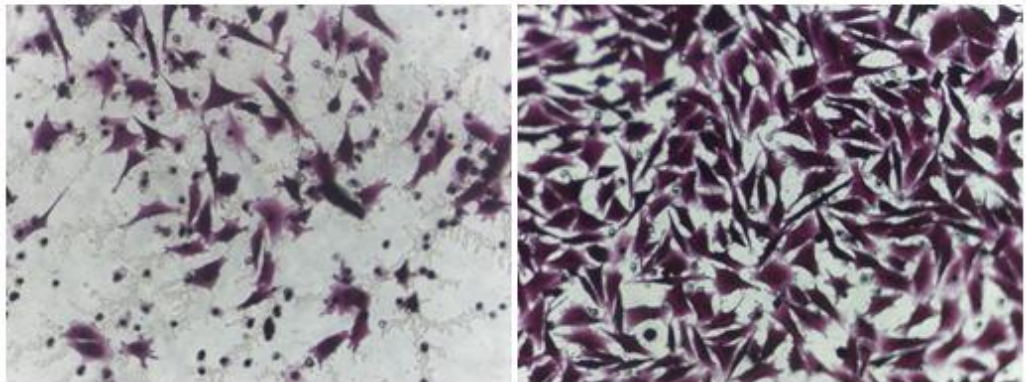
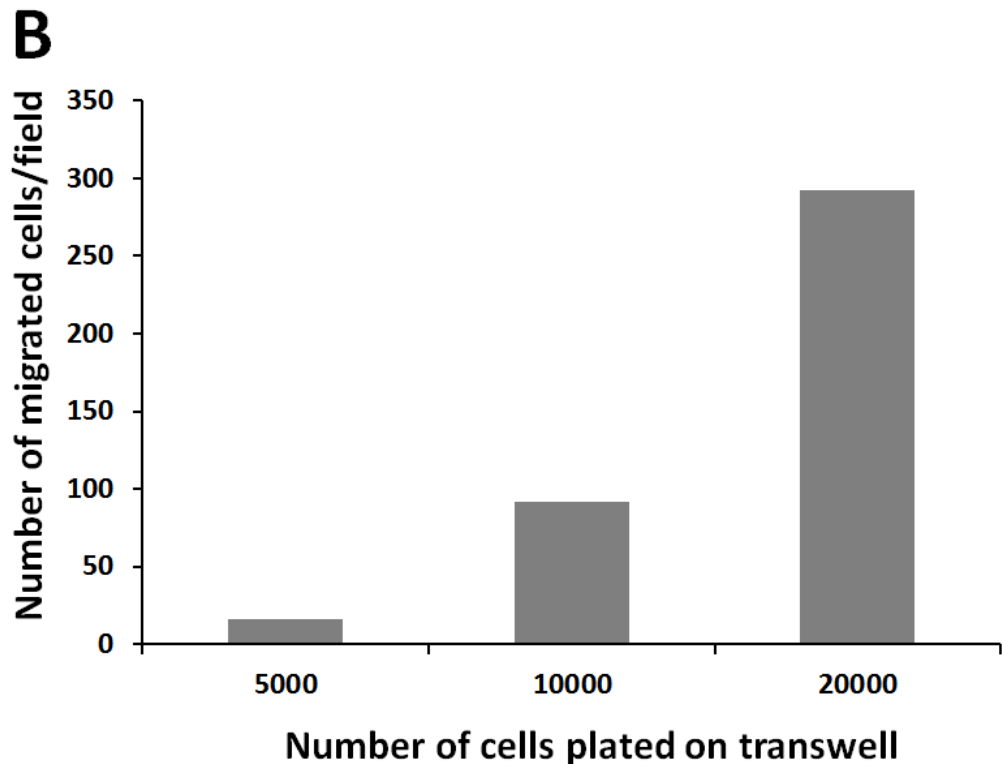


Figure legend next page



**Figure 3.1:** (A) Pictures of transwell inserts after fixing and staining with crystal violet. Representative fields of insert seeded with 5000 cells (left) and 20000 cells (right). (B) Quantification of migrating cells by cell counting and expressed as number of migrated cells per field. The graph represents one experiment performed in duplicate in order to optimize the experimental conditions.

### **3.2.1 PLC activity is essential for MDA-MB-231 fibronectin-induced migration**

In order to investigate the role of PLC $\gamma$ 1 in fibronectin-induced migration in MDA-MB-231 cells I decided to test the effect of the PLC inhibitor U73122 on cell migration. The inhibitor U73122 is a pan-PLC inhibitor that inhibits the lipase activity of all the PLC family components and has been shown to inhibit cell motility (Jones et al., 2005). Since PLC $\gamma$ 1 is activated by fibronectin, the inhibitor was a useful tool to start investigating the involvement of PLC $\gamma$ 1 in fibronectin-induced migration. MDA-MB-231 were serum starved overnight

and pre-treated with U73122 (5 $\mu$ M) for 30 minutes before being plated on transwell inserts in the presence or absence of the inhibitor. Cells were allowed to migrate for 4 hours before being fixed. Migration of cells treated with the inhibitor was compared to control cells treated with the inactive analogue U73343. Migration of cells treated with the drug carrier (DMSO) alone was also determined. Cell migration was completely inhibited in MDA-MB-231 treated with U73122 (p=0.001). No inhibition of cell migration was detected in cells treated with the inactive analogue U73343 compared to cells treated with vehicle alone. This data indicated that PLC activity is essential for fibronectin-induced migration in MDA-MB-231 (Figure 3.2).

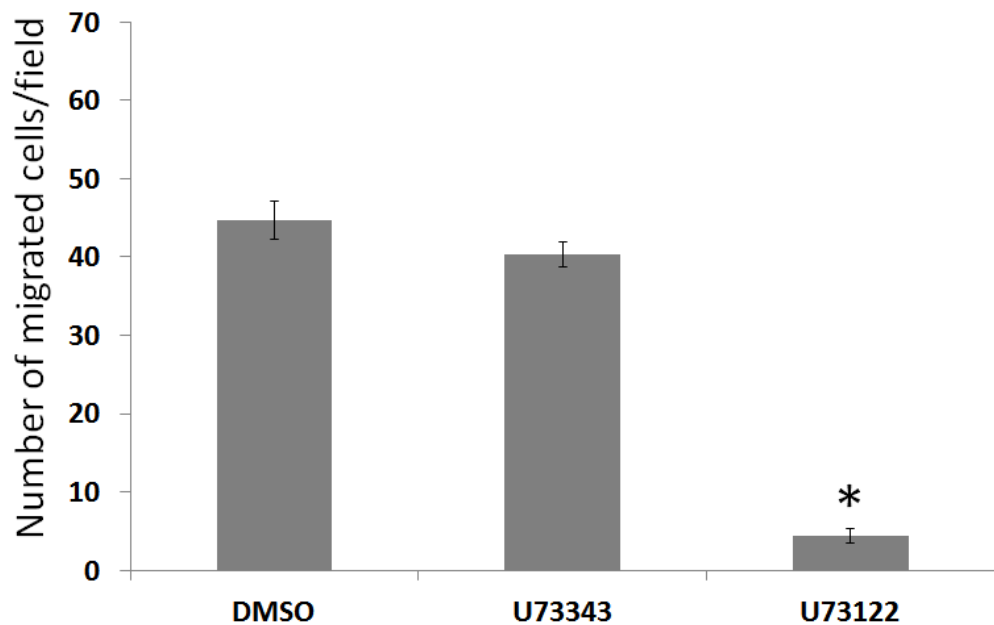


**Figure 3.2: Effect of PLC inhibition on fibronectin-induced cell migration.** Migration is expressed as migrated cells per field. Migration of MDA-MB-231 treated with U73122 was compared to cells treated with the inactive analogue U73343. Columns are the mean of 3 independent experiments performed in duplicate; bars S.E. \*p=0.001

### **3.2.2 Effect of a PLC $\gamma$ 1 mutant form constitutively recruited to the plasma membrane on fibronectin-induced cell migration.**

PLC $\gamma$ 1 plays an important role in cellular spreading on Matrigel in endothelial and cancer cells (Jones et al., 2005; Jones et al., 2007). As shown in Figure 3.2, inhibition of PLC activity leads to impaired fibronectin-induced migration in MDA-MB-231. PLC $\gamma$ 1 has been demonstrated to be involved in focal adhesion formation during cell motility and it is recruited to the leading edge of the cells during wound healing assay and cell migration (Piccolo et al., 2002). Therefore PLC $\gamma$ 1 recruitment at the leading edge of the cells is crucial to regulate cell motility and it is probably involved in controlling directional motility.

In order to assess the potential involvement of the PLC $\gamma$ 1 isoform in directional motility I decided to test the effect of overexpressing a constitutively membrane-recruited PLC $\gamma$ 1 mutant on fibronectin induced migration in MDA-MB-231. Since PLC $\gamma$ 1 is recruited to the plasma membrane at the leading edge, I hypothesised that a constitutively active form of PLC $\gamma$ 1 recruited all along the plasma membrane could affect directionality during the migration process. For this purpose MDA-MB-231 cells expressing a palmitoylated form of PLC $\gamma$ 1 (MDA-MB-231 PALM-PLC $\gamma$ 1), kindly provided by Dr. Bonvini, were analysed on fibronectin-induced cell migration transwell assay.

MDA-MB-231 cells expressing only the palmitoylation (MDA-MB-231 PALM) sequence were used as internal control in the migration experiments. Data indicated a significant reduction of fibronectin-induced migration in MDA-MB-231 PALM-PLC $\gamma$ 1 compared to MDA-MB-231 PALM (Figure 3.3), suggesting that overexpression of a mutant PLC $\gamma$ 1 constitutively associated to the plasma membrane affects the ability of cells to migrate towards fibronectin. These data further supported the hypothesis that recruitment of PLC $\gamma$ 1 to the leading edge of migrating cells is important for cell migration.

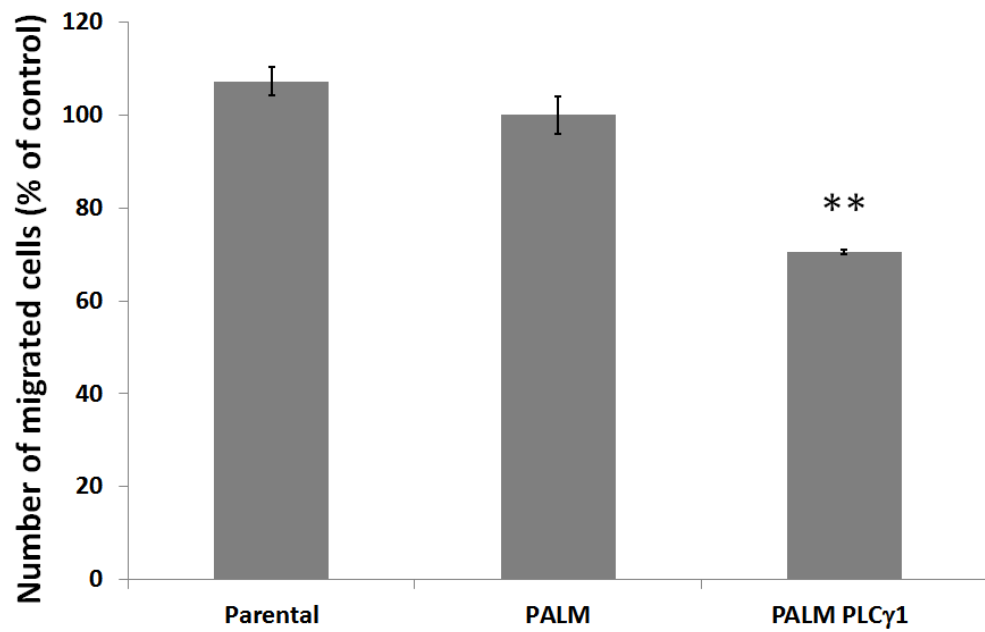


**Figure 3.3 Cell migration in MDA-MB-231 expressing PALM-PLC $\gamma$ 1:**

Number of migrated MDA-MB-231 (Parental) or cells expressing a palmytoylated PLC $\gamma$ 1 (PALM PLC $\gamma$ 1), or the palmytoylation sequence alone (PALM) is expressed as percentage of migrated MDA-MB-231 expressing the empty vector as control. Columns are the mean of three different experiments each of them performed in duplicate; bars S.E. \*\*p=0.005

### 3.2.3 Downregulation of PLC $\gamma$ 1 expression using a pSUPERIOR construct containing specific shRNA targeting PLC $\gamma$ 1.

Since no PLC $\gamma$ 1 specific inhibitors are available, the best available molecular approach to assess the role of PLC $\gamma$ 1 activity in different cellular function was the generation of stable cell lines downregulated for PLC $\gamma$ 1 using short hairpin RNA (shRNA). pSUPERIOR.retro.puro vector containing unique 19 nucleotides sequence complementary to the mRNA transcript of PLC $\gamma$ 1 was generated previously in the lab (Sala et al., 2008) (see chapter 2.2.2.3.1; 2.2.2.3.2). The resulting transcript of the recombinant vector is predicted to fold back on itself to form a 19-base pair loop structure (shRNA) which is then cleaved in the cell to produce a functional siRNA. Three-point mutations in the 19 nucleotides sequence were introduced to generate an appropriate pSUPERIOR.retro.puro vector control (3MUT) (Sala et al., 2008). MDA-MB-435 and TSA cell lines were infected with pSUPERIOR.retro.puro 3MUT and pSUPERIOR.retro.puro shPLC $\gamma$ 1. Infected cells were kept in culture in the presence of puromycin. Western Blot (WB) analysis of cell extracts was performed to assess the expression level of PLC $\gamma$ 1 in cells expressing the targeting sequence shPLC $\gamma$ 1 and control cells 3MUT (Figure 3.4). Cells expressing the shPLC $\gamma$ 1 sequence showed a significant reduction in PLC $\gamma$ 1 protein levels compared to the 3MUT control cells.

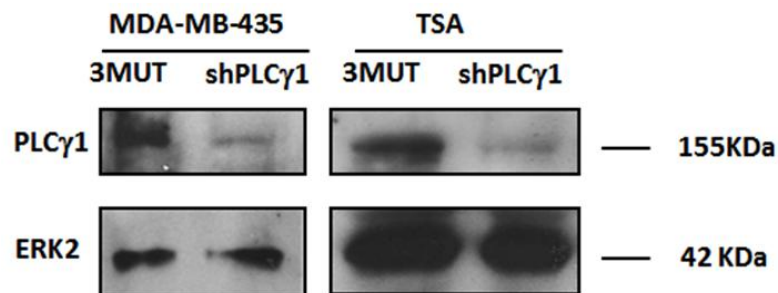


**Figure 3.4 WB analysis of stable protein downregulation of PLC $\gamma$ 1:** PLC $\gamma$ 1 protein level was assessed by WB in cell lysates of MDA-MB-435 and TSA cell lines expressing the specific shRNA targeting PLC $\gamma$ 1 (shPLC $\gamma$ 1) and compared to expression in cells expressing the non-targeting shRNA (3MUT). PLC $\gamma$ 1 expression was assessed by immunoblot using a specific anti-PLC $\gamma$ 1

antibody. Immunoblot for ERK2 was used as control for equal loading. The position of the bands correspond to 155 KDa for PLC $\gamma$ 1 and 42 KDa for ERK2.

### 3.2.4 Inducible downregulation of PLC $\gamma$ 1 expression using a pSUPERIOR construct

The pSUPERIOR.retro.puro vector can be used as an inducible vector to produce siRNA in mammalian cells. The vector contains a tetracycline operator 2 (TetO<sub>2</sub>) derived from E. Coli in the H1 promoter. The TetO<sub>2</sub> sequence acts as binding site for a homodimer of Tet repressor that, if present, blocks the transcription of the shRNAs. Therefore a previous transfection with the tetracycline repressor expressing vector is necessary to allow the binding of the Tet repressor to the TetO<sub>2</sub> operator. The tetracycline repressor binds with high affinity to the operator sequence in the absence of tetracycline. Upon addition, tetracycline binds to the Tet repressor causing conformational changes to the repressor that impair the operator-repressor binding, eventually resulting in the transcription of the shRNA duplex that, once processed from the RNAi machinery of the cell, provides functional siRNA (Figure 3.5).

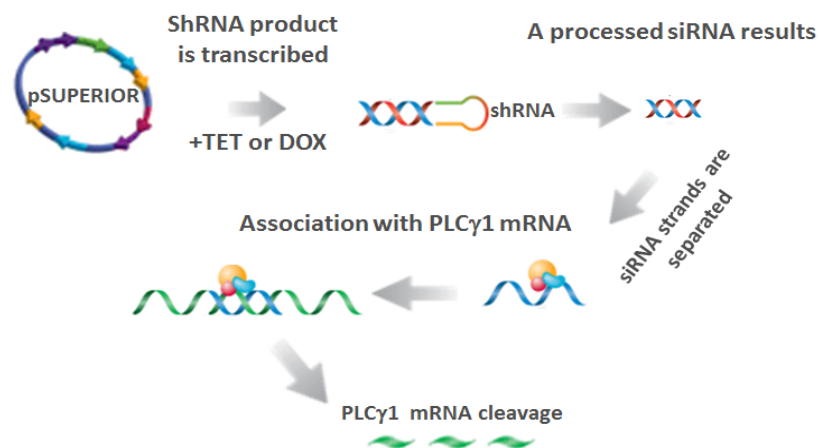


**Figure 3.5 Model of inducible protein downregulation using pSUPERIOR inducible system.** Figure adapted from Santa Cruz Biotechnology ([http://www.scbt.it/gene\\_silencers.html](http://www.scbt.it/gene_silencers.html)).

Therefore MDA-MB-231 cells were first transfected with a vector expressing the Tet repressor and selected to generate stable Tet repressor expressing clones. Subsequently, a selected clone was infected with the pSUPERIOR 3MUT and pSUPERIOR shPLC $\gamma$ 1 in order to generate cells with an inducible downregulation of PLC $\gamma$ 1 and the respective control. These cells were previously generated in the lab (Sala et al., 2008). As shown in Figure 3.6, MDA-MB-231 pSUPERIOR 3MUT cells show comparable PLC $\gamma$ 1 expression in the presence or absence of tetracycline addition indicating that the 3MUT sequence has no effect on the expression levels of PLC $\gamma$ 1. On the contrary, 24 hours of treatment with tetracycline of MDA-MB-231 pSUPERIOR shPLC $\gamma$ 1 cells induces a clear downregulation of PLC $\gamma$ 1 protein expression.

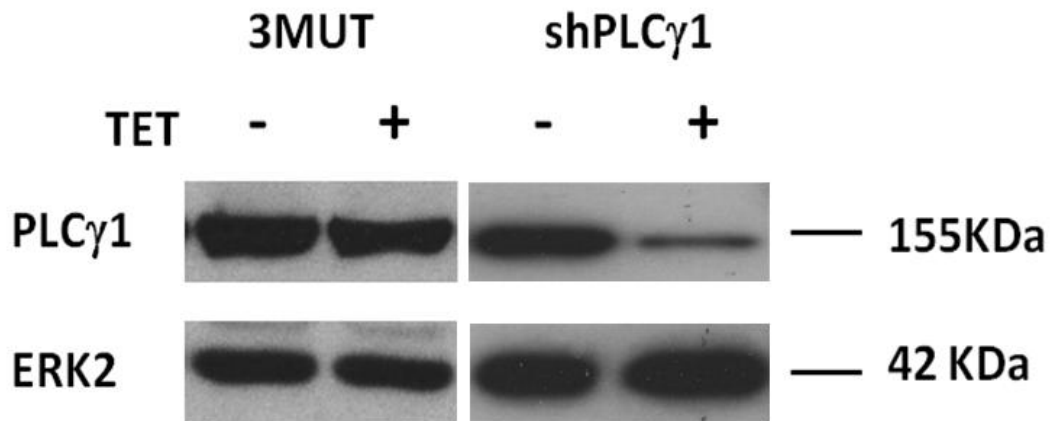


**Figure 3.6 Inducible downregulation of PLC $\gamma$ 1:** WB analysis of PLC $\gamma$ 1 protein level in cells expressing the TET repressor and a non-targeting shRNA (3MUT) or the targeting shRNA (shPLC $\gamma$ 1) in the presence or absence of tetracycline. ERK2 immunoblot was used as an equal loading control.

### **3.2.5 Cell invasion assay in breast cancer cells stably downregulated for PLC $\gamma$ 1 expression**

The experimental conditions used in the transwell assays are very different from the physiological conditions encountered by cancer cells during the metastatic process. ECM and the basal membranes of organs represent the main barriers that cancer cells need to cross in order to locally invade the tissue of origin or to initiate a secondary tumour in a distant organ.

The Matrigel cell invasion assay more closely mimics the physiological conditions encountered by the cancer cells during ECM invasion. Matrigel is a mixture of ECM components produced by the Engelbreth-Holm-Swarm (EHS) murine sarcoma that has been used to study cell morphology on ECM components and the three-dimensional architecture in normal and malignant cell lines. The main components of Matrigel are laminin, collagen IV, entactin and perlecan; growth factors are minor components. In particular Matrigel exists in a growth factor rich composition, or in growth factor reduced composition. Matrigel can be applied on the inserts in its cold liquid form over transwell inserts and allowed to polymerise to form a gel with a defined three dimensional structure.

The effect of PLC $\gamma$ 1 downregulation on three-dimensional invasion was investigated previously in the lab using MDA-MB-231 stably downregulated for PLC $\gamma$ 1 expression (Sala et al., 2008). I decided to perform Matrigel invasion experiments using other breast cancer cell models such as MDA-MB-435 and TSA stably downregulated for PLC $\gamma$ 1 expression. This allowed me to investigate the role of PLC $\gamma$ 1 in 3D invasion in different breast cancer cell lines. MDA-MB-435 and TSA expressing shRNA targeting PLC $\gamma$ 1 expression (shPLC $\gamma$ 1) or the 3MUT shRNA (sh3MUT) cloned in the pSUPERIOR.retro.puro were used for the assay. Cells were seeded on inserts pre-coated with Matrigel growth factor-reduced and fixed after the appropriate invasion time (see chapter 2.4.2.2). I observed that downregulation of PLC $\gamma$ 1 completely inhibited Matrigel invasion in MDA-MB-435 ( $p < 0.05$ ) and in TSA ( $p < 0.01$ ) compared to the respective controls. These data indicate that PLC $\gamma$ 1

is required for 3D-Matrigel invasion in the breast cancer cell lines analysed and that its downregulation severely impairs the cellular movements through the 3D-structure of the Matrigel (Figure 3.7).

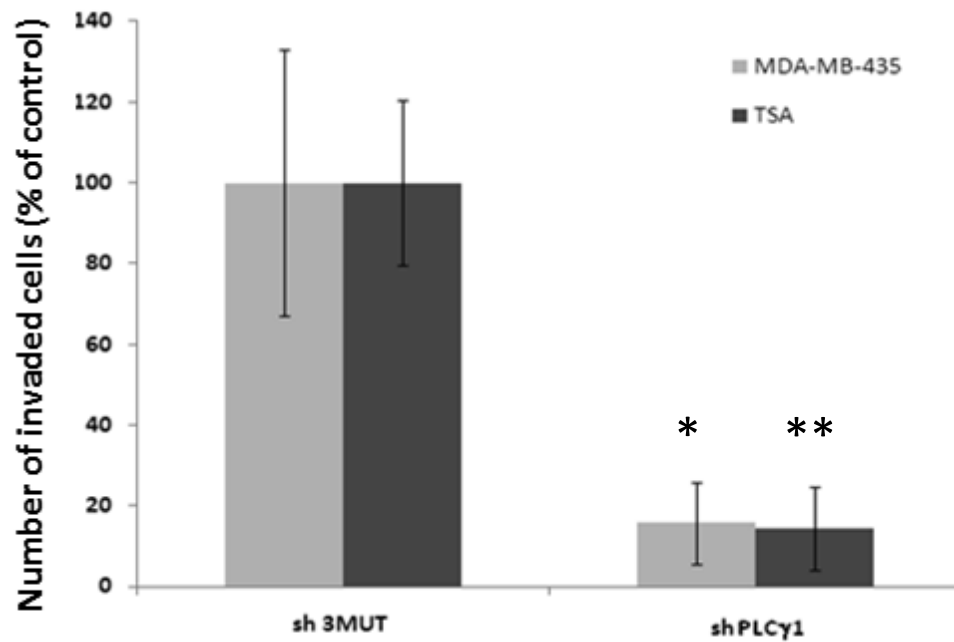


**Figure 3.7 Analysis of Matrigel invasion in breast cancer cell lines:** 10,000 cells were seeded on Matrigel and allowed to invade for 36 hours. Cells that have invaded were fixed, stained with crystal violet and counted. Quantification of Matrigel cell invasion is expressed as percentage of invading cells. Columns are the mean of three independent experiments each of them performed in duplicate; bars S.E. \* $p < 0.05$ ; \*\*  $p < 0.01$

### 3.2.6 Cell invasion assay in melanoma cells transiently downregulated for PLC $\gamma$ 1 expression

In order to determine whether PLC $\gamma$ 1 has a role in invasion of different cancer cells, the effect of PLC $\gamma$ 1 downregulation in the highly invasive melanoma cell line A375M was investigated. Since A375M cells stably downregulated for PLC $\gamma$ 1 expression were not available, I decided to downregulate PLC $\gamma$ 1 transiently using specific PLC $\gamma$ 1-targeting siRNA. A375M were transfected with Hiperfect transfecting reagent (Qiagen) (see chapter 2.2.2.2). Optimisation of the protocol transfection was necessary in order to setup the experimental conditions. Once the protocol was optimised, the invasion on Matrigel of A375M transfected with siRNA for PLC $\gamma$ 1 or a non-targeting sequence (Scrambled) was determined. WB analysis of lysates of transfected cells was performed in parallel to each invasion experiment at the end of the assay to evaluate the effective downregulation of PLC $\gamma$ 1 protein expression as shown in Figure 3.8A.

Analysis of cells that have invaded demonstrated that downregulation of PLC $\gamma$ 1 protein expression strongly inhibits Matrigel invasion in A375M ( $p=0.001$ ). These data confirm the importance of PLC $\gamma$ 1 in 3D cellular invasion and show that PLC $\gamma$ 1 is important for cell invasion not only in breast cancer cell lines but also in other models such as melanoma (Figure 3.8B).

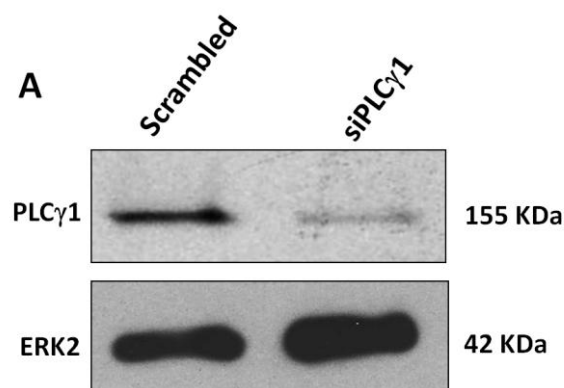
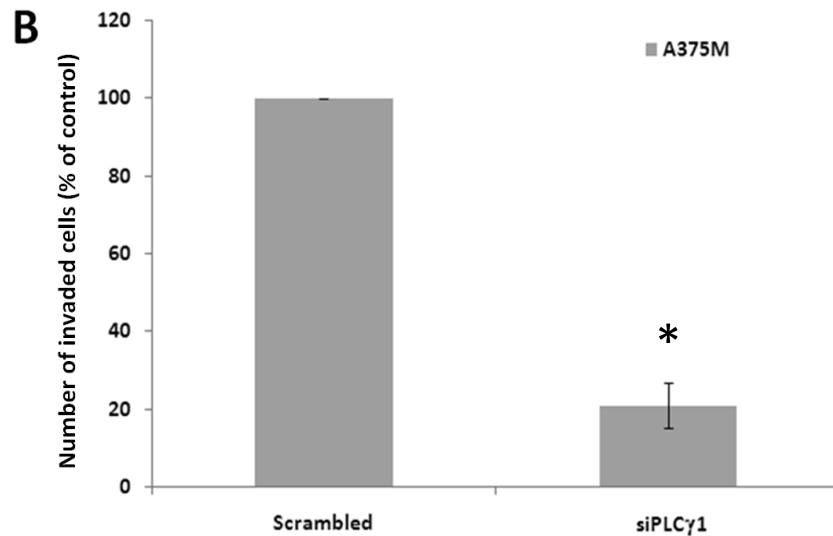


Figure legend next page...



**Figure 3.8 (A) PLC $\gamma$ 1 transient downregulation in A375M** assessed by WB using specific PLC $\gamma$ 1 antibody. **(B) Matrigel cell invasion assay** comparing A375M siPLC $\gamma$ 1 and A375 scrambled invasion rate. Cells were starved overnight 24 hours after transfection and then seeded on Matrigel-coated transwell for 36 hours before being fixed and stained. Columns are the mean of three different experiments performed in duplicate; bars S.E. \*P=0.001

### 3.2.7 Analysis of cytoskeleton remodelling in MDA-MB-435

As described in chapter 1.3.4, PLC $\gamma$ 1 is involved in cytoskeleton remodelling and its inhibition induces a rounded morphology in endothelial and cancer cell lines which fail to form cell protrusion and to undergo cell spreading in response to integrin engagement (Jones et al., 2005). Previous experiments performed in the lab showed that EGF-induced membrane ruffles are inhibited in MDA-MB-231 cells downregulated for PLC $\gamma$ 1 (Sala et al., 2008). Therefore I decided to investigate the effect of PLC $\gamma$ 1 downregulation on cytoskeleton remodelling in other breast cancer cell lines. The effect of PLC $\gamma$ 1 downregulation on cytoskeleton remodelling was investigated using immunofluorescence staining of actin with Alexa<sup>®</sup>Fluor 594 phalloidin. Phalloidin is a molecule with high affinity for actin, belonging to the family of

phallotoxins, which stabilizes F-actin preventing actin depolymerisation. Phalloidin-conjugated with the Alexa® Fluor 594 dye allows fluorescent visualization of actin cytoskeleton by excitation at 543 nm wavelength. MDA-MB-435 cells were serum starved overnight and then stimulated with EGF or media supplemented with 10% serum for 6 minutes before being fixed and examined with a confocal microscope. Serum and EGF stimulation induces formation of membrane ruffles and cytoskeleton protrusion (white arrows in Figure 3.9A) in both MDA-MB-435 3MUT and MDA-MB-435 shPLC $\gamma$ 1. However downregulation of PLC $\gamma$ 1 significantly reduced the percentage of cell processing membrane ruffles or cellular protrusion (Figure 3.9B). These data indicate that PLC $\gamma$ 1 is required for polymerization of new actin filaments underneath the plasma membrane, which is essential for membrane ruffling formation and growth factor-induced cytoskeleton remodelling.

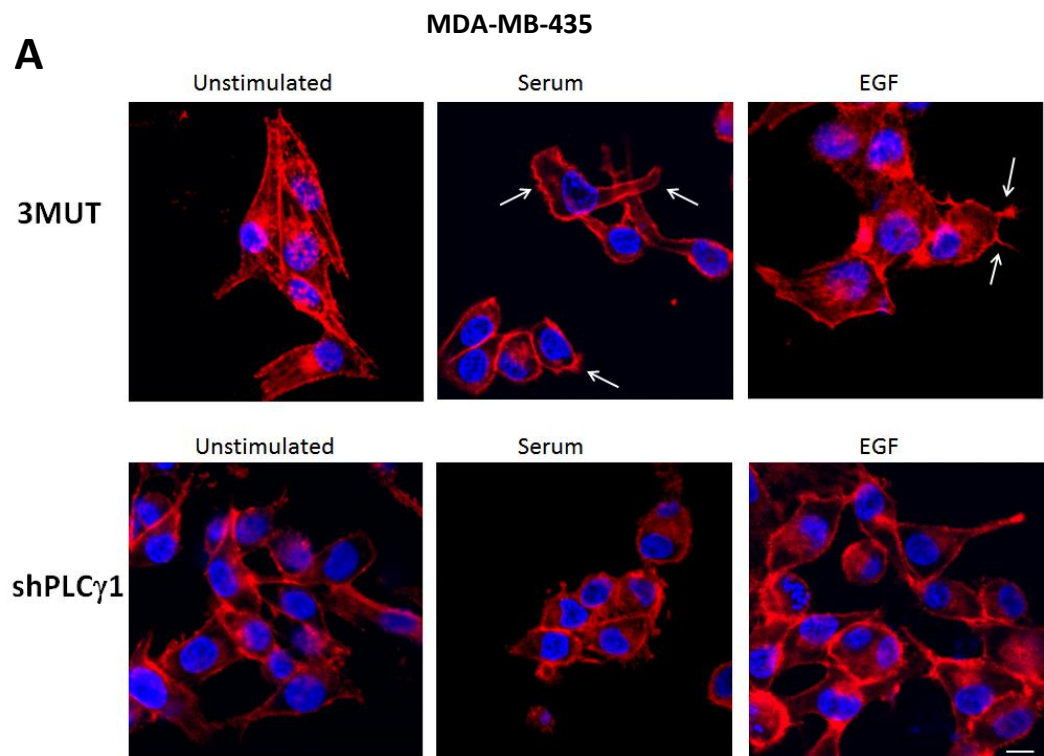
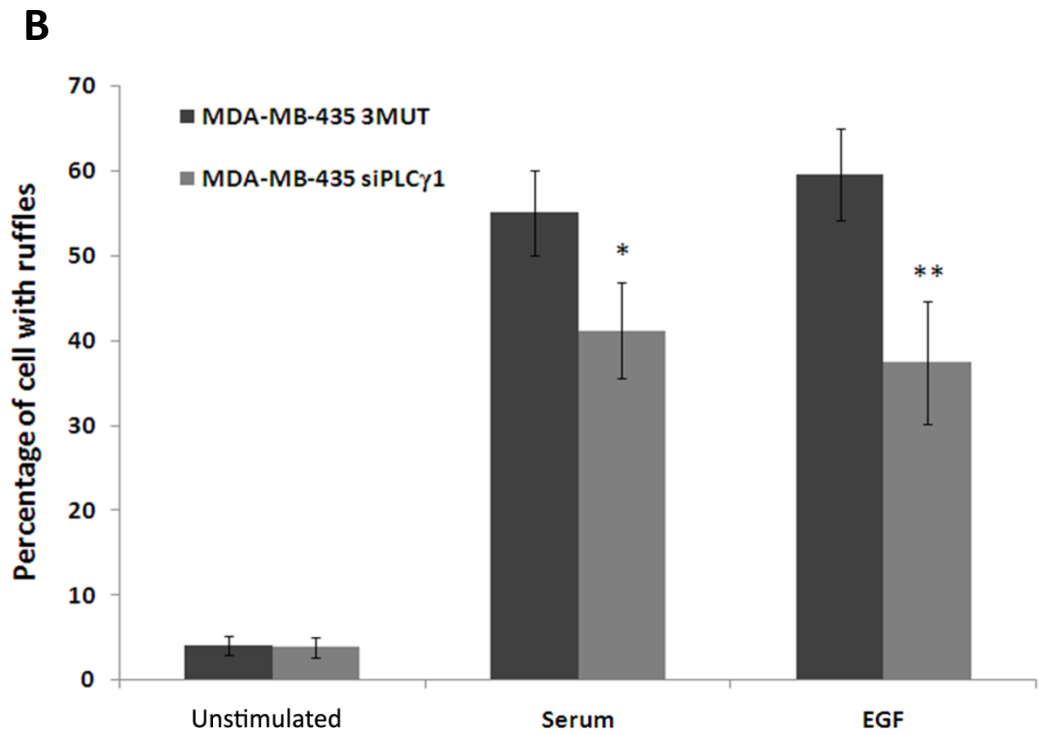


Figure legend next page...



**Figure 3.9: PLC $\gamma$ 1 is important for cytoskeleton remodelling:** (A) Phalloidin staining of actin cytoskeleton in unstimulated and EGF- or Serum-stimulated MDA-MB-435. Arrows indicate membrane ruffles. (B) Quantification of membrane ruffles was performed on 4 independent experiments. At least 100 cells per experiment were counted and classified according to the presence or absence of membrane ruffles. Columns represent the average of four independent experiments  $\pm$ SEM. Bar=10  $\mu$ m,\*p=0.05, \*\*p=0.01.

### 3.2.8 Analysis of cytoskeleton remodelling in TSA murine breast cancer cell line

To determine whether PLC $\gamma$ 1 has a role in actin remodelling in other breast cancer cell lines, actin cytoskeleton staining was performed in TSA cells. Data revealed that serum-induced and EGF-induced membrane ruffle formation was strongly inhibited in TSA shPLC $\gamma$ 1 compared to control TSA 3MUT (Figure 3.10). Inhibition of membrane ruffle formation was more evident in this cell line than in the MDA-MB-435 (Figure 3.9A) but data in both cell lines demonstrated the role of PLC $\gamma$ 1 in EGF- and serum-induced actin remodelling.

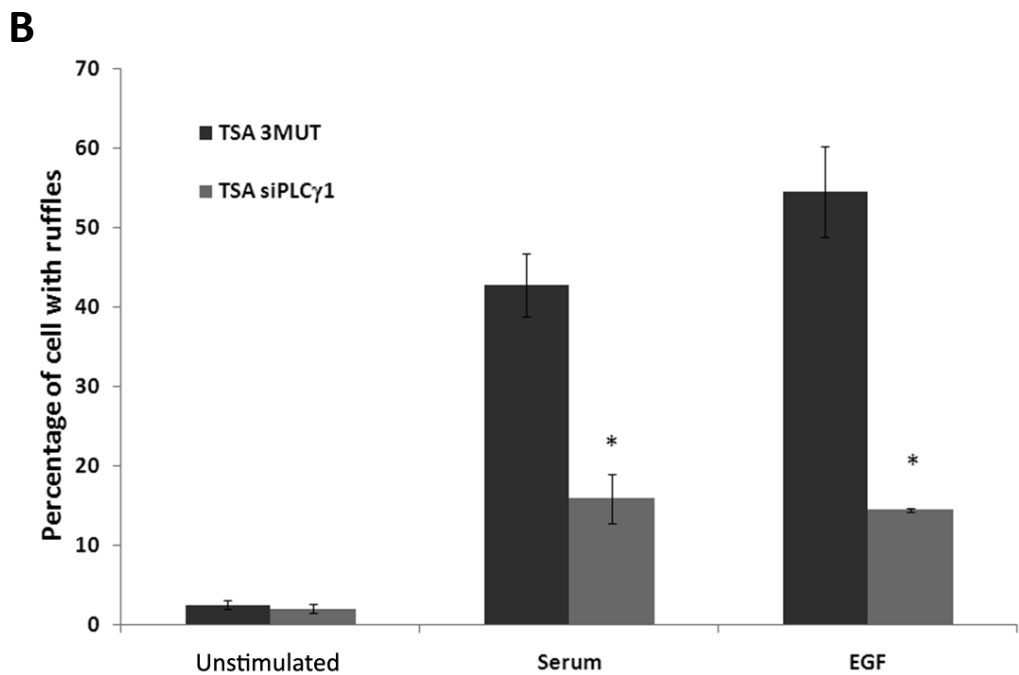
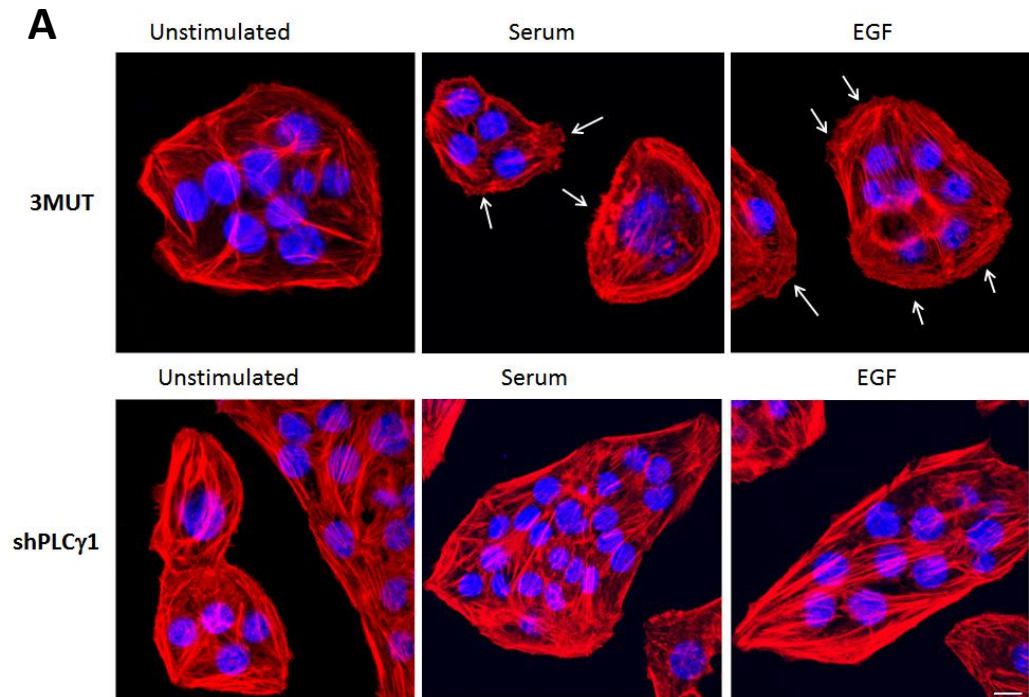


**Figure 3.10** (A) Phalloidin staining of actin cytoskeleton in unstimulated and EGF- or Serum-stimulated TSA. Arrows indicate membrane ruffles Bar=10 $\mu$ m. (B) Quantification of membrane ruffling was performed in 4

different experiments in duplicate. At least 100 cells per experiments were counted and classified according to the presence or absence of membrane ruffles. Columns represent the average of four independent experiments. bars S.E., \*p=0.05.

### 3.3 Discussion

The tumour is the second cause of death in adults. Surgical excision of the primary tumour can result in good prognosis. However, cancer cells can acquire metastatic capacity leading to the spreading of tumour in distant tissues often resulting in a poor prognosis. Metastatic tumours are often resistant to chemotherapy and non-responsive to treatment and therefore the metastatic stage in cancer disease represents the most serious condition. Cancer cells able to metastasise are the result of a selective process where cells with high ability to migrate and to invade the ECM are selected. Understanding the mechanism by which they migrate and can invade is therefore a key goal in cancer research. It has been widely accepted that PLC $\gamma$  is involved in cell migration and cell invasion *in vitro* and *in vivo*. Previous works investigated how integrins (Tvorogov et al. 2004) and EGF stimulate PLC $\gamma$ -mediated cell migration and invasion in different normal and cancer cell lines. Furthermore the use of specific siRNA targeting PLC $\gamma$ 1 expression underlined the importance of this specific isoform in cell spreading on different substrates such as fibronectin and Matrigel. The EGFR-PLC $\gamma$ 1 pathway plays an important role in cell motility and cancer invasion (Chen et al., 1994; Kassis et al., 1999). Indeed EGFR and ERB2 receptors have been linked to increased invasivity and poor prognosis in breast cancer patients, and inhibition of PLC using the pan-PLC inhibitor U73122 or EGFR inhibitor decreased breast cancer cell migration *in vitro* (Kassis et al., 1999) as confirmed in my experimental system (Figure 3.2).

Furthermore PLC $\gamma$ 1 is highly expressed in colon cancer, breast cancer and highly metastatic colorectal tumour cell lines (Nomoto et al., 1995; Smith et al., 1998). Especially, high levels of PLC $\gamma$ 1 were found in breast carcinoma

metastases compared to primary tumour (Sala et al, 2008), indicating that this enzyme is important for the metastatic process. Expression of a dominant-negative mutant of PLC $\gamma$ 1 in *de novo*-occurring carcinomas of the mammary or prostate gland mice models diminished lungs metastasis (Shepard et al., 2007). These data pointed at PLC $\gamma$  as an important regulator of metastasis dissemination and suggested PLC $\gamma$  as a potential therapeutic target to prevent metastasis formation. However it should be mentioned that all these studies were obtained using generic PLC inhibitors or a dominant negative mutant. My results were obtained using specific siRNA or shRNA that allowed the transient or stable downregulation of PLC $\gamma$ 1 expression in a panel of metastatic breast cancer cell lines and one cell line of a highly metastatic melanoma. The experiments described in this chapter were published in a Cancer Research paper together with parallel experiments performed by co-authors (Sala et al., 2008). Downregulation of PLC $\gamma$ 1 inhibited Matrigel cell invasion *in vitro* in all the cell lines, indicating that this enzyme has a role in cell motility and invasion in different cell lines (Figure 3.7; 3.8). It has been already shown that PLC $\gamma$ 1 is recruited to the leading edge of migrating cells in a PI3K dependent manner (Falasca et al., 1998; Piccolo et al., 2002) and that it is involved in integrin-induced cytoskeleton remodelling downstream of FAK activation (Zhang et al., 1999), which results in directional migration. In line with this, data in Figure 3.3 shows that the expression of a mutant PLC $\gamma$ 1 constitutively associated to the plasma membrane inhibits the fibronectin- induced cell migration, likely through a loss of cell directionality caused by lack of polarization of PLC $\gamma$ 1. Data in the literature have also demonstrated an important role of PLC $\gamma$ 1 in integrin-induced cell spreading and cytoskeleton remodelling. Mouse embryonic fibroblast (MEF) cells knocked-down for PLC $\gamma$ 1 showed rounded morphology and diminished RAC1 activation upon integrin engagement which is essential for membrane ruffles formation (Choi et al., 2007). Consistent with this we also reported a role of PLC $\gamma$ 1 in EGF-induced Rac1 activation (Sala et al., 2008). Similarly, I observed that downregulation of PLC $\gamma$ 1 in MDA-MB-435 and TSA breast cancer cells impaired ruffles formation upon EGF or serum stimulation (Figure 3.9-3.10),

indicating that PLC $\gamma$ 1 plays an essential role in cytoskeleton remodelling which is essential for protrusion formation in cancer cell lines in turn necessary to regulate cell motility. Taken together these studies highlighted PLC $\gamma$ 1 as a key molecular enzyme involved in cell motility in normal and in cancer cells. Interestingly PLC $\gamma$ 1 has been found overexpressed in different cancer type like prostate and breast cancer. Furthermore we reported that PLC $\gamma$ 1 was overexpressed in 50% of metastasis form breast cancer patients (Sala et al., 2008). Data showed in this chapter showed that PLC $\gamma$ 1 isoform is essential for cell invasion of breast cancer and melanoma cells on Matrigel. These data supported the hypothesis that PLC $\gamma$ 1 might have a role in the metastatic process. Indeed, based on these data, we performed *in vivo* metastasis assay using MDA-MB-231 cells expressing the stable and inducible system in order to downregulate PLC $\gamma$ 1 protein expression (Sala et al., 2008) and we demonstrated that PLC $\gamma$ 1 is important for both development and progression of metastasis (chapter 1.4).

### Summary

Taken together these data demonstrated the main role of PLC $\gamma$ 1 in cell migration and in particular in cancer cell invasion *in vitro*. Furthermore data showed that PLC $\gamma$ 1 has a main role in growth factor-induced cytoskeleton remodelling, which may explain the eventual inhibition of cell motility. These data, published in a Cancer Research paper, demonstrated the role of PLC $\gamma$ 1 in metastasis and highlighted PLC $\gamma$ 1 as a potential target for anti-metastatic drug development.

## **Chapter 4**

**PLC $\gamma$ 1 is the main PLC isoform  
involved in EGF- and FGF- induced  
calcium release and InsP<sub>3</sub> production  
in  
MDA-MB-231 and endothelial cells**

## 4.1 Introduction

The results described in chapter 3 demonstrated the essential role of PLC $\gamma$ 1 on cell migration, invasion and cytoskeleton remodelling. These data, together with our data indicating the key role in metastasis development and progression (Sala et al., 2008), suggested that targeting PLC $\gamma$ 1 may represent a novel key anti-metastatic strategy. In order to investigate the potential effect of PLC $\gamma$ 1 inhibition it was first necessary to find an unequivocal read out of the enzymatic activity of PLC $\gamma$ 1. PLC $\gamma$ 1 is activated by different growth factor like EGF, FGF and PDGF (Kim et al., 1990; Kim et al., 1991). Once activated PLC $\gamma$ 1 hydrolyzes PtdIns(4,5)P<sub>2</sub> leading to accumulation Ins(1,4,5)P<sub>3</sub> and diacylglycerol that in turn induce calcium release from internal stores and the activation of some protein kinase C (PKC) isoforms, respectively. Following the initial calcium release from the internal stores and plasma membrane depolarisation, store operating channels (SOC) situated on the plasma membrane allow the influx of calcium ions from the extracellular compartment providing a more sustained signal (Patterson et al., 2005M; Heo et al., 2006).

Analysis of cytoplasmic calcium variation provides an indirect read-out of IP<sub>3</sub> production which is dependent from PLC activity. Molecular probes are available to measure calcium concentration in a fluorescence assay. In particular the fluorescent calcium probe Fluo-4 AM is extensively used to measure variation in the cytoplasm calcium levels on time. This is obtained using a confocal time lapse analysis exciting the probe with a 488 nm wavelength laser and measuring the emission at 515 nm.

## 4.2 Results

### 4.2.1 Effect of PLC $\gamma$ 1 downregulation on EGF-induced calcium release in MDA-MB-231

EGFR and HerB family receptors are often overexpressed in breast cancer and EGF stimulates activation of PLC $\gamma$ 1 in different types of cancer (Thomas et al., 2003; Price et al., 1999). Based on this, the effect of PLC $\gamma$ 1 downregulation on calcium variation upon EGF stimulation was determined in MDA-MB-231 cells.

As shown in Figure 4.1, calcium measurements were performed in MDA-MB-231 cells expressing the inducible system, described in chapter 3.2.4, in the absence (PLC $\gamma$ 1 expressed) or presence (PLC $\gamma$ 1 downregulated) of tetracycline. Cells were stimulated with EGF (50 ng/ml) after a pre-acquisition of 1 minute and the fluorescence was monitored for 8 minutes. ATP was added at the end of the experiment as positive control in order to determinate cell viability. MDA-MB-231 not treated with tetracycline (-TET) responded in a fast-response-manner to EGF stimulation. In contrast MDA-MB-231 downregulated for PLC $\gamma$ 1 (+TET) did not show any fluorescence variations after EGF stimulation. The calcium response induced by ATP was comparable in both MDA-MB-231 (-TET) and MDA-MB-231 shPLC $\gamma$ 1 (+TET) indicating that cells were equally viable for the duration of the analysis. This data indicated that PLC $\gamma$ 1 is essential for EGF-induced calcium mobilisation in MDA-MB-231 and suggested that other PLC members are not involved in EGF-induced calcium release in this cell line.

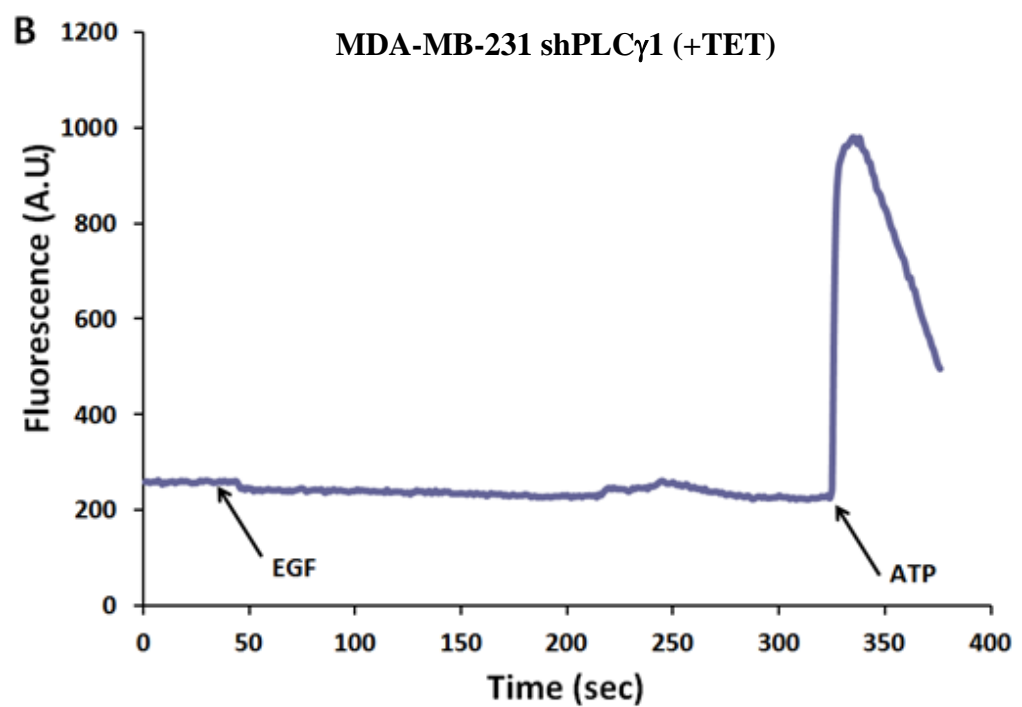
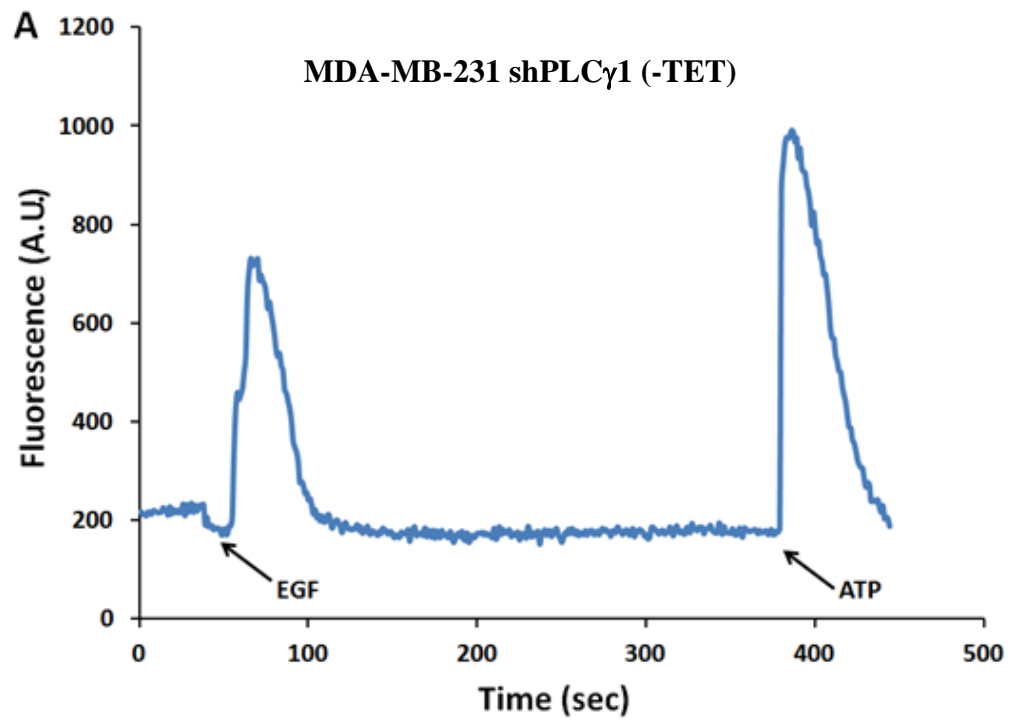


**Figure 4.1: PLC $\gamma$ 1 is essential for EGF-induced calcium mobilisation:** Calcium mobilisation assay upon EGF stimulation: **(A)** Calcium increase in EGF-stimulated-MDA-MB-231 when PLC $\gamma$ 1 is expressed. Arrows indicate the

time point of EGF or ATP treatment. **(B)** Calcium increase in EGF-stimulated-MDA-MB-231 when PLC $\gamma$ 1 expression is downregulated by tetracycline treatment is not expressed following the induction of transcription of the specific shRNA. Arrows indicate the time point of EGF or ATP treatment. Graph is the average of three independent experiments.

#### **4.2.2 Effect of PCL $\gamma$ 1 downregulation on EGF-dependent Inositol Phosphates accumulation**

In order to validate the calcium measurement data obtained in MDA-MB-231 expressing the inducible system targeting PLC $\gamma$ 1, I used a complementary approach to assess PLC $\gamma$ 1 activity. As described in introductory chapter 4.1 the hydrolysis of PtdIns(4,5)P<sub>2</sub> by PLC produces the second messengers Ins(1,4,5)P<sub>3</sub> and DAG. Measurement of inositol phosphates production represents a direct read-out of PLC activity upon cellular stimulation. The assay specifically used in this set of experiments measures the production of all inositol phosphates species. However, since the inositol phosphates variation is mainly due to the Ins(1,4,5)P<sub>3</sub> production generated by PLC activation and its degradation products, the assay is a direct read-out of PLC activation.

MDA-MB-231 cells expressing the inducible system were divided in two groups. One group was treated with tetracycline 24 hours before the labelling to induce PLC $\gamma$ 1 downregulation (+TET), whereas the second group was not treated with tetracycline and used as control (-TET). This second group therefore expressed PLC $\gamma$ 1 since the silencing system was not induced. Cells were then labelled using <sup>3</sup>H-*myo*-inositol for 24 hours in inositol free, serum free media and then stimulated with EGF at different time points. Cells were lysed, inositol phosphates were separated by anion exchange chromatography and the total amount was assessed by liquid radioactivity counting. Downregulation of PLC $\gamma$ 1 (MDA-MB-231 shPLC $\gamma$ 1 +TET) strongly inhibited the EGF-induced inositol phosphates production at all time points compared to the control MDA-MB-231 sh PLC $\gamma$ 1 -TET (Figure 4.2). Taken together

calcium measurement assay and inositol phosphates production assay indicate that EGF stimulation specifically activates the PLC $\gamma$ 1 isoform in MDA-MB-231 excluding any significant involvement of other PLC isoforms.

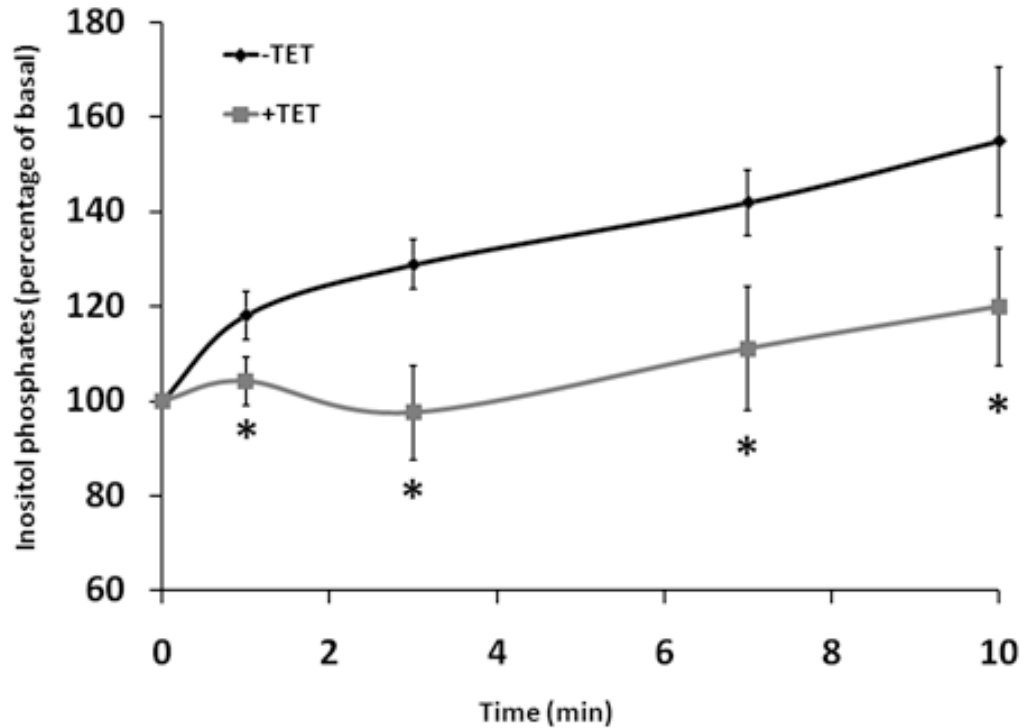


**Figure 4.2 Inositol phosphate assay:** MDA-MB-231 shPLC $\gamma$ 1 (-TET) and MDA-MB-231 shPLC $\gamma$ 1 (+TET) were stimulated with 50 ng/ml EGF for 1,3,5,7,10 minutes. Inositol phosphates accumulation was expressed as percentage of the respective basal. Graphs are the average of 4 independent experiments; bars S.E.; \*P<0.05

### 4.3 Discussion

In this chapter I described two assays used to analyse PLC $\gamma$ 1 activity: the calcium mobilisation assay and the inositol phosphates assay. The calcium assay using the confocal microscope in a time lapse mode was rigorously optimised since it is composed of a step of incorporation of the Fluo-4-AM probe, followed by a de-esterification step. The optimal concentration of Fluo-4 to be used was determined empirically evaluating the number of fluorescent

cells after 1 hour of incubation with a solution 2mM and 4mM of Fluo-4. Only cells incubated with 4 $\mu$ M Fluo-4 showed detectable fluorescence. The cells were incubated in presence or absence of calcium at 2mM concentration. The absence of calcium caused cell detachment from the bottom glassed plate, indicating that calcium was essential for cell adhesion in MDA-MB-231. Because of this all subsequent calcium measurement were performed in the presence of extracellular calcium, therefore the analysed calcium variations were due to the overall flux of calcium across the membranes (internal store and extracellular Ca<sup>2+</sup> influx). The inositol phosphate assay was used to validate data obtained by calcium release, since this method measures directly the production of inositol phosphates. Data obtained analysing the intracellular calcium mobilisation and the inositol phosphate production showed that down regulation of PLC $\gamma$ 1 completely inhibits EGF-induced calcium release in MDA-MB-231. As described in paragraph 1.2.5, PLC $\epsilon$  can also be activated by EGF. However the fact that PLC $\epsilon$  is mainly expressed in tissues such brain, colon and lungs and together with results obtained from calcium and inositol phosphates measurements rules out any contribution of this PLC isoform to the EGF-induced signalling in this particular model. Therefore PLC $\gamma$ 1 appears to be the only member of the PLC family necessary for EGF induced-calcium mobilisation in MDA-MB-231.

### Summary

Calcium release assay revealed that PLC $\gamma$ 1 is the only PLC isoform involved in the EGF-induced signalling in MDA-MB-231

## **4.4 PLC $\gamma$ 1 siRNA interference inhibits FGF-2 induced calcium release in HUVEC cells**

### **4.4.1 Calcium release assay upon FGF-2 addition**

Angiogenesis is involved in different processes such as development, wound healing and tissue regeneration. It plays also an important role in disease such as arteriosclerosis and tumour growth. This process involves endothelial cells which are able to organise three dimensional capillary structures. Different growth factors play an important role in angiogenesis. The most investigated growth factor, the vascular endothelial growth factor (VEGF), has been related to pathological angiogenesis and has been the targeted for development of anti-angiogenic agents. The fibroblast growth factor family (FGF) is composed of 22 different factors. In particular it has been reported that FGF-2 is upregulated in different cancers. FGF induces activation of PI3K/AKT pathway, Src family tyrosine kinases and Ras pathway and it has been shown to activate PLC $\gamma$ 1. It was previously observed in my laboratory that downregulation of PLC $\gamma$ 1 strongly reduces the FGF-induced inositol phosphates accumulation in Human umbilical vein cells (HUVEC) (Maffucci et al., 2009). To further investigate whether FGF-2 was able to activate PLC $\gamma$ 1, I decided to analyse FGF-2-induced calcium mobilisation. The assay was first optimized for this cell line. Cells were labelled with FLUO-4 and stimulated with FGF-2 using the two different concentrations (50ng/ml and 100ng/ml) in order to find the optimal concentration. Changes in fluorescence were measured for 20 minutes. The first concentration failed to induce any detectable intracellular calcium release whereas stimulation with 100ng/ml FGF-2 induced a spiked-shape response as indicated in Figure 4.3. Cell viability was assessed at the end of the acquisition time measuring the calcium release upon ATP stimulation.

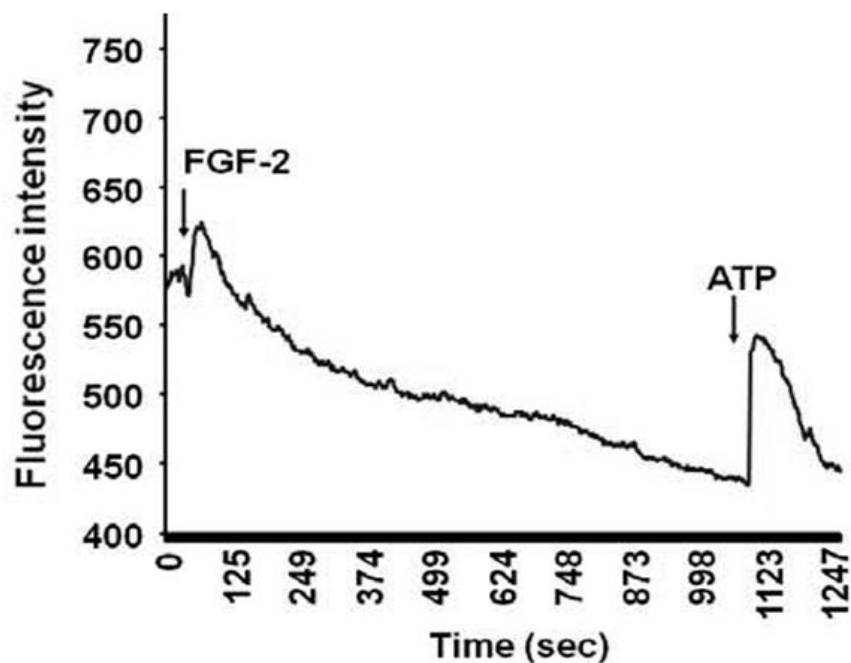


**Figure 4.3 Intracellular calcium** increase in serum starved HUVEC was determined as described in the Materials and Methods section. Cells were stimulated with 100 ng/ml FGF-2 and 1 mM ATP at the indicated times (arrows). Data are mean of values obtained from 4 independent experiments.

#### 4.4.2 PI3K is required for FGF-2-induced calcium release

To gain further insight into the mechanism of FGF-induced activation of PLC $\gamma$ 1, I decided to investigate the potential role of PI3K in this process in HUVEC cells. As described in chapter 1.3.2 PI3K activation is essential for PLC $\gamma$ 1 translocation to the plasma membrane (Falasca et al., 1998). Therefore, I decided to investigate the effect of the reversible PI3K inhibitor LY294002 on intracellular calcium mobilisation. HUVEC cells were serum starved overnight and pretreated with LY294002 (10  $\mu$ M) and FGF-induced calcium mobilisation was measured by confocal analysis. HUVEC cells treated with vehicle alone were used as control. Cell viability was assessed by ATP stimulation at the end of the assay. Data in Figure 4.4 shows that the FGF-2-induced calcium mobilisation was completely inhibited in HUVEC cells treated with LY294002 compared to control cells. These data indicate that PI3K is important also in FGF-2 induced PLC $\gamma$ 1 activation in endothelial cells.

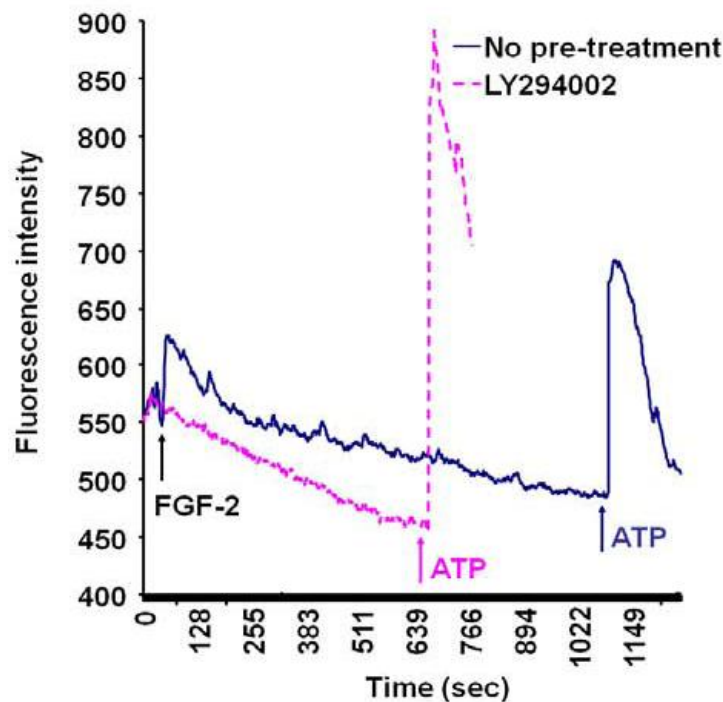


**Figure 4.4: PI3K is required for FGF-2-induced calcium release.** FGF-2-induced calcium release in serum starved HUVEC untreated (blue line) or treated (pink line) with LY294002 (10  $\mu$ M). Data are mean of values obtained from 2 independent experiments.

#### 4.4.3 Effect of PLC $\gamma$ 1 and PLC $\gamma$ 2 downregulation on endothelial cell proliferation

Previous experiments performed by others in my laboratory showed that downregulation of PLC $\gamma$ 1 inhibited inositol phosphates accumulation in endothelial cells. To investigate a potential aspecific effect of PLC $\gamma$ 1-targeting siRNA on PLC $\gamma$ 2 expression, I decide to investigate PLC $\gamma$ 2 levels in HUVEC cells transfected with siRNA targeting PLC $\gamma$ 1. In parallel, siRNA targeting PLC $\gamma$ 2 were used to evaluate the effect of PLC $\gamma$ 2 dowregulation in endothelial cells. Data in figure 4.5A-B show western blot analysis of HUVEC cells transfected with siRNA targeting PLC $\gamma$ 1 or PLC $\gamma$ 2 or with scrambled siRNA as control. Data showed that PLC $\gamma$ 1 was completely downregulated in cells transfected with siRNA targeting PLC $\gamma$ 1, while PLC $\gamma$ 2 levels were not affected. Similarly, transfection with siRNA targeting PLC $\gamma$ 2 had no effect on

PLC $\gamma$ 1 expression indicating that the siRNA sequences used were isoform specific. In order to investigate the role of the PLC $\gamma$ 1 and PLC $\gamma$ 2 on cell proliferation in endothelial cells, cell counting experiments were performed after 24 hours and 48 hours from transfection. Data in Figure 4.5C show that downregulation of PLC $\gamma$ 1 had no effect on cell proliferation. On the contrary, HUVEC transfected with siRNA targeting PLC $\gamma$ 2 showed a significant decrease in cell proliferation compared to control cells or cells transfected with siRNA targeting PLC $\gamma$ 1. These data indicated that PLC $\gamma$ 1 and PLC $\gamma$ 2 play different roles in endothelial cells, with a main role of PLC $\gamma$ 2 in cell proliferation.

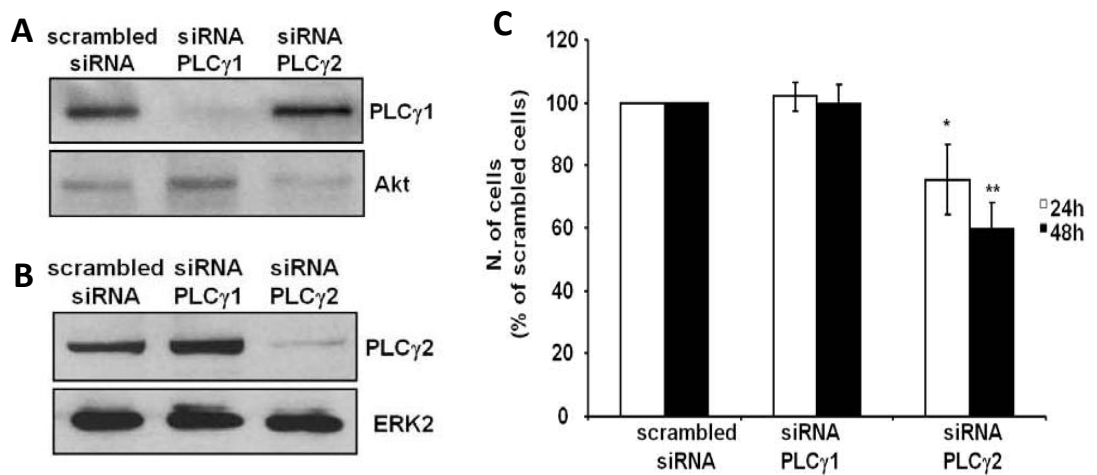


**Figure 4.5: PLC $\gamma$ 2 but not PLC $\gamma$ 1 affects cell proliferation in HUVEC cells: A,B)** Western blot analysis for PLC $\gamma$ 1 and PLC $\gamma$ 2 expression in HUVEC cells transfected with scramble, PLC $\gamma$ 1 or PLC $\gamma$ 2 siRNA. **C)** Cell counting of HUVEC transfected with scrambled, PLC $\gamma$ 1 or PLC $\gamma$ 2 siRNA after 24 and 48 hours of transfection. Data are expressed as percentage of scrambled cells and are mean  $\pm$ SEM of values from 6 independent experiments.

#### 4.5 Discussion

In this chapter I described experiments performed to understand the contribution of PLC $\gamma$ 1 signalling in endothelial cells (HUVEC). The mechanism of FGF-2-induced activation of PLC $\gamma$ 1 has been controversial.

Some studies reported a positive regulation of PLC $\gamma$ 1 phosphorylation by FGF-2 (Burgess et al., 1990), while other reported that FGF-2 is not able to phosphorylate PLC $\gamma$ 1 (McLaughlin et al., 2001). To investigate the FGF-2 induced PLC $\gamma$ 1 activation, I decided to measure the intracellular calcium mobilisation upon FGF-2 stimulation. FGF-2 stimulation induced an instant calcium increase in HUVEC cells. Furthermore, parallel experiments in my laboratory showed that downregulation of PLC $\gamma$ 1 inhibited inositol phosphates accumulation upon FGF-2 stimulation (Maffucci et al., 2009). Together these data demonstrated the main role of PLC $\gamma$ 1 in the FGF-2 response in endothelial cells. It was reported that PI3K activation is essential for PLC $\gamma$ 1 activation upon growth factor stimulation in cancer cells (Falasca et al., 1998; Piccolo et al., 2002). I therefore decided to investigate the potential role of PI3K in FGF-2-induced PLC $\gamma$ 1 activation. My data showed that treatment with PI3K inhibitors (LY294002 and Wortmannin) inhibited PLC $\gamma$ 1 activation. In particular LY294002 treatment inhibited intracellular calcium mobilization and experiments performed in my laboratory by others showed that treatment with wortmannin inhibited inositol phosphates accumulation in cells stimulated with FGF-2. Therefore this data demonstrated that PI3K is essential for the FGF-2-induced PLC $\gamma$ 1 activation. Since PLC $\gamma$ 2 is mainly expressed in the hematopoietic tissue, I investigated the effect of PLC $\gamma$ 1 and PLC $\gamma$ 2 downregulation on cell viability. The effect on cell proliferation observed in HUVEC cells downregulated for PLC $\gamma$ 2, but not in cells transfected with PLC $\gamma$ 1 siRNA, shows that PLC $\gamma$ 1 and PLC $\gamma$ 2 had different functions in endothelial cells. These results are in line with different reports that showed the differential and not overlapping role of the PLC $\gamma$ 1 isoforms in the immunitary system (Regunathan et al., 2006).

### Summary

Taken together these data demonstrate that FGF-2 induces PLC $\gamma$ 1 activation in a PI3K-dependent mechanism and identified the critical role of PLC $\gamma$ 1 in cell migration and tubulogenesis in endothelial cells and highlighted the non-overlapping functions of PLC $\gamma$ 1 and PLC $\gamma$ 2 (Maffucci et al., 2009).

**Chapter 5**  
**Effect of Ins(1,3,4,5,6)P<sub>5</sub> and 2-*O*-Bn-  
InsP<sub>5</sub> on cell migration, cell invasion  
and on PLCγ1 activity**

## 5.1 Introduction

Inositol 1,3,4,5,6 pentakisphosphates (InsP<sub>5</sub>) has been shown to possess anti angiogenic properties and to induce apoptosis in ovarian cancer, lung and breast cancer cell lines (Piccolo et al., 2004; Maffucci et al., 2005). This compound is able to inhibit activation of the PI3K/AKT pathway activation preventing AKT phosphorylation (see introduction chapter 1.8). Since AKT PH domain not only binds phosphoinositides but also inositol phosphates such as InsP<sub>4</sub>, it has been hypothesised that InsP<sub>5</sub> prevents AKT plasma membrane recruitment by binding to the AKT PH domain and therefore competing with PtdIns(3,4,5)P<sub>3</sub> and PtdIns(3,4)P<sub>2</sub> for the PH domain binding. As described in the introductory chapter 1.2.4, PLC $\gamma$ 1 possesses a PH domain reported to be important for its enzymatic activation. The PH domain of PLC $\gamma$ 1 recruits the enzyme to the plasma membrane in an essential step for its enzymatic activation, interacting with PtdIns(3,4,5)P<sub>3</sub> produced by PI3K. Therefore I hypothesized that InsP<sub>5</sub> could prevent PLC $\gamma$ 1 activation by competing with PLC $\gamma$ 1 PH domain binding to PtdIns(3,4,5)P<sub>3</sub> and therefore preventing its activation. As described in introduction chapter 1.3.4, PLC $\gamma$ 1 is involved in controlling cell migration and cytoskeleton remodelling and its pharmacological inhibition could block these processes. Therefore I decided to test the effects of InsP<sub>5</sub> on cell migration and Matrigel cell invasion on a panel of cancer cell lines.

## 5.2 Results

### 5.2.1 InsP<sub>5</sub> inhibits fibronectin-induced migration in MDA-MB-231

In order to determine the effect of InsP<sub>5</sub> on fibronectin-induced cell migration of MDA-MB-231, I performed migration assay using transwell inserts previously coated with fibronectin. MDA-MB-231 cells were serum starved overnight and then pre-treated with InsP<sub>5</sub> (50  $\mu$ M) for 30 minutes. Since InsP<sub>5</sub> is dissolved in H<sub>2</sub>O, MDA-MB-231 cells treated with the same volume of H<sub>2</sub>O were used as control. Cells were then seeded on the inserts and allowed to migrate for 4 hours before being fixed and counted. Data revealed that InsP<sub>5</sub> inhibits MDA-MB-231 fibronectin-induced migration by 60% indicating that InsP<sub>5</sub> inhibits the integrin-activated migration in this breast cancer cell line (Figure 5.1).

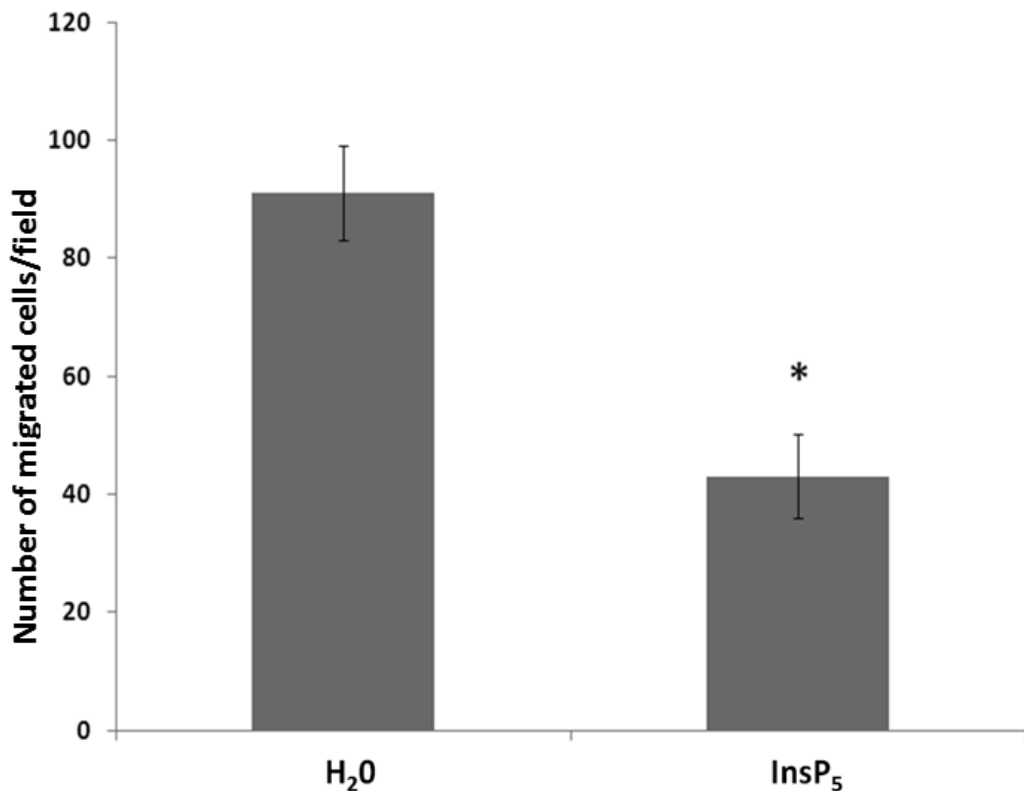


**Figure 5.1 InsP<sub>5</sub> inhibits fibronectin-induced migration:** Quantification of fibronectin-induced migration of MDA-MB-231 cells treated with InP<sub>5</sub>

(50 $\mu$ M) compared to control cells treated with vehicle alone. Data are means  $\pm$ SEM of values obtained from three independent experiments. \* $p$ <0.01

### 5.2.2 InsP<sub>5</sub> inhibits cell invasion on Matrigel of MDA-MB-231

To investigate the effects of InsP<sub>5</sub> on cancer cell invasion, Matrigel cell invasion assay was performed. MDA-MB-231 cells were serum deprived overnight and treated with the inhibitor for 30 minutes before being seeded on the transwell inserts pre-coated with Matrigel. Cells were allowed to invade the Matrigel for 36 hours before being fixed. InsP<sub>5</sub> was maintained for the duration of the invasion experiment. MDA-MB-231 cells treated with H<sub>2</sub>O were used as control. Data revealed that InsP<sub>5</sub> inhibits invasion of MDA-MB-231 cells on Matrigel by 38% compared to the control, indicating that InsP<sub>5</sub> is not only able to reduce cell migration but also to inhibit 3D-Matrigel cell invasion (Figure 5.2).

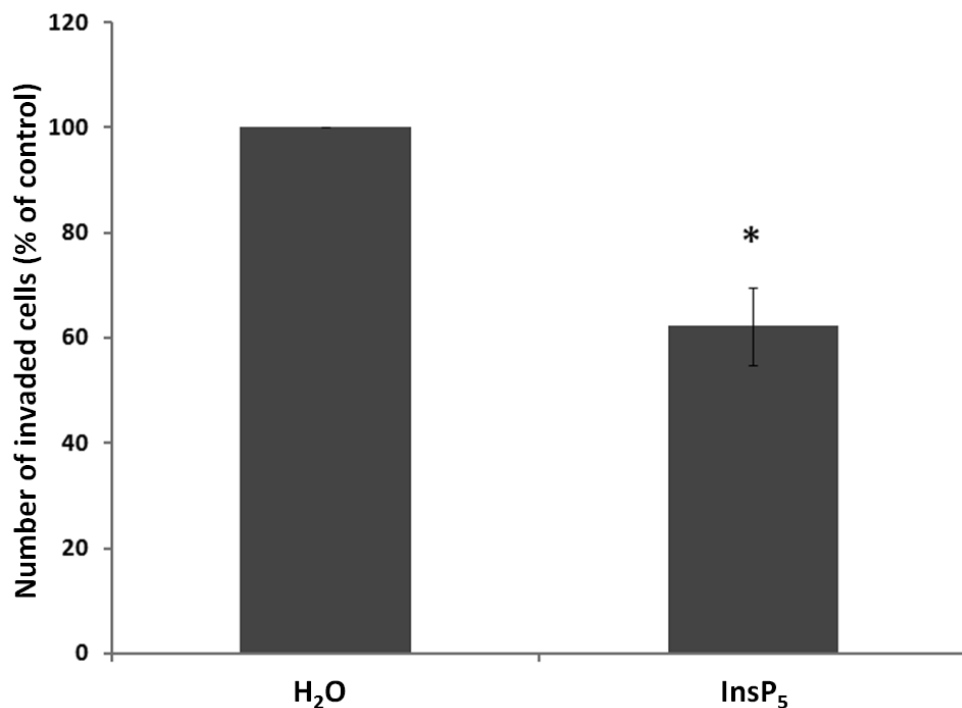


**Figure 5.2 InsP<sub>5</sub> inhibits Matrigel invasion:** Quantification of 3D-Matrigel invasion of MDA-MB-231 cells treated with InP<sub>5</sub> (50 $\mu$ M) compared to control

cells expressed as percentage of control cells which invaded the Matrigel. Data are means  $\pm$ S.E.M of values obtained from 3 independent experiments. \*p=0.01

### **5.2.3 Effect of InsP<sub>5</sub> on cell survival and proliferation in MDA-MB-231 Breast cancer cells**

Since InsP<sub>5</sub> inhibits migration and invasion in MDA-MB-231, I decided to investigate the effect of the compound on cell proliferation and cell survival since these processes may affect cell motility. Furthermore it has been previously shown that InsP<sub>5</sub> induces apoptosis in ovarian, lung cancer and some breast cancer cell lines (Piccolo et al., 2004). A potential pro-apoptotic effect in MDA-MB-231 could also result in the inhibition of cell invasion rate on Matrigel. In order to determine any potential effect of InsP<sub>5</sub> on cell proliferation and cell survival, I performed cell counting experiments in MDA-MB-231 after 72 hours of treatment with InsP<sub>5</sub> in serum free and in serum conditions. Cells treated with H<sub>2</sub>O were used as control. 15,000 cells per-well were seeded, treated with InsP<sub>5</sub> or carrier alone and counted after 72 hours treatment. Data shown in Figure 5.3 indicate that InsP<sub>5</sub> had no effect on MDA-MB-231 proliferation, in cells treated with InsP<sub>5</sub> in 10% serum for 72 hours of treatment. Similarly, no effect on cell survival was detected in cells treated with InsP<sub>5</sub> in serum free condition. These data indicate that InsP<sub>5</sub> does not affect cell proliferation and cell survival in MDA-MB-231 and that the effect seen on cell invasion is not dependent on changes in the proliferation or survival.

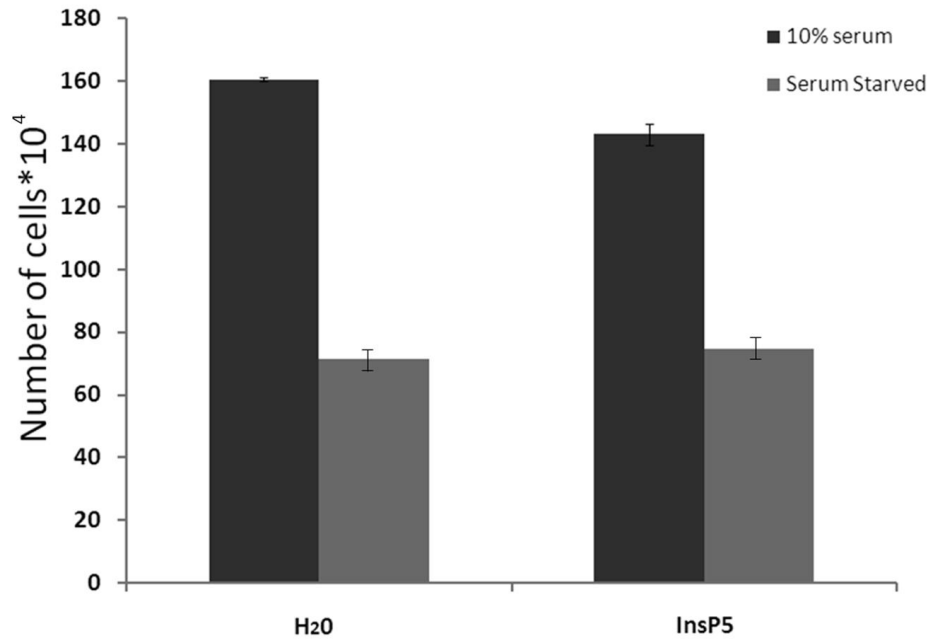


**Figure 5.3:** Cell counting of MDA-MB-231 after 72 hours of treatment with InsP<sub>5</sub> (50 $\mu$ M) in media supplemented with 10% serum or serum deprived media conditions. Data are means  $\pm$ SEM of values obtained from 3 independent experiments in duplicate. No significant difference was observed.

#### 5.2.4 InsP<sub>5</sub> inhibits Matrigel cell invasion in human and murine breast cancer cell lines

My previous experiments performed using MDA-MB-231 indicated that InsP<sub>5</sub> inhibits migration and invasion. I therefore decided to evaluate the effect of InsP<sub>5</sub> treatment on different cancer cell lines. I performed cell invasion assays on Matrigel using the human breast cancer cell line MDA-MB-435 and two syngenic mouse models of breast cancer cell lines (TSA and 4T1). InsP<sub>5</sub> was maintained for the duration of the invasion experiment. Cells treated with H<sub>2</sub>O for each cell line were used as internal controls. Data in Figure 5.4 show that InsP<sub>5</sub> decreased the percentage of cells that had invaded by 35% in MDA-MB-435 and TSA, compared to the respective control. Interestingly, 4T1 cells were more sensitive to the treatment with InsP<sub>5</sub> compared to the other cell lines

used, showing an inhibition of invasion of 76%. Overall these data demonstrated that InsP<sub>5</sub> inhibits invasion of a panel of breast cancer cell lines.

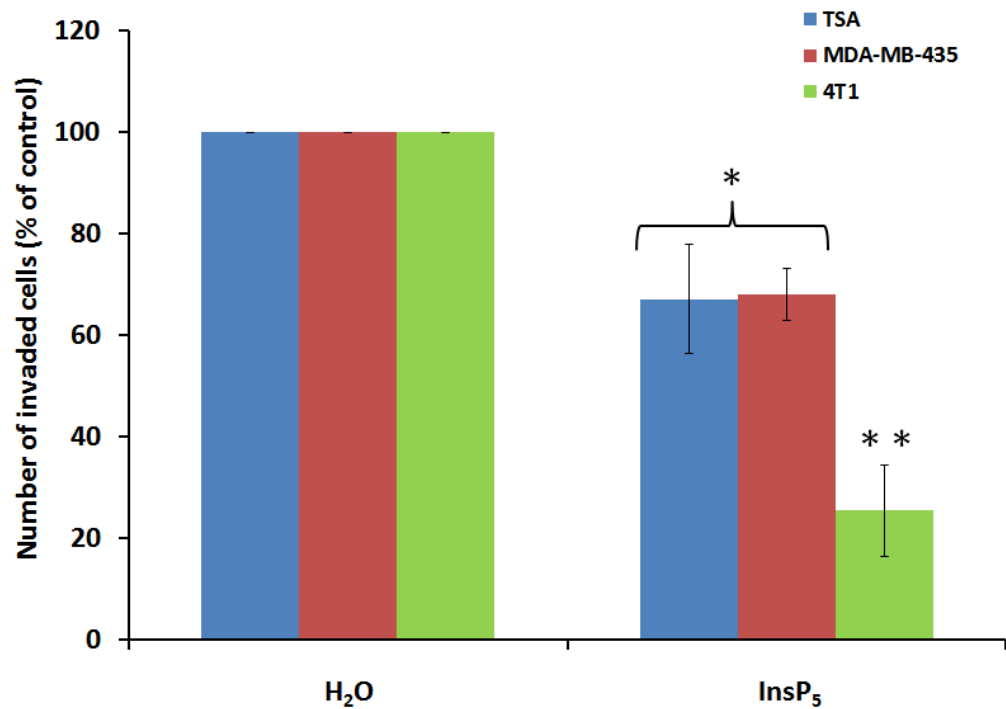


**Figure 5.4: InsP<sub>5</sub> inhibits cell invasion on Matrigel of MDA-MB-435, 4T1 and TSA treated with InsP<sub>5</sub>.** Invasion was expressed as percentage of cells treated with the vehicle alone which invaded the Matrigel (control). Data are means  $\pm$ SEM of values obtained from 3 independent experiments in duplicate. \*p=0.05; \*\*p=0.005

### 5.2.5 InsP<sub>5</sub> does not affect cell proliferation and cell survival of MDA-MB-435, 4T1 and TSA.

In order to evaluate any potential pro-apoptotic effect of InsP<sub>5</sub> on MDA-MB-435, 4T1 and TSA cell lines, I analysed cell proliferation and cell survival on these cell lines, as previously described. Cell counting experiments were performed on cells treated with InsP<sub>5</sub> in 10% serum media and on cells treated with InsP<sub>5</sub> in serum free condition. Cells treated with vehicle (H<sub>2</sub>O) alone

were used as controls for the experiments. Data in Figure 5.5 show that  $\text{InsP}_5$  did not affect proliferation and survival in MDA-MB-435 and TSA (panel A,B). Similarly, no effect on proliferation of TSA was observed in cells kept in 10% serum upon  $\text{InsP}_5$  (panel C, D). On the contrary the number of 4T1 cells after 48 hours or 72 hours treatment with  $\text{InsP}_5$  in serum free condition was clearly reduced, suggesting an effect of the inositol phosphate on cell survival in this particular cell type. Nevertheless, since Matrigel invasion assays were performed in the presence of serum and  $\text{InsP}_5$  does not affect cell proliferation in the presence of serum, we can conclude that the inhibition of invasion detected in the presence of  $\text{InsP}_5$  is exclusively due to an impaired cell migration.

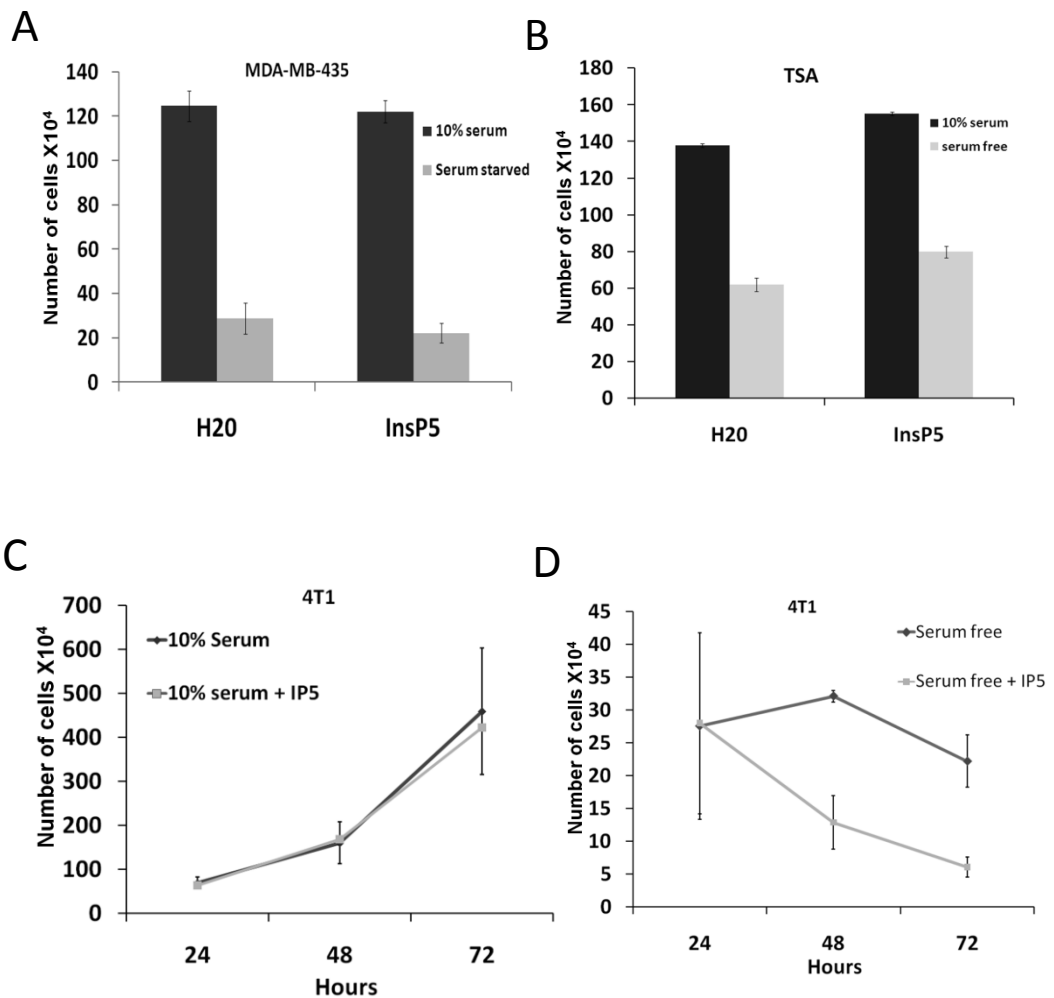


**Figure 5.5: Effect of  $\text{InsP}_5$  on cell proliferation/survival:** Cell counting experiment assessing cell proliferation (10% serum) and survival (Serum free

condition) in, MDA-MB.435 (A), TSA (B) and 4T1 (C,D) after 72 hours of treatment with 50  $\mu$ M InsP<sub>5</sub>. Data are means  $\pm$ SEM of values obtained from 3 independent experiments in duplicate.

### **5.2.6 InsP<sub>5</sub> inhibits internal calcium release In MDA-MB-231 and MDA-MB-435 cell lines.**

Our data so far indicated that InsP<sub>5</sub> inhibits cancer cell invasion primarily through inhibition of cell migration. Since we have shown that PLC $\gamma$ 1 has a key role in regulating cell migration, I hypothesised that InsP<sub>5</sub> could affect PLC $\gamma$ 1 activity. Therefore to test this hypothesis, a calcium release assay was performed using MDA-MB-231 and MDA-MB-435 treated with InsP<sub>5</sub> and stimulated with EGF, since I previously demonstrated that this process is completely dependent on PLC $\gamma$ 1 in MDA-MB-231 (Figure 4.1). Cells were pre-treated with InsP<sub>5</sub> and intracellular calcium variation was assessed with confocal microscope analysis, as before. Data in Figure 5.6A show the calcium response in control MDA-MB-231, treated with vehicle alone. EGF stimulation induced a rapid increase in fluorescence generating an initial Ca<sup>2+</sup> spike immediately after stimulation followed by calcium oscillations. In contrast, cells treated with InsP<sub>5</sub> showed a significant decrease of the initial spike and calcium oscillation, indicating that InsP<sub>5</sub> inhibits PLC $\gamma$ 1 activity (Figure 5.6B). Cell viability was assessed at the end of the assay by ATP stimulation (Figure 5.6C). Fold increase in fluorescence was calculated comparing the difference in fluorescence between basal and the highest fluorescence induced by EGF in three different experiments (Figure 5.6D) and confirming the strong inhibition upon InsP<sub>5</sub> treatment. Similarly, EGF induced a rapid increase in calcium in MDA-MB-435 (Figure 5.7A) which was completely inhibited in cells treated with InsP<sub>5</sub> (Figure 5.7B), indicating that InsP<sub>5</sub> inhibits EGF-induced intracellular calcium mobilization in different cell types. Fold increase in fluorescence was calculated as previously indicated (Figure 5.7D). Similarly, cell viability was assessed at the end of the assay by ATP stimulation (Figure 5.7C)

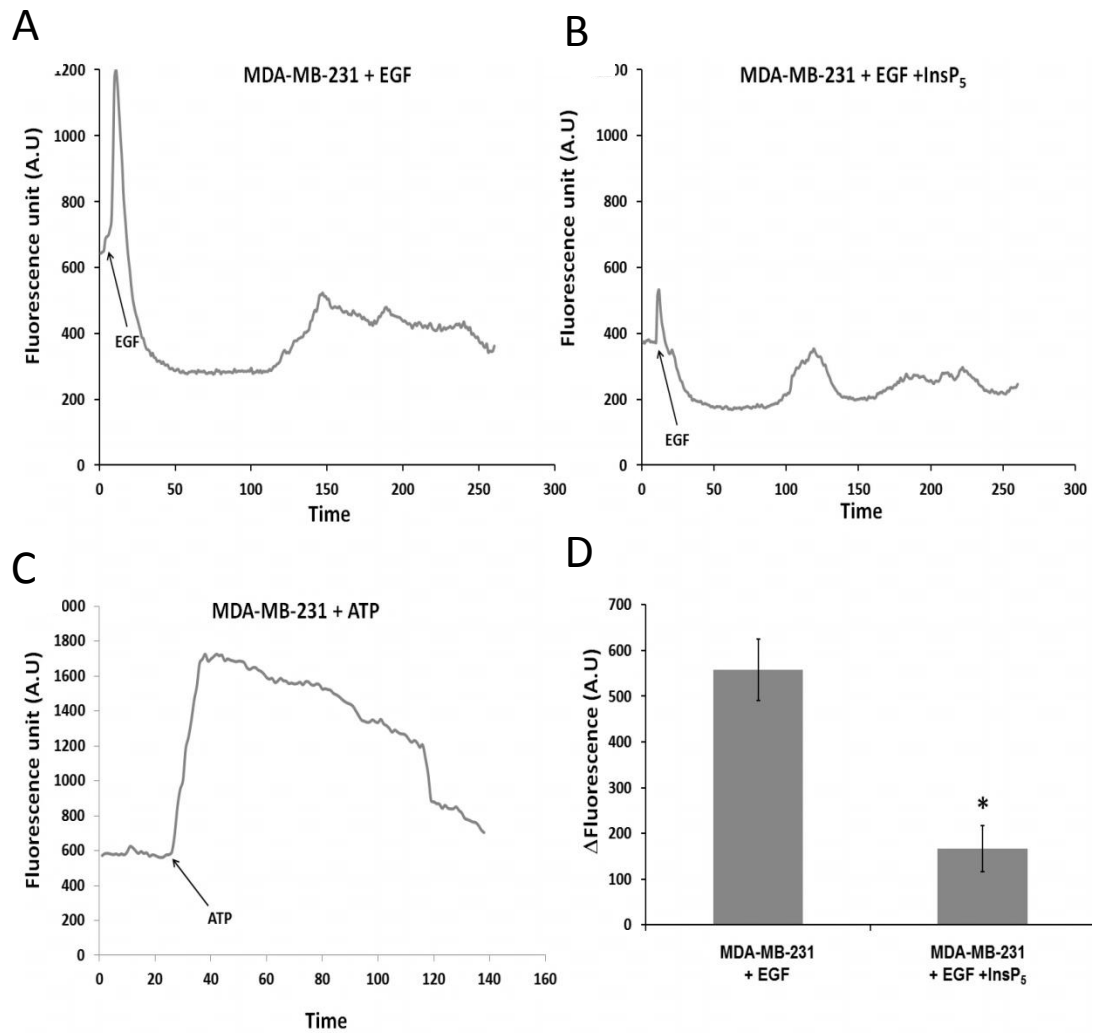


**Figure 5.6 Effect of InsP<sub>5</sub> on EGF-induced intracellular calcium mobilisation in MDA-MB-231:** **A, B)** Representative experiment of EGF-induced intracellular calcium mobilisation in untreated MDA-MB-231 and MDA-MB-231 treated with InsP<sub>5</sub> (50 μM). **C)** Representative ATP-induced intracellular calcium mobilisation. **D)** Quantification of intracellular calcium increase. Columns are the mean of three independent experiments; Bars S.E \*P=0.01

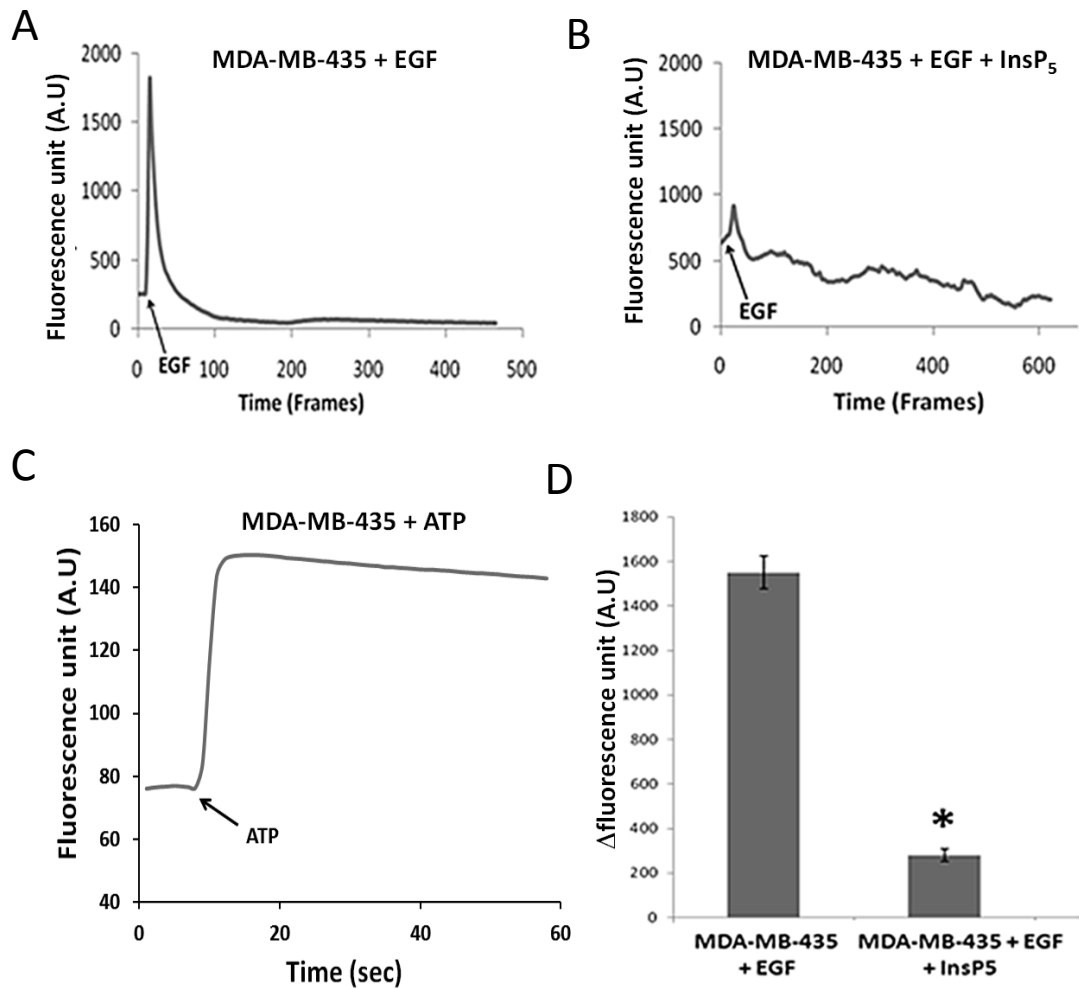


**Figure 5.7: Effect of InsP<sub>5</sub> on EGF-induced intracellular calcium mobilisation in MDA-MB-435:** **A,B)** Representative experiment of EGF-induced intracellular calcium mobilisation in untreated MDA-MB-435 and MDA-MB-435 treated with InsP<sub>5</sub> (50 μM). **C)** Representative ATP-induced intracellular calcium mobilisation. **D)** Quantification of intracellular calcium increase. Columns are the mean of three independent experiments; Bars S.E \*p=0.001

### 5.3 Discussion

Taken together these experiments demonstrated that InsP<sub>5</sub> is able to inhibit cell migration and Matrigel cell invasion *in vitro* in different metastatic cell lines. Furthermore Figure 5.6 and 5.7 showed that InsP<sub>5</sub> inhibits the EGF-induced intracellular calcium mobilization in breast cancer cell lines. Since, as shown in chapter 4.2.1 and 4.2.2 the EGF-induced calcium mobilization is completely dependent on PLC $\gamma$ 1 activity, it is possible to conclude that InsP<sub>5</sub> inhibits PLC $\gamma$ 1 activity. Due to the key role of PLC $\gamma$ 1 in cell motility, cytoskeleton remodelling and cell metastasis (Sala et al., 2008), it is tempting to speculate that InsP<sub>5</sub> may have anti-metastatic properties *in vivo*, since this compound is able to inhibit cell migration and invasion *in vitro* (Figure 5.1, 5.2, 5.4).

### 5.4 2-*O*-Bn-InsP<sub>5</sub> – a new synthetic compound based on InsP<sub>5</sub> structure

In the last years my lab has been focussed on finding alternative compounds based on InsP<sub>5</sub> structure, in collaboration with Professor Potter at the University of Bath. X-Ray crystallography data revealed that Akt PH domain possesses a tyrosine residue near the 6-OH of bound of Ins(1,3,4,5)P<sub>4</sub> that might interact with an aromatic group. Therefore InsP<sub>5</sub> analogues were designed not to alter the symmetry of the parental molecule. As described previously in the introduction chapter 1.8, 2-*O*-Bn-InsP<sub>5</sub> was more potent in inhibiting AKT phosphorylation and it was effective in cell lines resistant to InsP<sub>5</sub> treatment, indicating a more potent action of this synthetic InsP<sub>5</sub> derivative compared to its natural parental molecule.

Thus, I decided to test whether 2-*O*-Bn-InsP<sub>5</sub> was able to inhibit PLC $\gamma$ 1.

#### 5.4.1 2-*O*-Bn-InsP<sub>5</sub> inhibits fibronectin-induced cell migration in MDA-MB-231

Data presented in chapter 5.1 shows that InsP<sub>5</sub> inhibits MDA-MB-231 fibronectin-induced migration. Based on this, I decided to investigate the effect of 2-*O*-Bn-InsP<sub>5</sub> on cell migration. Fibronectin-induced cell migration was measured in the same experimental conditions described in chapter 5.1. Cells were serum starved overnight and pre-treated with 2-*O*-Bn-InsP<sub>5</sub> (50 $\mu$ M) for 30 minutes before being plated on fibronectin-coated transwell inserts and allowed to migrate for 4 hours and then fixed in presence of the compound. Cells treated with vehicle alone were used as control. Data in Figure 5.8 shows that 2-*O*-Bn-InsP<sub>5</sub> completely blocked fibronectin-induced cell migration in MDA-MB-231 and that 2-*O*-Bn-InsP<sub>5</sub> has a more potent effect in inhibiting cell migration compared to the parental molecule (InsP<sub>5</sub>) which inhibits fibronectin-induced migration by 60% (Figure 5.1).

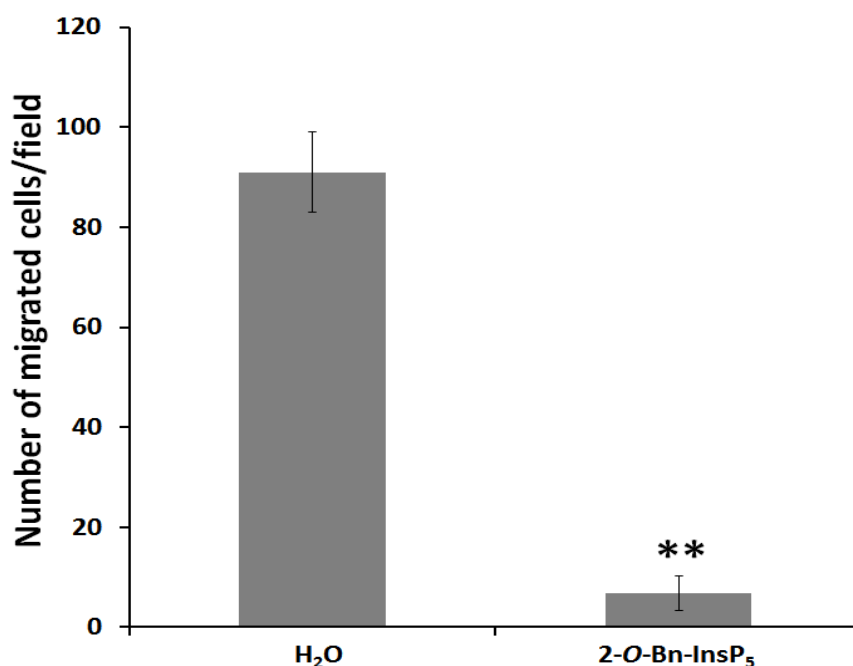


**Figure 5.8: 2-*O*-Bn-InsP<sub>5</sub> blocks fibronectin-induced migration:** fibronectin-induced migration of MDA-MB-231 cells treated with 2-*O*-Bn-InsP<sub>5</sub> (50 $\mu$ M) compared to control cells treated with vehicle alone. Data are

means  $\pm$ SEM of values obtained from 3 independent experiments.  
\*\*p=0.003

#### 5.4.2 2-*O*-Bn-InsP<sub>5</sub> inhibits cell migration in a dose-dependent manner

Considering that 2-*O*-Bn-InsP<sub>5</sub> show an inhibition of 90% in cell migration, I decided to test different concentrations of inhibitor on fibronectin-induced cell migration, to find the lower effective concentration. Experiments were performed using MDA-MB-231 treated with 2-*O*-Bn-InsP<sub>5</sub> at 5, 10, 25, 50  $\mu$ M. Cells treated with vehicle alone were used as control As shown in Figure 5.9 cells treated with 2-*O*-Bn-InsP<sub>5</sub> 10 $\mu$ M show already an inhibition of 80% compared to the control. These data demonstrate that 2-*O*-Bn-InsP<sub>5</sub> inhibit in a dose response manner and is already effective at the concentration of 10 $\mu$ M. Taken together these data showed that the synthetic InsP<sub>5</sub>-derivative compound, 2-*O*-Bn-InsP<sub>5</sub>, is more potent in inhibiting cell migration compared to the mother molecule.

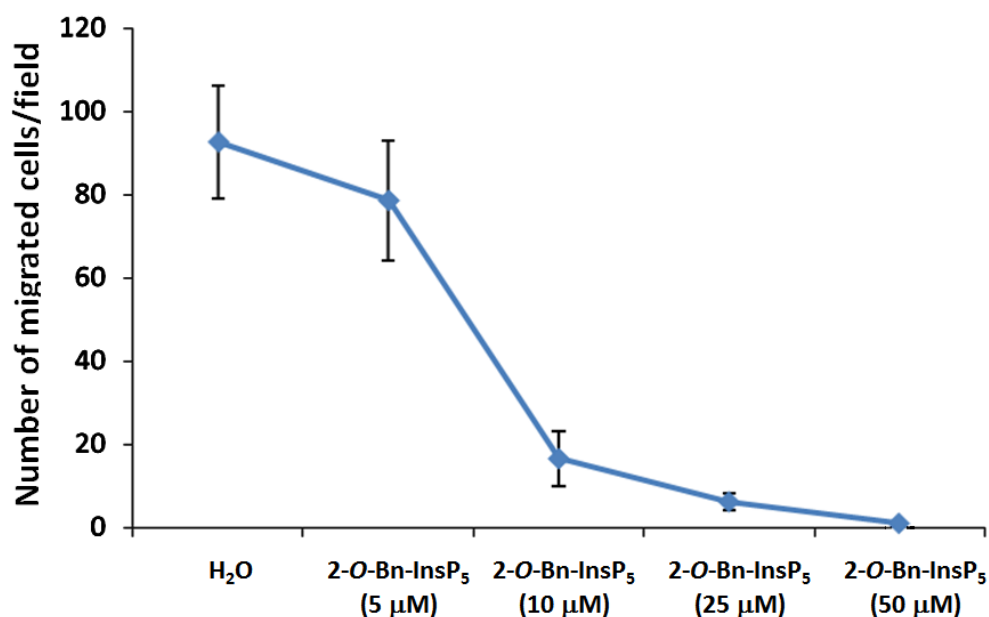


**Figure 5.9: 2-*O*-Bn-InsP<sub>5</sub> inhibits cell migration in a dose-dependent manner:** MDA-MB-231 were pre-treated with 2-*O*-Bn-InsP<sub>5</sub> at different concentration (5, 10, 25, 50  $\mu$ M). Control cells were pre-treated with H<sub>2</sub>O as control. Data are means  $\pm$ SEM of values obtained from 3 independent experiments.

### 5.4.3 2-*O*-Bn-InsP<sub>5</sub> inhibits cell invasion on Matrigel in different human and murine breast cancer cell lines

Data previously described showed that 2-*O*-Bn-InsP<sub>5</sub> inhibits fibronectin-induced cell migration in MDA-MB-231 more potently compared to InsP<sub>5</sub>. Therefore I decided to investigate the effect of 2-*O*-Bn-InsP<sub>5</sub> on cancer cell invasion on Matrigel. Invasion assays were performed using MDA-MB-231, MDA-MB-435, TSA and 4T1 cell lines. The same experimental conditions described in chapter 5.2.3 and 5.2.4 were used. Briefly, cells were serum starved and pre-treated with 2-*O*-Bn-InsP<sub>5</sub> for 30 minutes before being seeded on Matrigel-coated transwell inserts and allowed to invade for 36 hours before being fixed. The compound was maintained for the duration of the invasion experiment. Cells treated with H<sub>2</sub>O were used as control. Data in Figure 5.10 show that 2-*O*-Bn-InsP<sub>5</sub> strongly inhibits invasion on Matrigel in all the cell lines tested. In particular a 52.7%, 63.8%, 73.9%, 87.9% of inhibition was observed respectively in TSA, MDA-MB-435, MDA-MB-231 ad 4T1. As indicated in Table 5.1, it is worth noticing that in each cell line 2-*O*-Bn-InsP<sub>5</sub> inhibited cell invasion on Matrigel more potently than InsP<sub>5</sub>. Taken together these data suggested that 2-*O*-Bn-InsP<sub>5</sub> is able to inhibit cancer cell invasion even more efficiently than the parental molecule.

	H <sub>2</sub> O	InsP <sub>5</sub>	2- <i>O</i> -Bn-InsP <sub>5</sub>
TSA	100%	67.1%	47.3%
MDA-MB-435	100%	68.1%	36.2%
MDA-MB-231	100%	62.2%	26.1%
4T1	100%	25.4%	12.1%

Table 5.1: Percentage of MDA-MB-231, MDA-MB-435, 4T1, TSA treated with InsP<sub>5</sub> 50μM or 2-*O*-Bn-InsP<sub>5</sub> 50μM that have invaded after 36 hours \*p<0.05,\*\*p<0.005. Matrigel invasion expressed as percentage of control cells that had invaded the Matrigel layer (average of 3 independent experiments).

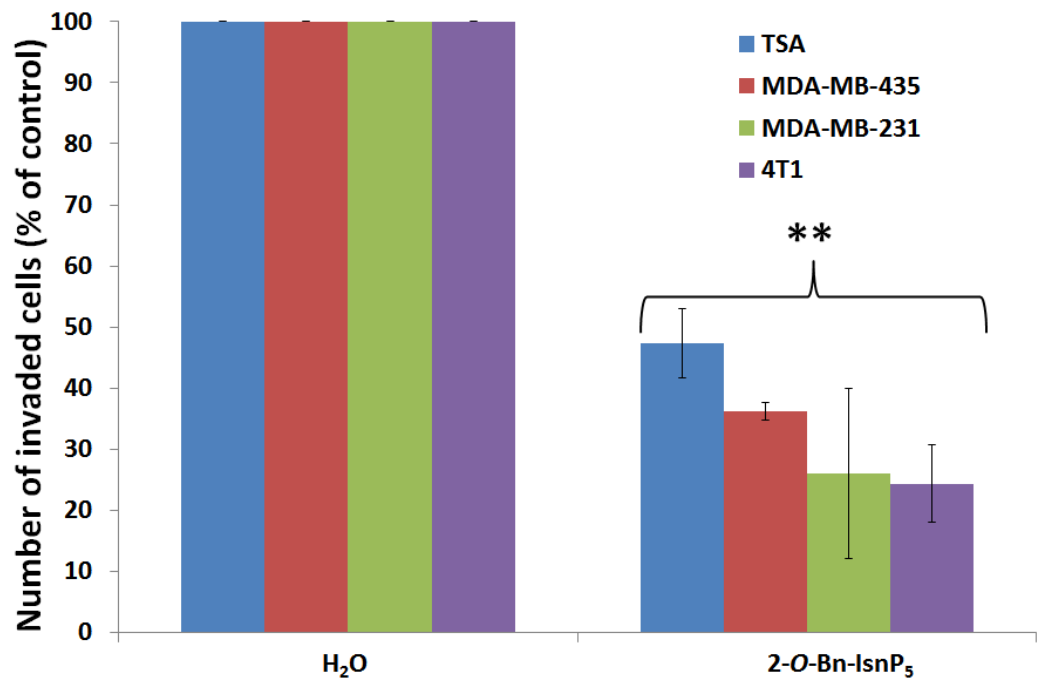


**Figure 5.10: 2-O-Bn-InsP<sub>5</sub> inhibits cell invasion on Matrigel:** Cell invasion assay on Matrigel, expressed as percentage of cells that had invaded, assessed in the indicated cell lines treated with 2-O-Bn-InsP<sub>5</sub>. Invasion was compared to control cells treated with H<sub>2</sub>O. Data are means  $\pm$ SEM of values obtained from 3 independent experiments. \*\*p=0.005

#### **5.4.4 2-*O*-Bn-InsP<sub>5</sub> does not affect cell proliferation and cell survival in MDA-MB-435, 4T1 and TSA cell lines.**

As discussed before for InsP<sub>5</sub>, the effect of 2-*O*-Bn-InsP<sub>5</sub> on cell invasion prompted us to evaluate a potential effect on cell proliferation and cell survival. Cell counting assay was performed on MDA-MB-231, MDA-MB-435, 4T1 and TSA after 72 hours of treatment with 2-*O*-Bn-InsP<sub>5</sub>. Cells were treated with 2-*O*-Bn-InsP<sub>5</sub> in 10% serum supplemented media condition to measure changes in proliferation and in serum free condition to evaluate effects on cell survival. Cells treated with H<sub>2</sub>O were used as control. Data in Figure 5.11A,B,E reveals that, similarly to InsP<sub>5</sub> treatment, 2-*O*-Bn-InsP<sub>5</sub> treatment had no effect on cell proliferation and cell survival in MDA-MB-231, MDA-MB-435 and TSA. Similarly, no change was observed in cell proliferation in 4T1 treated with 2-*O*-Bn-InsP<sub>5</sub> (Figure 5.11C). However, a decreased number of 4T1 cells was observed when treated in serum free condition (Figure 5.11D), indicating an effect on cell survival promoted by 2-*O*-Bn-InsP<sub>5</sub> treatment. Since the Matrigel cell invasion assay was performed in serum condition, I concluded that the effect seen upon 2-*O*-Bn-InsP<sub>5</sub> treatment on cell invasion was not due to effects on cell growth but to a decreased ability of the cells to invade.

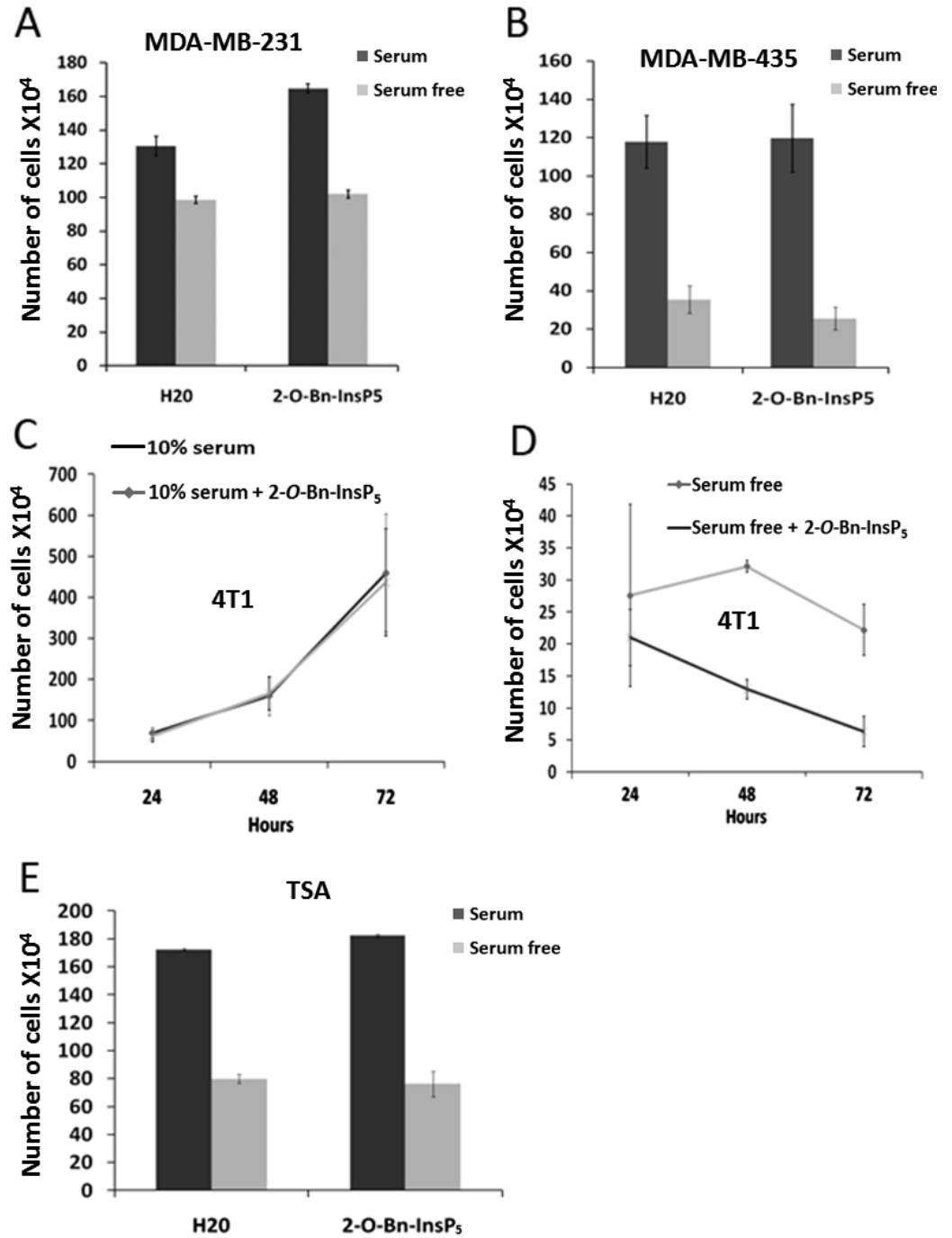


**Figure 5.11: Cell proliferation and cell survival upon 2-O-Bn-InsP<sub>5</sub> treatment:** Cell counting performed on MDA-MB-231 (A), MDA-MB-435 (B), 4T1 (C,D) and TSA (E) treated with 2-O-Bn-InsP<sub>5</sub> (50μM) in 10% serum or serum free condition. Cell counting was performed after 72 hours (48 hours and 72 hours in 4T1). Data are mean ±SEM of three independent experiments.

#### 5.4.5 2-O-Bn-InsP<sub>5</sub> inhibits calcium release response in MDA-MB-231 and MDA-MB-435 upon EGF stimulation.

To determine whether the effect of 2-O-Bn-InsP<sub>5</sub> on cell invasion is also due to inhibition of PLC $\gamma$ 1, as for InsP<sub>5</sub>, I decided to perform calcium release assay experiments on MDA-MB-231 and MDA-MB-435 treated with 2-O-Bn-InsP<sub>5</sub> and then stimulated with EGF. All experiments were performed following the same experimental conditions used to test the effect of InsP<sub>5</sub> described in chapter 5.2.6. Data in Figure 5.12 show that 2-O-Bn-InsP<sub>5</sub> completely inhibits the EGF-induced intracellular calcium variation in MDA-MB-231 (A) and MDA-MB-435 (B). These data indicate that 2-O-Bn-InsP<sub>5</sub> completely blocks PLC $\gamma$ 1 activity upon EGF stimulation in both cell lines. Furthermore data indicates that the inhibitory effect of 2-O-Bn-InsP<sub>5</sub> is more potent compared to InsP<sub>5</sub> (Chapter 5.2.6).

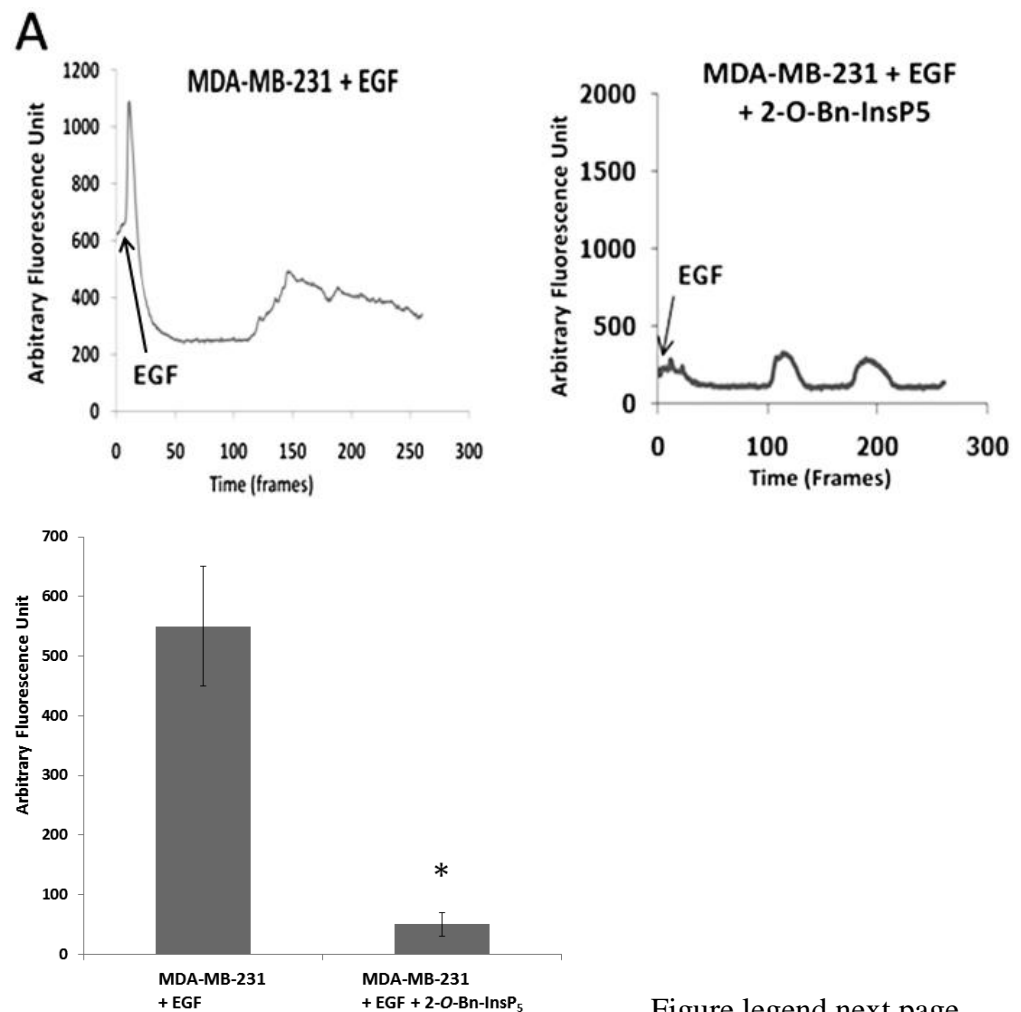
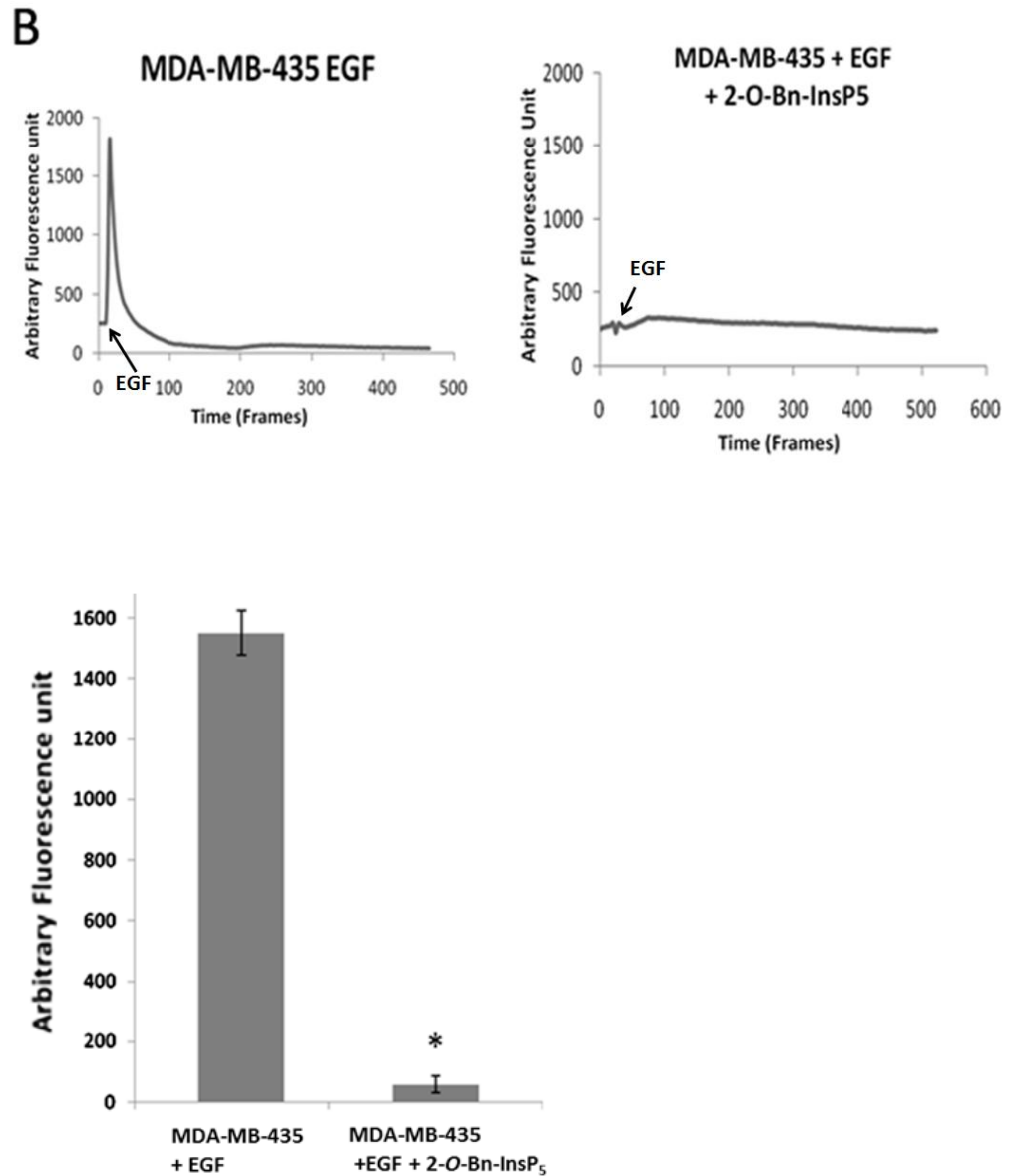


Figure legend next page



**Figure 5.12 Effects of 2-O-Bn-InsP<sub>5</sub> on intracellular calcium mobilisation.** **A)** EGF-induced intracellular calcium mobilisation in MDA-MB-231 untreated (left) or treated with 50  $\mu$ M 2-O-Bn-InsP<sub>5</sub> (right). Quantification of intracellular calcium increase (bottom). Columns are the mean of three independent experiments; Bars S.E \* $p=0.002$  **B)** Calcium release assay in MDA-MB-435 untreated (left) or treated with 50  $\mu$ M 2-O-Bn-InsP<sub>5</sub> (right). Quantification of intracellular calcium increase (bottom). Columns are the mean  $\pm$ SEM of four independent experiments; \* $p=0.001$ .

#### **5.4.6 2-*O*-Bn-InsP<sub>5</sub> inhibits PLC $\gamma$ 1 tyrosine phosphorylation upon EGF stimulation**

As discussed in chapter 1.3, different steps are involved in PLC $\gamma$ 1 activation. The recruitment to the plasma membrane is essential for PLC $\gamma$ 1 activation. Furthermore tyrosine phosphorylation of PLC $\gamma$ 1 is essential for its enzymatic activation. Since 2-*O*-Bn-InsP<sub>5</sub> showed the highest inhibitory effects on cell motility, Matrigel cell invasion and EGF-induced PLC $\gamma$ 1-mediated intracellular calcium release, I decided to focus on the mechanism through which 2-*O*-Bn-InsP<sub>5</sub> inhibits PLC $\gamma$ 1 activity. Therefore I decided to investigate the potential effect of 2-*O*-Bn-InsP<sub>5</sub> treatment on PLC $\gamma$ 1 tyrosine phosphorylation. In particular I decided to investigate the phosphorylation of the residue Y783 which is essential for PLC $\gamma$ 1 enzymatic activity (Sekiya et al, 2004).

MDA-MB-231 cells were serum starved overnight and then pre-treated with 2-*O*-Bn-InsP<sub>5</sub> for 30 minutes. Cells were then stimulated with EGF for 3 and 10 minutes and lysed for protein extraction. MDA-MB-231 cells treated with H<sub>2</sub>O were used as control. Western blot analysis was performed and phosphorylation of PLC $\gamma$ 1 at Y783 residue was assessed using a specific antibody. Western blot analysis generated two bands corresponding to the phosphorylated form of PLC $\gamma$ 1 as indicated by the manufacturer. GAPDH levels were measured in order to evaluate protein equal loading. A representative blot is shown in Figure 5.13. 2-*O*-Bn-InsP<sub>5</sub> strongly inhibits PLC $\gamma$ 1 phosphorylation upon EGF stimulation compared to untreated cells. These data indicates that 2-*O*-Bn-InsP<sub>5</sub> can inhibit PLC $\gamma$ 1 activation by blocking its tyrosine phosphorylation. Therefore the ability of 2-*O*-Bn-InsP<sub>5</sub> to inhibit PLC $\gamma$ 1 phosphorylation provides a molecular mechanism for the reduced Matrigel invasion detected in cancer cell lines treated with 2-*O*-Bn-InsP<sub>5</sub>, and possibly InsP<sub>5</sub>, explaining the decreased activity of the enzyme observed by the intracellular calcium mobilization assay.

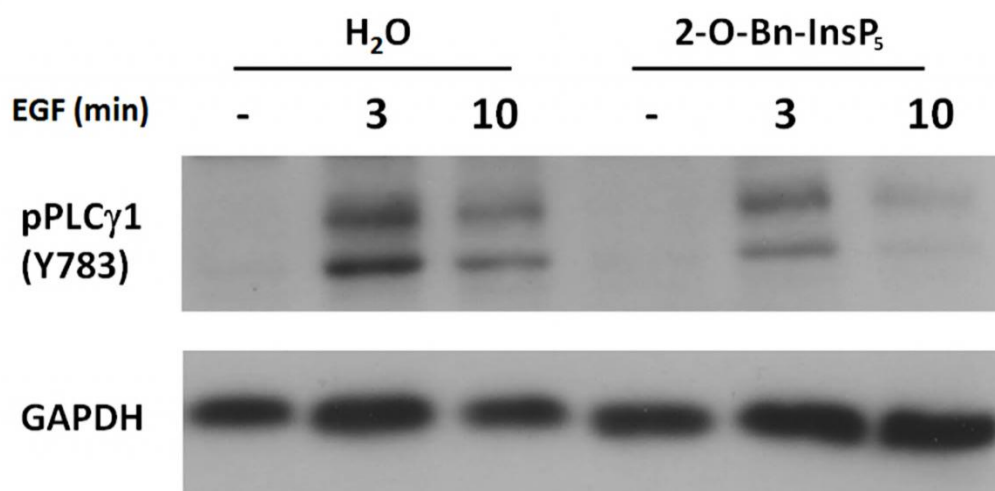


**Figure 5.13: PLC $\gamma$ 1 phosphorylation is inhibited by 2-O-Bn-InsP<sub>5</sub> treatment:** Western blot analysis of PLC $\gamma$ 1 phosphorylation at its residue Y783 in MDA-MB-231 untreated or pre-treated with 2-O-Bn-InsP<sub>5</sub> for 30 minutes before stimulation with 50 ng/ml EGF for 3 and 10 minutes. Blot representative of 4 independent experiments.

## 5.5 Discussion

As discussed in the introductory chapters increasing evidence showed that the inositol phosphates might compete with the binding of phosphoinositides to PH domains possessed by key proteins involved in cell proliferation, cell survival and motility such as AKT, preventing their activation. My laboratory has been focussed on developing inositol phosphates-based compounds and investigating their effects on the PI3K/AKT pathway. Data showed in chapter 3, together with data published in our recent report (Sala et al., 2008) demonstrate the pivotal role of PLC $\gamma$ 1 in cell migration and invasion and, more importantly, the requirement of PLC $\gamma$ 1 for metastases development and progression. In an effort to identify potential specific PLC $\gamma$ 1 inhibitors, I decided to investigate the effect on PLC $\gamma$ 1 activation of inositol phosphates treatment, hypothesising that they might compete with the PtdIns(3,4,5)P<sub>3</sub> for the binding of PLC $\gamma$ 1 PH domain, blocking the PI3K-dependent plasma membrane recruitment of PLC $\gamma$ 1 necessary for the activation of the enzyme.

This model was already demonstrated for AKT inhibition promoted by InsP<sub>5</sub> (Piccolo et al., 2004; Maffucci et al., 2005). I therefore investigated the effect of InsP<sub>5</sub> treatment on cell migration in MDA-MB-231 and cell invasion in a broader number of breast cancer cell lines (MDA-MB-231, MDA-MB-435, TSA, 4T1). Data showed a significant inhibition of cell invasion on Matrigel in all the cancer cell lines analysed (Figure 5.1, 5.2, 5.4). Noteworthy no difference in cell proliferation or cell survival (except 4T1 cell line) was observed in cells treated with InsP<sub>5</sub>, excluding therefore the possibility that the effect on cell migration and invasion was due to decreased cell viability (Figure 5.3, 5.5).

It has to be noted that InsP<sub>5</sub> induced apoptosis mostly in cell lines with high level of AKT activation while it had low or no effect in cell lines with normal level of activation of PI3K/AKT pathway (Piccolo et al., 2004). MDA-MB-231 for example shows low level of AKT activation and treatment with InsP<sub>5</sub> has no effect on cell proliferation and survival. On the contrary SKOV3 possesses elevated levels of AKT activation and treatment with Ins(1,3,4,5,6)P<sub>5</sub> affects cell proliferation and cell survival (Piccolo et al., 2004). To investigate the potential inhibition of PLC $\gamma$ 1 by InsP<sub>5</sub> treatment, I performed calcium mobilisation assays upon EGF stimulation in MDA-MB-231 and MDA-MB-435. EGF-induced calcium mobilisation was inhibited in cells upon treatment with InsP<sub>5</sub> compared to untreated cells (Figure 5.6, 5.7). No difference in ATP-induced calcium mobilisation was observed upon InsP<sub>5</sub> treatment compared to the control. Since the EGF-induced calcium migration in MDA-MB-231 is completely dependent on PLC $\gamma$ 1 (Figure 4.1, 4.2), these data strongly suggested that InsP<sub>5</sub> inhibits PLC $\gamma$ 1 activation directly or indirectly.

The effect of InsP<sub>5</sub> treatment on cell migration and invasion prompted my group, in collaboration with Professor Potter (University of Bath) to develop novel molecules based on InsP<sub>5</sub> structure in the effort to improve its potency and specificity. The derivative 2-*O*-Bn-InsP<sub>5</sub> showed enhanced inhibitory properties towards AKT. Invasion assay on Matrigel showed that 2-*O*-Bn-InsP<sub>5</sub> was more efficient in inhibiting invasion compared to InsP<sub>5</sub> (Figure 5.8,

5.9, 5.10) without affecting cell proliferation and cell survival (Figure 5.11). Intracellular calcium mobilisation showed that 2-*O*-Bn-InsP<sub>5</sub> completely blocked intracellular calcium release, indicating that this InsP<sub>5</sub> derivative was a more potent inhibitor towards PLC $\gamma$ 1 compared to the parental molecule (Figure 5.12). Since PLC $\gamma$ 1 phosphorylation status is essential for PLC $\gamma$ 1 activity, I investigated whether 2-*O*-Bn-InsP<sub>5</sub> was able to inhibit the phosphorylation status of PLC $\gamma$ 1. Analysis of EGF-induced tyrosine phosphorylation of PLC $\gamma$ 1 showed that 2-*O*-Bn-InsP<sub>5</sub> inhibited PLC $\gamma$ 1 phosphorylation at its residue Y783, which strictly correlates with the enzymatic activity (Figure 5.13). Taken together these data demonstrated that the inhibitor prevents PLC $\gamma$ 1 phosphorylation and the following activation of PLC $\gamma$ 1. However the mechanism by which 2-*O*-Bn-InsP<sub>5</sub> and InsP<sub>5</sub> inhibit PLC $\gamma$ 1 is not well understood and different hypotheses must be further investigated. For example it cannot be excluded that the inhibitors compete with EGF binding to the EGFR, resulting in an inhibition of the downstream pathway.

In an effort to determine specificity and targets of these two compounds, an *in vitro* kinase screening was performed on InsP<sub>5</sub> and 2-*O*-Bn-InsP<sub>5</sub> (Falasca et al., 2010). The screening was performed by Select Screen™ Kinase Profiling Service supplied by Invitrogen. InsP<sub>5</sub> and 2-*O*-Bn-InsP<sub>5</sub> were tested *in vitro* on over 60 different kinases in order to assess their specificity and their inhibitory activity. 2-*O*-Bn-InsP<sub>5</sub> inhibits PDK1 activity with an IC<sub>50</sub> of 26.5 nM towards PDK1. Both compounds showed no effect on AKT1 and AKT2 kinase activity. These results suggested a potential link between PDK1 and PLC $\gamma$ 1 in a mechanism that could involve PDK1 in PLC $\gamma$ 1 phosphorylation directly or indirectly. However since PDK1 is a serine/threonine kinase, a direct involvement is unlikely. A recent report showed that PDK1 is involved in ROCK1 regulation in a kinase-independent mechanism which involves the direct interaction of PDK1 with ROCK1 at the plasma membrane (Sahai et al., 2008) promoting ROCK1 activity. Therefore a similar mechanism might be involved in PLC $\gamma$ 1 regulation. This hypothesis was the basis for the experiments described in chapter 7.

## Summary

Ins(1,3,4,5,6)P<sub>5</sub> and 2-*O*-Bn-InsP<sub>5</sub> show inhibiting PLC $\gamma$ 1 activity. This was assessed by calcium release assay and inositol phosphates incorporation in MDA-MB-231. Moreover 2-*O*-Bn-InsP<sub>5</sub> inhibits PLC $\gamma$ 1 Y783 phosphorylation. Both compounds, but more 2-*O*-Bn-InsP<sub>5</sub>, inhibit cell migration and cancer cell invasion.

**Chapter 6**

**Potential involvement of ABC  
transporters on inositol  
polyphosphates transmembrane  
transport**

## 6.1 InsP<sub>5</sub> internalisation

My data so far demonstrated that 2-*O*-Bn-InsP<sub>5</sub> is able to inhibit PLC $\gamma$ 1 phosphorylation at residue Y783 and to inhibit its enzymatic activity. Furthermore InsP<sub>5</sub> and 2-*O*-Bn-InsP<sub>5</sub> block cell migration and invasion in the panel of breast cancer cell lines tested, indicating that they may have anti-metastatic properties *in vivo*. The mechanism by which inositol polyphosphates are transported across the membrane has not been characterised. It has to be noticed that Ins(1,3,4,5,6)P<sub>5</sub> possesses five phosphates groups that confer a high negative charge to the compound. Therefore it is unlikely that Ins(1,3,4,5,6)P<sub>5</sub> can be transported by passive diffusion across the plasma membrane. It has been demonstrated that Ins(1,3,4,5)P<sub>4</sub> and Ins(1,3,4,5,6)P<sub>5</sub> are internalized by cancer cells (Razzini et al., 2000; Maffucci et al., 2005), and preliminary data produced by my group shows that inositol polyphosphates uptake is inhibited at 4°C suggesting an active transport mechanism. In order to investigate inositol polyphosphates uptake I used the 2-fluorescein-conjugated-InsP<sub>5</sub> (2-FAM-InsP<sub>5</sub>) which was synthesized by our collaborator Professor Potter at the University of Bath. The fluorescein-conjugated compound gave the opportunity to follow its incorporation over time and visualise the dynamic of its incorporation inside the cells.

### 6.1.1 Time-course of InsP<sub>5</sub> uptake

MDA-MB-231 were seeded on coverslips and incubated with 25  $\mu$ M FAM-InsP<sub>5</sub> prepared in DMEM supplemented with 10% serum for the indicated time points. As controls MDA-MB-231 were incubated with 25 $\mu$ M fluorescein for the indicated time and then fixed. Fluorescence intensity was measured using confocal microscopy. Figure 6.1A shows that 2-FAM-InsP<sub>5</sub> entered the cells and it was already detectable intracellularly after 5 minutes. In contrast, control cells treated with fluorescein did not show intracellular fluorescence at any of the indicated time-points (Figure 6.1B). These results indicate that InsP<sub>5</sub> is able to enter MDA-MB-231 cells, despite its polar nature, as already demonstrated for the ovarian cancer cell line SKOV-3 and for the Small Cell Lung Cancer cell line (Maffucci et al., 2005; Razzini et al., 2000).

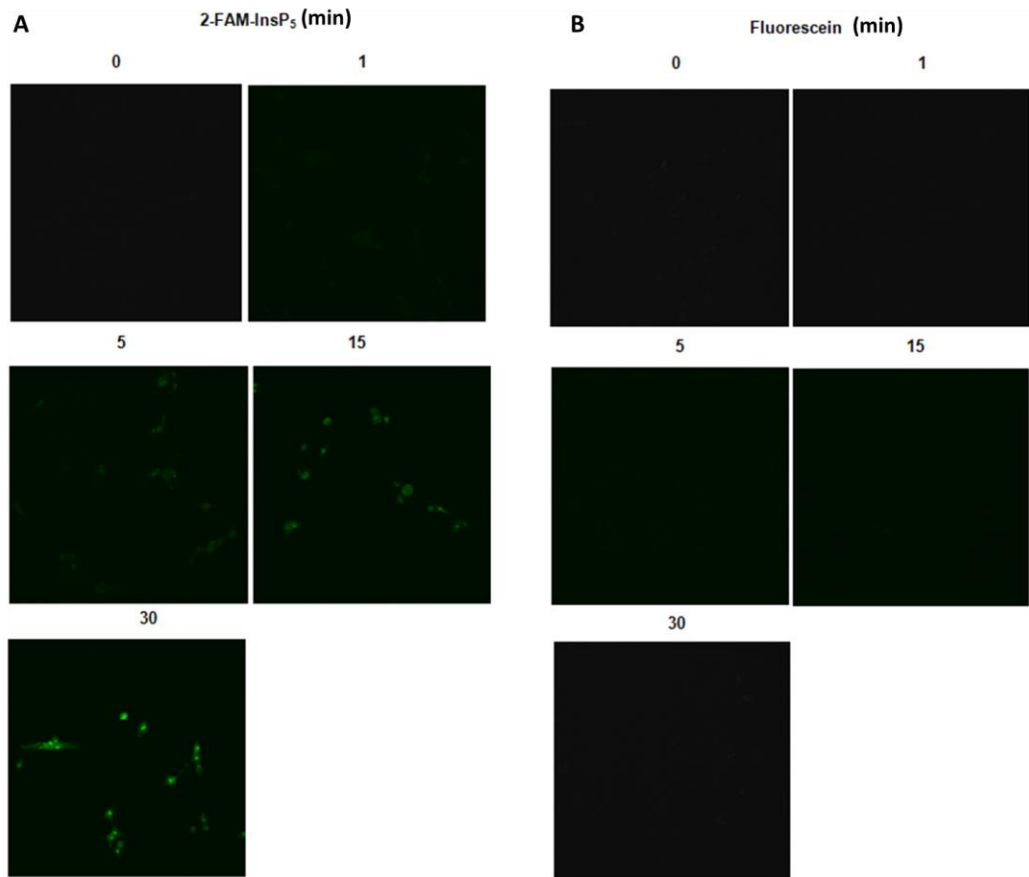


**Figure 6.1 Incorporation of 2-FAM-InsP<sub>5</sub>** A) MDA-MB-231 were seeded on coverslips in a 12-well plate and incubated with 2-FAM-InsP<sub>5</sub> (25  $\mu$ M) for the indicated times before being fixed. B) MDA-MB-231 cells were incubated with 25  $\mu$ M fluorescein as appropriate control for the 2-FAM-InsP<sub>5</sub> uptake.

### 6.1.2 Probenecid and Glibenclamide inhibit 2-FAM-InsP<sub>5</sub> uptake

In 2009 Nagy et al. identified in *Arabidopsis* a membrane transporter belonging to the ATP-binding-cassette (ABC) transporter, involved in the inositol hexakisphosphates transport. The ABC transporters are involved in the trafficking of many substances and several lines of evidence established their role in cancer drug resistance. Indeed the multidrug resistance in tumour is associated with overexpression of certain ABC transporters which, for this reason, are called Multidrug Resistance (MDR) protein or Multidrug Resistance Proteins (MRP) (Glavinas et al., 2004). In particular ABCC1/MRP1, ABCB1/MDR1 and ABCG2 are the transporters mainly involved in the drug resistance process. It has been recently reported that that inositol hexakisphosphate is actively exported from the cytoplasm to the vacuole by the ABCC5 transporter (Nagy et al., 2009). In order to assess the possibility that ABC transporters may also be involved in inositol polyphosphates uptake in mammalian cells, I decided to test the effect of probenecid and glibenclamide, which are two inhibitors of ABC transporters, on inositol phosphates uptake. MDA-MB-231 cells were treated with the inhibitors in a dose dependent manner in order to find highest non-toxic concentration (table 6.1). Treatment with probenecid 5mM and 10mM and glibenclamide 600  $\mu$ M and 1.5mM were toxic, resulting in cell death within one hour from the beginning of the treatment. Therefore hereafter the first effective non-toxic concentration was used for all the experiments. In particular cells were treated with probenecid 1mM and glibenclamide 150 $\mu$ M. MDA-MB-231 were pre-treated for 1 hour with probenecid and glibenclamide and then incubated with 2-FAM-InsP<sub>5</sub> for the indicated times in presence of the inhibitors before being fixed and fluorescence analysed by confocal microscopy. Figure 6.2 shows that treatment of MDA-MB-231 with both inhibitors reduced 2-FAM-InsP<sub>5</sub> intake for 5 and 10 minutes. This data indicated that transporters belonging to the ABC family could be involved in the uptake of InsP<sub>5</sub> in mammalian cells similarly to what was reported in *Arabidopsis*.

Table 6.1:

Concentration Tested					
Probenecid	500 $\mu$ M	1mM	3mM	5mM	10mM
Glibenclamide	75 $\mu$ M	150 $\mu$ M	450 $\mu$ M	600 $\mu$ M	1.5mM

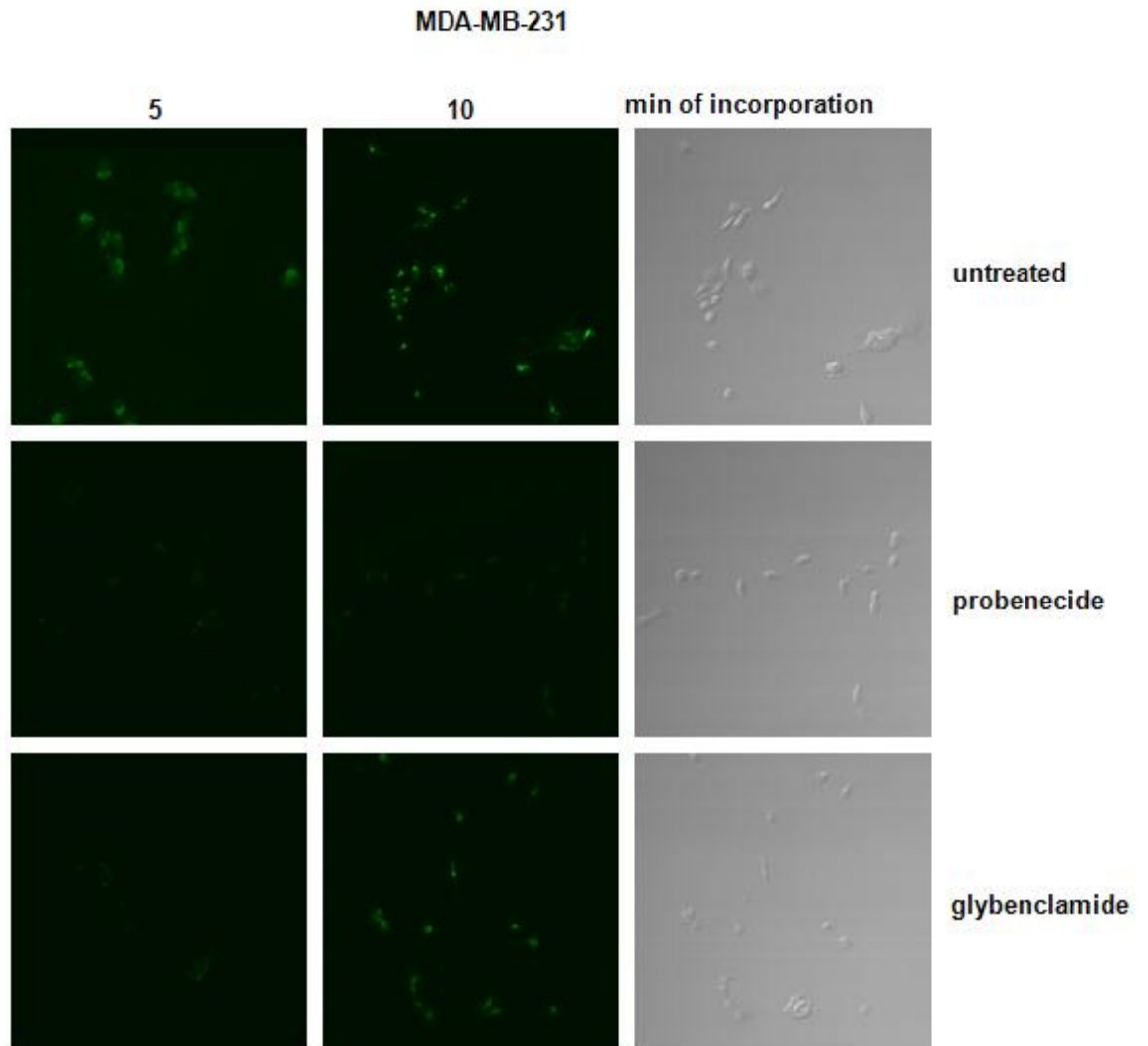


**Figure 6.2: Time course of 2-FAM-InsP<sub>5</sub> uptake** in untreated cells and in MDA-MB-231 treated with probenecid and glibenclamide. On the right a representative bright-field picture of untreated and treated cells is presented.

### 6.1.3 ABCC1 transporter is involved in 2-FAM-InsP<sub>5</sub> uptake

The ABC transporters are a family of trans-membrane transporters involved in export of different substances. Mice deficient in ABCG2, ABCB1 or ABCC1 are viable and fertile but are more sensitive to cytotoxic drugs, consistent with the role of ABC transporters in protecting cells from toxins (Wijnholds et al., 1998; Dean et al., 2005). At present no evidence shows that in mammalian cells ABC transporters are involved in the import process, but they have been characterised for their main role in drug export and multidrug resistance. The finding that ABC inhibition by probenecid and glibenclamide is able to block the uptake of 2-FAM-InsP<sub>5</sub> (Figure 6.2) showed that this class of transporter may be involved also in the import process of InsP<sub>5</sub>, supporting the hypothesis that ABC transporter may be involved in the import of certain substances rather than export alone.

In order to further investigate the role of ABC transporters in inositol polyphosphates intake, I decided to investigate the role of the ABCC family members. In particular ABCC1 has been found upregulated in a variety of solid tumour such as lung, breast and prostate and it constitutes a negative prognostic marker for early stage breast cancer (Kartenbeck et al., 1996; Rudas et al., 2003).

The first approach was to use the ABCC1 specific inhibitor MK-571. MDA-MB1-231 cells were pre-treated with 40 µM MK-571 for 1 hour before being incubated with 2-FAM-InsP<sub>5</sub> for the indicated minutes. Figure 6.3A shows images of a representative experiment of four experiments. Decreased fluorescence was observed at 10, 15 and 30 minutes of 2-FAM-InsP<sub>5</sub> incorporation in cells treated with MK-571 compared to untreated cells, indicating that ABCC1 transported is involved in FAM-InsP<sub>5</sub> uptake. However it is worth noticing that cells treated with MK-571 inhibitor were able to uptake 2-FAM-InsP<sub>5</sub>, although with a slower kinetic, indicating that ABCC1 is not the only transporter involved in the 2-FAM-InsP<sub>5</sub> intake (Figure 6.3B).

A

Untreated (minutes of 2-FAM-InsP<sub>5</sub>)

MK-571 (minutes of 2-FAM-InsP<sub>5</sub>)

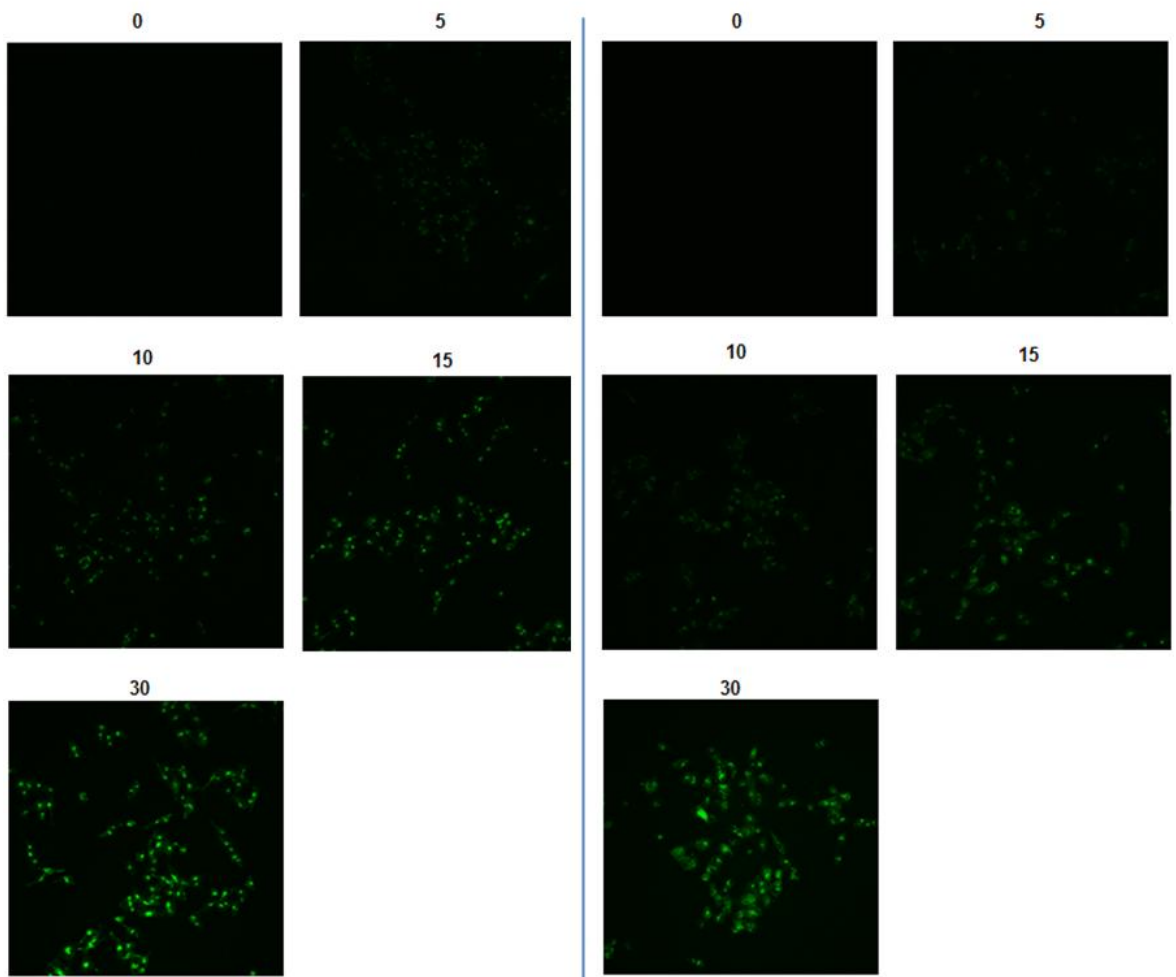
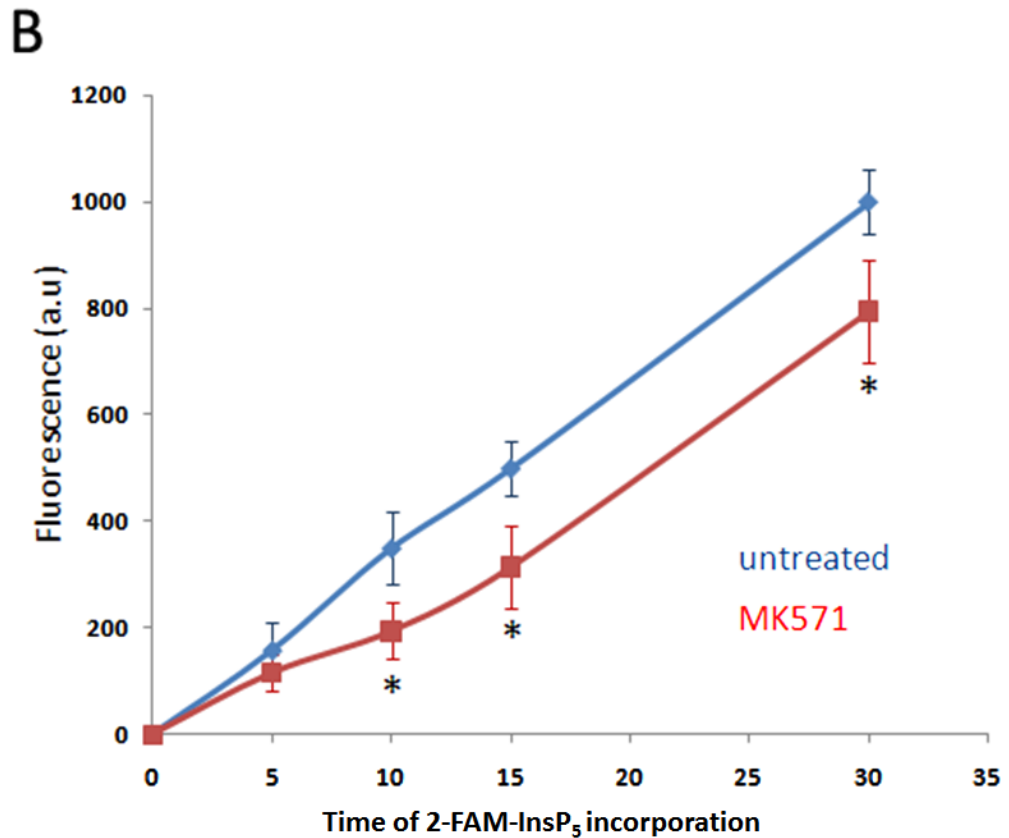


Figure legend next page



**Figure 6.3: 2-FAM-InsP<sub>5</sub> is inhibited by MK-571:** A) Images of MDA-MB-231 untreated or pre-treated with 40  $\mu$ M MK-571 and incubated with 2-FAM-InsP<sub>5</sub> at indicated time points. **B)** Quantification of 4 independent experiments. Graphs are means values  $\pm$ S.E; \*P<0.05

#### 6.1.4 ABCC1 is potentially involved in <sup>3</sup>H-InsP<sub>5</sub> uptake.

In order to validate the data obtained using 2-FAM-InsP<sub>5</sub> uptake, incorporation experiments of <sup>3</sup>H-labelled InsP<sub>5</sub> were performed. MDA-MB-231 were seeded on a 12 well plate and left untreated or pre-treated with 40  $\mu$ M MK-571 for 1 hour and then incubated with 50 $\mu$ M of “cold” InsP<sub>5</sub> supplemented with <sup>3</sup>H-InsP<sub>5</sub> (4,000 cpm/well) provided by our collaborator (Adolfo Saiardi, UCL). The amount of incorporated radioactivity was determined by liquid scintillation counting. The uptake of <sup>3</sup>H-InsP<sub>5</sub> was significantly decreased in cells pre-treated with the ABCC1 inhibitor compared to control cells (Figure 6.4). These data confirmed the results

obtained following the incorporation of the 2-FAM-InsP<sub>5</sub> and suggest that ABCC1 transporter is involved in the InsP<sub>5</sub> uptake.

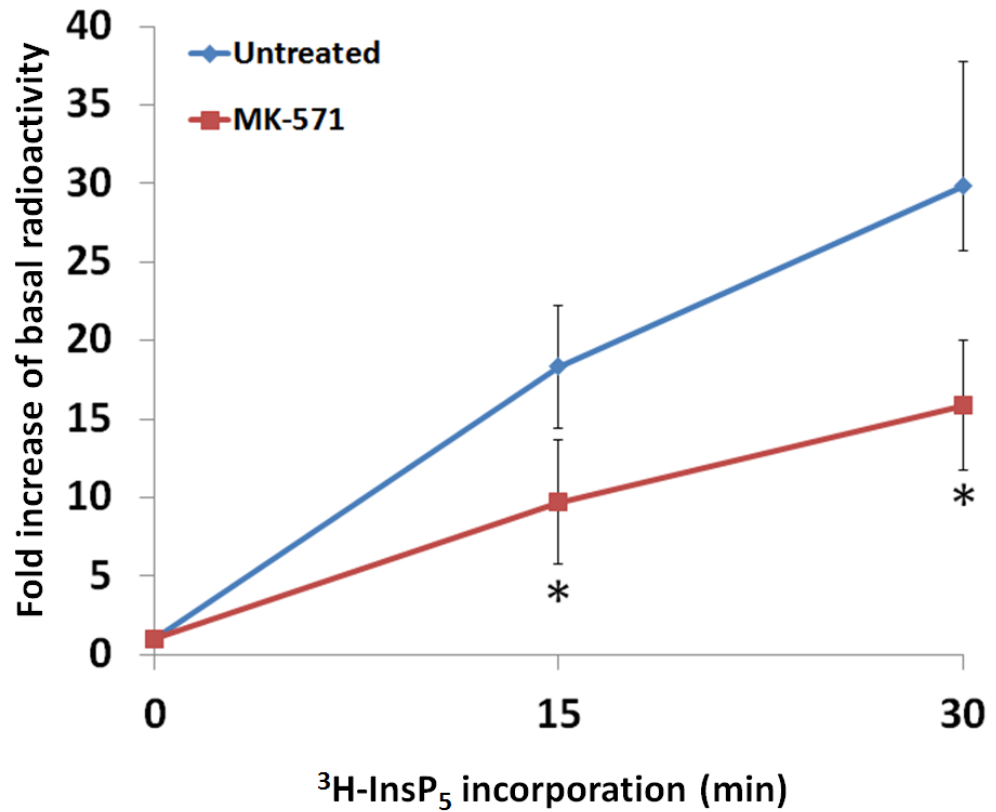


**Figure 6.4: <sup>3</sup>H-InsP<sub>5</sub> incorporation is inhibited by MK-571:** <sup>3</sup>H-InsP<sub>5</sub> incorporation in MDA-MB-231 untreated (blue line) or treated with the ABCC1 inhibitor MK-571 (red line). Graphs are the mean of 3 independent experiments; bars S.E.M; \*P<0.05

### **6.1.5 Downregulation of ABCC1, but not ABCC5, inhibits InsP<sub>5</sub> uptake in MDA-MB-231**

In order to further investigate the role of ABCC1 in InsP<sub>5</sub> transport, I decided to determine the effect of ABCC1 downregulation using specific siRNA in MDA-MB-231. The effect of ABCC5 downregulation (another member of the ABCC family) on 2-FAM-InsP<sub>5</sub> and <sup>3</sup>H-InsP<sub>5</sub> uptake was also investigated in order to assess the potential involvement of other family members in the uptake process.

MDA-MB-231 cells were transfected with siRNAs targeting ABCC1 or ABCC5 respectively. As controls, MDA-MB-231 transfected with a scrambled sequence were used. After 72 hours from transfection, cells were incubated with 2-FAM-InsP<sub>5</sub> for the indicated times before being fixed. Intracellular cell fluorescence was analysed in three independent experiments. Decreased fluorescence was observed in MDA-MB-231 transfected with siRNA targeting ABCC1 compared to cells transfected with scrambled siRNA. In particular a decrease of 50% was observed after 10 minutes of 2-FAM-InsP<sub>5</sub> incorporation. Representative images are showed in Figure 6.5A,B. MDA-MB-231 transfected with siRNA targeting ABCC5 transporter expression showed no difference in 2-FAM-InsP<sub>5</sub> incorporation compared to control (Figure 6.5C). These data suggest that ABCC1 is required for inositol pentakisphosphate transport and that its downregulation significantly decreases uptake of extracellular inositol pentakisphosphate (Figure 6.5D). Furthermore data suggest that ABCC1 may have a specific role in inositol pentakisphosphate active transport, since siRNA for ABCC5 does not affect its cellular intake.

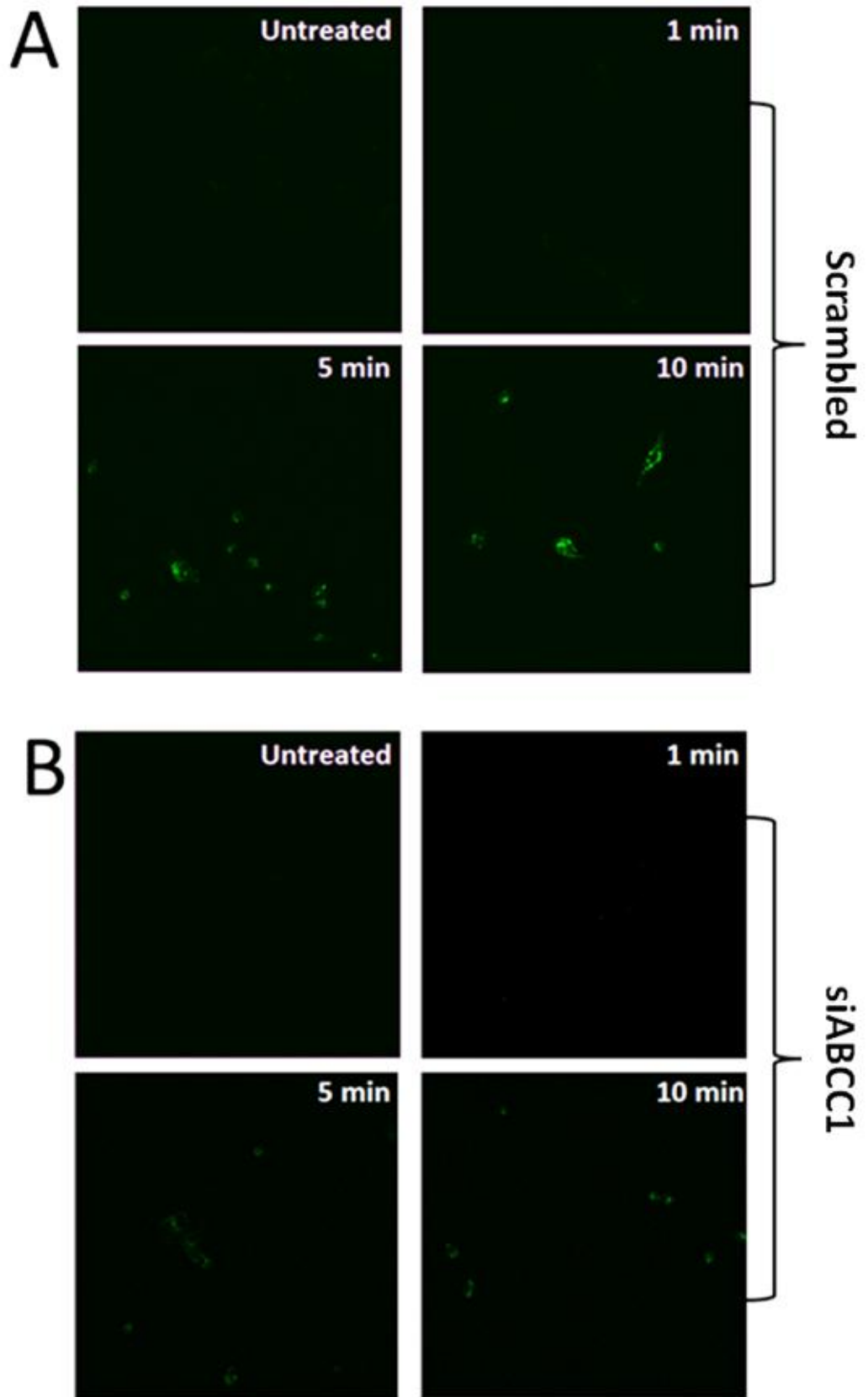
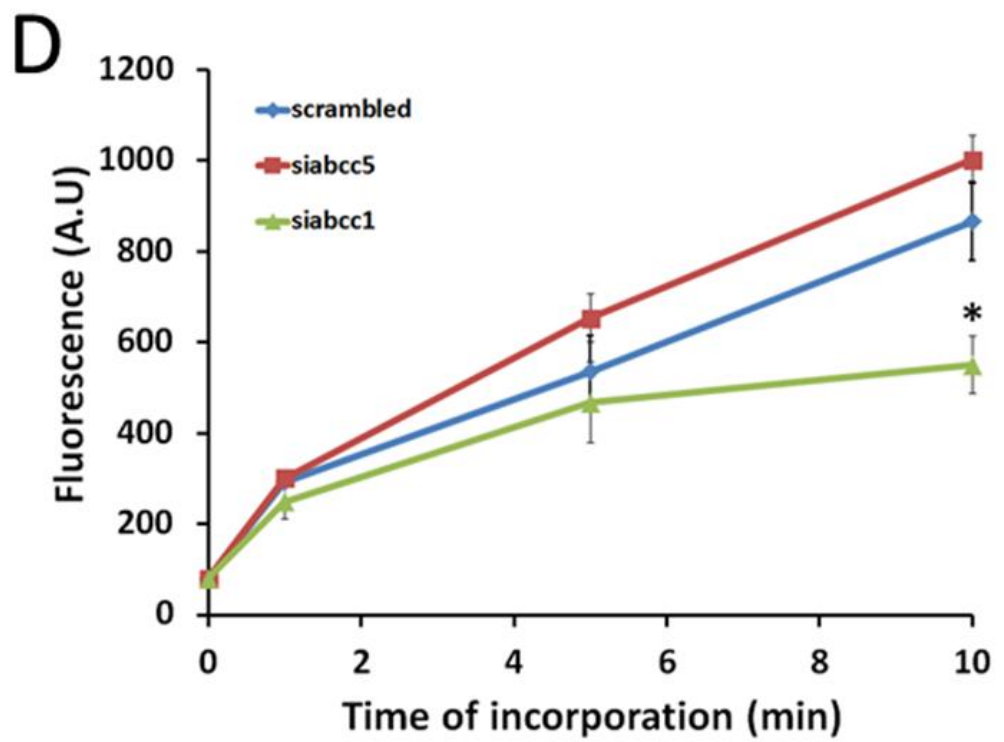
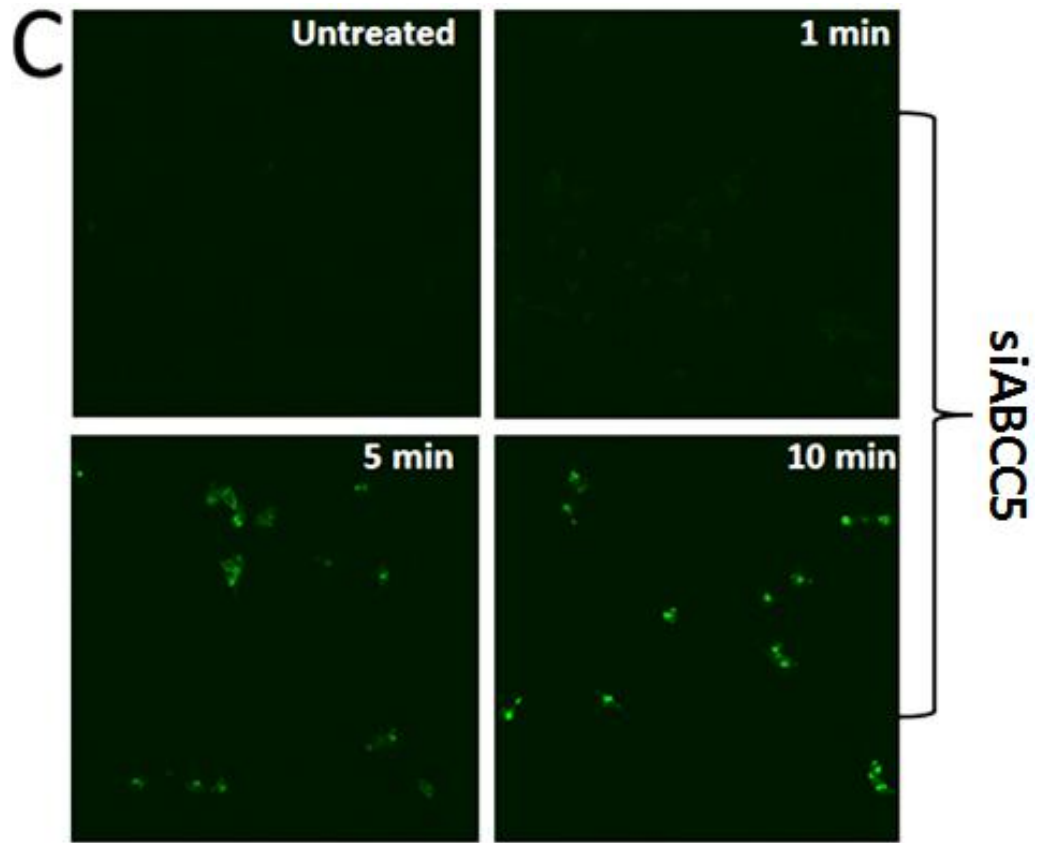


Figure legend next page



**Figure 6.5: Effect of siRNAs targeting ABCC1 or ABCC5 on 2-FAM-InsP<sub>5</sub> uptake:** Representative images of MDA-MB-231 transfected respectively with

scrambled siRNA (A), siRNA targeting ABCC1 (B) or siRNA targeting ABCC5 (C) incubated with 2-FAM-InsP<sub>5</sub> for 1, 5 and 10 minutes. Statistical analysis (D) was performed measuring fluorescence of 30 cells per sample for each time point. Plots are the mean of three independent experiments; bars S.E.M; \*p<0.05

### 6.1.6 Downregulation of ABCC1 expression inhibits <sup>3</sup>H-InsP<sub>5</sub> uptake

I then analysed the effect of ABCC1 downregulation on <sup>3</sup>H-InsP<sub>5</sub> incorporation in MDA-MB-231. Incorporation of <sup>3</sup>H-InsP<sub>5</sub> was assessed in parallel in MDA-MB-231 transfected with siRNA targeting the ABCC5 transporter. MDA-MB-231 transfected with a scrambled siRNA sequence were used as control. MDA-MB-231 were incubated for 1 hour with 50 μM “cold” InsP<sub>5</sub> and <sup>3</sup>H-InsP<sub>5</sub> (5000cpm/μl), then lysed and analysed by liquid scintillation counting. Cells downregulated for ABCC1 showed a significant decrease in <sup>3</sup>H-InsP<sub>5</sub> incorporation compared to scrambled cells. On the contrary ABCC5 knock down did not show any effect on the uptake process (Figure 6.6). These data confirmed the observation obtained by confocal fluorescence analysis suggesting the specific role of ABCC1 in InsP<sub>5</sub> uptake.

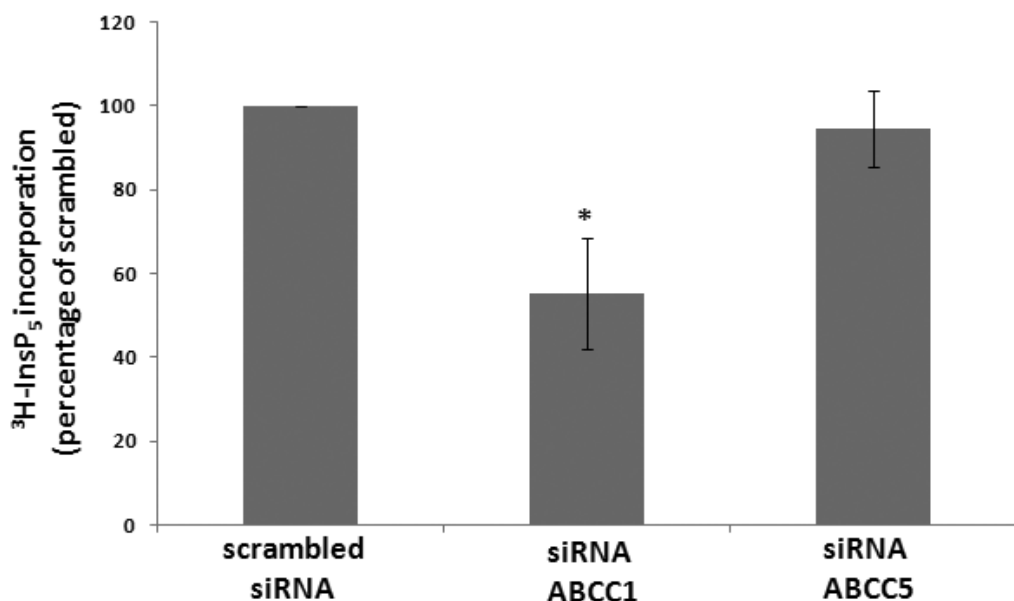
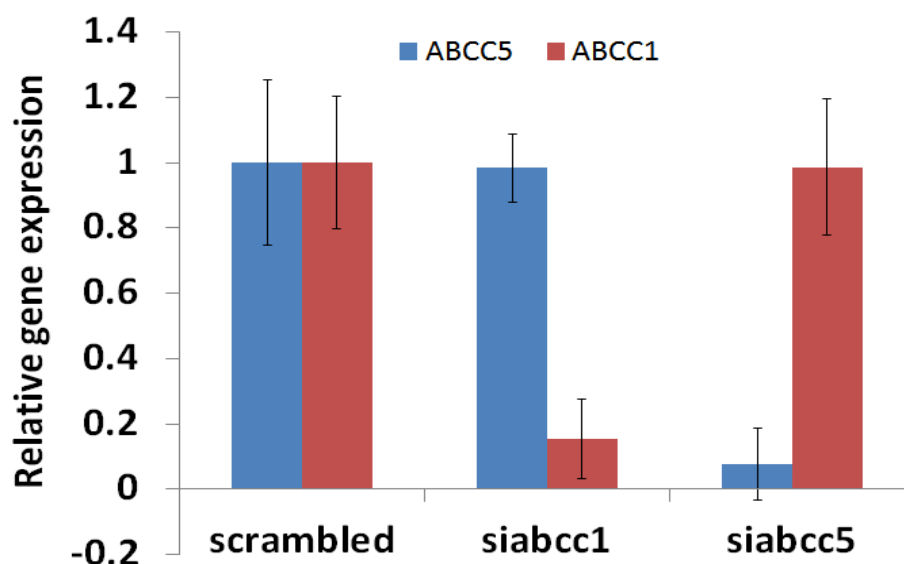


Figure legend next page

**Figure 6.6: Effect of siRNAs targeting ABCC1 or ABCC5 on <sup>3</sup>H-InsP<sub>5</sub> uptake**  
<sup>3</sup>H-InsP<sub>5</sub> incorporation analysis in MDA-MB-231 transfected with scrambled siRNA, ABCC1 siRNA or ABCC5 siRNA and incubated with <sup>3</sup>H-InsP<sub>5</sub> for 1 hour. Columns represent the mean average incorporation of 4 independent experiments, expressed as percentage of 3H-InsP<sub>5</sub> incorporation of scrambled cell lines; bars S.E.M; \*p<0.05

### 6.1.7 Downregulation of ABCC1 and ABCC5 protein levels in MDA-MB-231

Downregulation of ABCC1 and ABCC5 in MDA-MB-231 levels was checked by Real-Time PCR after 72 hours from transfection. A scrambled non-targeting sequence was used as control. Figure 6.7 shows more than 80% decrease of ABCC1 and ABCC5 mRNA levels in cells transfected with the respective siRNA when compared with expression of control scrambled cells. Furthermore, no decrease in ABCC5 mRNA levels was detected in cells transfected with siRNA targeting ABCC1 and vice versa, indicating that the sequences used are specific for each transporter and are able to downregulate them with high efficiency.



**Figure 6.7: Quantification of ABCC1 and ABCC5 expression:** RT-PCR analysis of ABCC1 and ABCC5 mRNA levels in cells transfected with siRNA for ABCC1 and ABCC5 and control scrambled siRNA. Relative gene expression was

calculated using scrambled samples as calibrators and actin as a housekeeping gene. Columns are the mean  $\pm$ SEM of three independent experiments

## 6.2 Discussion

Data presented in this chapter aimed to investigate the potential role of ABC transporters belonging to the ABCC family in inositol phosphate active transport in mammalian cells. My group showed that cancer cells uptake inositol polyphosphates (Razzini et al., 2000). Furthermore preliminary data show that inositol polyphosphates uptake is inhibited by incubating the cells at 4°C. However it is currently unknown which transporters are involved in this process. Although ABC transporters in mammals are involved in drug export and their overexpression confers drug resistance to cancer cells, it has been shown that ABCC family members are involved in the vacuole export of inositol pentakisphosphate (Nagy et al., 2009) in *Arabidopsis*. Furthermore evidence suggests that ABC transporters are involved in the import of anion abscisic acid into cells in *plantae*. Another report suggests the involvement of ABC transporters in the import of auxin (Terasaka K., et al., 2005). In principle there is no evidence suggesting that ABC transporters should not be involved in import/export process rather than export alone. Starting from this evidence, I decided to investigate the role of ABC transporters in inositol pentakisphosphates in cancer cells. Treatment of MDA-MB-231 with two generic ABC transporter inhibitors (probenecid and glibenclamide) inhibited 2-FAM-InsP<sub>5</sub> incorporation, indicating that ABC transporters may be involved in Ins(1,3,4,5,6)P<sub>5</sub> uptake (Figure 6.2). In particular treatment with MK-571, a specific inhibitor of ABCC1, inhibited uptake of 2-FAM-InsP<sub>5</sub> and of <sup>3</sup>H-InsP<sub>5</sub> (Figure 6.3, 6.4). Similar results were obtained using siRNA targeting ABCC1 (Figure 6.5). It has to be noted that neither MK-571 treatment nor downregulation of ABCC1 completely inhibited InsP<sub>5</sub> uptake indicating that ABCC1 is not the only ABC transporter involved in this process. However downregulation of ABCC5 had no effect on InsP<sub>5</sub> uptake indicating that the inhibition observed upon ABCC1 inhibition may be specific and not all the ABCC family members are involved in this process. Although a more complete screening is required to assess the role of the ABC

family members in inositol phosphates uptake, my data indicate for the first time that in mammalian cells ABC transporters may be involved in inositol phosphate uptake and therefore suggest a potential involvement of ABC transporters also in cellular import. These data may also have important relevance in cancer therapy. Indeed ABC transporters have been found overexpressed in several cancers including pancreatic cancer (Konig et al., 2005; Hagmann et al., 2009). This family of proteins has an established role in chemoresistance or multidrug resistance. Work in my laboratory has recently unravelled a novel involvement of these proteins in cancer progression. Indeed it has been reported that ABCC1 transporter is involved in an autocrine loop by which cancer cells can stimulate their proliferation (Pineiro et al., 2010). In particular the phospholipid lysophosphatidylinositol (LPI) is synthesized by cancer cells, through the action of the enzyme phospholipase A2 (PLA<sub>2</sub>), and exported by ABCC1. Once released, LPI can bind its receptor GPR55 (G-protein coupled receptor 55) and activate signalling pathways involved in cell proliferation (Pineiro et al., 2010). Inhibition of this ABC transporter-mediated autocrine loop can represent a novel strategy to block cancer cell proliferation. Indeed, blockage of activation of GPR55 or activity of the LPI transporter ABCC1 inhibits survival and proliferation of prostate and ovarian cancer cell lines. However, according to the data shown in this chapter, the overexpression of ABCC1 might increase the intracellular uptake of exogenous inositol phosphates such as InsP<sub>5</sub> or potential synthetic derivatives, resulting in increased sensitivity and cell death.

### Summary

Data shown in this chapter indicates for the first time a potential involvement of ABC transporters and in particular of ABCC1 transporter in inositol phosphate uptake in mammalian cells. Taken together this data show a potential novel role for ABCC transporters in active cellular import and suggest a novel way of thinking ABC transporters, not only as transporter involved in drug resistance or autocrine loop but also as potentially marker to identify tumour responsiveness to specific anti-cancer treatment, such as inositol phosphates.

## **Chapter 7**

### **PDK1-dependent PLC $\gamma$ 1 activation**

## **7.1 Transient downregulation of PDK1 in MDA-MB-231, MDA-MB-435 and A375M**

Results described in chapter 5.4.5 and 5.4.6 showed that 2-*O*-Bn-InsP<sub>5</sub> treatment is able to block PLC $\gamma$ 1 activity (Figure 5.13) and that it inhibits PLC $\gamma$ 1 phosphorylation at the residue Y783. Furthermore kinase profile assays provided *in vitro* evidence that 2-*O*-Bn-InsP<sub>5</sub> specifically inhibits PDK1. These data suggested that PDK1 might have a novel role on PLC $\gamma$ 1 regulation and activation. In order to investigate this hypothesis I decided to investigate the potential effect of PDK1 downregulation on PLC $\gamma$ 1 activity.

### **7.1.1 PDK1 protein downregulation in MDA-MB-231, MDA-MB-435 and A375M**

Transient downregulation of PDK1 was achieved using specific siRNA targeting PDK1. MDA-MB-231, MDA-MB-435 cells were transfected with Oligofectamine transfecting agent, while A375M were transfected using Hyperfect transfecting agent. In order to test the efficiency of PDK1 silencing, MDA-MB-231 lysates obtained after 48 hours and 72 hours from transfection were analysed by western blot analysis using a specific PDK1 antibody (Figure 7.1A). Efficiency of downregulation in A375M and MDA-MB-435 was assessed after 72 hours from transfection. Cells transfected with non-targeting siRNA were used as control. Western Blots in Figure 7.1B,C showed a reduced PDK1 expression after 48 hours compared to scrambled cells in MDA-MB-435 and A375M. PDK1 protein expression was downregulated after 72 hours from transfection in all the three cell lines, indicating that 72 hours are required for the efficient downregulation of this enzyme in all the three cell lines investigated.

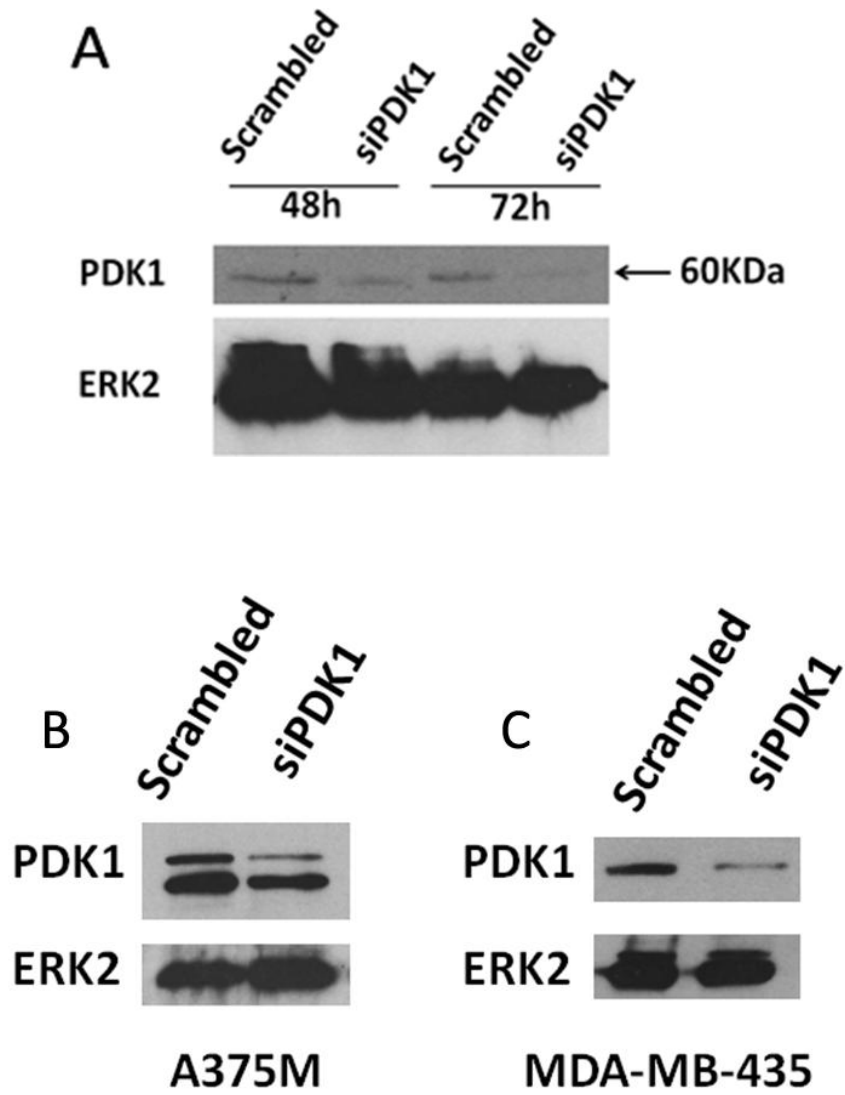


**Figure 7.1: Transient downregulation of PDK1:** Expression levels of PDK1 after 48 and 72 hours from transfection with specific siRNA targeting PDK1 in MDA-MB-231 and after 72 hours in A375M and MDA-MB-435 cells.

### **7.1.2 Transient downregulation of PDK1 protein expression inhibits calcium release upon EGF stimulation**

The observation that 2-*O*-Bn-InsP<sub>5</sub> inhibits PLCγ1 activity (as assessed by EGF-induced calcium release) and that kinase profiling analysis revealed that 2-*O*-Bn-InsP<sub>5</sub> is a specific PDK1 inhibitor, prompted me to investigate whether PDK1 had a role in PLCγ1 activation. Therefore I decided to determine the effect of PDK1 downregulation on PLCγ1 activity in MDA-MB-231 and A375M using the intracellular calcium measurement assay upon EGF stimulation. As indicated in chapter 7.1, the most efficient downregulation was obtained after 72 hours of transfection with the specific siRNAs. Therefore the calcium measurement was performed after 72 hours from transfection. MDA-MB-231 and A375M siPDK1 were serum-starved overnight and loaded with Fluo-4-AM before analysis of calcium mobilisation induced by EGF stimulation. MDA-MB-231 and A375M transfected with a scrambled sequence were used as controls. The chart shown in Figure 7.2 indicates that EGF stimulation induced a fast response in MDA-MB-231 and A375M scrambled cells, leading to the peaks in the calcium pattern. Cell viability was assessed adding ATP to the cells towards the end of the assay, which generated peak at the end of the chart. Strikingly, EGF-induced calcium mobilisation was completely abrogated in MDA-MB-231 and A375M transfected with siRNA targeting PDK1. ATP-induced calcium mobilisation was comparable in cells transfected with scrambled or PDK1 specific siRNA, indicating no significant difference in cell viability. These data revealed for the first time a role of PDK1 in PLCγ1 activation.

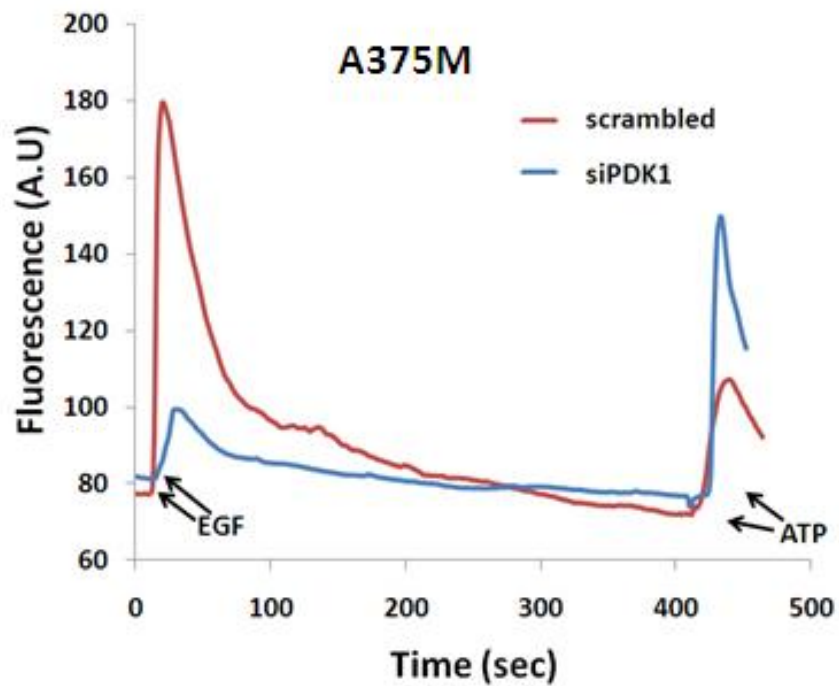
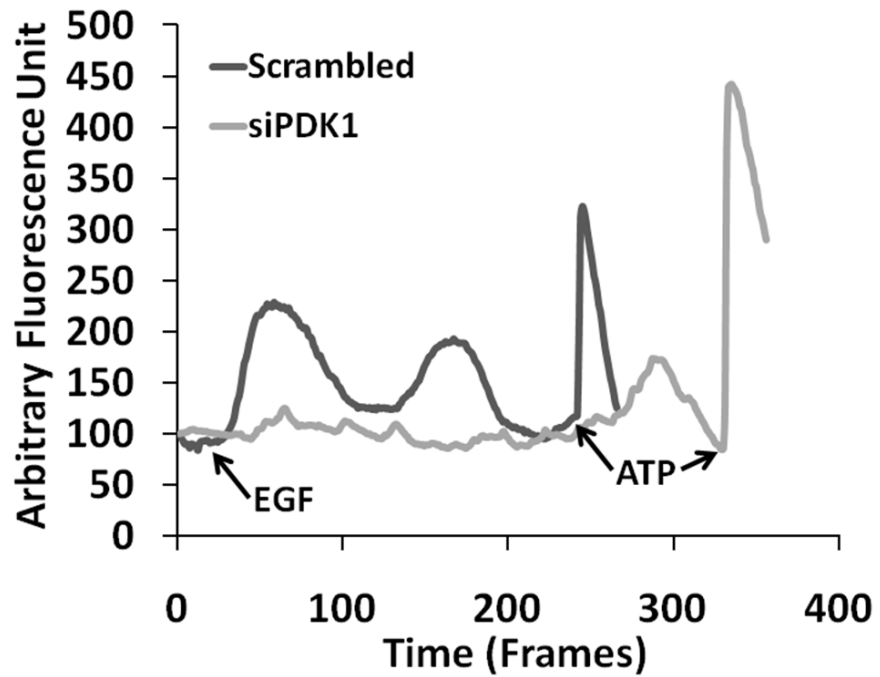


**Figure 7.2 PDK1 downregulation inhibits EGF-induced calcium release:** Calcium release assay performed on MDA-MB-231 and A375M transfected with siRNA specific for PDK1 or with a non-targeting sequence. Arrows indicate the time point of EGF and ATP stimulation. The chart is the mean of 4 independent experiments.

### **7.1.3 Matrigel cell invasion is inhibited in Breast cancer and Melanoma cell lines upon PDK1 downregulation.**

As described in the introductory chapter 1.7, PDK1 is a key enzyme involved in promoting cell invasion. Calcium measurement showed that siRNA for PDK1 inhibits PLC $\gamma$ 1 activity as assessed by intracellular calcium mobilisation upon EGF stimulation in MDA-MB-231. Since both enzymes play an important role in cell invasion, I decided to investigate the effects of PDK1 downregulation on cell invasion on Matrigel using different invasive cancer cell types. MDA-MB-231, MDA-MB-435 and A375M were transfected with scrambled siRNA and siRNA for PDK1 and 72 hours after transfection cells were plated on Matrigel pre-coated transwells and allowed to invade for 36 hours. An aliquot of cells was seeded in parallel on 6-well plates to perform western blot analysis at the end of the invasion assay. Cells transfected with a scrambled siRNA sequence were used as control. Cell invasion on Matrigel was inhibited in all three cell lines upon downregulation of PDK1 compared to their respective control. In particular invasion was inhibited by 50% and 52% in MDA-MB-231 and MDA-MB-435 upon PDK1 knock down respectively compared to MDA-MB-231 and MDA-MB-435 scrambled cells (Figure 7.3). A375M showed the highest inhibition with a decrease in cell invasion of 70% compared to scrambled cells, indicating that PDK1 plays an important role in Matrigel cell invasion in several cancer types, and the inhibition is independent of the cell type used (Figure 7.3). These data showed that PDK1 is an essential enzyme for promoting cancer cell invasion, consistent with data in the literature (Primo et al., 2007; Pinner and Sahai, 2008; Finlay et al., 2009).

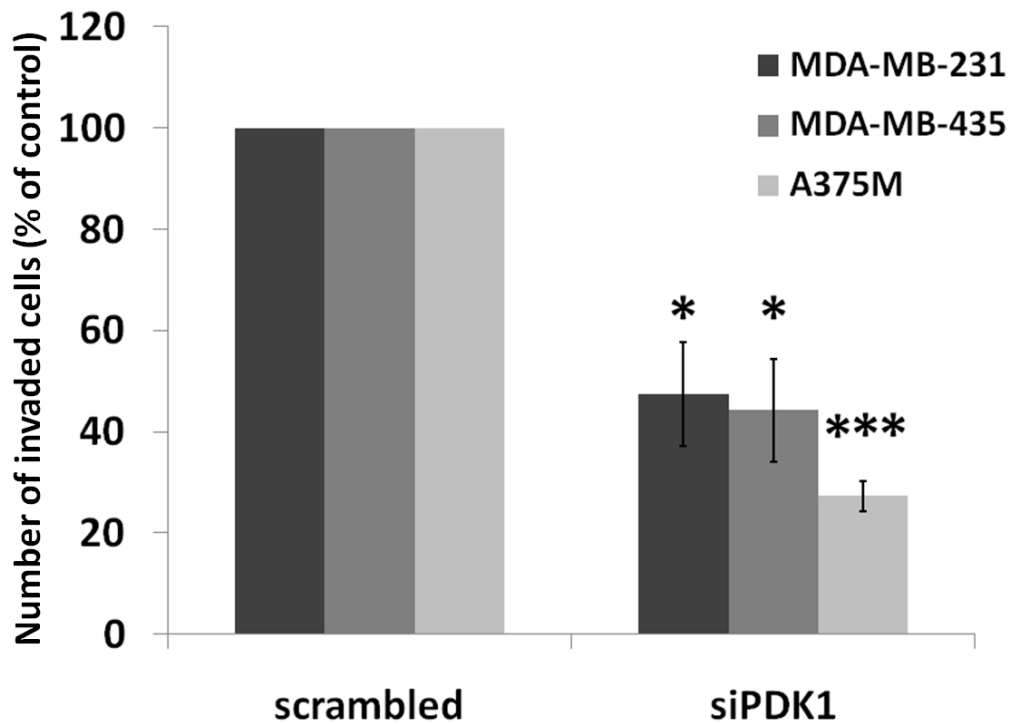


**Figure 7.3 Cell invasion on Matrigel of MDA-MB-231, MDA-MB-435 and A375M downregulated for PDK1 expression:** Invasion assay was performed after 72 hours from siRNA transfection and lasted 36 hours. Columns are mean of three independent experiments. Bars S.E; \* $p < 0.05$ ; \*\*\* $p < 0.001$

## 7.2 Generation of MDA-MB-231 stably downregulated for PDK1 expression

In order to further investigate the effect of PDK1 protein downregulation on PLC $\gamma$ 1 activation, I decided to generate stable MDA-MB-231 downregulated for PDK1. The rationale for this decision was the limitation of the transient transfection using siRNAs. Transient transfection interfering efficiency is variable among the different experiments. Furthermore transient interfering does not provide a homogenous population of cell downregulated for the targeted protein. In order to overcome these limitations I generated MDA-MB-231 cells expressing shRNA targeting PDK1 using specific targeting sequences cloned in the vector pSUPERIOR.retro.puro. Cells expressing the

construct were selected. This method allowed the selection of a more homogeneous population of cells downregulated for PDK1 expression.

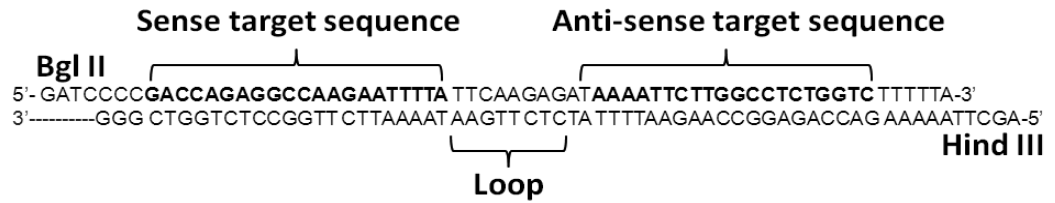
The pSUPERIOR vector was used in concert with a pair of custom oligonucleotides that contained a unique 22-nt sequence derived from the mRNA transcript of PDK1 in order to induce gene suppression. The target sequence corresponds to the sense strand of the pSUPERIOR-generated siRNA, which corresponds to the complementary sequence within the mRNA. The forward and reverse oligonucleotides were annealed and cloned into the vector, between the unique BglIII and HindIII enzyme sites. This strategy positions the forward oligonucleotides at the correct position downstream from the H1 promoter's TATA box to generate the desired siRNA duplex.

### **7.2.1 Design of 22-nucleotide targeting sequence cloned in pSUPERIOR.retro.puro vector**

The sequence of the targeting oligonucleotides includes the unique 22-nucleotide targeting sequence in both sense and antisense orientation, separated by a 9-nt spacer sequence. The 5' end corresponds to the BglIII site, while the 3' end contains the HindIII corresponding nucleotides. The resulting transcript of the recombinant vector is predicted to fold back on itself to form a 22-base pair stem-loop structure.

The 22-nucleotide targeting sequence was designed based on the sequence published by Sahai et al, 2008 used for siRNA (Figure 7.4). The sequence was modified in the last nucleotide in order to remove the fifth T that would be otherwise recognized as a stop by RNA polymerase III aborting the transcription of the shRNA. A 5 point mutated sequence was generated and cloned in the pSUPERIOR.retro.puro vector as closest control. The 5' end presents the BglIII restriction site, while the 3' end contains the HindIII corresponding nucleotides (Figure 7.4).

**shPDK1 targeting sequence:**



**5MUT sequence**

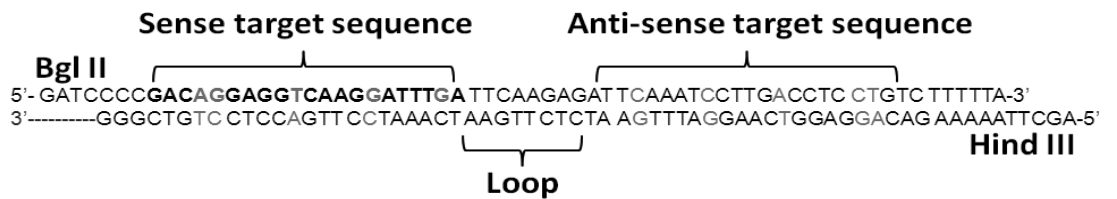


**Figure 7.4: Short hairpin constructs:** Cloning of shPDK1 targeting sequence (panel above) and 5 point mutated non-targeting sequence (panel below) in pSUPERIOR.retro.puro vector.

In order to insert the custom-designed oligonucleotides in the pSUPERIOR.retro.puro vector, I performed serial digestions of the pSUPERIOR.retro.puro vector with Hind III and BglIII restriction enzymes. The serial digestions were performed separately in order to be certain of the restriction activity of each enzyme. After each digestion, plasmids were loaded on 1% agarose gel and analysed by electrophoresis.

The vector was first digested with Hind III overnight. Figure 7.5 shows the uncut plasmid on the left and the vector upon overnight digestion on the right.

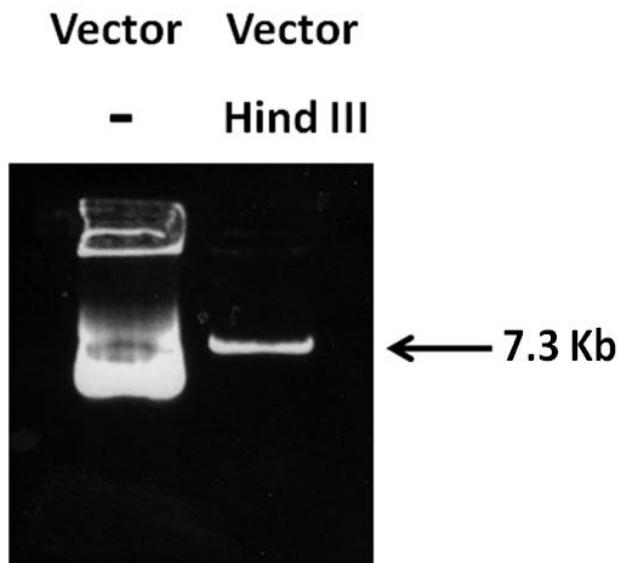


**Figure 7.5:** pSUPERIOR.retro.puro not digested and digested with HindIII restriction enzyme.

The digested vector was purified and digested a second time with restriction enzyme BglII, in order to create complementary extremities for the insertion of the annealed custom oligonucleotides. As a control the parental uncut vector was digested with BglII alone in order to verify the activity of the restriction enzyme. Figure 7.6 shows that the vector was successfully double digested with HindIII and BglII as indicated by the second band at 1kb in the third lane on the right at 6.3kb and at 1Kb.

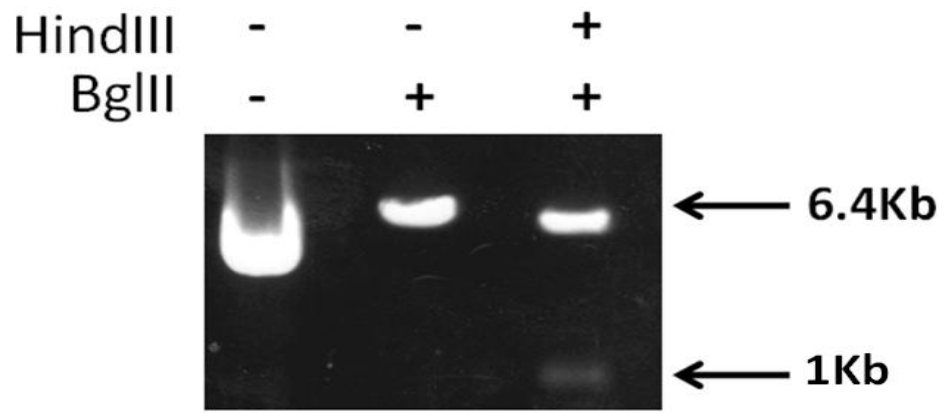


**Figure 7.6:** Digestion of the previously HindIII-digested pSUPERIOR.retro.puro using the restriction enzyme BglII (right lane). BglII activity was tested on uncut vector (middle lane).

### 7.2.2 Colony-PCR screening

In order to insert the 5Mut and the shPDK1 oligonucleotides in the vector, ligase reaction was performed overnight. Competent Top10™ bacterial cells (Invitrogen, UK) were transformed with the plasmids upon ligation. 20 Positive bacterial colonies for the 5MUT and 20 positive bacterial colonies for shPDK1 were picked up and screened by PCR. Primers provided by the manufacturer for PCR screening of positive colonies were used in order to screen the effective integration of the customer oligos in the double-cut plasmids. Positive colonies were predicted to give an amplification product of 482 bp. Figure 7.7 shows the amplification product of the 40 different colonies. Among the different positive colonies I choose the colonies listed in table 7.1 to proceed for plasmid purification and cell transfection.



**Figure 7.7 Colony PCR screening:** Screening of positive colonies shows an amplicon at the predicted size of 483bp.

<b>Colony number</b>	<b>Sequence</b>
<b>2</b>	<b>5MUT</b>
<b>8</b>	<b>5MUT</b>
<b>25</b>	<b>shPDK1</b>
<b>26</b>	<b>shPDK1</b>
<b>27</b>	<b>shPDK1</b>
<b>39</b>	<b>shPDK1</b>
<b>40</b>	<b>shPDK1</b>

**Table 7.1:** List of colonies chosen for plasmid purification and following transfection for generation of cells stably downregulated for PDK1 and respective control.

### **7.2.3 Clones selection**

MDA-MB-231 cells were transfected with plasmid constructs listed in table 7.1 and plated in selection media containing 1 $\mu$ g/ml puromycin after 48 hours after transfection. Five days later two clones from each transfection were picked up and plated in separate plate dishes and allowed to grow. Protein lysates obtained from the different clones were analysed for PDK1 protein expression levels by western blot using a specific PDK1 antibody. Only two clones (construct 39, clone number 1 and construct 39, clone number 2) showed a clear reduction in PDK1 expression, and will be referred to as shPDK1 Clone 1 and Clone 2. Construct 2 clone 1 and construct 8 clone 1 were chosen as scrambled and maintained in culture and will be referred to as 5MUT clone 1 and clone 2 (Figure 7.8A). Figure 7.8B shows a further western blot analysis of MDA-MB-231 5MUT clones and MDA shPDK1 clones after different passages in culture.

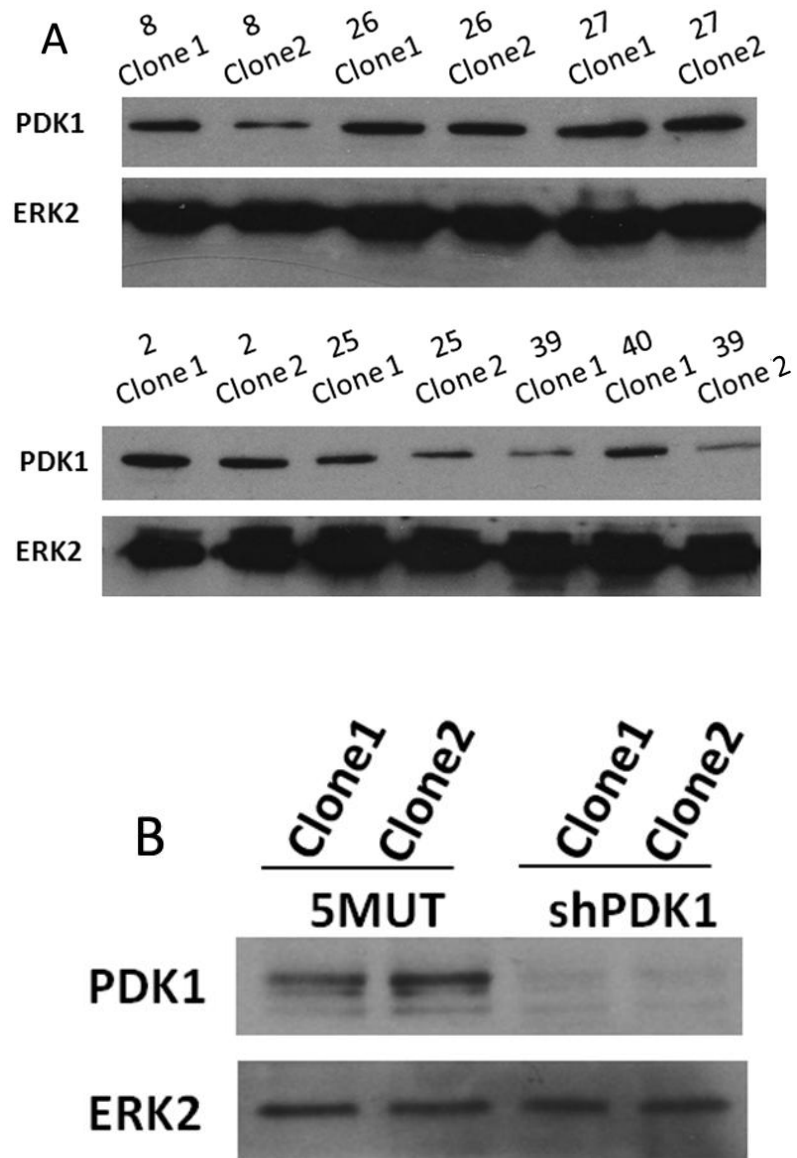


**Figure 7.8: Stable downregulation of PDK1.** A) Western blot analysis of PDK1 levels on the different clones at passage 1. B) Representative Western blot analysis of PDK1 after two cell passages in culture.

### **7.3 Effect of PDK1 protein downregulation on Inositol phosphates production**

Intracellular calcium analysis experiments showed that transient protein downregulation of PDK1 using siRNA interfering inhibits intracellular calcium mobilisation upon EGF stimulation in MDA-MB-231 (chapter 7.1.2). In order to validate these results, I decided to investigate the inositol phosphate production in MDA-MB-231 shPDK1 “MDA-MB-231 shPDK1”. MDA-MB-231 5MUT cells were used as control for the experiments. Experiments were performed using the two clones previously selected in order to avoid any clone-specific effect in the analysis.

Cells were labelled with a  $^3\text{H}$ -*myo*-inositol for 24 hours in inositol free, serum free media and then stimulated with EGF at different time points. Cells were lysed, and total inositol phosphates were separated by anion exchange chromatography and the total amount assessed by liquid radioactivity counting. Accumulation of inositol phosphates was inhibited in both clones MDA-MB-231 shPDK1 compared to MDA-MB-231 5MUT (Figure 7.9A). This data were consistent with results obtained in the calcium mobilization assay and identify PDK1 as a new key protein in regulating PLC $\gamma$ 1 activity.

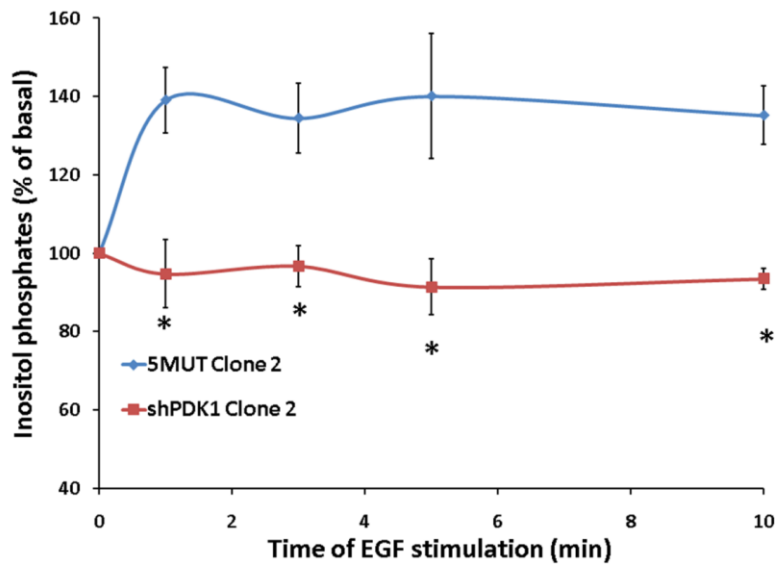
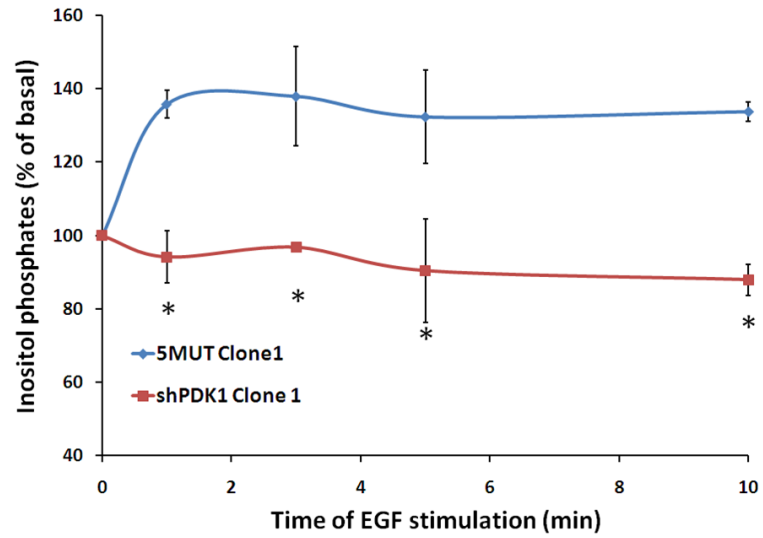


**Figure 7.9: Inositol phosphates levels in MDA-MB-231 stably downregulated for PDK1:** Inositol phosphates accumulation in MDA-MB-231 5MUT and shPDK1 previously incubated in  $^3\text{H}$ -*myo*-inositol for 24 hours in inositol free, serum free media and then stimulated with 50ng/ml EGF for the indicated times before being lysed and analysed by liquid radioactivity counting. Data are means  $\pm$ .SEM of 4 independent experiments.; \* $p < 0.05$

## **7.4 The PDK1-dependent PLC $\gamma$ 1 regulation**

### **7.4.1 Analysis of PLC $\gamma$ 1 protein level in MDA-MB-231 downregulated for PDK1**

In order to understand the mechanism of PDK1-dependent regulation of PLC $\gamma$ 1 activity, I first determined whether downregulation of PDK1 affected PLC $\gamma$ 1 protein expression in MDA-MB-231. This experiment aimed to investigate any potential effect of the absence of PDK1 on PLC $\gamma$ 1 protein level due to changes at transcription level or protein stability. After 48 hours from transfection with specific PDK1-targeting siRNA or scrambled siRNA, cells were starved overnight and then stimulated with EGF at different times. Since PDK1 phosphorylates AKT at threonine 308 (Thr 308), I decided to check AKT phosphorylation to validate the efficiency of PDK1 downregulation. Western blot analysis showed that the decreased levels of PDK1 expression in MDA-MB-231 was mirrored by the inhibition of the EGF-induced threonine phosphorylation of AKT in “MDA-MB-231 siPDK1” compared to scrambled cells (Figure 7.10). No change in PLC $\gamma$ 1 expression was observed between MDA-MB-231 siPDK1 and control cells, indicating that PDK1 protein downregulation does not affect PLC $\gamma$ 1 expression and that the inhibition of PLC $\gamma$ 1 previously observed is due to an impaired PLC $\gamma$ 1 activation.

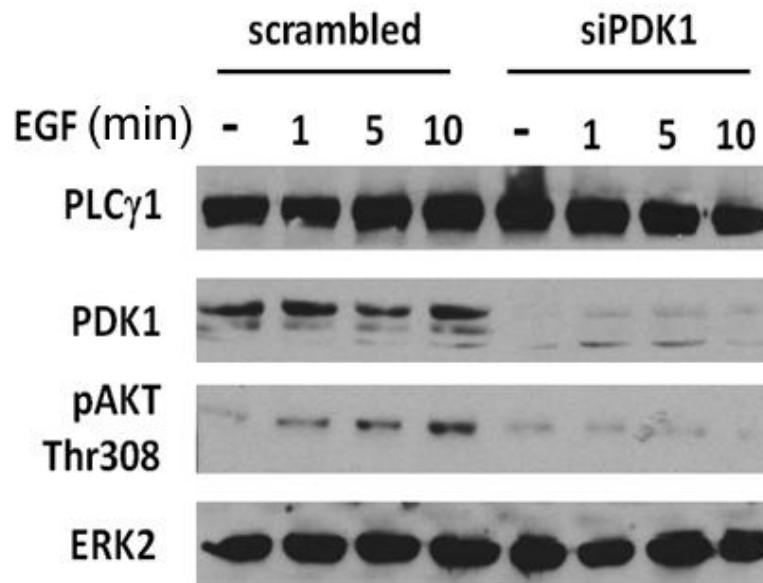


**Figure 7.10: PLC $\gamma$ 1 expression in cells downregulated for PDK1:** Western blot analysis of MDA-MB-231 transfected with scrambled siRNA or siRNA targeting PDK1 (siPDK1). Cells were treated with EGF for the indicated times 72h after transfection. Lysates were analysed using specific antibodies for the specified proteins. Blot representative of two independent experiments.

#### 7.4.2 Effect of downregulation of PDK1 on tyrosine phosphorylation of PLC $\gamma$ 1 in MDA-MB-231

To gain further insight into the mechanism of PDK1-dependent PLC $\gamma$ 1 activation, I decided to investigate any potential effect of PDK1 downregulation on PLC $\gamma$ 1 post-translational modifications. As described in chapter 1.3.1, PLC $\gamma$ 1 phosphorylation is required for its enzymatic activation. In particular phosphorylation of tyrosine 783 (Y783) correlates with PLC $\gamma$ 1 activation. MDA-MB-231 transfected with a control scrambled siRNA or siRNA targeting PDK1 were starved overnight 48 hours after transfection and then stimulated with EGF for 3 and 10 minutes. Western blot analysis showed that tyrosine phosphorylation of PLC $\gamma$ 1 was inhibited after 10 minutes of EGF stimulation in MDA-MB-231 compared to scrambled cells (Figure 7.11A). No

changes were observed after a short stimulation of 3 minutes, probably due to the not complete downregulation of PDK1. The efficiency of transfection was assessed using a specific PDK1 antibody to test protein expression levels of PDK1 in MDA-MB-231 and scrambled cells. These data indicate that downregulation of PDK1 inhibits the EGF-induced tyrosine phosphorylation of PLC $\gamma$ 1 at its residue Y783. Furthermore this data reveal a novel role for PDK1 in the regulation of PLC $\gamma$ 1 activity through modulation of its tyrosine phosphorylation. In order to validate the data obtained using transient siRNA similar experiments were performed in MDA-MB-231 stably downregulated for PDK1 expression. Cells were serum starved over-night, stimulated with EGF for 3 and 10 minutes before being lysed. Phosphorylation of PLC $\gamma$ 1 was strongly inhibited in cells expressing the shRNA targeting PDK1 compared to control cells (Figure 7.11B) at all time points of EGF stimulation. The discrepancy in the results obtained by transient and stable PDK1 downregulation may be explained by the partial silencing of PDK1 using transient RNA interfering. On the contrary, a more efficient PDK1 downregulation was achieved in MDA-MB-231 expressing the shRNA targeting PDK1, which showed a complete inhibition of PLC $\gamma$ 1 phosphorylation.

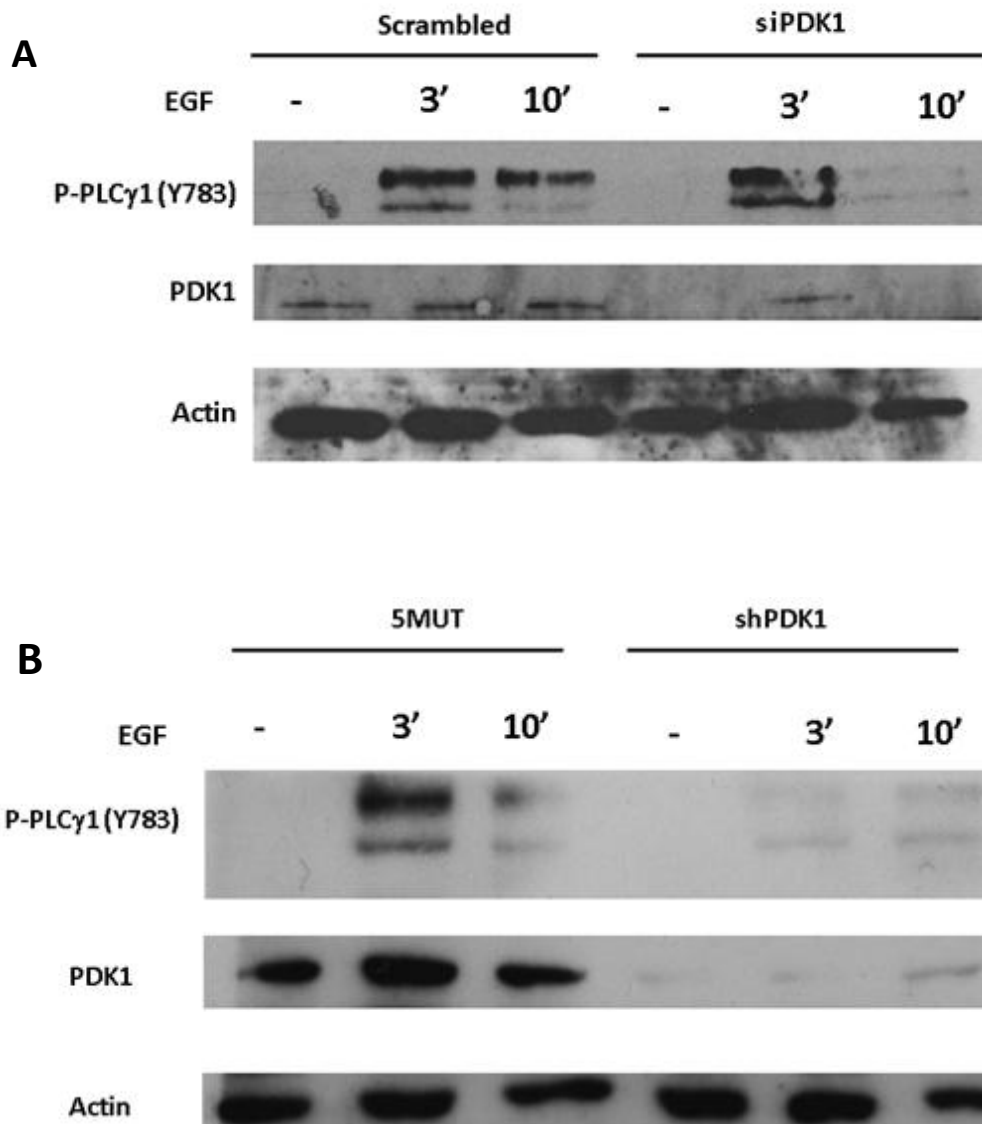


**Figure 7.11: Western blot analysis of MDA-MB-231 downregulated for PDK1 (siPDK1 or shPDK1):** **A)** Cells were treated with EGF 72 hours after transfection and overnight serum starvation. Phosphorylation of tyrosine 783 of PLC $\gamma$ 1 was assessed after 3 and 10 minutes of EGF stimulation (Representative Western blot of two independent experiments). **B)** MDA-MB-231 sh5MUT and MDA-MB-231 shPDK1 were treated with EGF for the indicated times and phosphorylation of PLC $\gamma$ 1 analysed. Lysates were analysed using specific antibodies for the specified proteins. Representative Western blot of 3 independent experiments.

## **7.5 Investigation of the mechanism of PDK1-mediated PLC $\gamma$ 1 activation**

In order to further investigate the mechanism through which PDK1 regulates PLC $\gamma$ 1 I decided to investigate the hypothesis that the two enzymes could interact. To test this hypothesis I used different complementary approaches. First I tested whether the two proteins, either endogenous or over-expressed could co-immunoprecipitate.

### **7.5.1 Overexpression of PLC $\gamma$ 1 and PDK1 in HEK293 cells**

To optimise the protocol of co-immunoprecipitation experiment, I first decided to perform the experiment using overexpressed PDK1 and PLC $\gamma$ 1. In these experiments HEK293 cells were chosen because of their high transfection efficiency. Cells were transfected using Lipofectamine (Invitrogen, UK) according to the manufacturer's instructions. 48 hours after transfection, proteins lysates were collected and expression of exogenous PLC $\gamma$ 1 and PDK1 assessed by western blot. HEK293 showed a high rate of transfection using both plasmids. Western blot analysis showed an increased expression of PLC $\gamma$ 1 in overexpressing HEK293 cells (HEK293-PLC $\gamma$ 1) compared to HEK293 transfected with the empty vector (HEK293). PLC $\gamma$ 1 was detected using specific anti-PLC $\gamma$ 1 antibody (Figure 7.12A).

The pOZ-PDK1 construct expresses an HA-FLAG tagged fusion protein. The HA and FLAG are two epitopes tags recognised by specific antibodies. Because of these flags the overexpressed PDK1 was predicted to be shifted compared to the wild type protein when run on acrylamide gel and then analysed by western blot.

Indeed Western blot analysis of HEK293 overexpressing PDK1 (HEK293-pOZ-PDK1) showed a high expression of the tagged PDK1 compared to control cells. Endogenous and exogenous PDK1 protein levels were assessed using a specific anti PDK1 and anti HA-antibody (Figure 7.12 B,C).

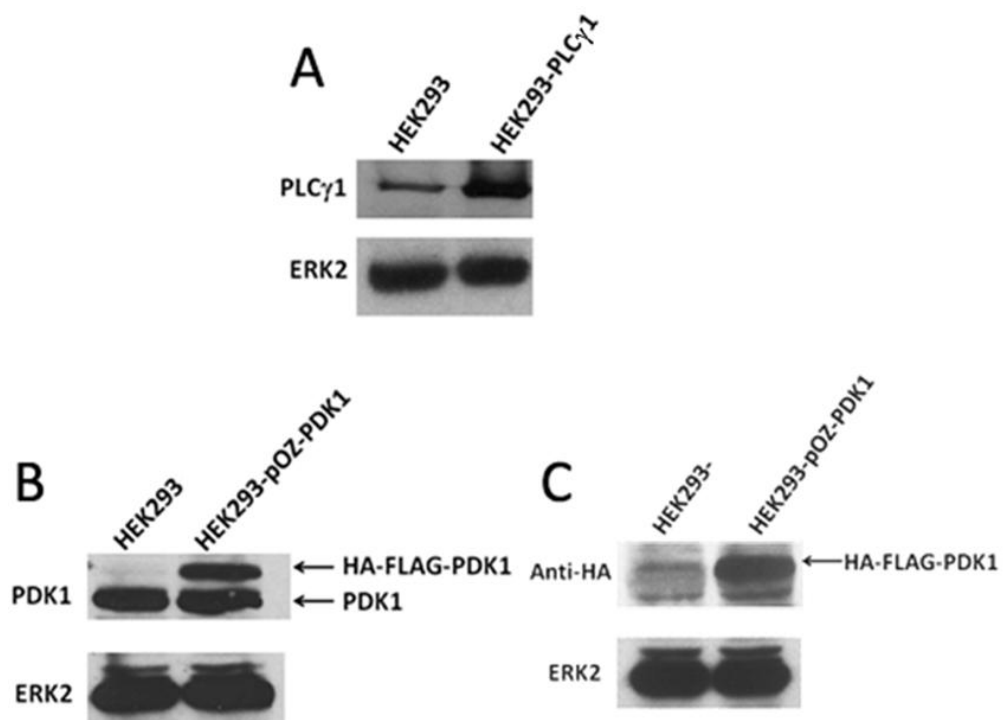


**Figure 7.12: Overexpression of PLC $\gamma$ 1 and HA-Flag-PDK1 in HEK293 cells:** **A)** Western blot analysis of HEK293 overexpressing PLC $\gamma$ 1 48 hours after transfection detected by a PLC $\gamma$ 1 specific antibody; **B)** Western analysis using the anti-PDK1 antibody of HEK293 expressing the HA-PDK1 tagged protein detected two bands which corresponded to the endogenous PDK1 (lower band) and to the recombinant protein HA-PDK1 (upper band); **C)** The overexpressed HA-PDK1 was detected using an anti-HA antibody in HEK293

### **7.5.2 Investigation of potential PLC $\gamma$ 1-PDK1 through co-immunoprecipitation analysis.**

Once optimized the protocol of overexpression, co-immunoprecipitation experiments were performed using HEK293 cells overexpressing both PLC $\gamma$ 1 and the tagged fusion protein HA-FLAG-PDK1. Cells were transfected and 48 hours after transfection cells were lysed and immunoprecipitation experiments were performed using the Catch and release 2.0® kit (Millipore, US) (chapter 2.2.1.2.1). This kit allows reducing troubleshooting in setting experimental conditions, since the IgG affinity beads are already in a column in a fixed amount decided by the manufacturer. I decided to perform immunoprecipitation experiments using the anti PLC $\gamma$ 1 antibody (Santa Cruz Biotechnology, USA) validated for immunoprecipitation analysis according to the manufacturer's datasheet. Immunoprecipitation with mouse IgG was performed in parallel as control. For each sample the lysates that did not bind to the PLC $\gamma$ 1 antibody-bead complex (unbound) was collected and loaded as a control. The immune-complex was detached from the beads using denaturing loading buffer after three washes, and loaded for western blot analysis (IP). Western blot analysis revealed an efficient immunoprecipitation of PLC $\gamma$ 1 in these experimental conditions. Furthermore the control IgG were unable to immunoprecipitate PLC $\gamma$ 1 (Figure 7.13). More importantly, a specific band recognised by the PDK1 antibody was detected in the PLC $\gamma$ 1-IP at the molecular weight of the HA-Flag-PDK1 fused protein. No PDK1 band was detectable in IgG-IP fraction indicating that the band was specific (Figure 7.13).

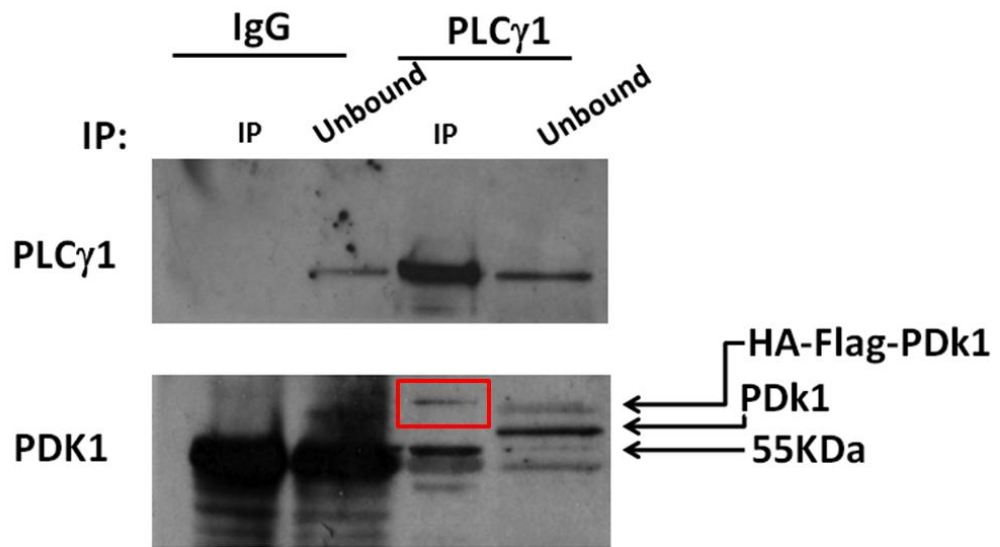


**Figure 7.13: Co-IP analysis of PDK1/ PLC $\gamma$ 1 upon overexpression:** Co-IP analysis of overexpressed PDK1 and PLC $\gamma$ 1 using anti-PLC $\gamma$ 1 or mouse-IgG to immunoprecipitate. Immunocomplexes were analysed for the presence of PDK1 and PLC $\gamma$ 1. Representative western blot of two independent experiments.

Data shown in Figure 7.13 suggested that a specific protein-protein interaction occurs between PLC $\gamma$ 1 and PDK1. However low amount of PDK1 was immunoprecipitated using the PLC $\gamma$ 1 antibody. Furthermore no endogenous PDK1 was detected in these experimental conditions indicating that the protocol needed to be further optimised. Using different amounts of protein lysates and antibody did not improve the co-immunoprecipitation rates, suggesting that conditions of lysis and wash buffers need to be optimised. It has to be noticed that the PDK1 band showed in IP-PLC $\gamma$ 1 samples presents a slight shift compared to the fusion protein of the unbound-PLC $\gamma$ 1, suggesting a potential post-translational modification of the protein. Further investigation could highlight a potential post-translational modification of PDK1 involved in the novel PDK1-PLC $\gamma$ 1 interaction and in PLC $\gamma$ 1 regulation.

### 7.5.3 GST pull-down experiments

The second approach that I decided to use in order to investigate a potential PLC $\gamma$ 1-PDK1 protein-protein interaction was the GST-pull down assay. This second approach is a complementary method to investigate protein-protein interactions in overexpressing conditions. The assay allows the pull-down of interacting protein without the use of specific antibodies. In this assay one of the two proteins whose interaction has to be tested is cloned in a Glutathione-S-Transferase (GST) expressing vector and the resulting GST-fused protein is immobilised on Glutathione agarose beads. Lysate containing the second protein of the potential interaction is loaded on the beads, and this allows the two proteins to interact. Finally the immobilised protein and the potential associated protein(s) can then be dissociated from the beads. Any potential interaction can then be analysed by western blot.

For these experiments, a pEBG2T vector expressing the coding sequence of PDK1 fused with GST at N-terminal (GST-PDK1) was used. This vector allowed the expression of GST-fusion protein directly in mammalian cells HEK293. Lysates from HEK293 overexpressing the empty vector pEBG2T-GST (GST) were used as control. The GST-PDK1 fusion protein presents a shift of ~26 KDa compared to the wild type protein. Figure 7.14 shows the western blot analysis of lysates from HEK293 overexpressing PLC $\gamma$ 1(HEK293-PLC $\gamma$ 1) and HEK293 overexpressing GST-PDK1 (HEK293-GST-PDK1). GST-PDK1 was efficiently overexpressed in HEK293 and recognised by a PDK1 specific antibody as a band at 85 KDa. In parallel HEK293-PLC $\gamma$ 1 showed increased levels of PLC $\gamma$ 1 compared to HEK293-GST-PDK1 used as control for PLC $\gamma$ 1 expression in this particular case.

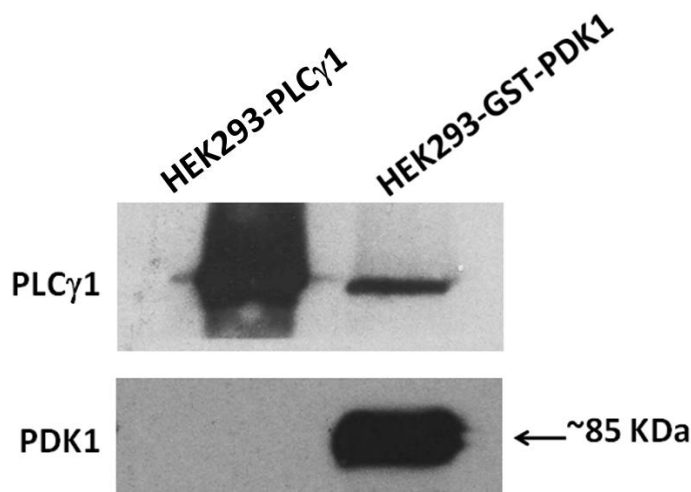


**Figure 7.14:** Overexpression of PLC $\gamma$ 1 and GST-PDK1 analysed by western blot using specific antibodies for PLC $\gamma$ 1 and PDK1. Note that addition of GST to PDK1 generates a band of ~85KDa.

#### 7.5.4 GST pull down analysis of PDK1-PLC $\gamma$ 1 interaction

The GST pull down assay was performed using protein lysates from HEK293-GST and HEK293-GST-PDK1. Lysate from HEK293-GST was used as negative control for the experiments, since the GST alone should not interact with PLC $\gamma$ 1. Briefly, lysates from HEK293-GST and HEK293-GST-PDK1 were incubated with the agarose-glutathione beads for 1 hour and then incubated overnight with lysed collected from HEK293 overexpressing PLC $\gamma$ 1. Beads were then washed and proteins bound to the agarose beads were harvested in denaturing condition and analyzed by western blot analysis. Figure 7.15 shows a representative western blot of experiments performed using lysis buffer (50mM Tris-pH 8.0, 50mM KCl, 1% NP-40) for collecting cell lysates and for the washing steps. A band recognised by PLC $\gamma$ 1 antibody was detected when lysates HEK293-PLC $\gamma$ 1 were incubated with GST-PDK1 previously immobilised on the agarose beads. However a small band recognised by PLC $\gamma$ 1 antibody was detected also in the negative control (HEK-GST). The limited amount of PLC $\gamma$ 1 interacting with PDK1, together with the signal detected in the control suggested me that the technique was not

optimised. Nevertheless the result was encouraging to further optimise the assay.

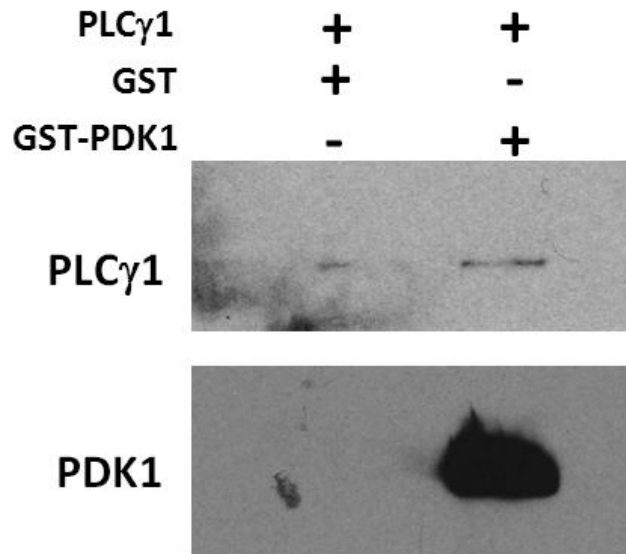


**Figure 7.15: GST pull down:** Western blot analysis of GST pull down assay of HEK293 overexpressing GST or GST-PDK1 incubated with lysate from HEK293 overexpressing PLC $\gamma$ 1. PLC $\gamma$ 1 and PDK1 were detected using specific antibodies. Representative western blot of 2 experiments.

In an effort to find the optimal condition to detect the interaction, I decided to test different buffers for the incubation step. Three different buffers were prepared changing the ionic and detergent concentration (Table 7.2). The aim of this optimisation protocol was to preserve the PLC $\gamma$ 1-PDK1 interaction and remove the aspecific binding observed in the control.

Table 7.2:

	Buffer 1	Buffer 2	Buffer 3
Tris pH 8.0	50 mM	50 mM	50 mM
NaCl	300 mM	150 mM	50mM
NP-40	0.1%	1%	2%

HEK293-GST and HEK293-GST-PDK1 were lysed in lysis buffer (50mM Tris-pH 8.0, 50mM KCl, 1% NP-40) and incubated with agarose-glutathione beads for 2 hours using one of the buffers listed in table 7.2. After three washes, performed in the chosen buffer, lysate from HEK293-PLC $\gamma$ 1 was incubated overnight with the beads-bound GST-fused protein, in the corresponding buffer. Complexes were eluted in denaturing conditions after three washes and analysed by western blot. As shown in Figure 7.16 PLC $\gamma$ 1 was not detected in the complex when the incubation was carried out in buffer 1 (lanes 2-3). On the contrary, a clear band was detected when HEK293-PLC $\gamma$ 1 lysate was incubated with GST-PDK1 using the buffer 2 (lanes 3-4) and buffer 3 (lane 5-6), indicating that PLC $\gamma$ 1-PDK1 complex was preserved in these conditions. Moreover a very low aspecific signal was detected following incubation with GST alone. Coomassie brilliant blue staining was performed in order to evaluate proteins levels in the different samples. The arrows indicate GST-PDK1 and GST. The staining revealed no major difference in protein levels among the different samples. Taken together these data demonstrated that PLC $\gamma$ 1 can associate with PDK1, at least *in vitro*.

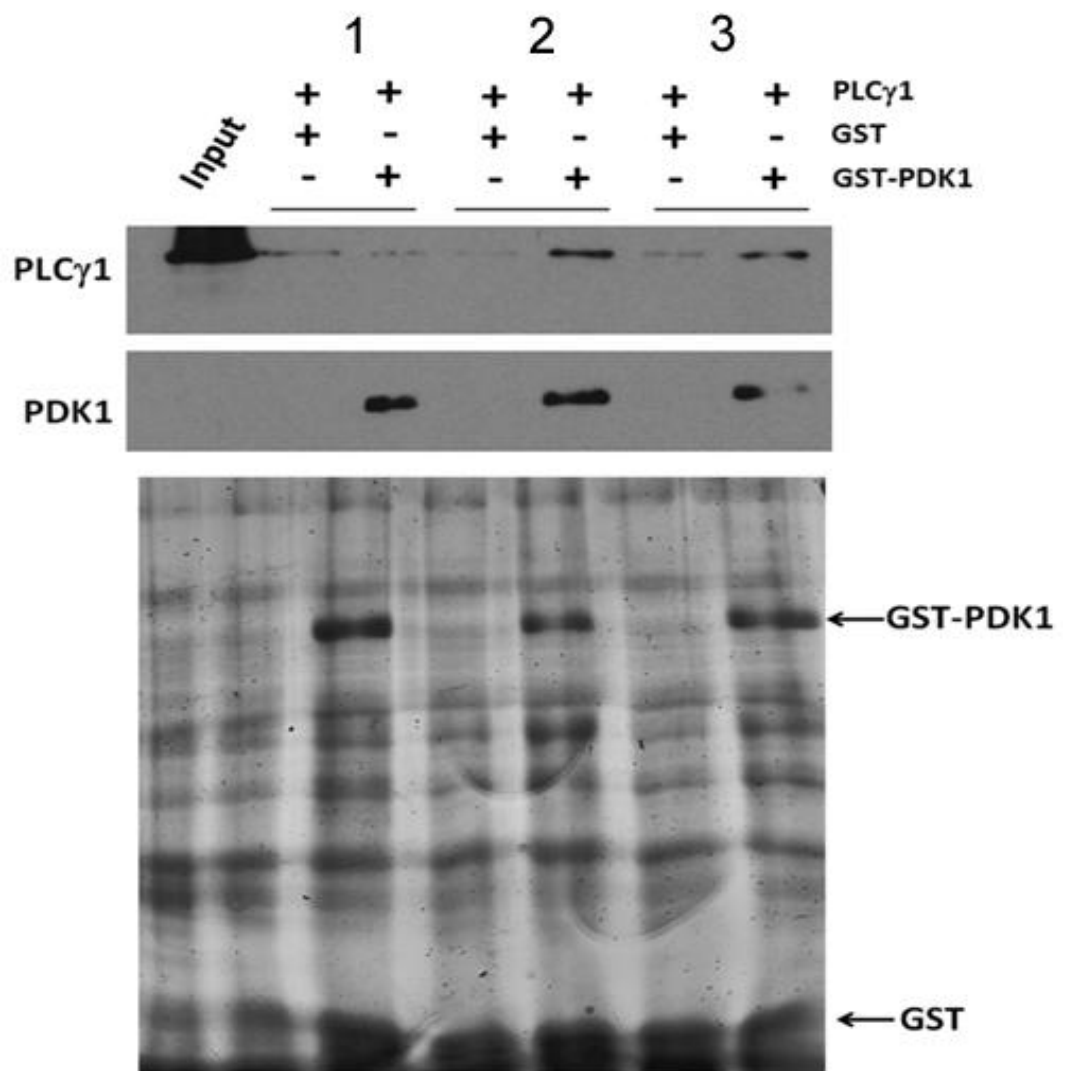


**Figure 7.16: GST Pull-down optimisation protocol:** WB analysis of GST pull down assay in cells expressing GST or GST-PDK1 and lysed with three different buffers (see table 3) (upper panel). Loading control was assessed by Coomassie staining of a gel run in parallel (lower panel). Representative Western blot of three independent experiments.

### 7.5.5 Co-immunoprecipitation analysis of endogenous PLC $\gamma$ 1 and PDK1 in MDA-MB-231

Co-immunoprecipitation and GST pull down experiments demonstrated for the first time that PLC $\gamma$ 1 can interact with PDK1 when overexpressed. To investigate the PDK1-PLC $\gamma$ 1 interaction at endogenous level, I decided to perform co-immunoprecipitation experiments of endogenous proteins from lysates of MDA-MB-231 stimulated with EGF and in full serum condition. Experimental conditions optimised in the pull-down assay were used. To this end, MDA-MB-231 were serum starved overnight and left untreated (control) or stimulated with EGF for 10 minutes. Alternatively, cells maintained in 10% serum supplied media were used. PLC $\gamma$ 1 and PDK1 were co-immunoprecipitated using the PLC $\gamma$ 1 antibody and immunocomplexes fractions assessed by western blot for PLC $\gamma$ 1 and PDK1. As shown in Figure 7.17, PDK1 was specifically immunoprecipitated by the anti-PLC $\gamma$ 1 in lysates from EGF-stimulated cells compared to non-stimulated cells or to cells maintained in serum condition. These data demonstrated that EGF induces association of PLC $\gamma$ 1 and PDK1. Data are consistent with previous results showing a reduced tyrosine phosphorylation of PLC $\gamma$ 1 after EGF stimulation in cells downregulated for PDK1 or treated with 2-*O*-Bn-InsP, suggesting that the interaction between PLC $\gamma$ 1 and PDK1 is necessary for PLC $\gamma$ 1 phosphorylation and the subsequent activation.

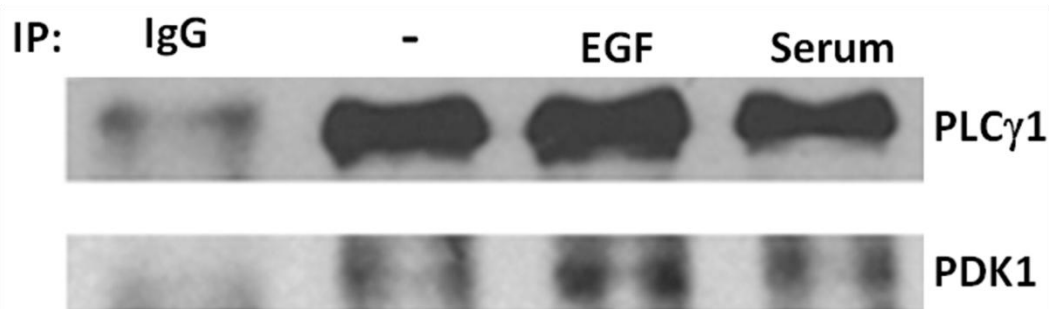


**Figure 7.17 Co-immunoprecipitation of endogenous PDK1 and PLC $\gamma$ 1:** MDA-MB-231 were left untreated or stimulated with EGF for 10 minutes or maintained in serum-supplemented media. Co-IP and western blot analysis

were performed using anti- PLC $\gamma$ 1 and anti-PDK1 antibodies. Representative Western blot of three independent experiments.

To further investigate the novel identified complex between PLC $\gamma$ 1 and PDK1, I decided to perform co-immunoprecipitation experiments in MDA-MB-435 downregulated for PLC $\gamma$ 1 expression (MDA-MB-435 shPLC $\gamma$ 1) and the respective control (MDA-MB-435 sh3MUT). The rationale was to investigate the potential PLC $\gamma$ 1/PDK1 complex in a second cell line and also to validate the specificity of the co-immunoprecipitation assay. Indeed, in principle, the co-immunoprecipitation analysis performed using the PLC $\gamma$ 1 antibody in cells lacking PLC $\gamma$ 1 should monitor potential aspecific immunoprecipitation. Cells were serum starved overnight and left untreated or stimulated with EGF for 10 minutes or with media containing 10% serum supplied media before being lysed. Immunoprecipitation assay was performed in the conditions previously described. Lysates were incubated with PLC $\gamma$ 1 antibody and immunoprecipitated fractions assessed by western blot for PLC $\gamma$ 1 and PDK1. Figure 7.18 shows that PLC $\gamma$ 1 was efficiently immunoprecipitated in MDA-MB-435 3MUT whereas no PLC $\gamma$ 1 (or reduced PLC $\gamma$ 1) was immunoprecipitated in MDA-MB-435 downregulated for PLC $\gamma$ 1 expression. These data demonstrate that PDK1 specifically interact with PLC $\gamma$ 1 and rule out any potential aspecific co-immunoprecipitation.

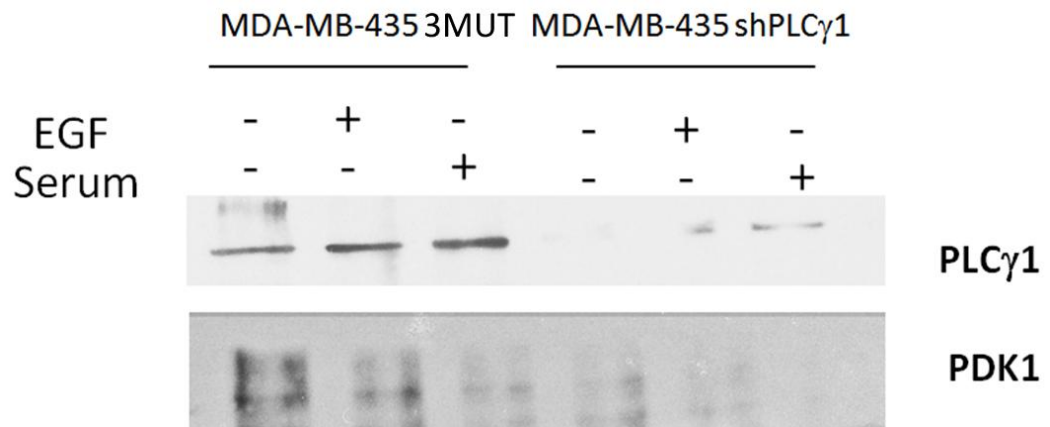
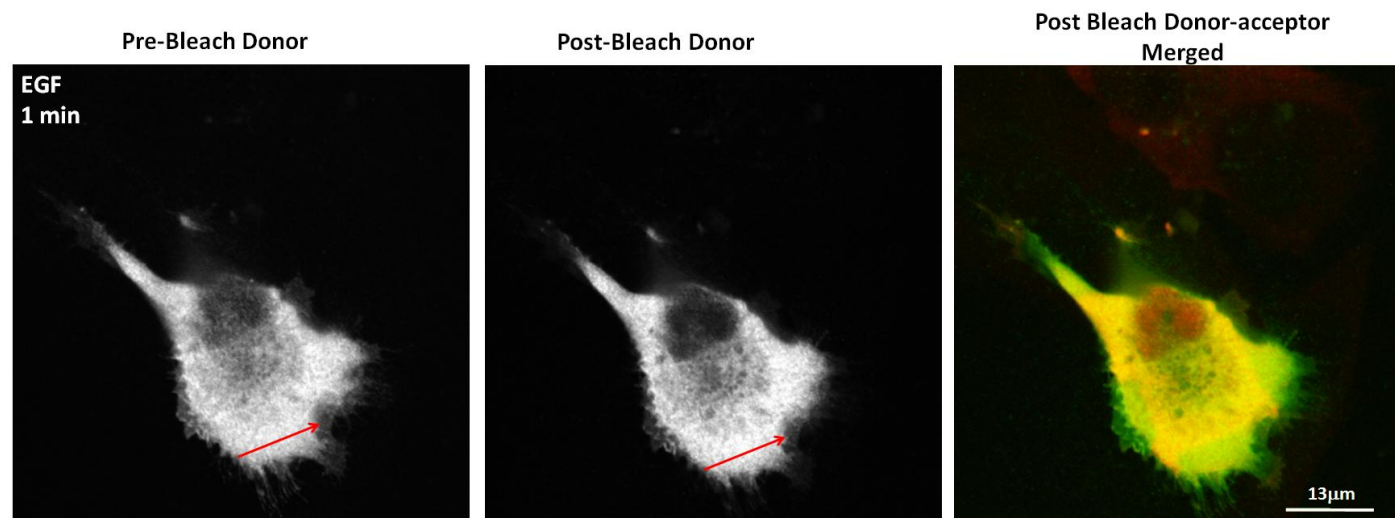
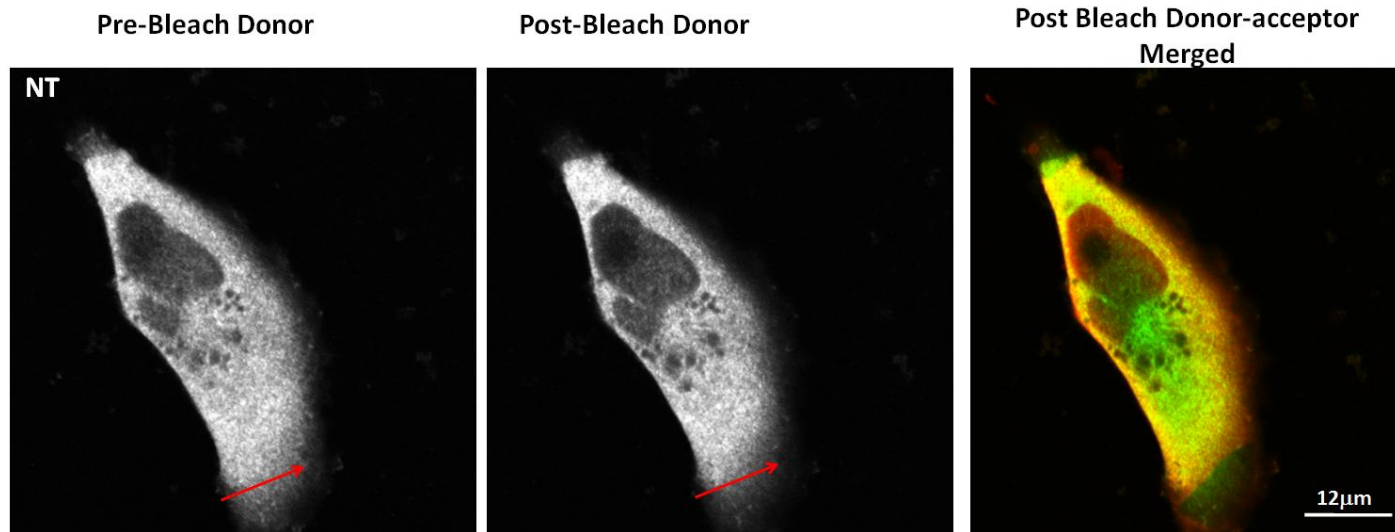


**Figure 7.18: Co-immunoprecipitation of PDK1 and PLC $\gamma$ 1 in MDA-MB-435:** MDA-MB-435 3MUT and MDA-MB-435 shPLC $\gamma$ 1 were left untreated or stimulated with EGF for 10 minutes or maintained in serum-supplemented media. Co-IP and western blot analysis are performed using anti- PLC $\gamma$ 1 and anti-PDK1 antibodies. Representative Western blot of three independent experiments.

### 7.5.6 FRET analysis of PLC $\gamma$ 1/PDK1 protein interaction by confocal imaging

To understand the dynamic of the interaction between PDK1 and PLC $\gamma$ 1, I decided to use the Fluorescence Resonance Energy Transfer (FRET) assay as described in chapter 2.3.4, in order to analyse the formation of the complex spatially and temporally. To this end MDA-MB-231 were co-transfected with plasmids to over-express both PLC $\gamma$ 1 and PDK1. As controls, MDA-MB-231 expressing a GFP-containing vector together with PLC $\gamma$ 1 plasmid and MDA-MB-231 expressing GFP-containing vector together with the pOZ-PDK1 plasmid were used. No FRET signal was expected to be detected in the control cells since no interaction occurs between GFP and PLC $\gamma$ 1 and between GFP and PDK1. Cells were starved overnight 24 hours after transfection and then left untreated or stimulated with EGF at different time points before being fixed. Immunofluorescence staining was performed using PLC $\gamma$ 1 and PDK1

specific antibodies (chapter 2.3.4) followed by FRET analysis. An increase in fluorescence in the donor channel was detected after acceptor's photo-bleaching. Donor fluorescence was measured at the level of membrane protrusions (when present after EGF stimulation) and also in more cytoplasmic regions. The rationale was that since PLC $\gamma$ 1 translocates to the plasma-membrane after EGF stimulation and also it is localised at the leading-edge of motile cells, the PDK1-PLC $\gamma$ 1 complex could be enriched in the EGF-induced cell protrusions. Donor fluorescence was measured also in more central cytoplasmic regions. Images in Figure 7.19 show the fluorescence intensity of the donor before and after the photo-bleaching for each time point in specific chosen regions. The merged channel shows where the acceptor was photo-bleached. The lines indicate representative regions where donor fluorescence change was measured and value collected for statistical analysis. In particular the chart in figure 7.20 shows the donor fluorescence (green line) before and after photobleaching of the acceptor (red line) of representative regions at all time points. FRET occurred after 1 minute and 3 minutes of EGF stimulation, since at these time-points acceptor's drop of fluorescence was coupled with an increased donor's fluorescence. As indicated in Figure 7.21, photo-bleaching of the donor caused a significant increase of fluorescence in the donor channel after 3 minutes of stimulation with EGF, indicative of FRET. No changes in donor fluorescence were revealed in the internal cytoplasmic region after acceptor photo-bleaching, and no FRET was detected when PLC $\gamma$ 1 or PDK1 were overexpressed together with a GFP-containing vector, indicating that PLC $\gamma$ 1 and PDK1 associated after EGF stimulation, in well-defined region corresponding to cellular protrusions induced by EGF.



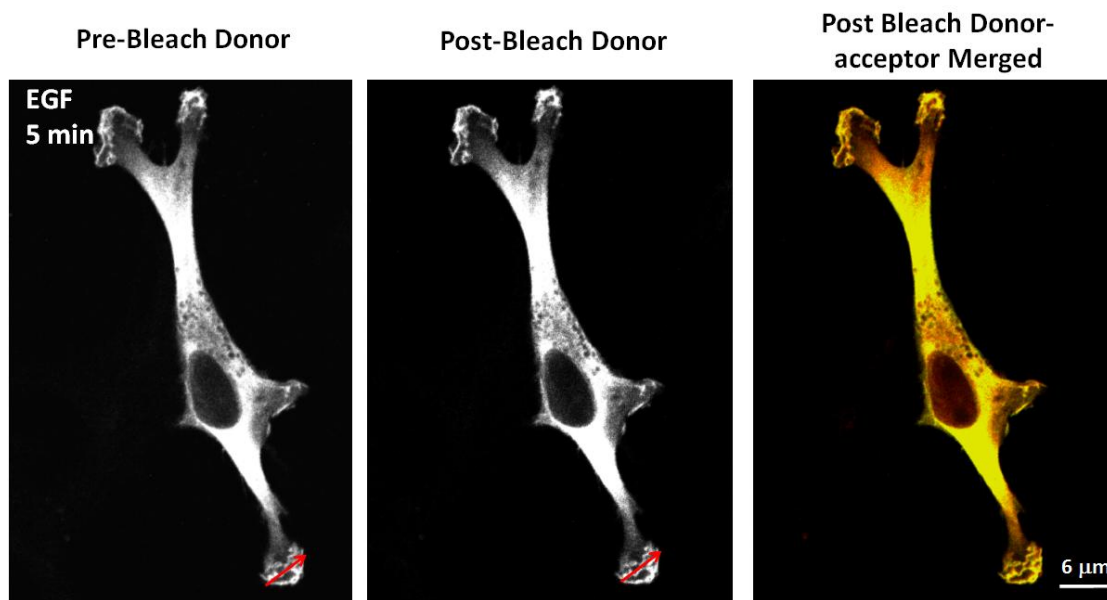
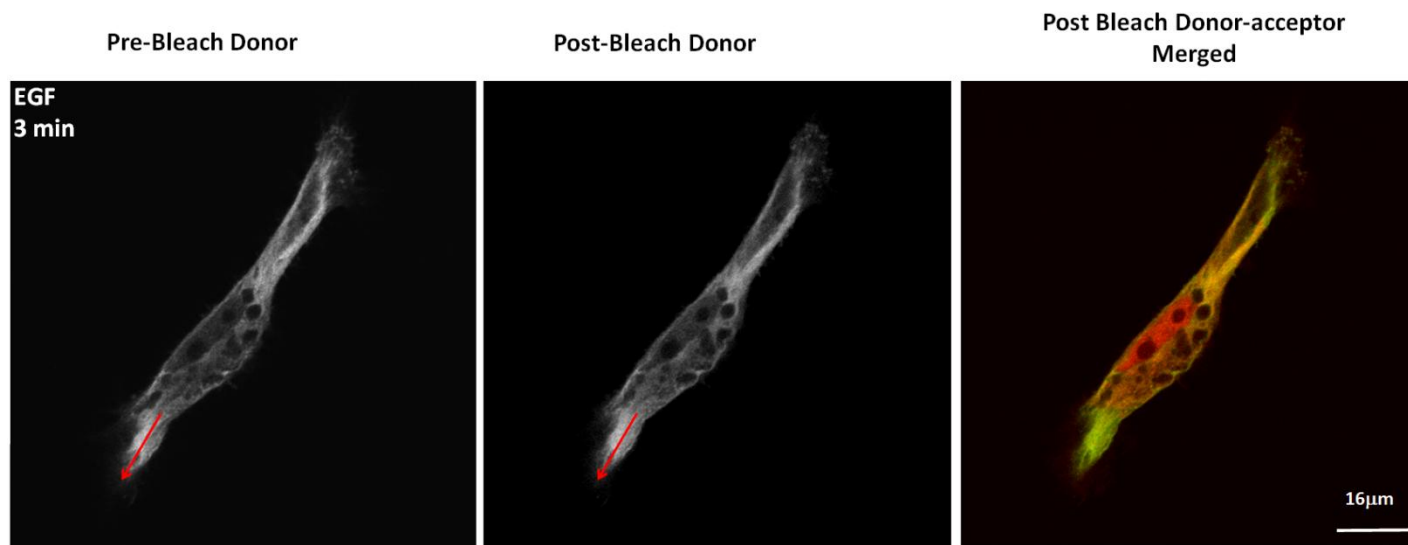




**Figure 7.19: FRET images of MDA-MB-231 expressing exogenous PLC $\gamma$ 1 and PDK1:** Donor pre-bleach and post-bleach fluorescence was measured in MDA-MB-231 overexpressing PLC $\gamma$ 1 and PDK1 after 1,3,5 and 10 minutes of stimulation with EGF in the areas indicated by the red line in each figure.

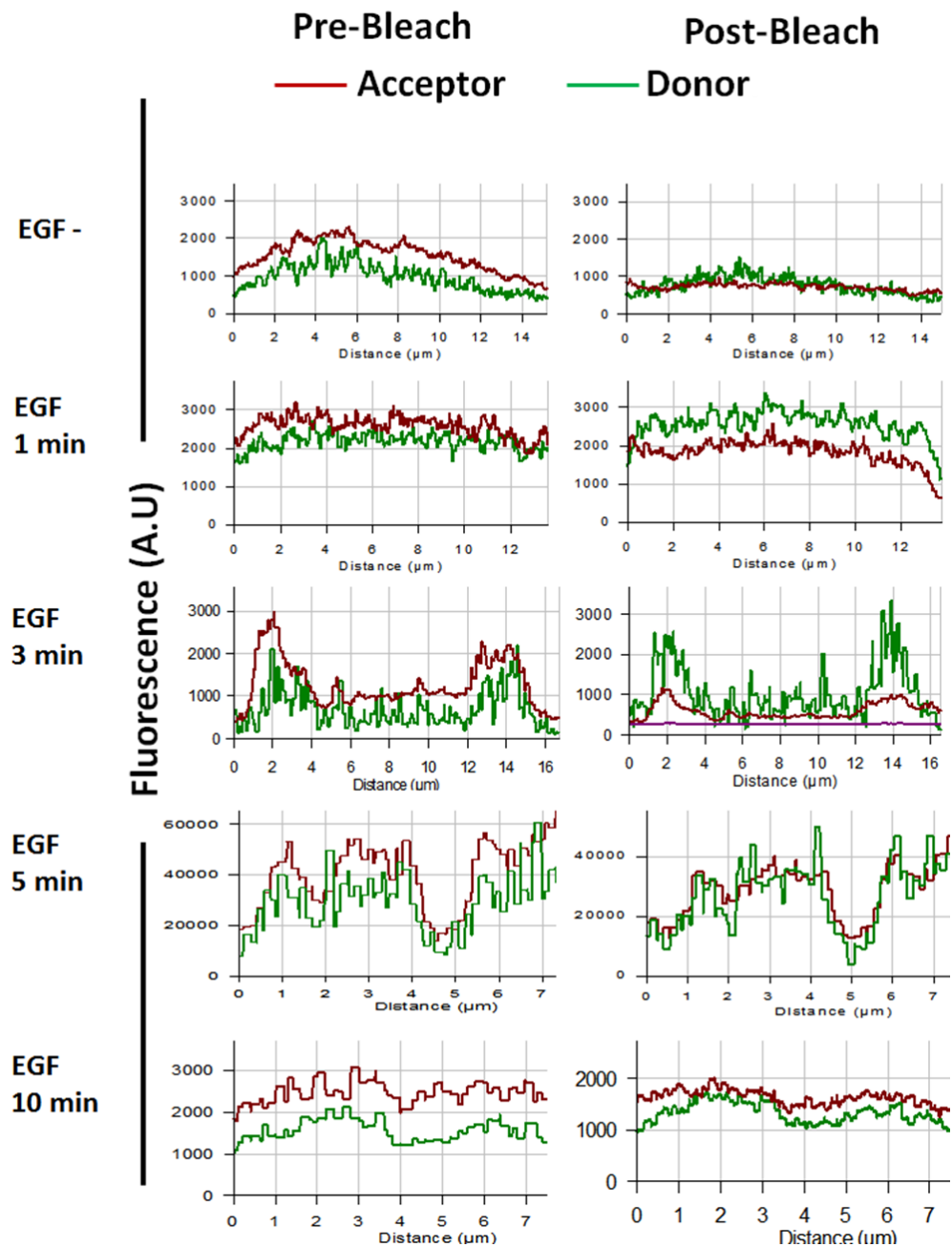


**Figure 7.20:** Graphs representing donor and acceptor fluorescence measured at each time points along the red line indicated in the corresponding figures showed in figure 7.19. Increased donor fluorescence after bleaching indicated FRET occurring in the measured area. Unstimulated MDA-MB-231 overexpressing PLC $\gamma$ 1 and PDK1 were used as control.

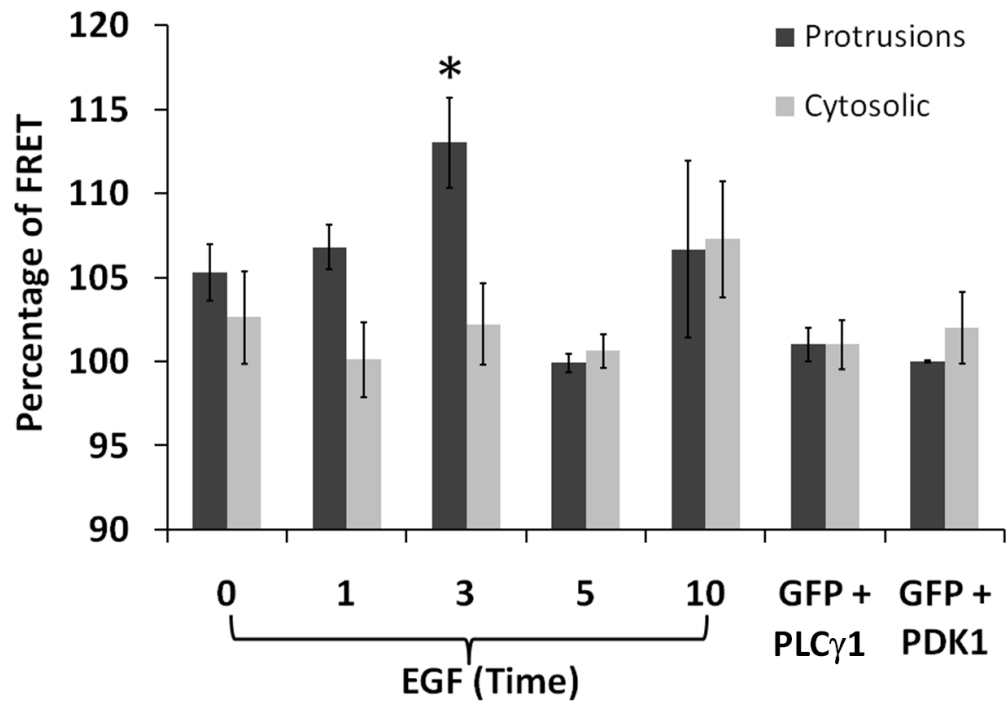


**Figure 7.21: Quantification of FRET in MDA-MB-231:** Chart indicates percentage of FRET in MDA-MB-231 expressing exogenous PLC $\gamma$ 1 and PDK1 at the indicate times of EGF stimulation. Percentage of FRET was calculated in three independent experiments measuring donor fluorescence of 10 cells per experiment before and after acceptor bleaching. Percentage of FRET in cells co-expressing PLC $\gamma$ 1 and GFP or PDK1 and GFP was used as basal FRET signal. Columns are the means  $\pm$ SEM of percentage of FRET measured at protrusion level or in more central cytosolic regions.

### **7.5.7 FRET analysis of PLC $\gamma$ 1/PDK1 protein interaction by FACS analysis**

To confirm the FRET data obtained by confocal analysis, I decided to perform FRET experiments using a different methodological approach. The FRET analysis described in chapter 7.5.6 was based on the increased fluorescence of the donor after photo-bleaching of the acceptor as read-out of occurring FRET. The methodology used to detect FRET using FACS analysis relies on increased fluorescence of the acceptor following donor excitation, without direct excitation of the acceptor itself. FRET occurs when donor's and acceptor's distance is less than 10 nm, resulting in increased fluorescence emission of the acceptor. Therefore the potential increase of acceptor fluorescence over background is due to FRET between donor and acceptor.

MDA-MB-231 cells were co-transfected with plasmids overexpressing PLC $\gamma$ 1 and PDK1. Cells were serum starved over night before being stimulated with 50ng/ml EGF. Background fluorescence of acceptor alone was measured as control. Furthermore acceptor fluorescence was measured in MDA-MB-231 expressing a GFP-containing vector together with PLC $\gamma$ 1 plasmid or pOZ-PDK1 plasmid, in order to calibrate the background fluorescence of the acceptor. Furthermore MDA-MB-231 cells were transfected with PLC $\gamma$ 1 or pOZ-PDK1 plasmid and labelled with donor or acceptor dye-conjugated antibodies. These measurements allowed the calibration of the instrument in order to avoid false-positive FRET signal from cross-talk artefacts. The acceptor emission profiles of untreated and EGF stimulated cells were compared to the acceptor profile obtained in cells stained for PDK1 and PLC $\gamma$ 1 respectively. As indicated in figure 7.22A unstimulated cells show an emission profile superimposable to the single positive sample. Cells stimulated with EGF present a shift in the acceptor emission profile indicating increased acceptor fluorescence subsequent to EGF stimulation. Analysis of the acceptor emission profiles shows that a slight increase in the acceptor fluorescence was detected in unstimulated MDA-MB-231 overexpressing PLC $\gamma$ 1 and PDK1 compared

to background level, although not statistically significant. On the contrary stimulation with EGF induced 30% increase of acceptor fluorescence (Figure 7.22B,C). These data indicate that EGF stimulation induces a fluorescence increase of the acceptor due to FRET occurring between PLC $\gamma$ 1 and PDK1, demonstrating that PLC $\gamma$ 1 and PDK1 interaction is induced by EGF stimulation.

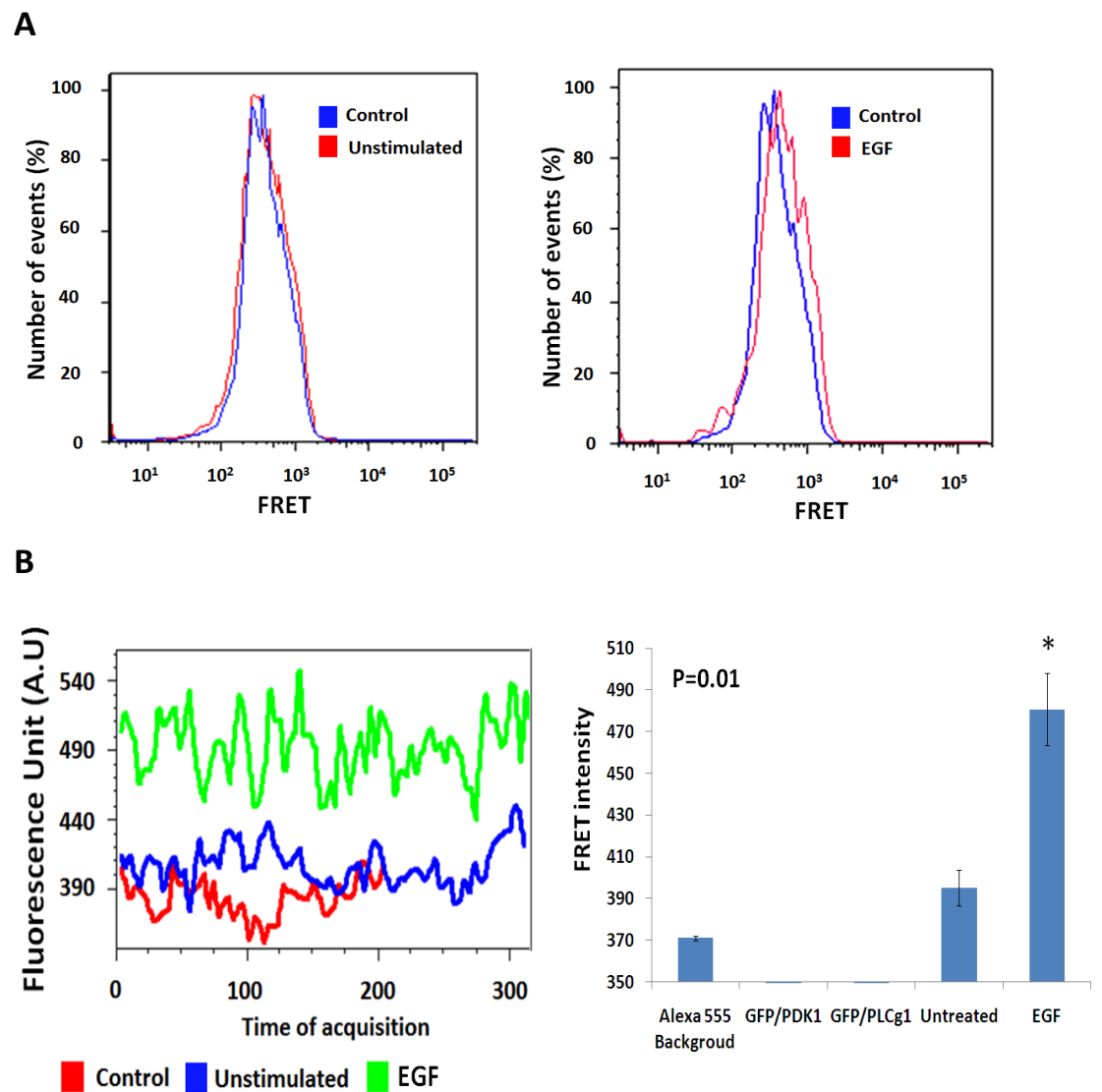


**Figure 7.22: Quantification of FRET by FACS analysis: A)** The data display acceptor fluorescence of control and unstimulated cells (left) and control and EGF-stimulated cells (right) after correction of spectral bleeding of donor into the FRET (550 nm) channel. **B)** Fluorescence intensity over

time of acquisition of control, unstimulated and EGF stimulated cells. C) **Quantification of fluorescence in the FRET channels in MDA-MB-231** transfected with PLC $\gamma$ 1 or pOZ-PDK1 plasmid and labeled with acceptor-dye-conjugated antibody, or expressing a GFP-containing vector (donor) together with PLC $\gamma$ 1 plasmid or pOZ-PDK1 plasmid labelled with acceptor-dye-conjugated antibody. FRET was quantified also in MDA-MB-231 co-expressing PLC $\gamma$ 1 and PDK1 untreated or stimulated with EGF. Graph is the average  $\pm$ SEM of three independent experiments.

## 7.6 Discussion

In order to test the hypothesis of a novel role of PDK1 in PLC $\gamma$ 1 regulation I decided first to investigate the role of PDK1 on PLC $\gamma$ 1 activation by measuring intracellular calcium and inositol phosphate accumulation upon EGF stimulation. Transient transfection of siRNAs is a powerful tool to downregulate the expression of targeted proteins. However, the results might be affected by intrinsic variability of the efficiency of transfection among different experiments and by a partial knock down. Therefore I decided to generate MDA-MB-231 expressing shRNA specific for downregulation of PDK1. The specific targeting sequence was cloned in the pSUPERIOR.retro.puro, which allows stable downregulation of the protein or inducible downregulation of the targeted protein if expressed in cells expressing the TET repressor. As described in the introductory chapter 1.7.2 increasing lines of evidence showed that PDK1 plays a main role in cell migration and invasion in normal and cancer cell lines. My data showed that transient downregulation of PDK1 inhibited cell invasion on Matrigel in MDA-MB-231, MDA-MB-435 and A375M indicating that PDK1 plays an important role in cell invasion in the cell systems used (Figure 7.3). Interestingly transient downregulation of PDK1 inhibited EGF-induced calcium mobilisation in MDA-MB-231 and A375M (Figure 7.2). Furthermore inositol phosphates accumulation assay was inhibited in two clones of MDA-MB-231 expressing shRNA targeting PDK1 (Figure 7.9). Since the EGF-induced calcium release is entirely dependent on PLC $\gamma$ 1 in

this cellular system, these data demonstrated that PDK1 is involved in PLC $\gamma$ 1 activity. Furthermore downregulation of PDK1 inhibited PLC $\gamma$ 1 phosphorylation in MDA-MB-231 which explains the inhibition of PLC $\gamma$ 1 activity (Figure 7.11). These data were consistent with the inhibition of PLC $\gamma$ 1 phosphorylation observed in cells treated with 2-*O*-Bn-InsP<sub>5</sub> upon EGF stimulation. These data therefore identified a novel role of PDK1 in PLC $\gamma$ 1 regulation and a common mechanism of regulation of cancer progression and metastasis development. Considering the importance of PLC $\gamma$ 1 in metastasis development and progression, the inhibiting effect of 2-*O*-Bn-InsP<sub>5</sub> on PLC $\gamma$ 1 activity and on cell invasion strongly suggests that this inhibitor might have anti-metastatic effects *in vivo*. PDK1 represents a good target in cancer and since it is involved in the regulation of proteins that have an important role in cancer cell biology such as AKT, S6K1, SGK1-3 and PKC. However for this reason PDK1 inhibition could result in side effects. Interestingly data in literature showed that hypomorphic mice did not show any specific phenotype but, when crossed with PTEN heterozygote mice are protected against tumour development (Bayascas et al., 2005). Therefore pharmacological PDK1 inhibition could result in primary tumour growth inhibition and more importantly in anti-metastatic effect.

Co-immunoprecipitation, GST pull-down and FRET analysis showed that PLC $\gamma$ 1 and PDK1 form a complex upon EGF stimulation, with an increased association upon growth factor stimulation. In particular confocal-based FRET analysis showed a significant increased association upon stimulation with EGF for 3 minutes in cell protrusion while FACS-based FRET analysis showed increased association upon EGF stimulation for 10 minutes. The different time response to EGF might be explained by the different conditions used for cell stimulation. Indeed for confocal-based FRET analysis adherent cells were stimulated at the different time points while for FACS-based FRET analysis cells were first detached and then stimulated with EGF in order to allow cell fixation for FACS analysis. Consistent with confocal-based FRET, co-immunoprecipitation analysis showed an increased association after 3 minutes stimulation with EGF. Taken together these data revealed a novel

protein-protein interaction between PLC $\gamma$ 1 and PDK1 essential for PLC $\gamma$ 1 activation and for cell motility.

### Summary

Data shown in this chapter reveal a novel role of PDK1 in PLC $\gamma$ 1 activation, and demonstrated that PDK1 is essential in PLC $\gamma$ 1 activation. In particular PLC $\gamma$ 1 and PDK1 interact upon EGF stimulation and FRET analysis revealed that this association is increased at protrusion level. Furthermore, inhibition of PDK1 blocks PLC $\gamma$ 1 activation and inhibits PLC $\gamma$ 1 tyrosine phosphorylation.

**Chapter 8**  
**Concluding discussion and future  
studies**

## 8.1 Discussion

The aim of my work was to investigate the role of PLC $\gamma$ 1 in cancer cell motility, with a particular interest in cancer cell migration and invasion, and the investigation of potential inhibitors that might prevent its activation. PLC $\gamma$ 1 has been extensively investigated in the literature and increasing lines of evidence suggested its role in cancer cell motility (Turner et al., 1997; Jonest et al., 2005; Shepard et al., 2007). Many previous reports used pan-PLC inhibitors or expression of a dominant negative mutants to understand the role of PLC $\gamma$  in cancer, especially in tumour local invasion and metastases. Our recent report demonstrated that PLC $\gamma$ 1 is overexpressed in lymph node metastases from breast cancer patients (Sala et al., 2008) and is required for metastasis development and progression.

The experiments performed in this thesis improved the understanding of the role of PLC $\gamma$ 1 in cancer cell motility and invasion *in vitro*. In particular I investigated the role of PLC $\gamma$ 1 in breast cancer and melanoma cancer cell migration and invasion *in vitro* using specific siRNA and shRNA to inhibit PLC $\gamma$ 1. This approach minimised aspecific effects compared to previous reports that used expression of dominant negative mutant to investigate PLC $\gamma$ 1 role in cancer. In accordance with previous observation using dominant negative mutant, my data showed that downregulation of PLC $\gamma$ 1 *in vitro* inhibited cancer cell migration and cell invasion *in vitro* and its downregulation affected membrane ruffles formation and growth factor-induced cytoskeleton remodelling. Failure in cytoskeleton remodelling is probably the main reason for the inhibition observed in cell migration and cell invasion. These *in vitro* data were the basis for experimental metastasis using MDA-MB-231 performed by my group. These experiments demonstrated that PLC $\gamma$ 1 is required for metastasis development and progression and identified PLC $\gamma$ 1 as a novel therapeutic target. Over the last 20 years successful strategies have been developed to treat different types of cancer, although cancer remains the second cause of death in adults. However no significant improvement has been achieved in treatment of metastasis, which most of the

time results in resistance to all the available treatment and represents the first cause of death in cancer patients. At present no antimetastatic drugs are available. Several papers produced by my laboratory demonstrated that inositol phosphates can be used to inhibit AKT by impairing the AKT PH/PtdIns(3,4,5)P<sub>3</sub> interaction, competing with PtdIns(3,4,5)P<sub>3</sub> for the PH domain binding (Piccolo et al., 2004; Maffucci et al., 2005). Similarly, since PLC $\gamma$ 1 possesses a PH domain responsible for its membrane recruitment, blocking the PH domain interaction with its substrate could be a good strategy to impair the activation of this enzyme. Considering that PH domains can bind different inositol phosphates with a different range of affinity ( Kavran et al., 1998; Maffucci and Falasca, 2001; Lemmon 2008), the hypothesis of finding inositol phosphates able to compete with the physiological substrate impairing the membrane recruitment, is extremely interesting.

For these reasons, in order to find specific inhibitors for PLC $\gamma$ 1, I tested the inositol pentakisphosphate InsP(1,3,4,5,6)P<sub>5</sub> and its derivative compound 2-*O*-Bn-InsP<sub>5</sub> on PLC $\gamma$ 1 activity. My data showed that 2-*O*-Bn-InsP<sub>5</sub>, and less potently InsP(1,3,4,5,6)P<sub>5</sub>, inhibit PLC $\gamma$ 1 activity upon EGF stimulation and that in MDA-MB-231, PLC $\gamma$ 1 is the only PLC isoform involved in EGF signalling. The effect observed in cancer cell migration and invasion, together with the potent PLC $\gamma$ 1 inhibition upon treatment with 2-*O*-Bn-InsP<sub>5</sub>, indicated that this compound might inhibit PLC $\gamma$ 1 *in vivo* and might have anti-metastatic activity. We recently reported that 2-*O*-Bn-InsP<sub>5</sub> is a specific and potent inhibitor for PDK1 with antitumor effect (Falasca et al., 2010). Therefore considering the role of PDK1 in cell migration and invasion and the effect observed upon 2-*O*-Bn-InsP<sub>5</sub> treatment in cancer cell migration and invasion and on PLC $\gamma$ 1 activation, I investigated a potential role of PDK1 in PLC $\gamma$ 1 activation. Strikingly, my data demonstrated a novel PDK1-dependent mechanism of PLC $\gamma$ 1 activation. Indeed transient or stable downregulation of PDK1 inhibited calcium mobilisation, inositol phosphates accumulation and PLC $\gamma$ 1 phosphorylation in Y783 upon EGF stimulation. Similarly, 2-*O*-Bn-InsP<sub>5</sub> treatment inhibited PLC $\gamma$ 1 tyrosine phosphorylation and PLC $\gamma$ 1 activity. Therefore these data demonstrated that PDK1 is essential for PLC $\gamma$ 1

phosphorylation, which is an essential step for PLC $\gamma$ 1 activation. However my data did not explain the mechanism by which PDK1 is involved in PLC $\gamma$ 1 phosphorylation. Indeed PDK1 is a threonine/serine kinase and therefore it is unlikely that the enzyme directly phosphorylates PLC $\gamma$ 1. To further gain insight into the novel identified PDK1-dependent mechanism, I decided to investigate the existence of a protein-protein complex between PLC $\gamma$ 1 and PDK1 which might be important for PLC $\gamma$ 1 activation independently of PDK1 kinase activity. Indeed a report showed that PDK1 association to ROCK1 regulates ROCK1 activity independently from PDK1 kinase activity (Pinner and Sahai, 2008). My data demonstrated not only the existence of a complex between PLC $\gamma$ 1 and PDK1 but also that this interaction is modulated upon EGF stimulation in breast cancer cells with an increased association in cellular protrusion. My work therefore identified a novel PDK1/PLC $\gamma$ 1 pathway, linking two major proteins involved in the regulation of cell motility and reported to play a major role in metastases. Moreover it improves the understanding of the molecular mechanism involved in the regulation of PLC $\gamma$ 1 in cancer. These data show that the PDK1/PLC $\gamma$ 1 is pharmacologically targetable and its inhibition may have antimetastatic effect *in vivo*. In particular these data indicate that 2-O-Bn-InsP<sub>5</sub> inhibits the PDK1/PLC $\gamma$ 1 pathway and is a promising anticancer and potential antimetastatic drug. My data strengthened the idea of PDK1 as a promising therapeutic target and suggest a major role of PDK1 in controlling metastasis development and progression by promoting PLC $\gamma$ 1 activation. Indeed PDK1 is overexpressed in breast cancer and increased copy number correlates with upstream lesion such as PTEN loss, PK3CA mutation and EGFR amplification which result in increased tumour growth, increased cell motility and poor prognosis (Maurer et al., 2009). In this scenario the novel PDK1/PLC $\gamma$ 1 might play an important role and could be an important therapeutic target for metastasis.

Data shown in this thesis highlighted the potential therapeutic properties of inositol phosphate compounds such as Ins(1,3,4,5,6)P<sub>5</sub> and 2-O-Bn-InsP<sub>5</sub>. However it is currently unknown how inositol phosphates are transported through the membrane. Recent evidence identified the role of ABCC family

members in inositol phosphates export, but no data are available in mammalian cells. My data showed for the first time that ABC transporters are involved in Ins(1,3,4,5,6)P<sub>5</sub> uptake in mammalian cells. In particular ABCC1 inhibition reduced Ins(1,3,4,5,6)P<sub>5</sub> uptake in breast cancer cells. The ABC transporters have a main role in chemoresistance and multidrug resistance. It was reported by my group that ABCC1 transporter promotes an autocrine loop by which cancer cells can stimulate their proliferation (Pineiro et al., 2010). Therefore this report suggests ABCC1 as a potential target to block cancer cell proliferation. However, according to the data showed in this thesis, the overexpression of ABCC1 might increase the intracellular uptake of exogenous inositol phosphates such as Ins(1,3,4,5,6)P<sub>5</sub> or potential synthetic derivative and could correlate with increased sensitivity showed by different cancer cell lines to inositol phosphates treatment. Therefore enhanced expression of ABCC1 might be used as potentially marker to identify tumour responsiveness to specific anti-cancer treatment, such as inositol phosphates.

## **8.2 Future work**

Several questions, arisen from the experiments showed in this thesis, remain pending.

Further work will focus on:

### **PDK1/PLC $\gamma$ 1**

Investigation of the mechanism by which PDK1 regulates PLC $\gamma$ 1 activity. Further experiments should investigate whether kinase activity of PDK1 is required for PLC $\gamma$ 1 activation or it is dispensable.

### **2-*O*-Bn-InsP<sub>5</sub> in metastases**

*In vitro* data showed that 2-*O*-Bn-InsP<sub>5</sub> inhibits PLC $\gamma$ 1 activity and cancer cell invasion. Further *in vivo* work is required to investigate the role in metastases development and progression and to investigate the pharmacokinetic of this compound.

### **ABC transporter and Inositol phosphates active transport**

Further work is required to investigate the role of ABC transporter family members. In particular, modulation of expression of different ABC transporters, especially ABCC and ABCG family members by overexpression or siRNAs could the contribution of ABC transporter in inositol phosphate intake. Furthermore, screening of ABCC and ABCG transporter expression in cancer cell could correlate their expression with increased sensitivity to Inositol phosphates treatment.

# **Bibliography**

- Agus, D. B., R. W. Akita, et al. (2002). "Targeting ligand-activated ErbB2 signaling inhibits breast and prostate tumor growth." *Cancer cell* **2**(2): 127-37.
- Alessi, D. R., S. R. James, et al. (1997). "Characterization of a 3-phosphoinositide-dependent protein kinase which phosphorylates and activates protein kinase B $\alpha$ ." *Current biology : CB* **7**(4): 261-9.
- Alessi, D. R., M. T. Kozlowski, et al. (1998). "3-Phosphoinositide-dependent protein kinase 1 (PDK1) phosphorylates and activates the p70 S6 kinase in vivo and in vitro." *Curr Biol* **8**(2): 69-81.
- Anderson, K. E., J. Coadwell, et al. (1998). "Translocation of PDK-1 to the plasma membrane is important in allowing PDK-1 to activate protein kinase B." *Curr Biol* **8**(12): 684-91.
- Andjelkovic, M., D. R. Alessi, et al. (1997). "Role of translocation in the activation and function of protein kinase B." *J Biol Chem* **272**(50): 31515-24.
- Andrianantoandro, E. and T. D. Pollard (2006). "Mechanism of actin filament turnover by severing and nucleation at different concentrations of ADF/cofilin." *Molecular cell* **24**(1): 13-23.
- Arteaga, C. L., M. D. Johnson, et al. (1991). "Elevated content of the tyrosine kinase substrate phospholipase C-gamma 1 in primary human breast carcinomas." *Proc Natl Acad Sci U S A* **88**(23): 10435-9.
- Bae, Y. S., L. G. Cantley, et al. (1998). "Activation of phospholipase C-gamma by phosphatidylinositol 3,4,5-trisphosphate." *The Journal of biological chemistry* **273**(8): 4465-9.
- Bauer, K. R., M. Brown, et al. (2007). "Descriptive analysis of estrogen receptor (ER)-negative, progesterone receptor (PR)-negative, and HER2-negative invasive breast cancer, the so-called triple-negative phenotype: a population-based study from the California cancer Registry." *Cancer* **109**(9): 1721-8.
- Bayascas, J. R., N. R. Leslie, et al. (2005). "Hypomorphic mutation of PDK1 suppresses tumorigenesis in PTEN(+/-) mice." *Curr Biol* **15**(20): 1839-46.
- Bayascas, J. R., S. Wullschleger, et al. (2008). "Mutation of the PDK1 PH domain inhibits protein kinase B/Akt, leading to small size and insulin resistance." *Molecular and cellular biology* **28**(10): 3258-72.
- Bellacosa, A., C. C. Kumar, et al. (2005). "Activation of AKT kinases in cancer: implications for therapeutic targeting." *Advances in cancer research* **94**: 29-86.
- Berridge, M. J. and R. F. Irvine (1989). "Inositol phosphates and cell signalling." *Nature* **341**(6239): 197-205.
- Berrie, C. P. and M. Falasca (2000). "Patterns within protein/polyphosphoinositide interactions provide specific targets for therapeutic intervention." *FASEB J* **14**(15): 2618-22.
- Biondi, R. M., D. Komander, et al. (2002). "High resolution crystal structure of the human PDK1 catalytic domain defines the regulatory phosphopeptide docking site." *EMBO J* **21**(16): 4219-28.
- Bunney, T. D. and M. Katan (2010). "Phosphoinositide signalling in cancer: beyond PI3K and PTEN." *Nat Rev Cancer* **10**(5): 342-52.

- Bunney, T. D. and M. Katan (2011). "PLC regulation: emerging pictures for molecular mechanisms." *Trends in biochemical sciences* **36**(2): 88-96.
- Burridge, K. and M. Chrzanowska-Wodnicka (1996). "Focal adhesions, contractility, and signaling." *Annu Rev Cell Dev Biol* **12**: 463-518.
- Burstein, H. J., A. Keshaviah, et al. (2007). "Trastuzumab plus vinorelbine or taxane chemotherapy for HER2-overexpressing metastatic breast cancer: the trastuzumab and vinorelbine or taxane study." *Cancer* **110**(5): 965-72.
- Calleja, V., D. Alcor, et al. (2007). "Intramolecular and intermolecular interactions of protein kinase B define its activation in vivo." *PLoS biology* **5**(4): e95.
- Carracedo, A. and P. P. Pandolfi (2008). "The PTEN-PI3K pathway: of feedbacks and cross-talks." *Oncogene* **27**(41): 5527-41.
- Chan, A. Y., S. Raft, et al. (1998). "EGF stimulates an increase in actin nucleation and filament number at the leading edge of the lamellipod in mammary adenocarcinoma cells." *J Cell Sci* **111** ( Pt 2): 199-211.
- Chang, J. S., S. K. Kim, et al. (2005). "Pleckstrin homology domains of phospholipase C-gamma1 directly interact with beta-tubulin for activation of phospholipase C-gamma1 and reciprocal modulation of beta-tubulin function in microtubule assembly." *The Journal of biological chemistry* **280**(8): 6897-905.
- Chattopadhyay, A., M. Vecchi, et al. (1999). "The role of individual SH2 domains in mediating association of phospholipase C-gamma1 with the activated EGF receptor." *The Journal of biological chemistry* **274**(37): 26091-7.
- Chen, P., H. Xie, et al. (1994). "Epidermal growth factor receptor-mediated cell motility: phospholipase C activity is required, but mitogen-activated protein kinase activity is not sufficient for induced cell movement." *J Cell Biol* **127**(3): 847-57.
- Cheng, H. F., M. J. Jiang, et al. (1995). "Cloning and identification of amino acid residues of human phospholipase C delta 1 essential for catalysis." *The Journal of biological chemistry* **270**(10): 5495-505.
- Choi, J. H., J. B. Park, et al. (2004). "Phospholipase C-gamma1 is a guanine nucleotide exchange factor for dynamin-1 and enhances dynamin-1-dependent epidermal growth factor receptor endocytosis." *J Cell Sci* **117**(Pt 17): 3785-95.
- Choi, J. H., Y. R. Yang, et al. (2007). "Phospholipase C-gamma1 potentiates integrin-dependent cell spreading and migration through Pyk2/paxillin activation." *Cell Signal* **19**(8): 1784-96.
- Citro, S., S. Malik, et al. (2007). "Phospholipase Cepsilon is a nexus for Rho and Rap-mediated G protein-coupled receptor-induced astrocyte proliferation." *Proceedings of the National Academy of Sciences of the United States of America* **104**(39): 15543-8.
- Clarke, J. H., M. Wang, et al. (2010). "Localization, regulation and function of type II phosphatidylinositol 5-phosphate 4-kinases." *Adv Enzyme Regul* **50**(1): 12-8.
- Cleator, S., W. Heller, et al. (2007). "Triple-negative breast cancer: therapeutic options." *The lancet oncology* **8**(3): 235-44.

- Cooper, G. M. (2000). *The Cell*, 2nd edition. A molecular approach, Sinauer Associates.
- Courtney, K. D., R. B. Corcoran, et al. (2010). "The PI3K pathway as drug target in human cancer." *J Clin Oncol* **28**(6): 1075-83.
- Currie, R. A., K. S. Walker, et al. (1999). "Role of phosphatidylinositol 3,4,5-trisphosphate in regulating the activity and localization of 3-phosphoinositide-dependent protein kinase-1." *Biochem J* **337** ( Pt 3): 575-83.
- Di Paolo, G. and P. De Camilli (2006). "Phosphoinositides in cell regulation and membrane dynamics." *Nature* **443**(7112): 651-7.
- Duronio, V. (2008). "The life of a cell: apoptosis regulation by the PI3K/PKB pathway." *The Biochemical journal* **415**(3): 333-44.
- Essen, L. O., O. Perisic, et al. (1996). "Crystal structure of a mammalian phosphoinositide-specific phospholipase C delta." *Nature* **380**(6575): 595-602.
- Essen, L. O., O. Perisic, et al. (1997). "Structural mapping of the catalytic mechanism for a mammalian phosphoinositide-specific phospholipase C." *Biochemistry* **36**(7): 1704-18.
- Falasca, M., D. Chiozzotto, et al. (2010). "A novel inhibitor of the PI3K/Akt pathway based on the structure of inositol 1,3,4,5,6-pentakisphosphate." *Br J Cancer* **102**(1): 104-14.
- Falasca, M., S. K. Logan, et al. (1998). "Activation of phospholipase C gamma by PI 3-kinase-induced PH domain-mediated membrane targeting." *The EMBO journal* **17**(2): 414-22.
- Fidler, I. J. (2003). "The pathogenesis of cancer metastasis: the 'seed and soil' hypothesis revisited." *Nat Rev Cancer* **3**(6): 453-8.
- Filippa, N., C. L. Sable, et al. (2000). "Effect of phosphoinositide-dependent kinase 1 on protein kinase B translocation and its subsequent activation." *Mol Cell Biol* **20**(15): 5712-21.
- Finlay, D. K., L. V. Sinclair, et al. (2009). "Phosphoinositide-dependent kinase 1 controls migration and malignant transformation but not cell growth and proliferation in PTEN-null lymphocytes." *J Exp Med* **206**(11): 2441-54.
- Frame, M. C., H. Patel, et al. (2010). "The FERM domain: organizing the structure and function of FAK." *Nat Rev Mol Cell Biol* **11**(11): 802-14.
- Franke, T. F., D. R. Kaplan, et al. (1997). "Direct regulation of the Akt proto-oncogene product by phosphatidylinositol-3,4-bisphosphate." *Science* **275**(5300): 665-8.
- Friedl, P. and K. Wolf (2003). "Tumour-cell invasion and migration: diversity and escape mechanisms." *Nat Rev Cancer* **3**(5): 362-74.
- Garcia, P., R. Gupta, et al. (1995). "The pleckstrin homology domain of phospholipase C-delta 1 binds with high affinity to phosphatidylinositol 4,5-bisphosphate in bilayer membranes." *Biochemistry* **34**(49): 16228-34.
- Gibson, T. J., M. Hyvonen, et al. (1994). "PH domain: the first anniversary." *Trends in biochemical sciences* **19**(9): 349-53.
- Gonzalez-Angulo, A. M., J. Ferrer-Lozano, et al. (2011). "PI3K Pathway Mutations and PTEN Levels in Primary and Metastatic Breast Cancer." *Mol Cancer Ther.*

- Gresset, A., S. N. Hicks, et al. (2010). "Mechanism of phosphorylation-induced activation of phospholipase C-gamma isozymes." *The Journal of biological chemistry* **285**(46): 35836-47.
- Guillaud, L., R. Wong, et al. (2008). "Disruption of KIF17-Mint1 interaction by CaMKII-dependent phosphorylation: a molecular model of kinesin-cargo release." *Nat Cell Biol* **10**(1): 19-29.
- Haendeler, J., G. Yin, et al. (2003). "GIT1 mediates Src-dependent activation of phospholipase Cgamma by angiotensin II and epidermal growth factor." *The Journal of biological chemistry* **278**(50): 49936-44.
- Hagmann, W., R. Jesnowski, et al. (2009). "ATP-binding cassette C transporters in human pancreatic carcinoma cell lines. Upregulation in 5-fluorouracil-resistant cells." *Pancreatology : official journal of the International Association of Pancreatology* **9**(1-2): 136-44.
- Hammond, G. R., S. K. Dove, et al. (2006). "Elimination of plasma membrane phosphatidylinositol (4,5)-bisphosphate is required for exocytosis from mast cells." *Journal of cell science* **119**(Pt 10): 2084-94.
- Hammond, G. R. and G. Schiavo (2007). "Polyphosphoinositol lipids: under-PPIning synaptic function in health and disease." *Developmental neurobiology* **67**(9): 1232-47.
- Harlan, J. E., P. J. Hajduk, et al. (1994). "Pleckstrin homology domains bind to phosphatidylinositol-4,5-bisphosphate." *Nature* **371**(6493): 168-70.
- Heasman, S. J. and A. J. Ridley (2008). "Mammalian Rho GTPases: new insights into their functions from in vivo studies." *Nat Rev Mol Cell Biol* **9**(9): 690-701.
- Heo, J. S., Y. J. Lee, et al. (2006). "EGF stimulates proliferation of mouse embryonic stem cells: involvement of Ca<sup>2+</sup> influx and p44/42 MAPKs." *Am J Physiol Cell Physiol* **290**(1): C123-33.
- Hokin, M. R. and L. E. Hokin (1953). "Enzyme secretion and the incorporation of P32 into phospholipides of pancreas slices." *The Journal of biological chemistry* **203**(2): 967-77.
- Holbro, T., R. R. Beerli, et al. (2003). "The ErbB2/ErbB3 heterodimer functions as an oncogenic unit: ErbB2 requires ErbB3 to drive breast tumor cell proliferation." *Proceedings of the National Academy of Sciences of the United States of America* **100**(15): 8933-8.
- Hondal, R. J., Z. Zhao, et al. (1998). "Mechanism of phosphatidylinositol-specific phospholipase C: a unified view of the mechanism of catalysis." *Biochemistry* **37**(13): 4568-80.
- Hooper, S., J. F. Marshall, et al. (2006). "Tumor cell migration in three dimensions." *Methods Enzymol* **406**: 625-43.
- Huang, P. S., L. Davis, et al. (1995). "An SH3 domain is required for the mitogenic activity of microinjected phospholipase C-gamma 1." *FEBS Lett* **358**(3): 287-92.
- Iorns, E., C. J. Lord, et al. (2009). "Parallel RNAi and compound screens identify the PDK1 pathway as a target for tamoxifen sensitization." *Biochem J* **417**(1): 361-70.
- Irvine, R. F., K. D. Brown, et al. (1984). "Specificity of inositol trisphosphate-induced calcium release from permeabilized Swiss-mouse 3T3 cells." *Biochem J* **222**(1): 269-72.

- Irvine, R. F., A. J. Letcher, et al. (1986). "Specificity of inositol phosphate-stimulated Ca<sup>2+</sup> mobilization from Swiss-mouse 3T3 cells." *The Biochemical journal* **240**(1): 301-4.
- Jackson, S. G., Y. Zhang, et al. (2007). "Structural analysis of the carboxy terminal PH domain of pleckstrin bound to D-myo-inositol 1,2,3,5,6-pentakisphosphate." *BMC Struct Biol* **7**: 80.
- Ji, Q. S., S. Ermini, et al. (1998). "Epidermal growth factor signaling and mitogenesis in Plcg1 null mouse embryonic fibroblasts." *Molecular biology of the cell* **9**(4): 749-57.
- Ji, Q. S., G. E. Winnier, et al. (1997). "Essential role of the tyrosine kinase substrate phospholipase C-gamma1 in mammalian growth and development." *Proceedings of the National Academy of Sciences of the United States of America* **94**(7): 2999-3003.
- Jin, T. G., T. Satoh, et al. (2001). "Role of the CDC25 homology domain of phospholipase Cepsilon in amplification of Rap1-dependent signaling." *The Journal of biological chemistry* **276**(32): 30301-7.
- Jones, N. P. and M. Katan (2007). "Role of phospholipase Cgamma1 in cell spreading requires association with a beta-Pix/GIT1-containing complex, leading to activation of Cdc42 and Rac1." *Mol Cell Biol* **27**(16): 5790-805.
- Jones, N. P., J. Peak, et al. (2005). "PLCgamma1 is essential for early events in integrin signalling required for cell motility." *J Cell Sci* **118**(Pt 12): 2695-706.
- Kang, Y., P. M. Siegel, et al. (2003). "A multigenic program mediating breast cancer metastasis to bone." *Cancer Cell* **3**(6): 537-49.
- Kassis, J., J. Moellinger, et al. (1999). "A role for phospholipase C-gamma-mediated signaling in tumor cell invasion." *Clin Cancer Res* **5**(8): 2251-60.
- Katan, M. and R. L. Williams (1997). "Phosphoinositide-specific phospholipase C: structural basis for catalysis and regulatory interactions." *Seminars in cell & developmental biology* **8**(3): 287-296.
- Kavran, J. M., D. E. Klein, et al. (1998). "Specificity and promiscuity in phosphoinositide binding by pleckstrin homology domains." *The Journal of biological chemistry* **273**(46): 30497-508.
- Kelley, G. G., S. E. Reks, et al. (2001). "Phospholipase C(epsilon): a novel Ras effector." *The EMBO journal* **20**(4): 743-54.
- Khoshyomn, S., P. L. Penar, et al. (1999). "Inhibition of phospholipase C-gamma1 activation blocks glioma cell motility and invasion of fetal rat brain aggregates." *Neurosurgery* **44**(3): 568-77; discussion 577-8.
- Kim, H. K., J. W. Kim, et al. (1991). "PDGF stimulation of inositol phospholipid hydrolysis requires PLC-gamma 1 phosphorylation on tyrosine residues 783 and 1254." *Cell* **65**(3): 435-41.
- Kim, J. K., J. W. Choi, et al. (2011). "Phospholipase C-eta1 is activated by intracellular Ca(2+) mobilization and enhances GPCRs/PLC/Ca(2+) signaling." *Cellular signalling* **23**(6): 1022-9.
- Kim, J. W., S. S. Sim, et al. (1990). "Tyrosine residues in bovine phospholipase C-gamma phosphorylated by the epidermal growth factor receptor in vitro." *The Journal of biological chemistry* **265**(7): 3940-3.

- Kim, M. J., J. S. Chang, et al. (2000). "Direct interaction of SOS1 Ras exchange protein with the SH3 domain of phospholipase C-gamma1." *Biochemistry* **39**(29): 8674-82.
- Kim, M. J., E. Kim, et al. (2000). "The mechanism of phospholipase C-gamma1 regulation." *Exp Mol Med* **32**(3): 101-9.
- Kok, K., B. Geering, et al. (2009). "Regulation of phosphoinositide 3-kinase expression in health and disease." *Trends in biochemical sciences* **34**(3): 115-27.
- Kolsch, V., P. G. Charest, et al. (2008). "The regulation of cell motility and chemotaxis by phospholipid signaling." *J Cell Sci* **121**(Pt 5): 551-9.
- Komander, D., A. Fairservice, et al. (2004). "Structural insights into the regulation of PDK1 by phosphoinositides and inositol phosphates." *The EMBO journal* **23**(20): 3918-28.
- Konig, J., M. Hartel, et al. (2005). "Expression and localization of human multidrug resistance protein (ABCC) family members in pancreatic carcinoma." *International journal of cancer. Journal international du cancer* **115**(3): 359-67.
- Langholz, O., D. Roeckel, et al. (1997). "Cell-matrix interactions induce tyrosine phosphorylation of MAP kinases ERK1 and ERK2 and PLCgamma-1 in two-dimensional and three-dimensional cultures of human fibroblasts." *Exp Cell Res* **235**(1): 22-7.
- Lassing, I. and U. Lindberg (1985). "Specific interaction between phosphatidylinositol 4,5-bisphosphate and profilactin." *Nature* **314**(6010): 472-4.
- Lawlor, M. A., A. Mora, et al. (2002). "Essential role of PDK1 in regulating cell size and development in mice." *EMBO J* **21**(14): 3728-38.
- Lawson, N. D., J. W. Mugford, et al. (2003). "phospholipase C gamma-1 is required downstream of vascular endothelial growth factor during arterial development." *Genes & development* **17**(11): 1346-51.
- Lemmon, M. A. (2008). "Membrane recognition by phospholipid-binding domains." *Nature reviews. Molecular cell biology* **9**(2): 99-111.
- Lemmon, M. A. and K. M. Ferguson (1998). "Pleckstrin homology domains." *Curr Top Microbiol Immunol* **228**: 39-74.
- Lemmon, M. A., K. M. Ferguson, et al. (1995). "Specific and high-affinity binding of inositol phosphates to an isolated pleckstrin homology domain." *Proceedings of the National Academy of Sciences of the United States of America* **92**(23): 10472-6.
- Lemmon, M. A., K. M. Ferguson, et al. (1996). "PH domains: diverse sequences with a common fold recruit signaling molecules to the cell surface." *Cell* **85**(5): 621-4.
- Li, S., Q. Wang, et al. (2009). "PLC-gamma1 and Rac1 coregulate EGF-induced cytoskeleton remodeling and cell migration." *Molecular endocrinology* **23**(6): 901-13.
- Liao, H. J., T. Kume, et al. (2002). "Absence of erythropoiesis and vasculogenesis in Plcg1-deficient mice." *The Journal of biological chemistry* **277**(11): 9335-41.
- Lim, M. A., L. Yang, et al. (2004). "Roles of PDK-1 and PKN in regulating cell migration and cortical actin formation of PTEN-knockout cells." *Oncogene* **23**(58): 9348-58.

- Liu, Y., J. Wang, et al. (2009). "Down-regulation of 3-phosphoinositide-dependent protein kinase-1 levels inhibits migration and experimental metastasis of human breast cancer cells." *Mol Cancer Res* **7**(6): 944-54.
- M, A. L., F. M., et al. (1997). "Regulatory recruitment of signalling molecules to the cell membrane by pleckstrin homology domains." *Trends Cell Biol* **7**(6): 237-42.
- Maffucci, T. and M. Falasca (2001). "Specificity in pleckstrin homology (PH) domain membrane targeting: a role for a phosphoinositide-protein cooperative mechanism." *FEBS Lett* **506**(3): 173-9.
- Maffucci, T., E. Piccolo, et al. (2005). "Inhibition of the phosphatidylinositol 3-kinase/Akt pathway by inositol pentakisphosphate results in antiangiogenic and antitumor effects." *Cancer Res* **65**(18): 8339-49.
- Maffucci, T., C. Raimondi, et al. (2009). "A phosphoinositide 3-kinase/phospholipase C $\gamma$ 1 pathway regulates fibroblast growth factor-induced capillary tube formation." *PloS one* **4**(12): e8285.
- Manning, B. D. and L. C. Cantley (2007). "AKT/PKB signaling: navigating downstream." *Cell* **129**(7): 1261-74.
- Martin, T. F. (2001). "PI(4,5)P<sub>2</sub> regulation of surface membrane traffic." *Current opinion in cell biology* **13**(4): 493-9.
- Masters, T. A., V. Calleja, et al. (2010). "Regulation of 3-phosphoinositide-dependent protein kinase 1 activity by homodimerization in live cells." *Sci Signal* **3**(145): ra78.
- Maurer, M., T. Su, et al. (2009). "3-Phosphoinositide-dependent kinase 1 potentiates upstream lesions on the phosphatidylinositol 3-kinase pathway in breast carcinoma." *Cancer Res* **69**(15): 6299-306.
- Michell, R. H. (1975). "Inositol phospholipids and cell surface receptor function." *Biochimica et biophysica acta* **415**(1): 81-47.
- Mills, S. J., D. Komander, et al. (2007). "Novel inositol phospholipid headgroup surrogate crystallized in the pleckstrin homology domain of protein kinase B $\alpha$ ." *ACS Chem Biol* **2**(4): 242-6.
- Minn, A. J., G. P. Gupta, et al. (2007). "Lung metastasis genes couple breast tumor size and metastatic spread." *Proc Natl Acad Sci U S A* **104**(16): 6740-5.
- Mohammadi, M., C. A. Dionne, et al. (1992). "Point mutation in FGF receptor eliminates phosphatidylinositol hydrolysis without affecting mitogenesis." *Nature* **358**(6388): 681-4.
- Molina, M. A., J. Codony-Servat, et al. (2001). "Trastuzumab (herceptin), a humanized anti-Her2 receptor monoclonal antibody, inhibits basal and activated Her2 ectodomain cleavage in breast cancer cells." *Cancer research* **61**(12): 4744-9.
- Mora, A., D. Komander, et al. (2004). "PDK1, the master regulator of AGC kinase signal transduction." *Semin Cell Dev Biol* **15**(2): 161-70.
- Mouneimne, G., L. Soon, et al. (2004). "Phospholipase C and cofilin are required for carcinoma cell directionality in response to EGF stimulation." *J Cell Biol* **166**(5): 697-708.
- Murthy, K. S., H. Zhou, et al. (2004). "Activation of PLC- $\delta$ 1 by Gi/o-coupled receptor agonists." *American journal of physiology. Cell physiology* **287**(6): C1679-87.

- Musacchio, A., T. Gibson, et al. (1993). "The PH domain: a common piece in the structural patchwork of signalling proteins." *Trends in biochemical sciences* **18**(9): 343-8.
- Nagashima, K., S. D. Shumway, et al. "Genetic and pharmacological inhibition of PDK1 in cancer cells: characterization of a selective allosteric kinase inhibitor." *J Biol Chem* **286**(8): 6433-48.
- Nagy, R., H. Grob, et al. (2009). "The Arabidopsis ATP-binding cassette protein AtMRP5/AtABCC5 is a high affinity inositol hexakisphosphate transporter involved in guard cell signaling and phytate storage." *The Journal of biological chemistry* **284**(48): 33614-22.
- Najafov, A., E. M. Sommer, et al. "Characterization of GSK2334470, a novel and highly specific inhibitor of PDK1." *Biochem J* **433**(2): 357-69.
- Nakashima, S., Y. Banno, et al. (1995). "Deletion and site-directed mutagenesis of EF-hand domain of phospholipase C-delta 1: effects on its activity." *Biochemical and biophysical research communications* **211**(2): 365-9.
- Newton, A. C. (1995). "Protein kinase C. Seeing two domains." *Current biology : CB* **5**(9): 973-6.
- Nguyen, D. X., P. D. Bos, et al. (2009). "Metastasis: from dissemination to organ-specific colonization." *Nat Rev Cancer* **9**(4): 274-84.
- Nurnberg, A., T. Kitzing, et al. (2011). "Nucleating actin for invasion." *Nat Rev Cancer* **11**(3): 177-87.
- Patterson, R. L., D. B. van Rossum, et al. (2002). "Phospholipase C-gamma is required for agonist-induced Ca<sup>2+</sup> entry." *Cell* **111**(4): 529-41.
- Patterson, R. L., D. B. van Rossum, et al. (2005). "Phospholipase C-gamma: diverse roles in receptor-mediated calcium signaling." *Trends Biochem Sci* **30**(12): 688-97.
- Pavlov, D., A. Muhlrad, et al. (2007). "Actin filament severing by cofilin." *Journal of molecular biology* **365**(5): 1350-8.
- Pearce, L. R., D. Komander, et al. (2010). "The nuts and bolts of AGC protein kinases." *Nat Rev Mol Cell Biol* **11**(1): 9-22.
- Peifer, C. and D. R. Alessi (2009). "New anti-cancer role for PDK1 inhibitors: preventing resistance to tamoxifen." *Biochem J* **417**(1): e5-7.
- Perou, C. M., T. Sorlie, et al. (2000). "Molecular portraits of human breast tumours." *Nature* **406**(6797): 747-52.
- Piccolo, E., P. F. Innominato, et al. (2002). "The mechanism involved in the regulation of phospholipase Cgamma1 activity in cell migration." *Oncogene* **21**(42): 6520-9.
- Piccolo, E., S. Vignati, et al. (2004). "Inositol pentakisphosphate promotes apoptosis through the PI 3-K/Akt pathway." *Oncogene* **23**(9): 1754-65.
- Pineiro, R., T. Maffucci, et al. (2011). "The putative cannabinoid receptor GPR55 defines a novel autocrine loop in cancer cell proliferation." *Oncogene* **30**(2): 142-52.
- Pinner, S. and E. Sahai (2008). "PDK1 regulates cancer cell motility by antagonising inhibition of ROCK1 by RhoE." *Nat Cell Biol* **10**(2): 127-37.
- Poulin, B., F. Sekiya, et al. (2000). "Differential roles of the Src homology 2 domains of phospholipase C-gamma1 (PLC-gamma1) in platelet-

- derived growth factor-induced activation of PLC-gamma1 in intact cells." *The Journal of biological chemistry* **275**(9): 6411-6.
- Price, J. T., T. Tiganis, et al. (1999). "Epidermal growth factor promotes MDA-MB-231 breast cancer cell migration through a phosphatidylinositol 3'-kinase and phospholipase C-dependent mechanism." *Cancer Res* **59**(21): 5475-8.
- Primo, L., L. di Blasio, et al. (2007). "Essential role of PDK1 in regulating endothelial cell migration." *J Cell Biol* **176**(7): 1035-47.
- Pullen, N., P. B. Dennis, et al. (1998). "Phosphorylation and activation of p70s6k by PDK1." *Science* **279**(5351): 707-10.
- Raina, K., S. Rajamanickam, et al. (2008). "Chemopreventive efficacy of inositol hexaphosphate against prostate tumor growth and progression in TRAMP mice." *Clin Cancer Res* **14**(10): 3177-84.
- Rameh, L. E., S. G. Rhee, et al. (1998). "Phosphoinositide 3-kinase regulates phospholipase C-gamma-mediated calcium signaling." *The Journal of biological chemistry* **273**(37): 23750-7.
- Rameh, L. E., K. F. Toliyas, et al. (1997). "A new pathway for synthesis of phosphatidylinositol-4,5-bisphosphate." *Nature* **390**(6656): 192-6.
- Razzini, G., C. P. Berrie, et al. (2000). "Novel functional PI 3-kinase antagonists inhibit cell growth and tumorigenicity in human cancer cell lines." *FASEB J* **14**(9): 1179-87.
- Rebecchi, M. J. and S. N. Pentylala (2000). "Structure, function, and control of phosphoinositide-specific phospholipase C." *Physiol Rev* **80**(4): 1291-335.
- Regunathan, J., Y. Chen, et al. (2006). "Differential and nonredundant roles of phospholipase C-gamma2 and phospholipase C-gamma1 in the terminal maturation of NK cells." *J Immunol* **177**(8): 5365-76.
- Rhee, S. G. (2001). "Regulation of phosphoinositide-specific phospholipase C." *Annual review of biochemistry* **70**: 281-312.
- Rhee, S. G. and Y. S. Bae (1997). "Regulation of phosphoinositide-specific phospholipase C isozymes." *J Biol Chem* **272**(24): 15045-8.
- Ridley, A. J. and A. Hall (1992). "The small GTP-binding protein rho regulates the assembly of focal adhesions and actin stress fibers in response to growth factors." *Cell* **70**(3): 389-99.
- Ridley, A. J., H. F. Paterson, et al. (1992). "The small GTP-binding protein rac regulates growth factor-induced membrane ruffling." *Cell* **70**(3): 401-10.
- Saarikangas, J., H. Zhao, et al. (2010). "Regulation of the actin cytoskeleton-plasma membrane interplay by phosphoinositides." *Physiological reviews* **90**(1): 259-89.
- Sahai, E. (2007). "Illuminating the metastatic process." *Nat Rev Cancer* **7**(10): 737-49.
- Sakamoto, K., I. Vucenik, et al. (1993). "[3H]phytic acid (inositol hexaphosphate) is absorbed and distributed to various tissues in rats." *J Nutr* **123**(4): 713-20.
- Sala, G., F. Dituri, et al. (2008). "Phospholipase C-gamma1 is required for metastasis development and progression." *Cancer Res* **68**(24): 10187-96.

- Sarbassov, D. D., D. A. Guertin, et al. (2005). "Phosphorylation and regulation of Akt/PKB by the rictor-mTOR complex." *Science* **307**(5712): 1098-101.
- Scagliotti, G. V., G. Selvaggi, et al. (2004). "The biology of epidermal growth factor receptor in lung cancer." *Clinical cancer research : an official journal of the American Association for Cancer Research* **10**(12 Pt 2): 4227s-4232s.
- Shamsuddin, A. M., I. Vucenik, et al. (1997). "IP6: a novel anti-cancer agent." *Life Sci* **61**(4): 343-54.
- Shepard, C. R., J. Kassis, et al. (2007). "PLC gamma contributes to metastasis of in situ-occurring mammary and prostate tumors." *Oncogene* **26**(21): 3020-6.
- Sieg, D. J., C. R. Hauck, et al. (2000). "FAK integrates growth-factor and integrin signals to promote cell migration." *Nat Cell Biol* **2**(5): 249-56.
- Singh, R. P., C. Agarwal, et al. (2003). "Inositol hexaphosphate inhibits growth, and induces G1 arrest and apoptotic death of prostate carcinoma DU145 cells: modulation of CDKI-CDK-cyclin and pRb-related protein-E2F complexes." *Carcinogenesis* **24**(3): 555-63.
- Snyder, J. T., A. U. Singer, et al. (2003). "The pleckstrin homology domain of phospholipase C-beta2 as an effector site for Rac." *The Journal of biological chemistry* **278**(23): 21099-104.
- Song, C., T. Satoh, et al. (2002). "Differential roles of Ras and Rap1 in growth factor-dependent activation of phospholipase C epsilon." *Oncogene* **21**(53): 8105-13.
- Sorlie, T., C. M. Perou, et al. (2001). "Gene expression patterns of breast carcinomas distinguish tumor subclasses with clinical implications." *Proc Natl Acad Sci U S A* **98**(19): 10869-74.
- Stephens, L. M., Al Hawkins, P. (2000). *Biology of phosphoinositides*. Ed. Cockcroft, S.
- Stoica, B., K. E. DeBell, et al. (1998). "The amino-terminal Src homology 2 domain of phospholipase C gamma 1 is essential for TCR-induced tyrosine phosphorylation of phospholipase C gamma 1." *Journal of immunology* **160**(3): 1059-66.
- Streb, H., R. F. Irvine, et al. (1983). "Release of Ca<sup>2+</sup> from a nonmitochondrial intracellular store in pancreatic acinar cells by inositol-1,4,5-trisphosphate." *Nature* **306**(5938): 67-9.
- Suh, P. G., J. I. Park, et al. (2008). "Multiple roles of phosphoinositide-specific phospholipase C isozymes." *BMB Rep* **41**(6): 415-34.
- Swairjo, M. A., N. O. Concha, et al. (1995). "Ca(2+)-bridging mechanism and phospholipid head group recognition in the membrane-binding protein annexin V." *Nature structural biology* **2**(11): 968-74.
- Szwergold, B. S., R. A. Graham, et al. (1987). "Observation of inositol pentakis- and hexakis-phosphates in mammalian tissues by <sup>31</sup>P NMR." *Biochem Biophys Res Commun* **149**(3): 874-81.
- Tantivejkul, K., I. Vucenik, et al. (2003). "Inositol hexaphosphate (IP6) enhances the anti-proliferative effects of adriamycin and tamoxifen in breast cancer." *Breast Cancer Res Treat* **79**(3): 301-12.

- Terasaka, K., J. J. Blakeslee, et al. (2005). "PGP4, an ATP binding cassette P-glycoprotein, catalyzes auxin transport in Arabidopsis thaliana roots." *The Plant cell* **17**(11): 2922-39.
- Thomas, C. C., M. Deak, et al. (2002). "High-resolution structure of the pleckstrin homology domain of protein kinase b/akt bound to phosphatidylinositol (3,4,5)-trisphosphate." *Curr Biol* **12**(14): 1256-62.
- Thomas, J. W., B. Ellis, et al. (1998). "SH2- and SH3-mediated interactions between focal adhesion kinase and Src." *J Biol Chem* **273**(1): 577-83.
- Thomas, S. M., F. M. Coppelli, et al. (2003). "Epidermal growth factor receptor-stimulated activation of phospholipase Cgamma-1 promotes invasion of head and neck squamous cell carcinoma." *Cancer Res* **63**(17): 5629-35.
- Torres, J., S. Dominguez, et al. (2005). "Solution behaviour of myo-inositol hexakisphosphate in the presence of multivalent cations. Prediction of a neutral pentamagnesium species under cytosolic/nuclear conditions." *J Inorg Biochem* **99**(3): 828-40.
- Touhara, K., J. Inglese, et al. (1994). "Binding of G protein beta gamma-subunits to pleckstrin homology domains." *The Journal of biological chemistry* **269**(14): 10217-20.
- Tsukada, S., M. I. Simon, et al. (1994). "Binding of beta gamma subunits of heterotrimeric G proteins to the PH domain of Bruton tyrosine kinase." *Proceedings of the National Academy of Sciences of the United States of America* **91**(23): 11256-60.
- Turner, T., M. V. Epps-Fung, et al. (1997). "Molecular inhibition of phospholipase cgamma signaling abrogates DU-145 prostate tumor cell invasion." *Clin Cancer Res* **3**(12 Pt 1): 2275-82.
- Tvorogov, D., X. J. Wang, et al. (2005). "Integrin-dependent PLC-gamma1 phosphorylation mediates fibronectin-dependent adhesion." *J Cell Sci* **118**(Pt 3): 601-10.
- Ullah, A. and A. M. Shamsuddin (1990). "Dose-dependent inhibition of large intestinal cancer by inositol hexaphosphate in F344 rats." *Carcinogenesis* **11**(12): 2219-22.
- van den Bout, I. and N. Divecha (2009). "PIP5K-driven PtdIns(4,5)P2 synthesis: regulation and cellular functions." *Journal of cell science* **122**(Pt 21): 3837-50.
- van Rheenen, J. and K. Jalink (2002). "Agonist-induced PIP(2) hydrolysis inhibits cortical actin dynamics: regulation at a global but not at a micrometer scale." *Molecular biology of the cell* **13**(9): 3257-67.
- van Rheenen, J., X. Song, et al. (2007). "EGF-induced PIP2 hydrolysis releases and activates cofilin locally in carcinoma cells." *J Cell Biol* **179**(6): 1247-59.
- van Rossum, D. B., R. L. Patterson, et al. (2005). "Phospholipase Cgamma1 controls surface expression of TRPC3 through an intermolecular PH domain." *Nature* **434**(7029): 99-104.
- Vasudevan, K. M., D. A. Barbie, et al. (2009). "AKT-independent signaling downstream of oncogenic PIK3CA mutations in human cancer." *Cancer Cell* **16**(1): 21-32.

- Vecchi, M., S. Confalonieri, et al. (2008). "Breast cancer metastases are molecularly distinct from their primary tumors." *Oncogene* **27**(15): 2148-58.
- Vucenik, I. and A. M. Shamsuddin (2003). "Cancer inhibition by inositol hexaphosphate (IP6) and inositol: from laboratory to clinic." *J Nutr* **133**(11 Suppl 1): 3778S-3784S.
- Vucenik, I., G. Y. Yang, et al. (1995). "Inositol hexaphosphate and inositol inhibit DMBA-induced rat mammary cancer." *Carcinogenesis* **16**(5): 1055-8.
- Walliser, C., M. Retlich, et al. (2008). "rac regulates its effector phospholipase Cgamma2 through interaction with a split pleckstrin homology domain." *J Biol Chem* **283**(44): 30351-62.
- Wang, W., R. Eddy, et al. (2007). "The cofilin pathway in breast cancer invasion and metastasis." *Nat Rev Cancer* **7**(6): 429-40.
- Waugh, C., L. Sinclair, et al. (2009). "Phosphoinositide (3,4,5)-triphosphate binding to phosphoinositide-dependent kinase 1 regulates a protein kinase B/Akt signaling threshold that dictates T-cell migration, not proliferation." *Molecular and cellular biology* **29**(21): 5952-62.
- Wells, A. and J. R. Grandis (2003). "Phospholipase C-gamma1 in tumor progression." *Clin Exp Metastasis* **20**(4): 285-90.
- Wen, W., J. Yan, et al. (2006). "Structural characterization of the split pleckstrin homology domain in phospholipase C-gamma1 and its interaction with TRPC3." *The Journal of biological chemistry* **281**(17): 12060-8.
- Wick, M. J., F. J. Ramos, et al. (2003). "Mouse 3-phosphoinositide-dependent protein kinase-1 undergoes dimerization and trans-phosphorylation in the activation loop." *J Biol Chem* **278**(44): 42913-9.
- Wijnholds, J., G. L. Scheffer, et al. (1998). "Multidrug resistance protein 1 protects the oropharyngeal mucosal layer and the testicular tubules against drug-induced damage." *J Exp Med* **188**(5): 797-808.
- Wise, A. and D. J. Gilbert (1982). "Phytate hydrolysis by germfree and conventional rats." *Appl Environ Microbiol* **43**(4): 753-6.
- Wong, K. K., J. A. Engelman, et al. (2010). "Targeting the PI3K signaling pathway in cancer." *Curr Opin Genet Dev* **20**(1): 87-90.
- Wymann, M. P. and R. Schneider (2008). "Lipid signalling in disease." *Nature reviews. Molecular cell biology* **9**(2): 162-76.
- Yamaguchi, H. and J. Condeelis (2007). "Regulation of the actin cytoskeleton in cancer cell migration and invasion." *Biochim Biophys Acta* **1773**(5): 642-52.
- Ye, K., B. Aghdasi, et al. (2002). "Phospholipase C gamma 1 is a physiological guanine nucleotide exchange factor for the nuclear GTPase PIKE." *Nature* **415**(6871): 541-4.
- Yin, J. J., K. Selander, et al. (1999). "TGF-beta signaling blockade inhibits PTHrP secretion by breast cancer cells and bone metastases development." *J Clin Invest* **103**(2): 197-206.
- Yuan, T. L. and L. C. Cantley (2008). "PI3K pathway alterations in cancer: variations on a theme." *Oncogene* **27**(41): 5497-510.
- Zamir, E. and B. Geiger (2001). "Molecular complexity and dynamics of cell-matrix adhesions." *J Cell Sci* **114**(Pt 20): 3583-90.

- Zhang, X., A. Chattopadhyay, et al. (1999). "Focal adhesion kinase promotes phospholipase C-gamma1 activity." *Proc Natl Acad Sci U S A* **96**(16): 9021-6.
- Zhang, X., N. Tang, et al. (2011). "Akt, FoxO and regulation of apoptosis." *Biochimica et biophysica acta*.

# Appendices

**1.1 5X denaturing sample buffer (per 16 ml)**

6.8 ml of ddH<sub>2</sub>O  
2 ml of 0.5M tris-HCl pH 6.8  
4 ml of Glycerol 87%  
1.6 ml of SDS 20%  
1.6 ml of bromophenol blue

**1.2 10% separating gel solution (per 5 ml)**

1.7 ml of Acrylamide mix [Protogel 30% (w/v) acrylamide: 0.8% (w/v) stock solution (37.5:1)]  
1.9 ml of ddH<sub>2</sub>O  
1.3 ml of 1.5M Tris, pH 8.8  
0.05 ml of 10% SDS  
0.05 ml of 10% APS  
0.02 ml of TEMED

**1.3 5% stacking gel solution (per 1 ml)**

0.17 ml of Acrylamide mix [Protogel 30% (w/v) acrylamide: 0.8% (w/v) stock solution (37.5:1)]  
0.68 ml of ddH<sub>2</sub>O  
0.13 ml of 1.0M Tris, pH 6.8  
0.01 ml of 10% SDS  
0.01 ml of 10% APS  
0.01 ml of TEMED

**1.4 1X running buffer**

25 mM tris, pH 8.9  
192 mM glycine  
0.2% SDS

**1.5 1X Transfer buffer**

25 mM Tris, pH 8.3  
192 mM Glycine

**1.6 1X TAE buffer**

96.8 g Tris  
22.84 mL Acetic Acid  
14.88 g EDTA

## 2. Map of pSUPERIOR.retro.puro used for generation of PDK1 targeting shRNA

### 2.2



pSUPER RNAi System™

VECTOR: pSUPERIOR.retro.puro  
CATALOG#: VEC-IND-0009/0010

Length: 7296 bp

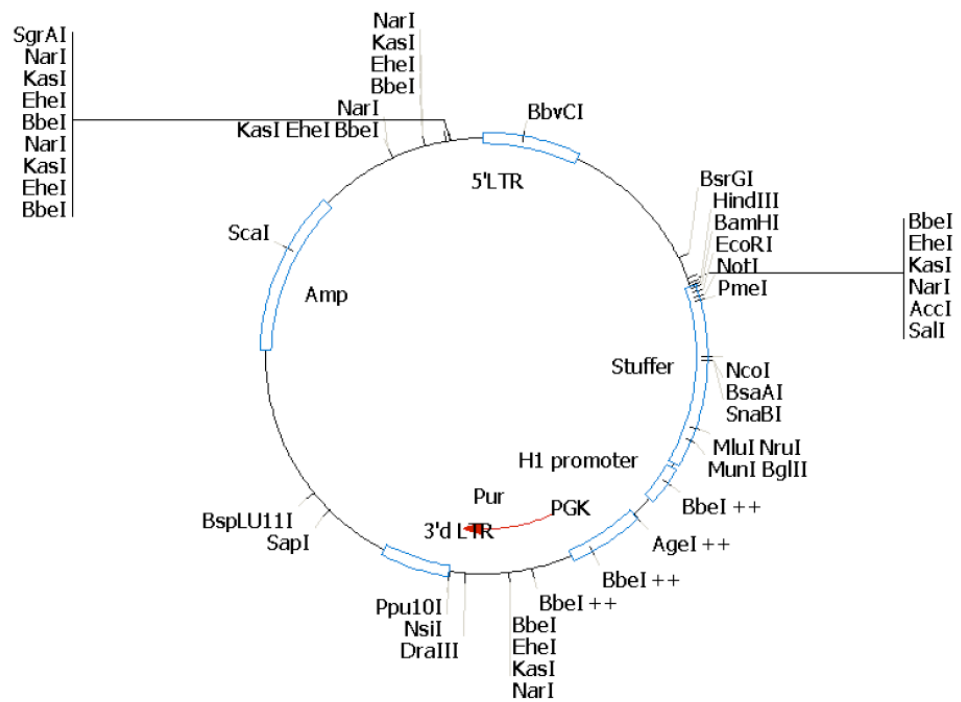
#### Key Sites

BglII: 2424  
HindIII: 1441  
EcoRI: 2646  
Sall: 1426  
XhoI: 1420

#### Vector Features

PGK promoter: 2767-3165  
Puro ORF: 3180-3779  
H1 promoter: 2651-2444  
Stuffer: 1447-2423  
Ampicillin resistance ORF: 6368-5502  
3' delta LTR: 3835-4202  
5' delta LTR: 7294-513

Sequencing primer 5'-GGAAGCCTTGGCTTTTG-3' binding site: 1241-1257  
Sequencing primer 5'-GATGACGTCAGCGTTCG-3' binding site: 2646-2630



## 2.1 Plasmids:

Plasmid	Selection	Provided by
pEGFP	Kanamycin	Clontech, US
PRK5-PLC $\gamma$ 1	Ampicillin	Prof. M. Falasca (BD, UK)
PALM-PLC $\gamma$ 1	Kanamycin	Dr. E. Bonvini (Macrogenics Inc., US)
pEBG2t-GST-PDK1	Ampicillin	Dr. D. Alessi
pOZ-PDK1	Kanamycin	Prof. R. Parsons
pCDNA	Ampicillin	Invitrogen, UK

## 2.2 siRNA

### 2.2.1 siRNA SMARTpool siRNA D-003017-02-0010, PDK1

target sequence 1: CAAGAGACCUCGUGGAGAA  
target sequence 2: GACCAGAGGCCAAGAAUUU  
target sequence 3: GGAAACGAGUAUCUUAUUAU  
target sequence 4: UGGCCAAAUUGCACGGAAU

### 2.2.3 siRNA SMARTpool siRNA D-003559-01-0010, PLC $\gamma$ 1

target sequence 1: CCAACCAGCUUAAGAGGAA  
target sequence 2: GAAGUGAACAUGUGGAUCA  
target sequence 3: GAGCAGUGCCUUUGAAGAA  
target sequence 4: CCAAGAAGGACUCGGGUCA

## 2.3 Primers

ABCC1 forward: 5-AGTGGAACCCCTCTCTGTTT-3'  
ABCC1 reverse: 5-CCTGATACGTCTTGGTCTTC-3'  
ABCC5 forward: 5-GGAGCTCTCAATGGAAGACG-3'  
ABCC5 reverse: 5-GTTTCACCATGAAGGCTGGT-3'  
 $\beta$ -actin forward: 5'-CTGGCACCACCTTCTACAATG-3'  
 $\beta$ -actin reverse: 5'-TCCAAAGGACAGGCTGGATG-3'